

AD-A242 015



2

NAVSWC TR 91-16

**BOLTZMANN TRANSPORT EQUATION
ALGORITHMS FOR INFINITE-SLAB BUILDUP
AND ALBEDO FACTORS**

BY W. L. DUNN, A. M. YACOUT, AND F. O'FOGHLUDHA
QUANTUM RESEARCH SERVICES, INC.

FOR NAVAL SURFACE WARFARE CENTER
RESEARCH AND TECHNOLOGY DEPARTMENT

DTIC
ELECTE
OCT 21 1991

S D D

30 SEPTEMBER 1990

Approved for public release; distribution is unlimited.

91-13595



NAVAL SURFACE WARFARE CENTER

Dahlgren, Virginia 22448-5000 • Silver Spring, Maryland 20903-5000

**BOLTZMANN TRANSPORT EQUATION
ALGORITHMS FOR INFINITE-SLAB BUILDUP AND
ALBEDO FACTORS**

**BY
W. L. DUNN, A. M. YACOUT, AND F. O'FOGHLUDHA
QUANTUM RESEARCH SERVICES INC.
FOR
NAVAL SURFACE WARFARE CENTER
RESEARCH AND TECHNOLOGY DEPARTMENT**

30 SEPTEMBER 1990

Approved for public release; distribution is unlimited.

NAVAL SURFACE WARFARE CENTER
Dahlgren, Virginia 22448-5000 • Silver Spring, Maryland 20903-5000

EXECUTIVE SUMMARY

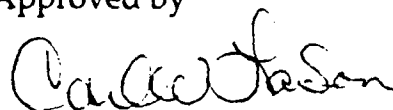
This report describes the development of improved algorithms for use in the Mathematical Radiation Environment Model for Ships (MREMS) code, which estimates dose equivalent at a matrix of many detector points due to a set of gamma-ray and neutron emitting source points. The algorithms consist of models with adjustable parameters, which are averageable over arbitrary source spectra, for buildup and albedo factors; these models can be used directly in the point-kernel model that MREMS employs. Buildup and albedo factors were calculated for six materials in a point-source, slab, point-detector geometry using a decomposition of the solution to the Boltzmann transport equation (and appropriate boundary conditions) into single- and multiple-scatter components. A rigorous solution for the single-scatter component was used that improves the efficiency of the calculations. A detailed model-fitting procedure was employed to fit these factors to simplified models, and the model constants were evaluated for each of several source energies. Finally, a procedure was implemented to determine average model constants for arbitrary source spectra. Slab buildup and albedo factors are presented for various source-slab-detector configurations, both in tabular form and in graphs that also show the fitted models.

FOREWORD

This work was sponsored by the Naval Surface Warfare Center (NAVSWC), under Contract N60921-88-C-0175. The purpose of the study was to develop improved point-kernel algorithms for shipboard radiation dosimetry calculations using the Mathematical Radiation Environment Model for Ships code. The particular emphasis in this research was the construction of simplified models for gamma-ray and neutron buildup and albedo factors representative of point-source, infinite-slab, point-detector geometries for six materials relevant to the ship environment. An efficient method of calculating the buildup and albedo factors using a unique single-scatter model was developed.

The authors thank G. Riel and N. Rao of NAVSWC's White Oak Laboratory for useful review of intermediate results and for several helpful suggestions during the course of the research. The assistance of C. Eisenhauer, of the National Institute of Standards and Technology, is gratefully acknowledged for supplying results of independent calculations and for technical review and advice. Also, review of an early version of this report by D. Trubey, of Oak Ridge National Laboratory, is appreciated.

Approved by



CARL W. LARSON, Head
Physics Technology Division



Accession For	
NTIS GRA&I	<input checked="" type="checkbox"/>
DTIC TAB	<input type="checkbox"/>
Unannounced	<input type="checkbox"/>
Justification	
By _____	
Distribution/	
Availability Codes	
Dist	Avail and/or Special
A-1	

CONTENTS

<u>Chapter</u>		<u>Page</u>
1	INTRODUCTION	1
2	OBJECTIVES	3
3	BUILDUP FACTOR CALCULATIONS	9
	SINGLE-SCATTER MODEL	11
	MULTIPLE-SCATTER MODEL	16
	SAMPLE RESULTS	20
4	SIMPLIFIED MODEL RESULTS	29
	MODEL FITTING PROCEDURE	29
	MODELS AS FUNCTIONS OF SOURCE ENERGY	31
	ENERGY AVERAGING PROCEDURE	50
5	ALBEDO CALCULATIONS	53
	ALGORITHMS	53
	SAMPLE RESULTS	55
	SIMPLIFIED MODELS	57
6	SAMPLE PROBLEM ANALYSIS	73
	CORRECTION FOR SOURCE-DETECTOR SEPARATION	73
	SINGLE SLABS	77
	INTERSECTING WALLS	81
7	SUMMARY AND CONCLUSIONS	93
	REFERENCES	97
	NOMENCLATURE	99
	DISTRIBUTION	(1)

CONTENTS (Cont.)

<u>Appendix</u>		<u>Page</u>
A	COMPUTER CODE DOCUMENTATION	A-1
B	GAMMA-RAY BUILDUP FACTOR TABLES, GEOMETRIES A-D	B-1
C	NEUTRON BUILDUP FACTOR TABLES, GEOMETRIES A-D	C-1
D	GAMMA-RAY ALBEDO FACTOR TABLES, GEOMETRIES B-D	D-1
E	NEUTRON ALBEDO FACTOR TABLES, GEOMETRIES B-D	E-1
F	GAMMA-RAY BUILDUP FACTOR TABLES, GEOMETRIES E-H.....	F-1
G	NEUTRON BUILDUP FACTOR TABLES, GEOMETRIES E-H.....	G-1
H	GAMMA-RAY ALBEDO FACTOR TABLES, GEOMETRIES F-H	H-1
I	NEUTRON ALBEDO FACTOR TABLES, GEOMETRIES F-H	I-1

ILLUSTRATIONS

<u>Figure</u>		<u>Page</u>
1	THE BASIC SOURCE-SLAB-DETECTOR GEOMETRY	4
2	THE ALBEDO GEOMETRY	5
3	SIMPLIFIED DESCRIPTION OF THE MREMS GEOMETRY	10
4	THE GEOMETRY FOR Ω , ω , AND ρ	12
5	THE SINGLE-SCATTER GEOMETRY FOR THE CASE $h_s = h_D = 0$	14
6	NEUTRON CROSS SECTION LIBRARY FILE STRUCTURE	19
7	THE VARIABLES DEFINING SPECIFIC CONFIGURATIONS	23
8	MODEL FITS TO GAMMA-RAY BUILDUP FACTOR DATA FOR ALUMINUM, GEOMETRY A	32
9	MODEL FITS TO GAMMA-RAY BUILDUP FACTOR DATA FOR IRON, GEOMETRY A	33
10	MODEL FITS TO GAMMA-RAY BUILDUP FACTOR DATA FOR LEAD, GEOMETRY A	34
11	MODEL FITS TO GAMMA-RAY BUILDUP FACTOR DATA FOR WATER, GEOMETRY A	35
12	MODEL FITS TO GAMMA-RAY BUILDUP FACTOR DATA FOR POLYETHYLENE, GEOMETRY A	36
13	MODEL FITS TO GAMMA-RAY BUILDUP FACTOR DATA FOR CONCRETE, GEOMETRY A	37
14	MODEL FITS TO NEUTRON BUILDUP FACTOR DATA FOR ALUMINUM, GEOMETRY A	38
15	MODEL FITS TO NEUTRON BUILDUP FACTOR DATA FOR IRON, GEOMETRY A	39

ILLUSTRATIONS (Cont.)

<u>Figure</u>		<u>Page</u>
16	MODEL FITS TO NEUTRON BUILDUP FACTOR DATA FOR LEAD, GEOMETRY A	40
17	MODEL FITS TO NEUTRON BUILDUP FACTOR DATA FOR WATER, GEOMETRY A	41
18	MODEL FITS TO NEUTRON BUILDUP FACTOR DATA FOR POLYETHYLENE, GEOMETRY A	42
19	MODEL FITS TO NEUTRON BUILDUP FACTOR DATA FOR CONCRETE, GEOMETRY A	43
20	THE THREE ALBEDO FACTOR CONFIGURATIONS	54
21	MODEL FITS TO GAMMA-RAY ALBEDO FACTOR DATA FOR ALUMINUM, GEOMETRY B	58
22	MODEL FITS TO GAMMA-RAY ALBEDO FACTOR DATA FOR IRON, GEOMETRY B	59
23	MODEL FITS TO GAMMA-RAY ALBEDO FACTOR DATA FOR LEAD, GEOMETRY B	60
24	MODEL FITS TO GAMMA-RAY ALBEDO FACTOR DATA FOR WATER, GEOMETRY B	61
25	MODEL FITS TO GAMMA-RAY ALBEDO FACTOR DATA FOR POLYETHYLENE, GEOMETRY B	62
26	MODEL FITS TO GAMMA-RAY ALBEDO FACTOR DATA FOR CONCRETE, GEOMETRY B	63
27	MODEL FITS TO NEUTRON ALBEDO FACTOR DATA FOR ALUMINUM, GEOMETRY B	64
28	MODEL FITS TO NEUTRON ALBEDO FACTOR DATA FOR IRON, GEOMETRY B	65
29	MODEL FITS TO NEUTRON ALBEDO FACTOR DATA FOR LEAD, GEOMETRY B	66
30	MODEL FITS TO NEUTRON ALBEDO FACTOR DATA FOR WATER, GEOMETRY B	67

ILLUSTRATIONS (Cont.)

<u>Figure</u>		<u>Page</u>
31	MODEL FITS TO NEUTRON ALBEDO FACTOR DATA FOR POLYETHYLENE, GEOMETRY B	68
32	MODEL FITS TO NEUTRON ALBEDO FACTOR DATA FOR CONCRETE, GEOMETRY B	69
33	MREMS TREATMENT OF OBLIQUE INCIDENCE ON SLABS	74
34	APPROXIMATE BEHAVIOR OF B VERSUS S	76
35	PLOTS OF $B_0 g_M(S a)$ VERSUS S FOR FOUR CASES	78
36	GEOMETRICAL ARRANGEMENT FOR SAMPLE PROBLEM 5	80
37	SAMPLE PROBLEM 6 DESCRIPTION	83
38	ENERGY SPECTRA FOR SAMPLE PROBLEM 6	85
39	SCHEMATIC OF THE LOCAL GEOMETRY ALONG THE LOS FOR SAMPLE PROBLEM 6	86
40	A HYPOTHETICAL PROBLEM WHICH WOULD BE MODELED AS SHOWN IN FIGURE 39(b)	91

TABLES

<u>Table</u>		<u>Page</u>
1	NUMERICAL COMPARISON OF THE SINGLE-SCATTER MODEL OF EQUATION (9) WITH INDEPENDENT RESULTS, FOR $c = 0.8$	21
2	COMPARISON OF FLUX RATIOS FOR 1.25 MEV GAMMA RAYS AND A 5.08-CM IRON SLAB.....	22
3	SAMPLE RESULTS FOR INFINITE-MEDIUM GAMMA-RAY ENERGY ABSORPTION BUILDUP FACTORS IN IRON.....	22
4	THE SIX MATERIALS AND THEIR DENSITIES AND ELEMENTAL COMPOSITIONS.....	24
5	THE INITIAL FOUR BUILDUP FACTOR CONFIGURATIONS.....	24
6	CALCULATED TOTAL CROSS SECTIONS FOR THE SIX MATERIALS...	25
7	GAMMA-RAY BUILDUP FACTORS FOR ALUMINUM, GEOMETRY A ($h_s=0, \rho_D=0, z_D=a$).....	27
8	NEUTRON BUILDUP FACTORS FOR ALUMINUM, GEOMETRY A ($h_s=0, \rho_D=0, z_D=a$).....	28
9	GAMMA-RAY BUILDUP FACTOR MODEL CONSTANTS AND LEAST-SQUARES FUNCTION VALUES FOR ALUMINUM, GEOMETRY A.....	44
10	GAMMA-RAY BUILDUP FACTOR MODEL CONSTANTS AND LEAST-SQUARES FUNCTION VALUES FOR IRON, GEOMETRY A.....	44
11	GAMMA-RAY BUILDUP FACTOR MODEL CONSTANTS AND LEAST-SQUARES FUNCTION VALUES FOR LEAD, GEOMETRY A.....	45
12	GAMMA-RAY BUILDUP FACTOR MODEL CONSTANTS AND LEAST-SQUARES FUNCTION VALUES FOR WATER, GEOMETRY A.....	45

TABLES (Cont.)

<u>Table</u>		<u>Page</u>
13	GAMMA-RAY BUILDUP FACTOR MODEL CONSTANTS AND LEAST-SQUARES FUNCTION VALUES FOR POLYETHYLENE, GEOMETRY A	46
14	GAMMA-RAY BUILDUP FACTOR MODEL CONSTANTS AND LEAST-SQUARES FUNCTION VALUES FOR CONCRETE, GEOMETRY A	46
15	NEUTRON BUILDUP FACTOR MODEL CONSTANTS AND LEAST-SQUARES FUNCTION VALUES FOR ALUMINUM, GEOMETRY A...	47
16	NEUTRON BUILDUP FACTOR MODEL CONSTANTS AND LEAST-SQUARES FUNCTION VALUES FOR IRON, GEOMETRY A	47
17	NEUTRON BUILDUP FACTOR MODEL CONSTANTS AND LEAST-SQUARES FUNCTION VALUES FOR LEAD, GEOMETRY A	48
18	NEUTRON BUILDUP FACTOR MODEL CONSTANTS AND LEAST-SQUARES FUNCTION VALUES FOR WATER, GEOMETRY A	48
19	NEUTRON BUILDUP FACTOR MODEL CONSTANTS AND LEAST-SQUARES FUNCTION VALUES FOR POLYETHYLENE, GEOMETRY A	49
20	NEUTRON BUILDUP FACTOR MODEL CONSTANTS AND LEAST-SQUARES FUNCTION VALUES FOR CONCRETE, GEOMETRY A	49
21	BUILDUP FACTORS IN WATER FOR SOURCE-DETECTOR SEPARATION OF 40 MFP	50
22	GAMMA-RAY ALBEDO FACTORS FOR ALUMINUM, GEOMETRY B	56
23	NEUTRON ALBEDO FACTORS FOR ALUMINUM, GEOMETRY B	56
24	GAMMA-RAY ALBEDO FACTOR MODEL CONSTANTS AND LEAST-SQUARES FUNCTION VALUES FOR GEOMETRY B	70
25	NEUTRON ALBEDO FACTOR MODEL CONSTANTS AND LEAST-SQUARES FUNCTION VALUES FOR GEOMETRY B	71
26	THE SAMPLE PROBLEM GEOMETRIES	74
27	THE PARAMETER VALUES FOR γ AND ν IN THE MODEL OF EQUATION (54) FOR g_M	77

TABLES (Cont.)

<u>Table</u>		<u>Page</u>
28	DESCRIPTION OF SAMPLE PROBLEM 5	79
29	MODEL CONSTANTS OBTAINED BY THE WBAR CODE FOR THE SPECTRA OF TABLE 28	81
30	MODEL AND MONTE CARLO RESULTS FOR SAMPLE PROBLEM 5	82
31	ASSUMED SPECTRA FOR SAMPLE PROBLEM 6	84
32	MODEL CONSTANTS OBTAINED BY THE WBAR CODE FOR SAMPLE PROBLEM 6	87
33	MODEL AND MONTE CARLO RESULTS FOR SAMPLE PROBLEM 6(a)	87
34	MODEL AND MONTE CARLO RESULTS FOR SAMPLE PROBLEM 6(b)	90

CHAPTER 1

INTRODUCTION

This report documents the results of research carried out under Contract N60921-88-C-0175, which was funded by the Naval Surface Warfare Center (NAVSWC), White Oak Laboratory. The period of performance was November 1988 – June 1990.

The basic requirement (Item 0001) was to construct improved gamma-ray and neutron buildup factor models for use in the existing Mathematical Radiation Environment Model for Ships (MREMS) code. Option 1 (Item 0002) was concerned with constructing similar algorithms for gamma-ray and neutron albedo, and option 2 (Item 0003) involved construction of computer codes to implement the developed algorithms. Options 3 and 4 (Items 0004 and 0005) called, respectively, for treatment of six sample problems and preparation of a manuscript suitable for journal publication.

The research described in this report achieved the following general results:

- slab-geometry algorithms were developed for both gamma-ray and neutron buildup and albedo factors, for monoenergetic point sources using a decomposition into single- and multiple-scatter components;
- simplified parametric models were fit to the buildup and albedo factors as functions of slab thickness for various source energies and each of six slab materials;
- a scheme to develop a model and calculate parameters for arbitrary source spectra was developed;
- three FORTRAN computer codes were developed and documented to evaluate gamma-ray and neutron buildup and albedo factors and to calculate the parameters for the source energy spectrum-averaged model;
- through evaluation of the sample problems, a correction factor to adjust for source-detector separation was constructed.

The distinguishing features of this work were the use of an efficient and accurate single-scatter model, applicable to both transmission (buildup) and reflection (albedo), and the calculation of factors for slabs as opposed to infinite media.

The studies undertaken as part of this research provide an analysis of one approach for estimating dose equivalent that is subject to certain assumptions, which were defined by the project statement of work. The results of this study will allow NAVSWC to evaluate the adequacy of this approximate methodology and to compare it with other approaches in order to develop a rational strategy for upgrading the MREMS code to meet the needs of the Navy.

The units for flux (by which we mean scalar flux) are $\text{cm}^{-2}\text{-sec}^{-1}$ and for fluence are cm^{-2} ; angular flux, Ψ , is expressed in $\text{cm}^{-2}\text{-sec}^{-1}\text{-ster}^{-1}$. The slab buildup and albedo factors are ratios of dose equivalent quantities. We express dose, D , in units of mrad and dose equivalent, H , in units of mrems; the two are related by the quality factor, Q , through the expression $H=QD$. We actually compute dose equivalent directly from fluence through an energy-dependent conversion factor h_ϕ . For gamma rays, the conversion is effected by calculating the energy deposition per gram of water at the detector point and assuming a quality factor of unity at all energies. For neutrons, the conversion factor is determined from the table on p. 616 of Schaeffer.¹ We use the symbol Φ for flux and F for fluence. We denote by Φ_1 the single-scatter flux due to a point source and by Φ_{10} the single-scatter flux due to a beam incident on a slab in unique direction Ω_0 . Slab thicknesses expressed in mean free paths (mfp) at the source energy are given the symbol a ; the symbol T is used for physical slab thickness and has units of cm.

Chapter 2 discusses research objectives; Chapters 3 and 4 report on the work to construct simplified buildup factor algorithms (Item 0001); Chapter 5 describes the albedo calculations (Item 0002); Chapter 6 gives a discussion of the analysis of sample problems and details the development of the source-detector separation correction factor; Chapter 7 summarizes the results of the entire project. The documentation for the computer codes (Item 0003) is given in Appendix A; tables of gamma-ray and neutron buildup factors for four configurations in the slab geometry are given in Appendices B and C; similar results for gamma-ray and neutron albedo factors appear in Appendices D and E, respectively; tables of gamma-ray and neutron buildup factors for four sample-problem geometries are given in Appendices F and G; and albedo factors for three sample problems are given in Appendices H and I.

CHAPTER 2

OBJECTIVES

The general objective of Item 0001 was to develop slab buildup factor algorithms that would be consistent with the point kernel model used in the MREMS code to see if they improve the accuracy of the code in typical ship dosimetry problems. MREMS treats point sources and point detectors, both of which are enclosed in compartments; therefore, the line of sight (LOS) between source and detector typically intersects one or more "walls." Currently, the slant distances through each material are calculated and summed by material and used in simple models that approximate infinite-medium buildup factors; these buildup factors are then used to estimate dose equivalent at each detector point. In Item 0001 of this research, Quantum sought to develop buildup factor models for the semi-infinite slab geometry of Figure 1 (in this geometry, the source is always at the origin of the coordinate system). Simplified models were then fit to the slab buildup factors, which can be used in MREMS in place of the infinite-medium buildup factor models.

For Item 0002, the overall objective was to construct albedo factor models for the same semi-infinite slab geometry. In the reflection case, both source and detector points are located on the same side of the slab, and albedo is defined solely in terms of the geometric spreading factor, $1/(4\pi r^2)$, from an "image source," reflected about the centerline of the slab, as shown in Figure 2. Again, simplified models were fit to the slab albedo factors. The general objective of Item 0003 was to develop codes to calculate the slab buildup and albedo factors and to average the constants of the simplified models over arbitrary source spectra.

Quantum's approach was to decompose the buildup and albedo factors into single- and multiple-scatter components. The single-scatter component was accurately represented as a definite integral and calculated using an efficient quadrature, and the multiple-scatter component was estimated by Monte Carlo models developed for this purpose. Two separate codes were developed, one for gamma rays and one for neutrons; both evaluate either buildup or albedo factors, depending on input, and give single-scatter, multiple-scatter, and total buildup or albedo factors.

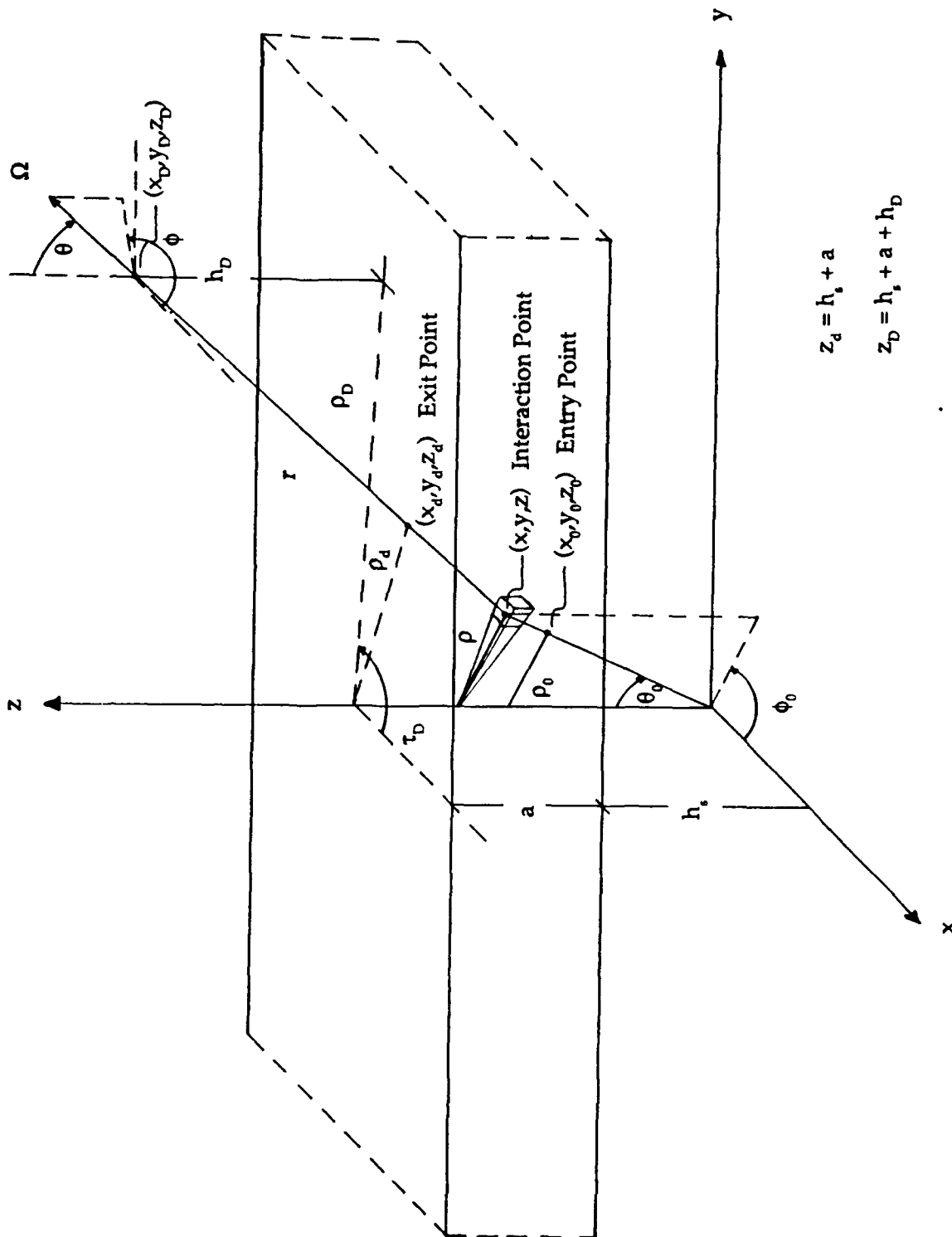
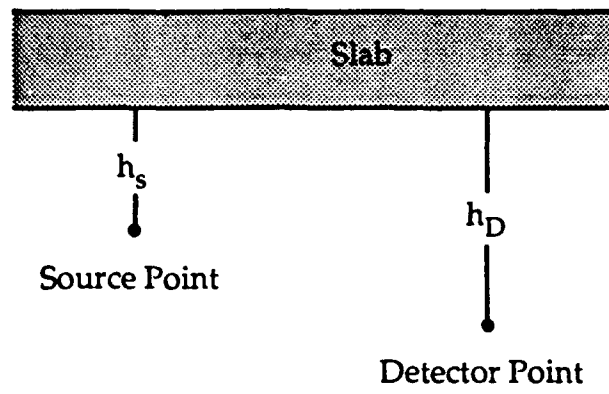
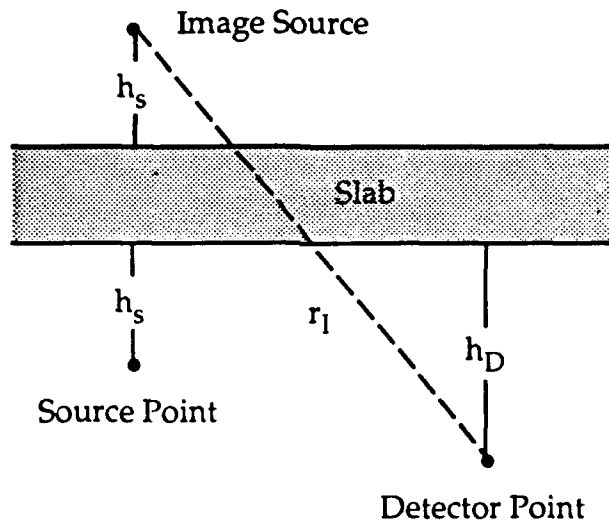


FIGURE 1. THE BASIC SOURCE-SLAB-DETECTOR GEOMETRY



(a) Actual source-detector arrangement



(b) Image source-detector arrangement

FIGURE 2. THE ALBEDO GEOMETRY

Item 0001

The specific objectives under Item 0001 can be stated as:

- Construct models to evaluate the single-scatter buildup, with respect to the uncollided dose equivalent, H_0 , for the single-source-point, single-detector-point, semi infinite-slab geometry of Figure 1. In particular, calculate the buildup factor

$$B_1 = 1 + \frac{H_1}{H_0} \quad (1)$$

as a function of h_s , ρ_D , z_D , a , source energy (E_0), and slab material, where H_1 is dose equivalent in tissue at the detector point (ρ_D , τ_D , z_D) due to single scatters in the slab. Both photon and neutron sources were considered, and the slab may consist of any of the following six materials: aluminum, iron, lead, water, polyethylene, and concrete. The buildup factors are evaluated for a monoenergetic source energy, E_0 .

- Construct codes to estimate the total buildup factor

$$B = B_1 + \frac{H_n}{H_0} = 1 + \frac{H_1 + H_n}{H_0} \quad (2)$$

for the same geometries and materials as above, where H_n is dose equivalent at (ρ_D , τ_D , z_D) due to radiation that scatters more than once in the slab.

- Fit the total buildup factor, B , to simplified models with adjustable parameters.

Item 0002

Under Item 0002 (Option 1), Quantum was to perform the following:

- For the geometry of Figure 2(a) and the same materials as above, construct models to estimate the single-scatter albedo, defined as

$$A_1 = \frac{4\pi r_1^2 H_1}{h_\phi} , \quad (3)$$

for neutron and photon sources of constant E_0 , where H_1 is dose equivalent in tissue at the detector point due to single scatters in the slab, r_1 is the image source-detector distance (see Figure 2(b)), and h_ϕ is a fluence-to-dose equivalent conversion factor.

- Construct a model for total albedo, i.e., estimate

$$A = \frac{4\pi r_1^2 (H_1 + H_n)}{h_\phi} , \quad (4)$$

where H_n is the dose at the detector point due to radiation that scatters more than once in the slab.

- Fit simple models with adjustable parameters to the total albedo factor.

Item 0003

Under Item 0003 (Option 2), the objectives were to construct codes that can be used by NAVSWC for the following:

- to estimate B and A, as described above; the codes were written in FORTRAN 77 and require input of h_s , ρ_D , z_D , a , E_0 , and slab material. They should apply for thicknesses over the range $0 < a \leq 7$ mean free paths (mfp).
- to perform spectrum averaging of the developed models; this code should construct model constants that are averaged over arbitrary source spectra, $S(E_0)$, defined on the intervals

$0.01 \text{ MeV} \leq E_0 \leq 7 \text{ MeV}$, for photons

$\text{thermal} \leq E_0 \leq 14 \text{ MeV}$, for neutrons.

Item 0004

The objective of Item 0004 (Option 3) was to consider six sample problems. The first four sample problems provide a means to refine the buildup and albedo models for axial and radial offset effects; the last two sample problems test the models against independent results for complex geometries, one of which was identified by NAVSWC.

Item 0005

The objective of Item 0005 (Option 4) was to prepare a manuscript that was suitable for journal publication. A manuscript entitled Gamma-Ray and Neutron Dose-Equivalent Buildup Factors for Infinite Slabs was prepared and separately provided to NAVSWC.

CHAPTER 3

BUILDUP FACTOR CALCULATIONS

In the MREMS code, dose equivalent is calculated at a number (typically, hundreds or thousands) of detector points by summing the contributions from many source points. The actual geometry is three-dimensional and quite complex (a simplified version is shown in Figure 3). Therefore, it is not possible to use a rigorous solution procedure, and the MREMS code is based on the point-kernel method. In this method, the uncollided dose equivalent, H_0 , at each detector point due to a particular source point is first calculated as

$$H_0 = \frac{S_0 h_\phi(E_0) e^{-\sum_{i=1}^m \sigma_i T_i}}{4\pi R^2}, \quad (5)$$

where S_0 is source strength, E_0 is source energy, $h_\phi(E_0)$ is a fluence-to-dose equivalent conversion factor, σ_i is the total macroscopic cross section of material i at E_0 , m is the total number of different materials encountered along the LOS, T_i is the linear distance through material i , and R is the source-detector separation. The total dose equivalent is then estimated as

$$H = B H_0, \quad (6)$$

where B is the dose-equivalent buildup factor, which accounts for the "extra" dose due to scattered radiation that reaches the detector point.

Rather than use infinite-medium buildup factors, we calculated buildup factors for the slab geometry of Figure 1. For our purposes, the basic problem reduces to solving the Boltzmann transport equation for the point-source, single-slab, point-detector geometry of Figure 1. We chose to do this by solving the problem of a directed beam incident on the slab from the source point at an arbitrary angle and then integrating that result over all incident directions.

Thus, we solved the Boltzmann transport equation in the form

$$\left[\mu \frac{\partial}{\partial z} + \omega \cdot \frac{\partial}{\partial \rho} + \sigma \right] \Psi(\rho, z, E, \Omega) = \frac{1}{2\pi} \int \int \Psi(\rho, z, E', \Omega') \sigma_s(E') f(E' \rightarrow E, \Omega' \rightarrow \Omega) d\Omega' dE' \quad (7)$$

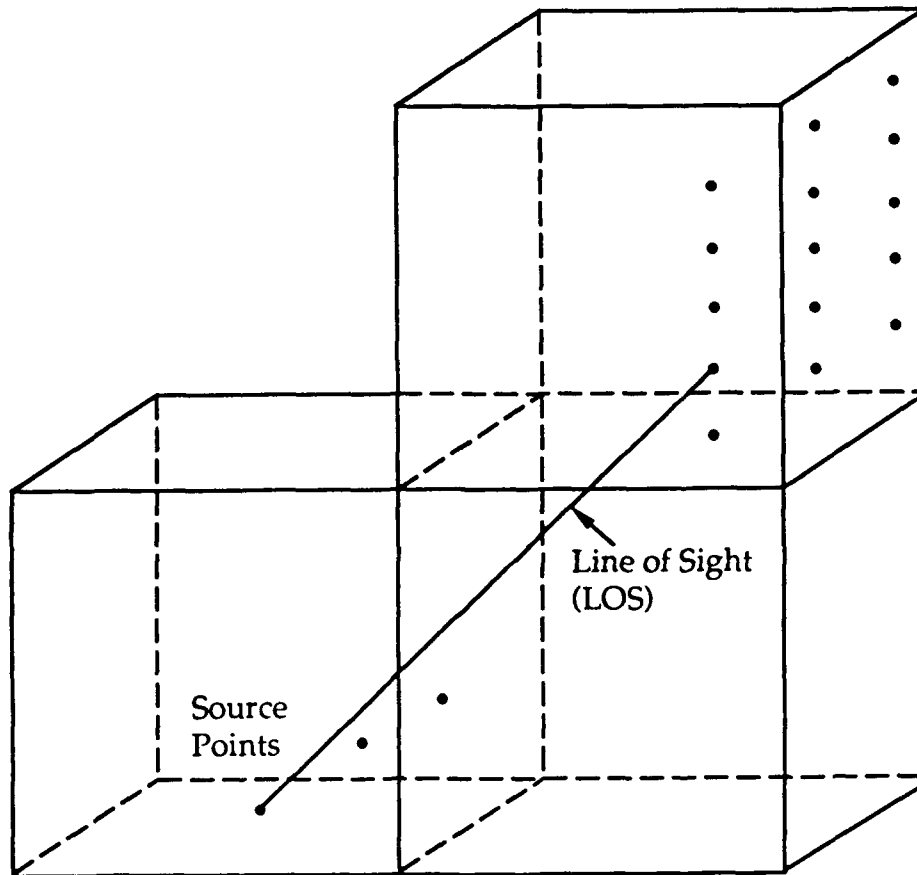


FIGURE 3. SIMPLIFIED DESCRIPTION OF THE MREMS GEOMETRY

subject to the boundary conditions

$$\Psi[\rho, h_s, E, \Omega(\mu, \phi)] = \delta\left(x - h_s, \frac{\sqrt{1-\mu_0^2} \cos \phi}{\mu_0}\right) \delta\left(y - h_s, \frac{\sqrt{1-\mu_0^2} \sin \phi}{\mu_0}\right) \delta(\mu - \mu_0) \delta(\phi - \phi_0) \delta(E - E_0) \quad (8a)$$

and

$$\Psi[\rho, h_s + T, E, \Omega(-\mu, \phi)] = 0 \quad (8b)$$

for $\mu \in [0, 1]$ and $\phi \in [0, 2\pi]$. Here ρ specifies lateral position in Cartesian (x, y) or cylindrical (ρ, τ) coordinates, $z \in [h_s, h_s + T]$ is depth in the slab, E is radiation energy, Ω defines in spherical coordinates (θ, ϕ) the direction of propagation, ω is the projection of Ω in the x - y plane (see Figure 4), σ_s and σ are the macroscopic scatter and total cross sections, respectively, and Ψ is the angular radiation flux. Further, $\mu = \cos \theta$ is the z -direction cosine of the propagating radiation, $f(E' \rightarrow E, \Omega' \rightarrow \Omega)$ is the probability density function for scattering from energy E' and direction Ω' to energy E and direction Ω , and all distances are in physical units of cm.

Previous research by the investigators²⁻⁴ to solve the searchlight problem for isotropic scattering led to a natural decomposition of the solution into single- and multiple-scatter components. The searchlight problem is basic to the considered slab problem, and so, extending the earlier work, we consider a similar decomposition here.

SINGLE-SCATTER MODEL

For the slab geometry of Figure 1 and the problem defined by Equations (7) and (8), a single-scatter model can be constructed by integrating, over path length in the slab, the standard Monte Carlo statistical estimator [e.g., see Reference 1]. This leads to the following model for the single-scatter contribution, Φ_{10} , to the flux at the detector point (ρ_D, τ_D, z_D) for radiation incident on the slab with direction $\Omega_0 = (\mu_0, \phi_0)$

$$\Phi_{10}(\mu_0, \phi_0) = \frac{\sigma_s(E_0)}{2\pi} \int_{h_s}^{h_s+T} \frac{e^{-\sigma_0 \zeta / \mu_0} e^{-\sigma q}}{r^2} f(E_0 \rightarrow E, \mu_0 \rightarrow \mu) d\zeta, \quad (9)$$

where $\sigma_0 = \sigma(E_0)$,

$$r = [(z_D - z)^2 + \rho_D^2 + \rho^2 - 2\rho_D \rho \cos(\tau_D - \phi_0)]^{1/2}, \quad (10a)$$

$$q = \frac{r(z_D - z)}{z_D - z}, \quad (10b)$$

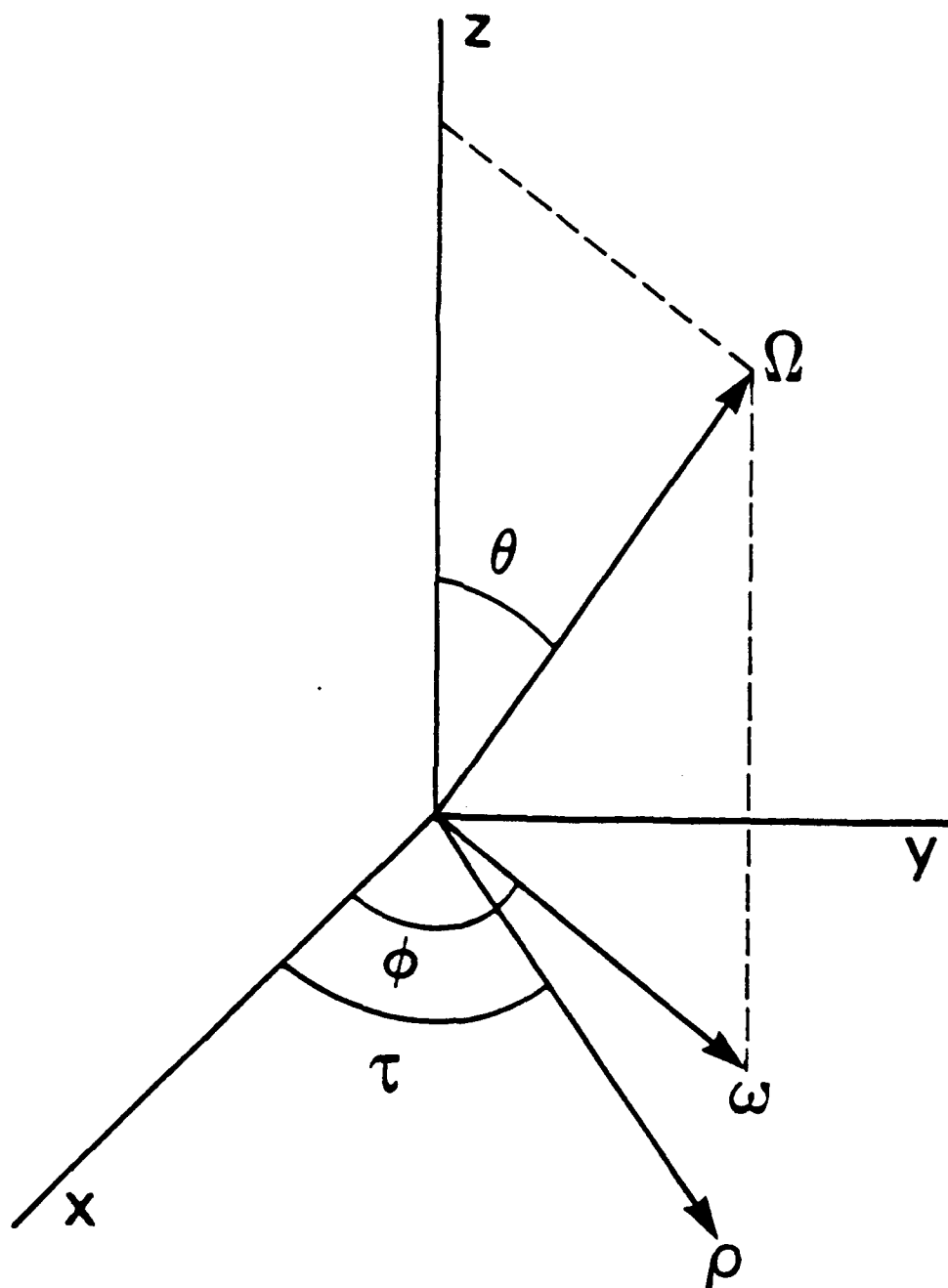


FIGURE 4. THE GEOMETRY FOR Ω , ω , AND ρ

and

$$\mu = \frac{z_D - z}{r} \quad (10c)$$

The total single-scatter flux can then be obtained by integration over all source emission directions that intersect the slab (i.e., over 2π steradians), viz.,

$$\Phi_1 = \frac{\sigma_s(E_0)}{2\pi} \int_0^1 \int_0^{2\pi} \int_{h_s}^{h_s+T} \frac{e^{-\sigma_0 \zeta / \mu_0 - \sigma q}}{r^2} f(E_0 \rightarrow E, \mu_0 \rightarrow \mu) d\zeta d\phi_0 d\mu_0 \quad (11)$$

Equation (11) is the complete model for the single-scatter flux, and thus for the fluence over a one-sec interval.

We were able to verify the formulation of Equation (9) for the special case of mono-energetic transport, isotropic scattering, and the simplified case where $h_s = h_D = 0$ (see Figure 5). For this case, Equation (9) takes the form

$$\Phi_{10} = \frac{\sigma_s}{4\pi} \int_{h_s}^{h_s+T} \frac{e^{-\sigma(\zeta/\mu_0 + q)}}{r^2} d\zeta \quad (12)$$

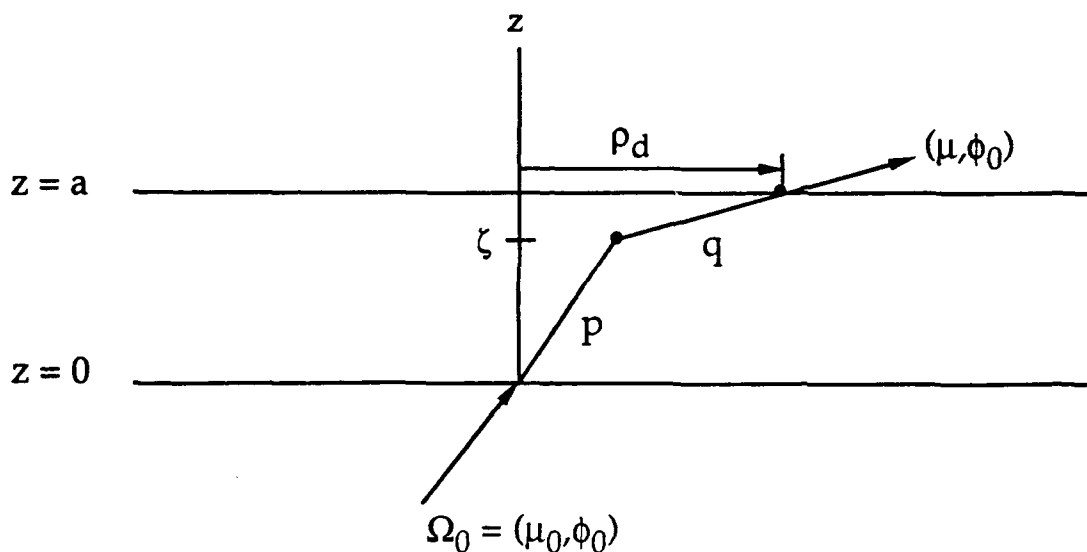
Two independent derivations were constructed. In the first derivation, the solution for the case $\tau_D = \phi_0$ was built up from a combination of the following factors:

- the equivalent surface source strength (μ_0)
- the probability that the particle would interact in the slab between path length p and $p+dp$ ($\sigma e^{-\sigma p} dp$)
- the probability of scatter ($c = \sigma_s / \sigma$)
- the probability that the direction after scatter would be toward the detector point [$d\mu d\phi / (4\pi)$]
- the probability of escaping the slab ($e^{-\sigma q}$)
- the boundary crossing estimator [$1 / (\mu \rho_d d\rho_d d\tau)$]

Combining these factors, we obtain the following general form

$$\Phi_1 = \mu_0 \int_0^{T/\mu_0} c \frac{d\mu}{2} \frac{d\phi}{2\pi} e^{-\sigma q} \frac{e^{-\sigma p} \sigma dp}{\mu \rho_d d\rho_d d\tau} \quad (13)$$

where q in this case assumes the simplified form


 FIGURE 5. THE SINGLE-SCATTER GEOMETRY FOR THE CASE $h_s = h_D = 0$

$$q = \left[(T - \zeta)^2 + \left(\rho_d - \frac{\zeta \sqrt{1 - \mu_0^2}}{\mu_0} \right)^2 \right]^{1/2} \quad (14)$$

Rewriting Equation (13) as

$$\Phi_1 = \frac{\sigma_s \mu_0}{4\pi \rho_d} \int_0^{T/\mu_0} \frac{e^{-\sigma(p+q)}}{\mu} \frac{d\mu}{d\rho_d} \frac{d\phi}{d\tau} dp, \quad (15)$$

where

$$\frac{d\phi}{d\tau} = \frac{\rho_d}{\rho_d - \frac{\zeta \sqrt{1 - \mu_0^2}}{\mu_0}}, \quad (16)$$

and changing the variable of integration from p to ζ , we obtain

$$\Phi_{10} = \frac{\sigma_s}{4\pi} \int_0^T \frac{e^{-\sigma(\zeta/\mu_0 + q)}}{q^2} d\zeta, \quad (17)$$

which is the same as Equation (12), since $(\rho_d, \tau_d, z_d) = (\rho_D, \tau_D, z_D)$ for $h_D = 0$, and so $q = r$.

The other derivation involves formally solving Equations (7) and (8). The general procedure can be reduced to the following steps:

- Express Equations (7) and (8) in optical units and apply a two-dimensional Fourier transform;
- Relate the transforms of the desired quantities to the solution of an appropriate pseudo problem;
- Convert the integrodifferential pseudo problem to a set of singular integral equations and integral constraints;
- Decompose the solution to the pseudo problem into $c=0$ and $c \neq 0$ components;
- Express the transform of the desired single-scatter solution in terms of the solution to the pseudo problem, and apply a two-dimensional Fourier inversion;
- Simplify the resulting inversion integral.

Detailed analysis, along the lines described in Reference 4, is required to complete most of these steps. Eventually, we obtain a solution, for the case $\tau_D = \phi_0$, of the form

$$\Phi_{10} = \frac{c}{4\pi} \frac{e^{-a/\mu_0}}{|\rho^*|} [I_1 + I_2 + I_3] \quad (18a)$$

where

$$\rho^* = \rho_D - \frac{a\sqrt{1-\mu_0^2}}{\mu_0} \quad (18b)$$

and the I behave as

$$I \sim \int_{\alpha}^{\beta} \frac{\gamma(\mu) e^{-\rho^* \delta(\mu, \mu_0)}}{\sqrt{1-\mu_0^2}} d\mu \quad (18c)$$

with α , β , δ , and γ assuming different forms for different values of ρ_D , which is here expressed in mfp. For arbitrary τ_D but $\rho_D \cos(\tau_D - \phi_0) > a\sqrt{1-\mu_0^2}/\mu_0$ we obtain the specific form

$$\Phi_{10} = \frac{c}{4\pi} e^{-a/\mu_0} \int_0^{\frac{a}{\sqrt{\rho_D^2 + a^2}}} \exp \left[\frac{t_0 G + u}{t^2 - t_0^2} \left(\frac{1}{\mu_0} - \frac{1}{\mu} \right) \right] \frac{d\mu}{u\mu}, \quad (19a)$$

where

$$t = \frac{\sqrt{1-\mu^2}}{\mu}, \quad (19b)$$

$$t_0 = \frac{\sqrt{1-\mu_0^2}}{\mu_0}, \quad (19c)$$

$$G = \rho_D \cos(\tau_D - \phi_0) - a t_0, \quad (19d)$$

$$u = [t_0^2 (G^2 - \rho_D^2) + (\rho_D t)^2]^{1/2}, \quad (19e)$$

and

$$\rho^* = [\rho_D^2 + (a t_0)^2 - 2 \rho_D a t_0 \cos(\tau_D - \phi_0)]^{1/2}. \quad (19f)$$

We are able to show (see SAMPLE RESULTS) that Equations (17) and (19) give identical numerical results to Equation (9). Since Equation (11) is merely the integral of Equation (9) over those directions that lead to incidence on the slab, this also verifies Equation (11), for the simplified case of monoenergetic transport and isotropic scattering.

MULTIPLE-SCATTER MODEL

We solve the Boltzmann equation for multiple scatters by the Monte Carlo method. A typical history proceeds according to the following steps:

1. Sample source emission angles toward the slab.
2. Sample a track length to the first interaction point and force a scatter; no detector score is required, since this is included in the single scatter model.
3. Sample the type of scatter, the scatter angles, and new energy, E . Except for the case of thermal neutron scattering, we first select the azimuthal angle, ϕ , according to

$$\phi = 2\pi \xi \quad (20)$$

where ξ is an uniform pseudorandom variate taken from the unit interval, and then select the cosine of the scattering angle, using the appropriate probability density function (pdf), and the post-interaction energy. We then update the direction cosines that define the new direction, Ω .

4. Sample a track length to next interaction point.

5. Score the contributions to the flux and dose equivalent at the detector:

For element i and scatter type j , the flux and dose equivalent are estimated, respectively, by

$$\Phi_{ij} = \frac{f_{ij}(\theta_s | E)}{2\pi} \frac{\sigma_{ij}(E)}{\sigma(E)} \frac{e^{-\sigma(E'_{ij})q}}{r^2} \quad (21)$$

and

$$H_{ij} = h_\phi(E'_{ij}) \Phi_{ij} t \quad (22)$$

where

$f_{ij}(\theta_s | E)$ = normalized differential probability to scatter at angle θ_s (angle between incident particle direction and the ray from the interaction point to the detector) at the incident particle energy E ,

E'_{ij} = scattered particle energy,

σ_{ij} = macroscopic cross section for the j^{th} type of interaction in element i ,

σ = slab total macroscopic cross section,

r = distance between interaction point and detector,

q = distance from interaction point to slab exit face towards the detector,

h_ϕ = appropriate flux to dose equivalent conversion factor (for neutrons, the conversion procedure described on p. 616 of Reference 1 was used), and

t = exposure time.

The contributions to the flux and dose equivalent are obtained by summing Φ_{ij} and H_{ij} for all elements and interaction types at each interaction point.

6. Terminate the history if the particle weight is below an input cutoff value, if particle energy is less than a specified value, or if the particle escapes the slab. Otherwise, force a scatter (type and element selected at random), and go to step 3 to determine new direction and energy.
7. Repeat steps 3 through 6 until particle termination, and then start a new history.

After all histories have been completed, the ensemble averages and their estimated standard deviations are determined.

In step 1 the initial particle weight is 0.5, since the polar angle is selected between 0 and $\pi/2$ instead of 0 and π . In steps 2 and 6 the particle weight is adjusted by the ratio of

the total scattering cross section to the total cross section. In sampling track length, there is an option that allows the user to force the particle to interact in the slab. In steps 2 and 3, if this option is selected, the particle weight is adjusted by the factor

$$(1 - e^{-L_{\max} \sigma}) ,$$

where L_{\max} is the maximum track length to escape the slab, i.e., the distance from the interaction point (or entry point) to the slab boundary along the direction of propagation.

For gamma rays the scattering interactions considered are incoherent, using Klein Nishina (KN); coherent (Rayleigh), if requested by the user; and pair production (PP) for photons above 1.25 MeV. In the case of PP, the original photon is replaced by two 0.511 MeV photons in opposite directions, each tracked separately. Cubic splines were fit to tabulated^{5,6} values of gamma-ray cross sections (coherent, incoherent, photoelectric, and pair production) in the energy range from 10 keV to 20 MeV. Plots of the cubic spline fits to the data are given in Reference 7, for most of the elements of interest in this study. The spline coefficients and energies where spline knots are located are stored in a library together with an optional element index (atomic number is used), and keys that indicate whether the energy scale is linear or logarithmic and the resulting cross sections are calculated as linear or logarithmic values. The current library contains 10 elements: H, C, O, Na, Al, Si, K, Ca, Fe, and Pb. There is no limit on the number of element cross sections that can be stored in the library, but these 10 allow the six materials of interest to be analyzed. The Rayleigh (coherent) cross sections for all elements are included in the library. However, a user option is available as an input to the program to suppress Rayleigh interactions.

For neutrons, the code considers both elastic scattering (including thermal elastic scatter) and inelastic scattering (if the neutron energy is above the inelastic threshold energy). Isotropic scatter is used for all energies in the center of mass system.⁸ Tabulated neutron cross sections vs energy were obtained from the ENDF/B-V files for the same 10 elements as in the gamma cross section library. The cross sections for each element were preprocessed in the following way: cross section data points were generated and retabulated to allow linear-linear energy versus cross section interpolation over the energy range available, thus eliminating computationally lengthy logarithmic interpolations. The number of data points in the thermal energy range and the threshold energy for each interaction type available were identified and stored in the element file. Next, the element cross sections were stored in a data library using a simplified data base management program.

The library, structured as shown in Figure 6, is a direct-access file in a binary format. Each record is eight bytes long; the left column shows the contents of the first four bytes and the right, the second four bytes. This structure reduces the required disk storage and minimizes the read time requirements of the program. An efficient binary (half-interval) search is used by the cross section evaluation routine to locate energy-cross

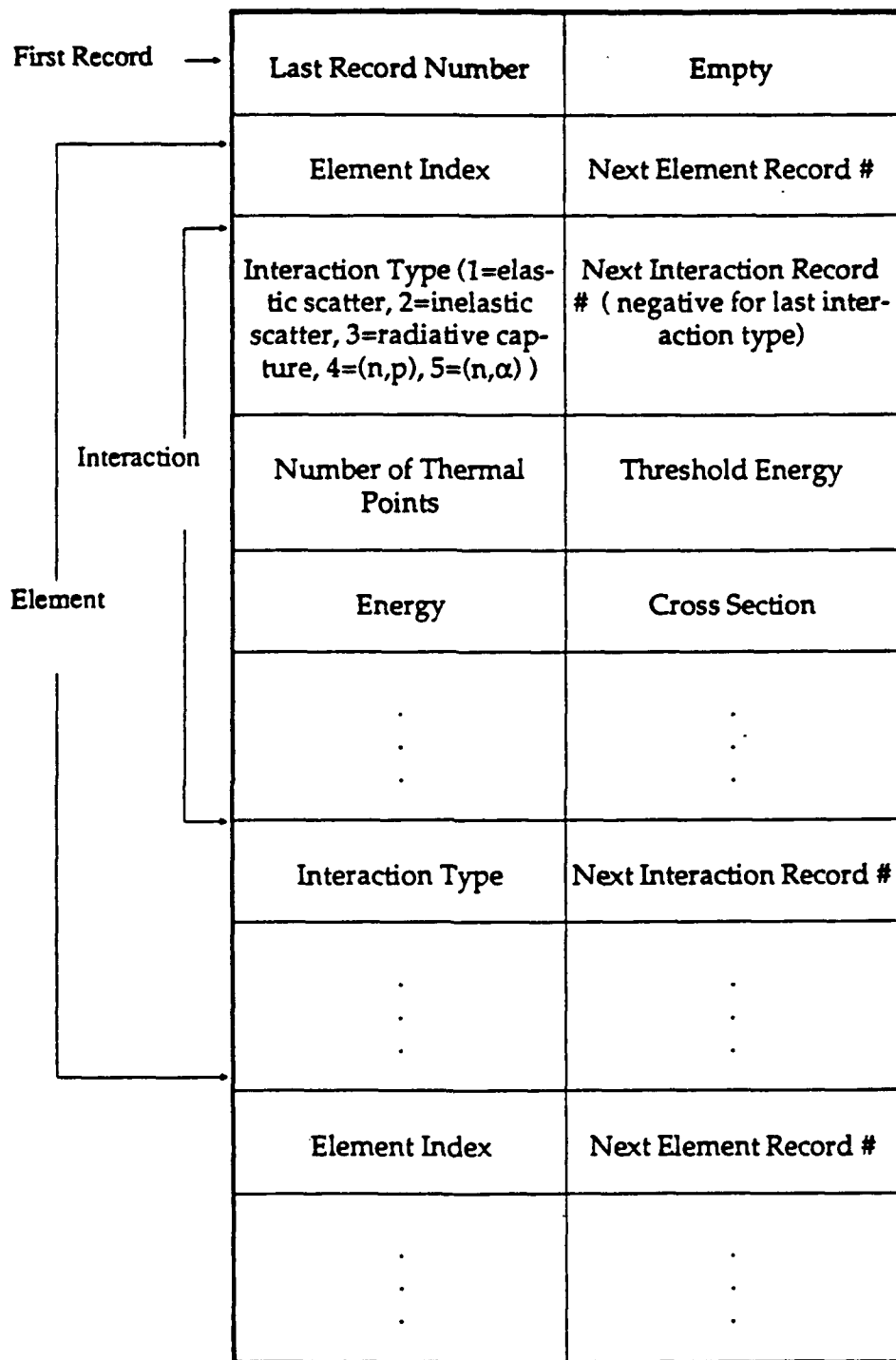


FIGURE 6. NEUTRON CROSS SECTION LIBRARY FILE STRUCTURE

section table entries containing the neutron energy at which interpolation is desired. To reduce table search time, the routine retains the last interval used, recognizing that the neutron energy decreases after a scatter, except in the thermal region.

SAMPLE RESULTS

The single- and multiple-scatter models were coded into two codes: GBAS and NBAS, for gamma-ray and neutron calculations, respectively. The codes were tested, first by generating numerical single-scatter results that were compared with results from the alternative single-scatter models of Equations (9), (17) and (19); excellent agreement was obtained, as shown in Table 1(a). Then, the single-scatter results of Equation (9) were tested against a single-scatter Monte Carlo calculation and an alternative numerical integration along the line of sight (LOS), or path length. Representative results from this comparison are shown in Table 1(b). Both the results using Equation (9) and those for the LOS integration were calculated using a composite Gaussian-Legendre quadrature. The significant reduction in run time (by factors of more than 20) of the quadrature method over Monte Carlo is apparent.

As a further test (that includes the multiple-scatter model), the ratios of scattered and unscattered fluxes to the free-field flux, Φ_f , were compared to results obtained from the MCNP code.⁹ Table 2 compares our flux ratios with those obtained using MCNP for a 5.08-cm thick iron slab for various angles of incidence (β) and various h_D/h_S . Again, the agreement is quite good. With respect to this test, we note that our results were generated using 10,000 histories (requiring less than 5 minutes run time on a Compaq 386/25, each) for all cases except $\cos \beta = 0.1961$, for which 100,000 histories were run (~30 minutes run time). It is also significant that the results appear to be relatively insensitive to the ratio h_D/h_S .

A further comparison was made with MCNP, comparing flux values directly, as shown below. The difference between the uncollided fluxes is due to minor differences in the photon cross sections used in the two codes. In these cases, coherent scattering was ignored.

	Total flux ($\text{cm}^{-2} \cdot \text{sec}^{-1}$)	Uncollided flux ($\text{cm}^{-2} \cdot \text{sec}^{-1}$)
MCNP (40,000 histories)*	1.1477×10^{-5}	3.037×10^{-6}
GBAS (10,000 histories)	1.1465×10^{-5}	3.059×10^{-6}

* Results supplied by C. Eisenhauer

The buildup factor calculation was checked by generating infinite-medium buildup factors and comparing with the ANS-6.4.3 Standard reference data of Trubey;¹⁰ typical results for iron are shown in Table 3.

TABLE 1. NUMERICAL COMPARISON OF THE SINGLE-SCATTER MODEL OF EQUATION (9) WITH INDEPENDENT RESULTS, FOR $c = 0.8$

 (a) Sample results for the case $a=1.0$ mfp, $h_s=h_D=0$, and $\mu_0=0.8$

$\tau_D=\phi_0$		Flux ($\text{cm}^{-2}\text{-sec}^{-1}$)		
ρ_D (mfp)	Equation (17)	Equations (19)	Equation (9)	
1.0	4.66690×10^{-2}	4.66690×10^{-2}	4.66690×10^{-2}	
2.0	2.22640×10^{-3}	2.22640×10^{-3}	2.22640×10^{-3}	
3.0	3.28221×10^{-4}	3.28221×10^{-4}	3.28221×10^{-4}	
4.0	6.49572×10^{-5}	6.49572×10^{-5}	6.49572×10^{-5}	

 $\tau_D-\phi_0=0.5$ radians

ρ_D (mfp)	Equations (19)	Equation (9)
1.0	2.31557×10^{-2}	2.31557×10^{-2}
5.0	1.38827×10^{-5}	1.38827×10^{-5}

 (b) Sample single-scatter results for the case $T=2.54$ cm, $h_s=2.54$ cm, $\rho_D=0$, $h_D=2.54$ cm

Energy (MeV)	Equation (9)		Numerical LOS Integration		Monte Carlo	
	Flux ($\text{cm}^{-2}\text{-sec}^{-1}$)	CPU (sec)	Flux ($\text{cm}^{-2}\text{-sec}^{-1}$)	CPU (sec)	Flux ($\text{cm}^{-2}\text{-sec}^{-1}$)	CPU (sec)
0.05	0.10426×10^{-5}	4.17	0.10426×10^{-5}	2.74	0.10705×10^{-5}	125.23
0.1	0.10395×10^{-3}	4.29	0.10395×10^{-3}	2.80	0.10388×10^{-3}	127.75
1.0	0.13861×10^{-3}	4.56	0.13861×10^{-3}	3.00	0.13845×10^{-3}	134.02
10.0	0.75513×10^{-4}	5.00	0.75296×10^{-4}	3.35	0.75108×10^{-4}	141.98
20.0	0.78980×10^{-4}	5.05	0.78704×10^{-4}	3.41	0.78530×10^{-4}	142.15

TABLE 2. COMPARISON OF FLUX RATIOS FOR 1.25-MEV GAMMA RAYS AND A 5.08-CM IRON SLAB

h_D/h_s ($h_s=101.6$ cm)	$\cos \beta$	Flux ratio Φ/Φ_f					
		Scattered		Uncollided		Total	
		GBAS	MCNP*	GBAS	MCNP*	GBAS	MCNP*
1	1.000	0.3257	0.3324	0.1200	0.1192	0.4457	0.4516
	0.7071	0.1943	0.2034	0.0499	0.0494	0.2441	0.2528
	0.4472	0.0761	0.0786	0.0087	0.0086	0.0848	0.0872
	0.1961	0.0161	0.0150	0.0000	0.0000	0.0161	0.0150
2	1.000	0.3285	0.3292	0.1200	0.1192	0.4485	0.4484
	0.7071	0.1934	0.1870	0.0499	0.0494	0.2433	0.2364
	0.4472	0.0781	0.0752	0.0087	0.0086	0.0868	0.0838
	0.1961	0.0172	0.0239	0.0000	0.0000	0.0172	0.0239
3	1.000	0.3278	0.3363	0.1200	0.1192	0.4478	0.4555
	0.7071	0.1879	0.1850	0.0499	0.0494	0.2388	0.2343
	0.4472	0.0781	0.0758	0.0087	0.0086	0.0868	0.0844
	0.1961	0.0191	0.0222	0.0000	0.0000	0.0191	0.0222

* Results supplied by C. Eisenhauer

TABLE 3. SAMPLE RESULTS FOR INFINITE-MEDIUM GAMMA-RAY ENERGY ABSORPTION BUILDUP FACTORS IN IRON

(a) Photon energy = 0.5 MeV

Source-detector distance (mfp)	B_1 Equation (11)	B_1 (MC)	B	ANS-6.4.3 ¹⁰
0.5	1.428	1.424	1.676± 2%	1.79
1.0	1.701	1.625	2.536± 6%	2.66
2.0	2.106	2.020	4.258± 8%	4.57
4.0	2.659	2.530	8.267±17%	9.25

(b) Photon energy = 4.0 MeV

Source-detector distance (mfp)	B_1 Equation (11)	B_1 (MC)	B	ANS-6.4.3 ¹⁰
0.5	1.182	1.157	1.226± 2%	1.31
1.0	1.316	1.247	1.546± 5%	1.59
2.0	1.532	1.415	1.784± 6%	2.12
4.0	1.891	1.833	2.784±15%	3.27

The NBAS code transport model is identical to that in the GBAS code, except for the treatment of scattering laws, cross sections, and flux-to-dose conversion. Following thorough individual tests of these items, the NBAS code was compared with MCNP for neutrons (^{252}Cf source) incident on polyethylene slabs; a representative comparison of scattered and uncollided flux and dose ratios (with respect to free-field values) follows, for the case $h_D/h_s=1.0$ and $\rho_D=0$:

T (cm)	Φ_s/Φ_f		Φ_0/Φ_f		D_s/D_f		D_0/D_f	
	NBAS	MCNP*	NBAS	MCNP*	NBAS	MCNP*	NBAS	MCNP*
1.27	0.457	0.476	0.604	0.599	0.266	0.237	0.637	0.640
2.54	0.648	0.671	0.399	0.379	0.356	0.314	0.435	0.420
5.08	0.588	0.593	0.167	0.167	0.329	0.291	0.190	0.193

* Results supplied by C. Eisenhauer

This comparison and the previous series of tests conclusively demonstrate the accuracy and efficiency of the GBAS and NBAS codes.

The GBAS and NBAS codes, which are documented in Appendix A, were used to generate buildup factors for various source-slab-detector configurations, various source energies, and all six of the materials of interest. The assumed densities and compositions of the six materials are described in Table 4. The configuration geometry is depicted in Figure 7, and Table 5 identifies the first four specific configurations that were considered. All distances (such as h_s , ρ_D , z_D , and a) were expressed in mfp of the slab material at the source energy. Since calculated photon buildup factors depend on the cross section data base used, we present in Table 6 the calculated total cross sections for all six materials at all the source energies considered.

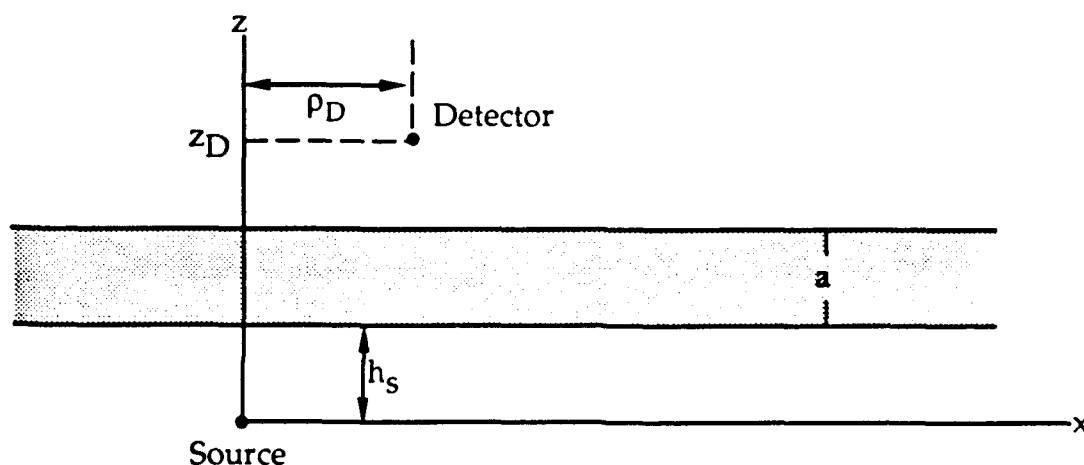


FIGURE 7. THE VARIABLES DEFINING SPECIFIC CONFIGURATIONS

TABLE 4. THE SIX MATERIALS AND THEIR DENSITIES AND ELEMENTAL COMPOSITIONS

Material	Density (gm/cc)	Element	Z _i	Weight fraction w _i
Aluminum	2.694	Al	13	1.0
Iron	7.86	Fe	26	1.0
Lead	11.33	Pb	82	1.0
Water	1.0	H	1	0.11190
		O	8	0.88810
Polyethylene	0.95	H	1	0.14380
		C	6	0.85620
Concrete	2.3	H	1	0.00562
		O	8	0.50010
		Na	11	0.01716
		Al	13	0.04577
		Si	14	0.31694
		K	19	0.01927
		Ca	20	0.08290
		Fe	26	0.01224

TABLE 5. THE INITIAL FOUR BUILDUP FACTOR CONFIGURATIONS

Geometry	h _s	ρ _D	z _D
A	0	0	a
B	0	0	2a
C	a	0	2a
D	0	a	a

TABLE 6. CALCULATED TOTAL CROSS SECTIONS FOR THE SIX MATERIALS

E_0 (MeV)	Aluminum	Iron	Lead	Water	Polyethylene	Concrete
(a) Gamma Ray						
0.10	0.4354	2.700	59.39	0.1672	0.1614	0.3914
0.15	0.3605	1.446	21.41	0.1488		
0.20	0.3236	1.092	10.66	0.1362	0.1328	0.2876
0.30	0.2788	0.8398	4.338	0.1185		
0.40	0.2493	0.7264	2.509	0.1063	0.1038	0.2210
0.50	0.2273	0.6537	1.746	0.09701		
0.60	0.2100	0.6001	0.1352	0.08969	0.08760	0.1862
0.80	0.1841	0.5230	0.9647	0.07866	0.07683	0.1632
1.0	0.1652	0.4682	0.7756	0.07061	0.06896	0.1465
1.5	0.1344	0.3814	0.5761	0.05735		
2.0	0.1160	0.3332	0.5118	0.04920		
3.0	0.09507	0.2836	0.4750	0.03956	0.03832	0.08367
4.0	0.08352	0.2595	0.4721	0.03397		
5.0	0.07633	0.2469	0.4813	0.03030	0.02891	0.06659
6.0	0.07156	0.2402	0.4961	0.02772		
7.0	0.06821	0.2369	0.5129	0.02581	0.02424	0.05892
(b) Neutron						
10^{-7}	0.08870	1.075	0.3794	34.60	34.67	34.68
10^{-5}	0.08176	0.9772	0.3753	1.501	1.873	0.3734
10^{-3}	0.08109	0.9772	0.3750	1.484	1.853	0.3711
0.1	0.2998	0.3219	0.3338	0.9731	1.222	0.2965
1.0	0.1424	0.3649	0.1469	0.5605	0.4544	0.4731
10.0	0.1035	0.2650	0.1327	0.1081	0.1251	0.1104
14.0	0.1018	0.2395	0.1092	0.1001	0.1101	0.1130

Single-scatter and total buildup factors for geometries A, B, C, and D are tabulated in Appendix B for gamma rays and in Appendix C for neutrons. For consistency of presentation, we show four significant figures in all our tables, even though we know that some of the results are not that accurate. (In general, the single-scatter factors are more accurate than the total.) We have also employed the convention of aligning the decimal points in each column so that order-of-magnitude changes are easy to detect. We note that in all geometries, the buildup factors are presented as functions of thickness of the slab along the LOS between source and detector. In Geometries A, B, and C, this is the same as slab thickness; in Geometry D, the slab thickness is $1/\sqrt{2}$ times the LOS thickness.

Table 7 gives the gamma-ray buildup factors for aluminum in geometry A, as an illustration. It can be seen that the single-scatter contribution to the total buildup factor is generally rather significant and, in some cases, is well above 90%. Table 8 gives neutron buildup factors for aluminum in geometry A. The single-scatter component for neutrons is typically a smaller fraction of the total than for gamma rays, although at 14 MeV, the single-scatter buildup factors are >40% of the total for slab thicknesses ≤ 2 mfp.

TABLE 7. GAMMA-RAY BUILDUP FACTORS FOR ALUMINUM, GEOMETRY A
 $(h_s = 0, \rho_D = 0, z_D = a)$

(a) Single-scatter

Thickness, a (mfp)	0.5	1.0	2.0	3.0	4.0	5.0	6.0	7.0
Energy (Mev)								
0.10	1.356	1.614	2.005	2.304	2.548	2.753	2.930	3.085
0.15	1.361	1.635	2.064	2.400	2.678	2.915	3.121	3.303
0.20	1.353	1.628	2.064	2.408	2.695	2.941	3.155	3.344
0.30	1.337	1.605	2.033	2.374	2.659	2.902	3.115	3.303
0.40	1.323	1.582	1.998	2.328	2.603	2.839	3.045	3.227
0.50	1.312	1.563	1.964	2.283	2.549	2.775	2.973	3.148
0.60	1.303	1.546	1.935	2.242	2.498	2.716	2.906	3.074
0.80	1.288	1.518	1.884	2.172	2.411	2.614	2.791	2.947
1.0	1.277	1.496	1.844	2.115	2.340	2.530	2.696	2.843
1.5	1.256	1.457	1.770	2.012	2.212	2.382	2.529	2.660
2.0	1.241	1.428	1.716	1.940	2.123	2.280	2.416	2.537
3.0	1.216	1.381	1.635	1.832	1.996	2.135	2.257	2.365
4.0	1.196	1.344	1.572	1.752	1.901	2.029	2.141	2.241
5.0	1.179	1.312	1.521	1.687	1.826	1.946	2.051	2.146
6.0	1.163	1.285	1.478	1.633	1.764	1.877	1.978	2.068
7.0	1.150	1.262	1.441	1.587	1.710	1.819	1.915	2.002

(b) Total

Energy (Mev)								
0.10	1.492	2.075	3.393	4.994	6.275	8.262	9.846	12.44
0.15	1.496	2.105	3.685	5.685	8.253	10.55	15.69	17.31
0.20	1.480	2.088	3.639	5.902	8.207	11.16	15.50	17.81
0.30	1.452	2.019	3.514	5.365	8.000	15.31	13.15	16.36
0.40	1.426	1.966	3.392	5.421	7.756	9.416	17.45	17.18
0.50	1.412	1.946	3.145	4.936	7.059	9.866	11.18	12.38
0.60	1.397	1.888	3.119	5.241	6.555	8.012	17.00	13.02
0.80	1.373	1.825	2.967	4.392	6.244	7.213	8.583	9.417
1.0	1.355	1.781	2.814	5.111	5.475	6.774	8.698	8.012
1.5	1.332	1.695	2.614	3.405	4.188	4.683	5.527	6.183
2.0	1.312	1.653	2.408	3.209	4.308	4.816	5.710	6.041
3.0	1.289	1.565	2.193	2.866	3.353	4.011	4.808	4.783
4.0	1.262	1.521	2.078	2.528	2.958	3.148	3.345	3.797
5.0	1.231	1.450	1.994	2.349	2.801	2.942	3.496	3.312
6.0	1.211	1.418	1.856	2.225	2.627	2.686	3.014	3.640
7.0	1.196	1.403	1.743	2.103	2.338	2.427	2.829	2.912

TABLE 8. NEUTRON BUILDUP FACTORS FOR ALUMINUM, GEOMETRY A
($h_s = 0$, $\rho_D = 0$, $z_D = a$)

(a) Single-scatter

Thickness, a (mfp)	0.5	1.0	2.0	3.0	4.0	5.0	6.0	7.0
Energy (Mev)								
10^{-7}	1.427	1.723	2.139	2.432	2.655	2.833	3.003	3.128
10^{-5}	1.465	1.788	2.242	2.562	2.806	3.002	3.163	3.299
10^{-3}	1.456	1.775	2.225	2.544	2.788	2.984	3.146	3.283
0.1	1.327	1.478	1.651	1.752	1.819	1.866	1.901	1.926
1.0	1.407	1.649	1.924	2.060	2.132	2.172	2.196	2.213
10.0	1.355	1.572	1.833	1.989	2.093	2.168	2.224	2.268
14.0	1.299	1.487	1.722	1.867	1.967	2.041	2.097	2.141

(b) Total

Energy (Mev)								
10^{-7}	1.647	2.550	5.458	12.43	25.61	39.58	96.60	146.3
10^{-5}	1.736	2.832	7.903	18.97	43.43	103.6	257.6	490.6
10^{-3}	1.708	2.810	6.860	15.39	36.08	75.05	148.6	304.9
0.1	1.819	3.146	8.125	20.29	51.50	128.9	363.1	990.5
1.0	1.693	2.697	6.154	12.79	25.85	44.13	72.35	125.4
10.0	1.571	2.395	5.268	10.87	18.67	27.05	38.76	134.8
14.0	1.462	2.065	4.121	7.118	11.03	17.30	35.20	49.26

CHAPTER 4

SIMPLIFIED MODEL RESULTS

Geometry A was taken as the basic geometry, and so the calculated buildup factors of Tables B-1 through B-6 in Appendix B and Tables C-1 through C-6 in Appendix C were fit to simplified parametric models, as functions of slab thickness for each material and each source energy. Then, the effects of source and detector axial offset ($h_s > 0$, $h_D > 0$) and detector radial offset ($\rho_D > 0$) were studied by comparison of the geometry A results with the results of calculations for Geometries B-D and with other single-scatter results.

Consistent with this approach, we first express the buildup factor for material M in the form

$$B = G_M(a) g_M(S|a) \quad (23)$$

where M is a material designator (A for aluminum, I for iron, and so on); a is slab thickness, in mfp at the source energy, E_0 , in material M; $G_M(a)$ is a simplified model for the buildup factor of geometry A; $g_M(S|a)$ is a correction factor, to adjust the model for axial offset effects; S is total distance between source and detector points expressed as multiples of slab thickness; and the parameters of G_M and g_M are functions of E_0 . Note that for this model, $G_M(0) = g_M(1|a) = 1$.

Our model-fitting procedure then consists of the following three steps:

- Fit models for $G_M(a)$ to the total buildup factor data, for Geometry A.
- Construct a correction factor, g_M , that adjusts the model for source-detector separation effects.
- Construct a procedure to average the model over arbitrary source spectra.

MODEL FITTING PROCEDURE

In Equation (23), G_M is dependent on a set of parameters, i.e.,

$$G_M(a) = G_M(a|\lambda) \quad (24)$$

where λ is a vector of the model parameters; thus, if there are p model parameters, λ is a p -vector. The solution for the unknown parameters λ can be obtained by the weighted least-squares approach. A computer code, ABFIT, was constructed for this purpose; it is an adaptation of the FITIT code of Dunn and Dunn¹¹, which was based on the CURFIT code of Bevington¹². It is designed to find a minimum of the weighted least-squares function

$$E^2(\lambda) = \frac{1}{v} \sum_{k=1}^K [B_k - G_M(a_k | \lambda)]^2 W_k \quad (25)$$

where K is the number of data points (in this case, slab thicknesses), v is the number of degrees of freedom,

$$v = K - p, \quad (26)$$

$B_k = B(E_0, a_k)$, and W_k is a weight for the k^{th} data point. We note that if $W_k = 1/\sigma_k^2$, with σ_k^2 the variance of B_k , then $E^2 = \chi^2_v$, the reduced chi-square statistic. The code allows constraints to be imposed on any of the model parameters. The model parameters may be linear, nonlinear, or mixed (i.e., some of each). The vector λ is ordered so that the first q elements are the nonlinear parameters and the last $p-q$ elements are the linear parameters.

For each material and E_0 , the fitting procedure involves first inputting the k data pairs (a_k, B_{Mk}) and initial estimates of the nonlinear parameter values. Then, the linear parameters are found by matrix inversion, using the input values for the nonlinear parameters. Next, the constraints are checked, any necessary adjustments made, and a value of E^2 is computed. Then, the nonlinear parameters are incremented according to a modified gradient search algorithm, the constraints are satisfied, and a new E^2 is determined. If this E^2 is smaller than the first, the nonlinear parameters are updated and the entire process is repeated; if not, the step size is adjusted and a new set of nonlinear parameters is obtained. This establishes an iterative procedure that is terminated when the relative difference between successive E^2 values is less than a specified tolerance, or when a specified number of iterations is exceeded. Once the search is completed, a final iteration is carried out, treating all parameters as nonlinear, in order to estimate the uncertainties in the obtained values of the parameters. This is a very useful device, since it can be used to indicate the validity of the model. If the uncertainties are relatively small, the selected model is probably a good one; if, on the other hand, the uncertainties are large (say $> 50\%$), then consideration should be given to trying a model having a different form.

MODELS AS FUNCTIONS OF SOURCE ENERGY

We tried various forms for G and found that the model

$$G_M(a) = e^{\alpha(E_0)} [1 - e^{-\beta(E_0)a}] \quad (27)$$

has the following desirable features:

- it goes to unity as a goes to zero;
- it is monotonically increasing and well behaved;
- it is simple, having only two parameters, α and β ;
- it asymptotically approaches a constant, $e^{\alpha(E_0)}$, as $a \rightarrow \infty$
- it fits the data fairly well for all materials and all source energies.

By fitting to the logarithm of the buildup factor, this model can be considered to be linear in α and nonlinear in β ; thus, for the ABFIT code, $p=2$, $q=1$ and the vector of parameters is

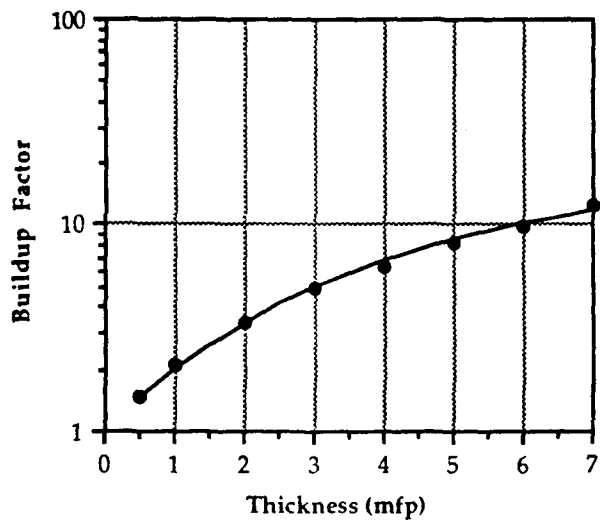
$$\lambda = (\beta, \alpha) \quad (28)$$

We used the procedure described in the previous section to fit the model of Equation (27) to the buildup factor data of Tables B-1 through B-6 in Appendix B and C-1 through C-6 in Appendix C. Results at four source energies are plotted for each of the six materials in Figures 8-13 for gamma rays and in Figures 14-19 for neutrons. The calculated model constants for all the materials and energies are tabulated in Tables 9-14 for gamma rays and in Tables 15-20 for neutrons.

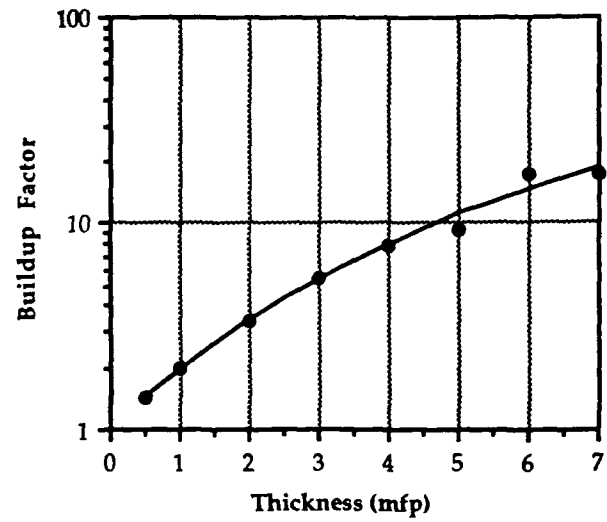
Thus, the buildup factor model is given by

$$B(E_0) = e^{\alpha(E_0)} [1 - e^{-\beta(E_0)a}] g_M(S|a) \quad (29)$$

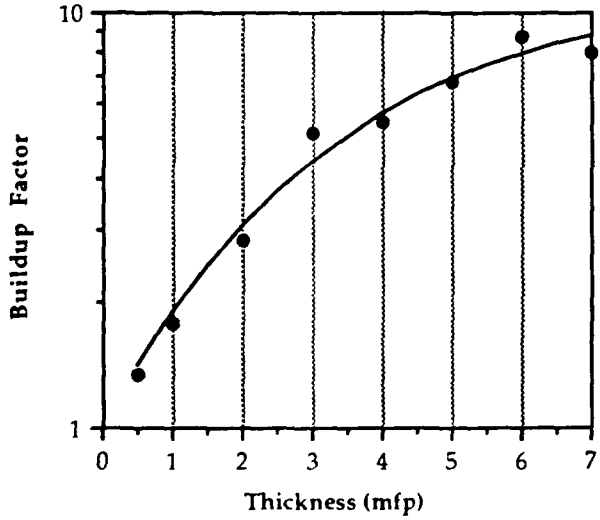
where E_0 is source energy, a is slab thickness in mfp at the source energy, α and β are model constants that depend on the specific material in the slab, S is the total source-detector separation, and g_M is a correction factor (see Chapter 6).



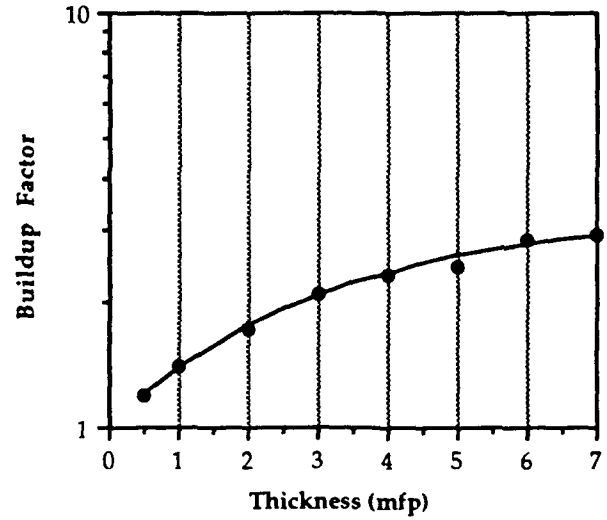
(a) $E_0 = 0.1$ MeV



(b) $E_0 = 0.4$ MeV

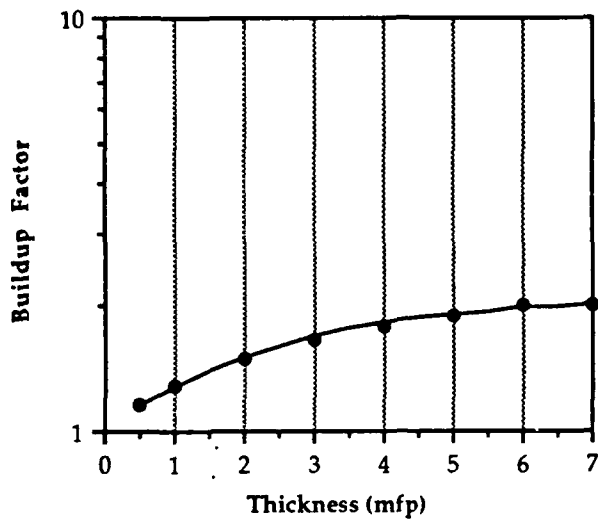


(c) $E_0 = 1.0$ MeV

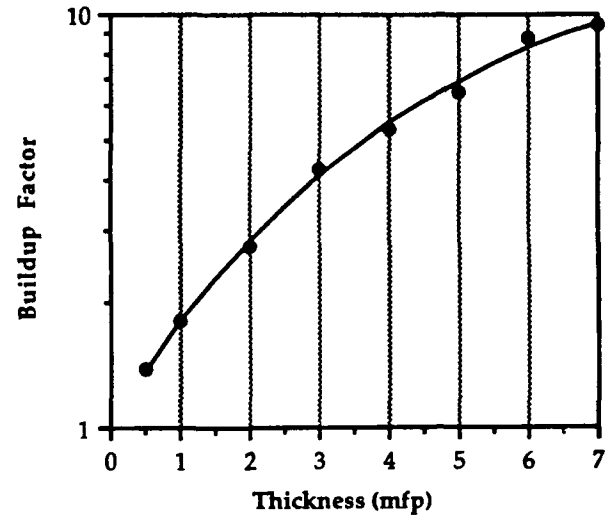


(d) $E_0 = 7.0$ MeV

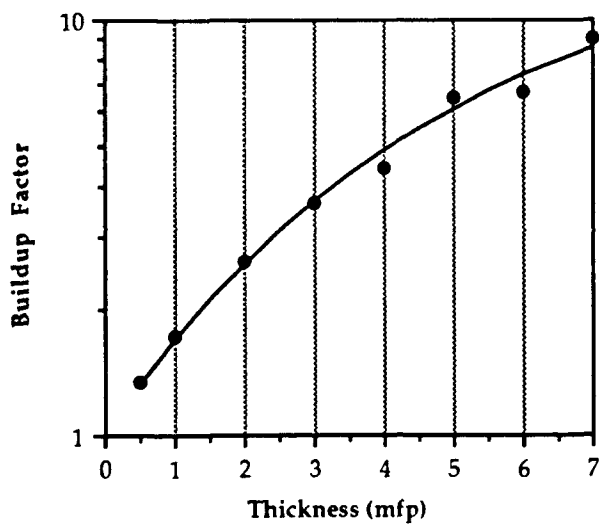
FIGURE 8. MODEL FITS TO GAMMA-RAY BUILDUP FACTOR DATA FOR ALUMINUM, GEOMETRY A



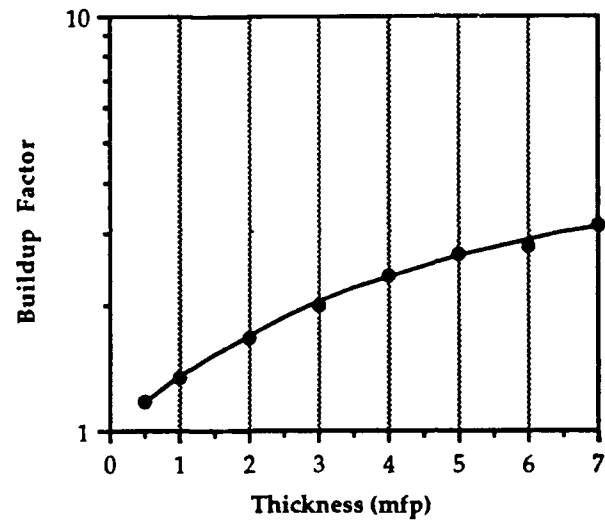
(a) $E_0 = 0.1$ MeV



(b) $E_0 = 0.4$ MeV

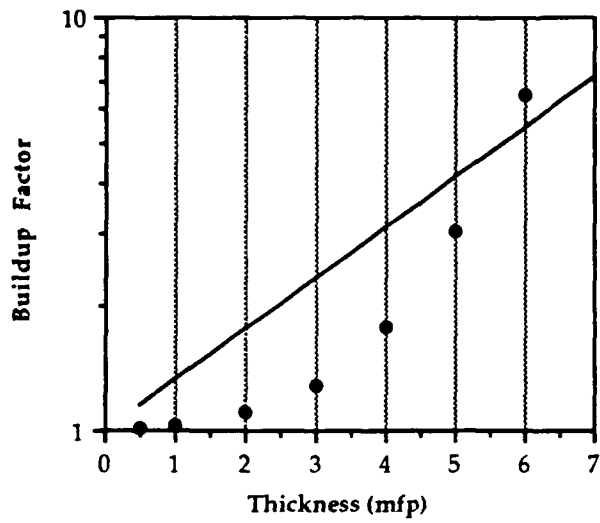


(c) $E_0 = 1.0$ MeV

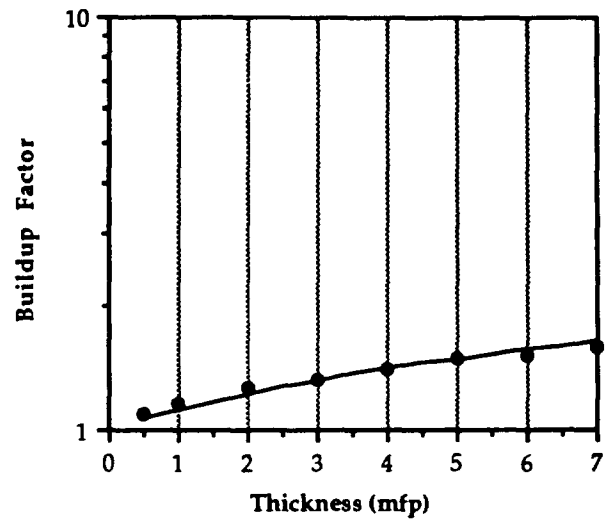


(d) $E_0 = 7.0$ MeV

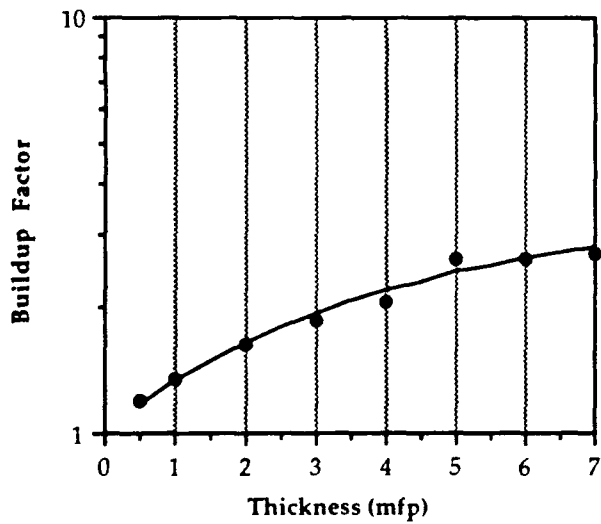
FIGURE 9. MODEL FITS TO GAMMA-RAY BUILDUP FACTOR DATA FOR IRON, GEOMETRY A



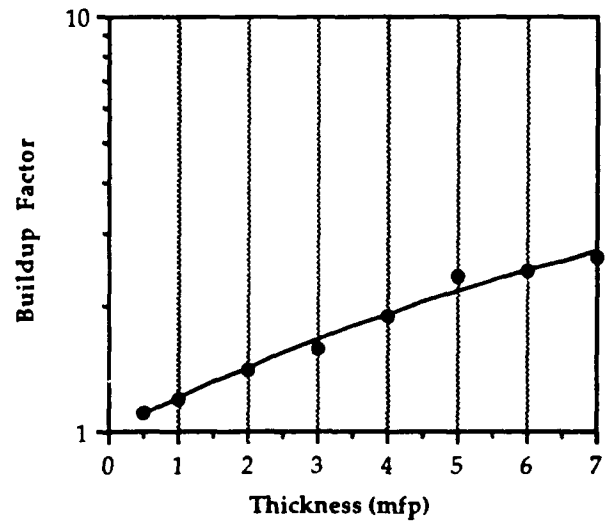
(a) $E_0 = 0.1$ MeV



(b) $E_0 = 0.4$ MeV

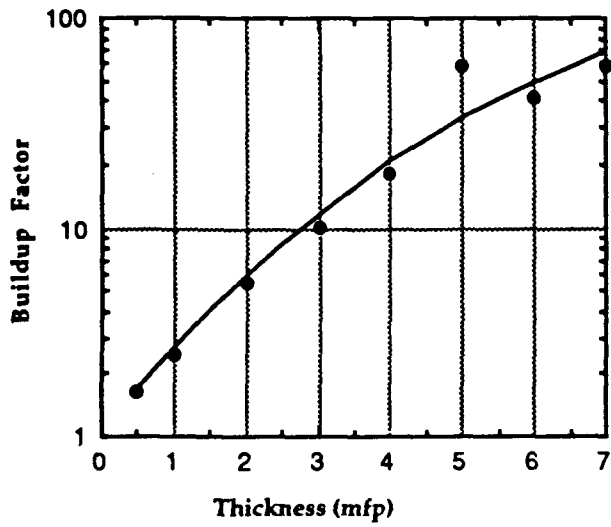


(c) $E_0 = 1.0$ MeV

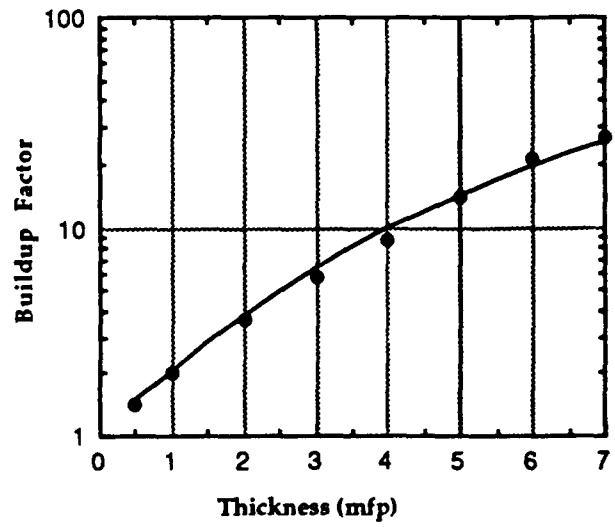


(d) $E_0 = 7.0$ MeV

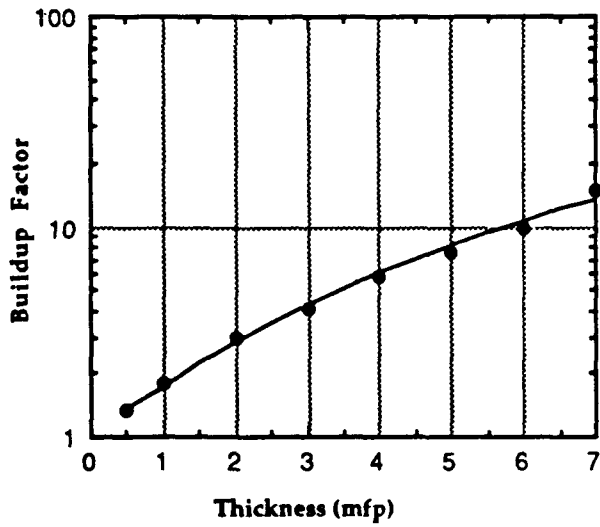
FIGURE 10. MODEL FITS TO GAMMA-RAY BUILDUP FACTOR DATA FOR LEAD, GEOMETRY A



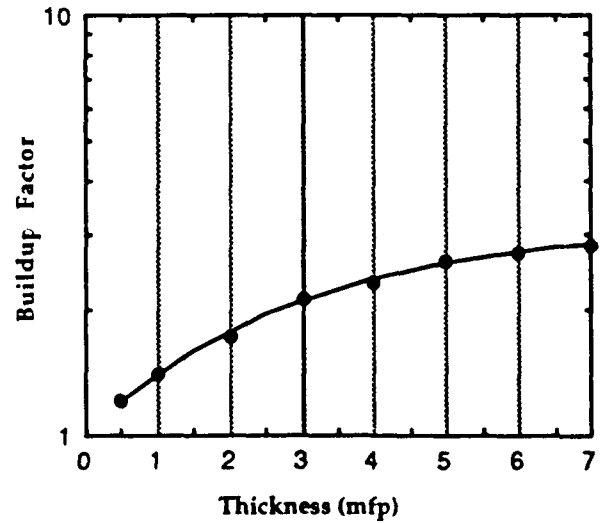
(a) $E_0 = 0.1$ MeV



(b) $E_0 = 0.4$ MeV

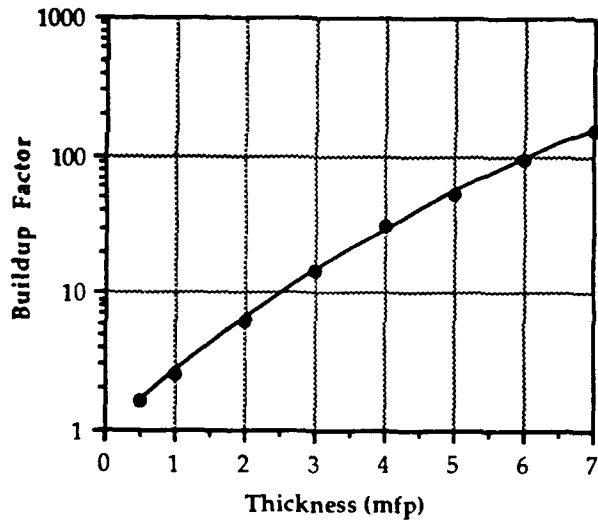


(c) $E_0 = 1.0$ MeV

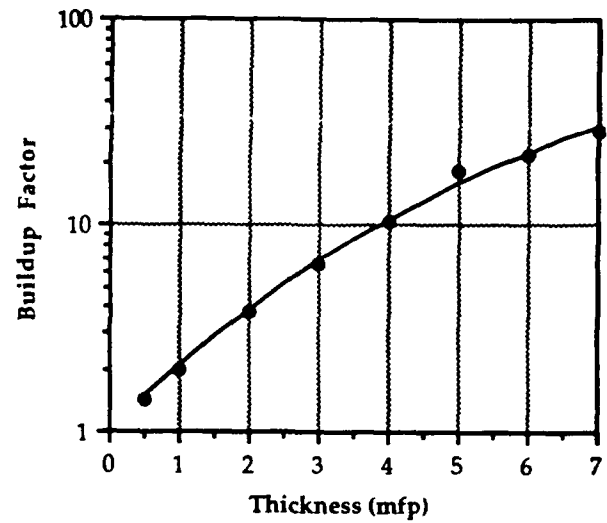


(d) $E_0 = 7.0$ MeV

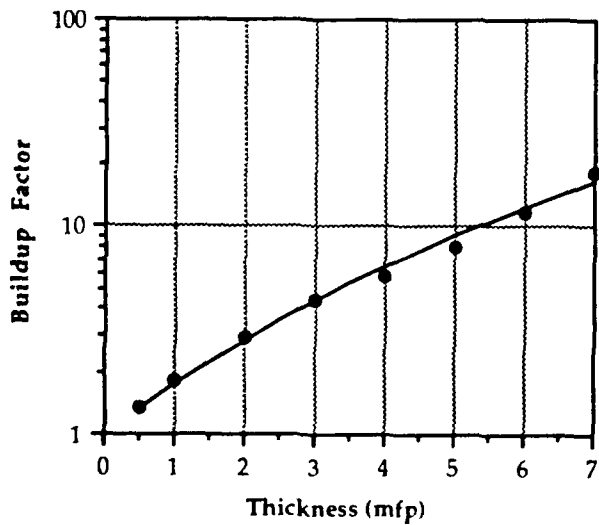
FIGURE 11. MODEL FITS TO GAMMA-RAY BUILDUP FACTOR DATA FOR WATER, GEOMETRY A



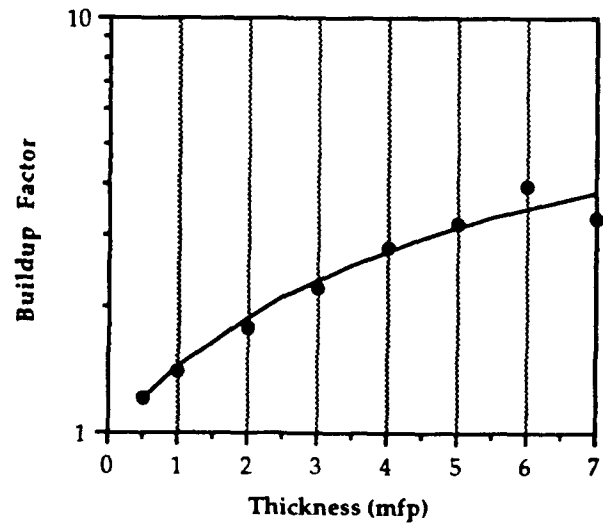
(a) $E_0 = 0.1$ MeV



(b) $E_0 = 0.4$ MeV

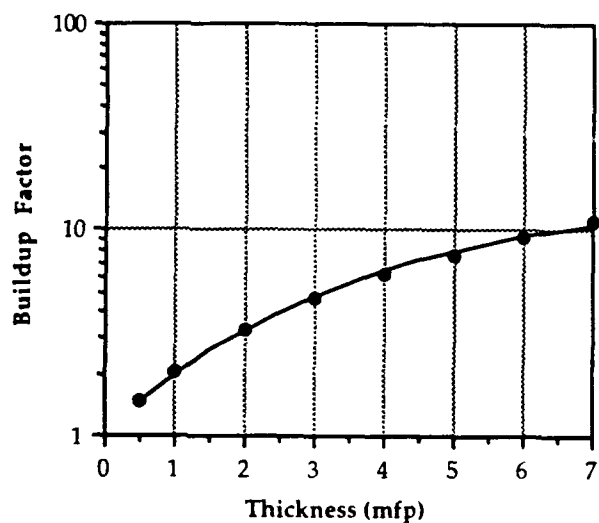


(c) $E_0 = 1.0$ MeV

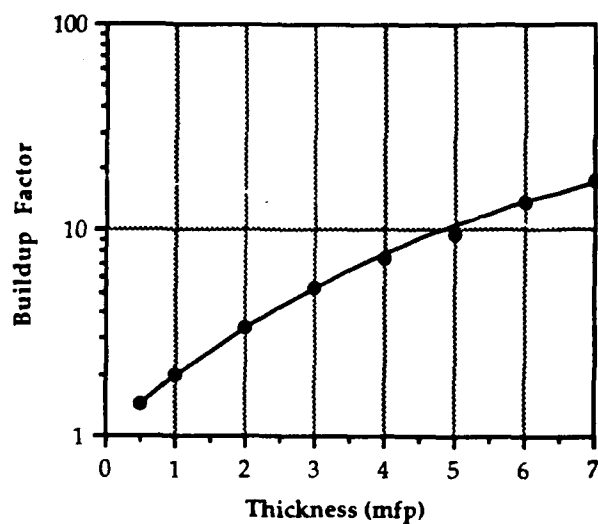


(d) $E_0 = 7.0$ MeV

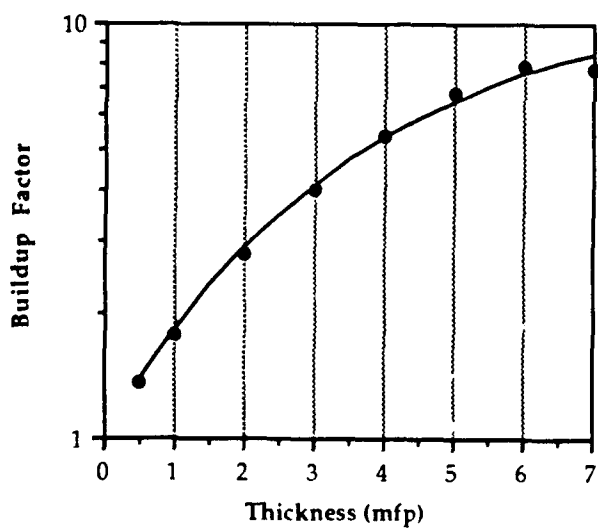
FIGURE 12. MODEL FITS TO GAMMA-RAY BUILDUP FACTOR DATA FOR POLYETHYLENE, GEOMETRY A



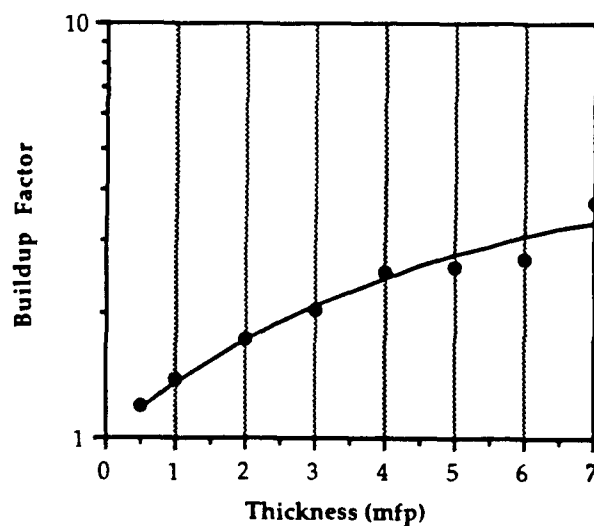
(a) $E_0 = 0.1$ MeV



(b) $E_0 = 0.4$ MeV

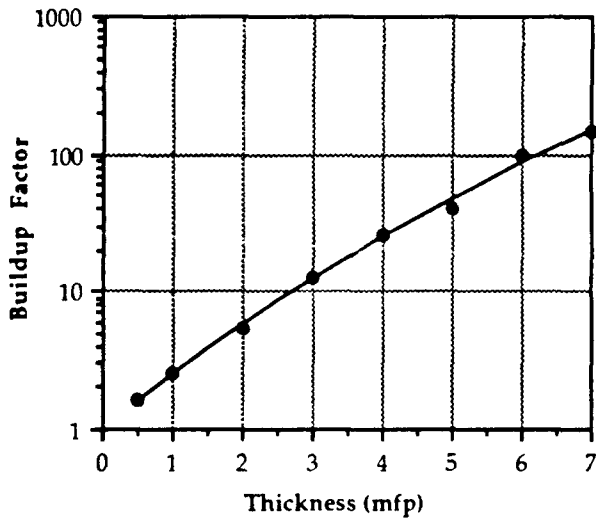


(c) $E_0 = 1.0$ MeV

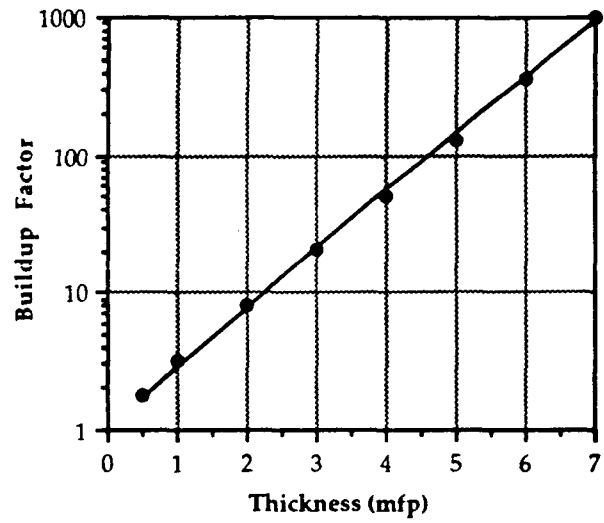


(d) $E_0 = 7.0$ MeV

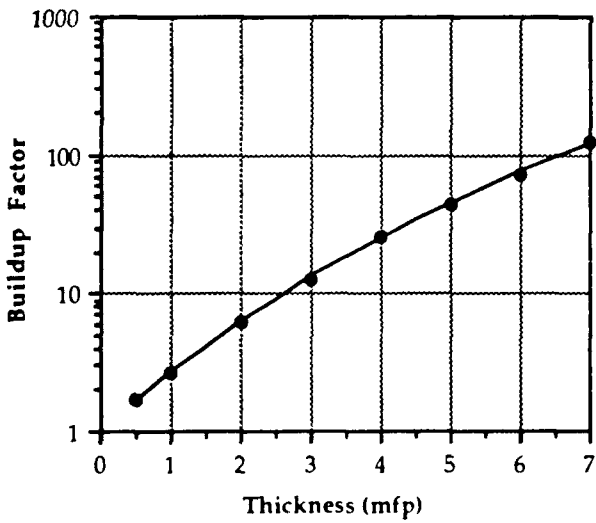
FIGURE 13. MODEL FITS TO GAMMA-RAY BUILDUP FACTOR DATA FOR CONCRETE, GEOMETRY A



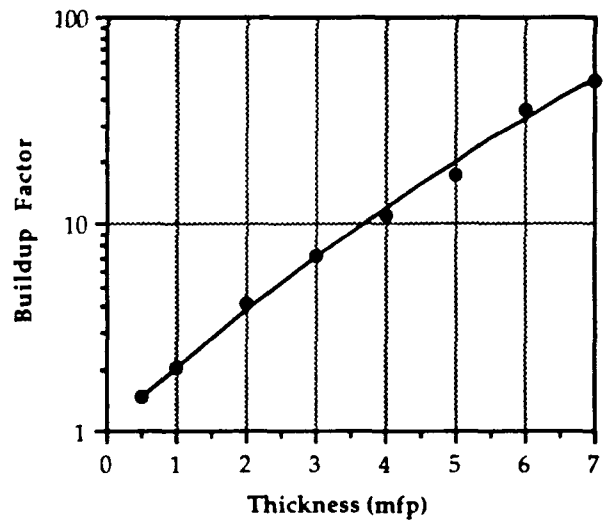
(a) $E_0 = 10^{-7}$ MeV



(b) $E_0 = 0.1$ MeV

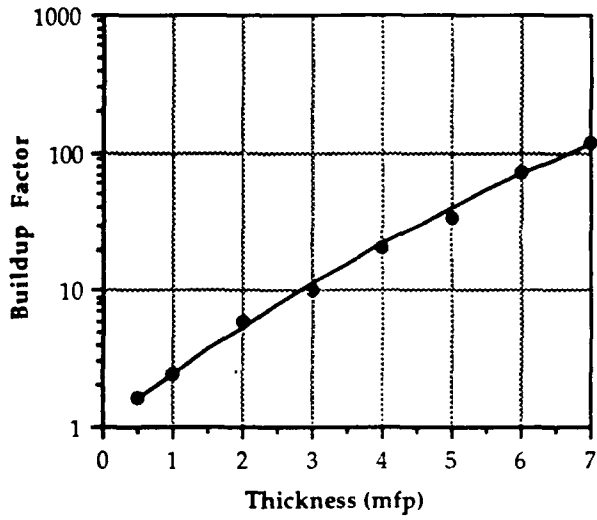


(c) $E_0 = 1.0$ MeV

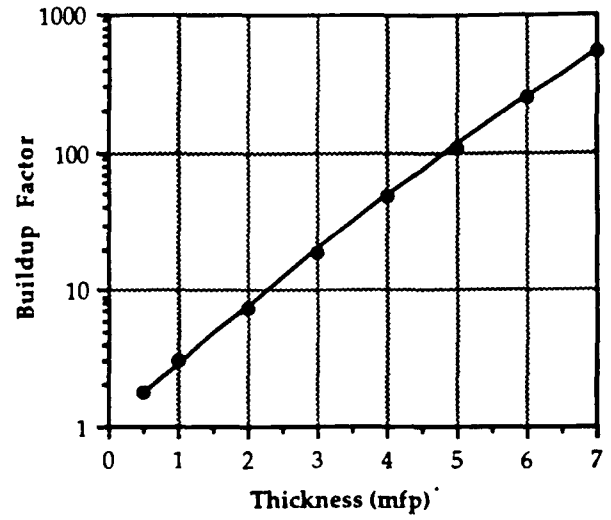


(d) $E_0 = 14$ MeV

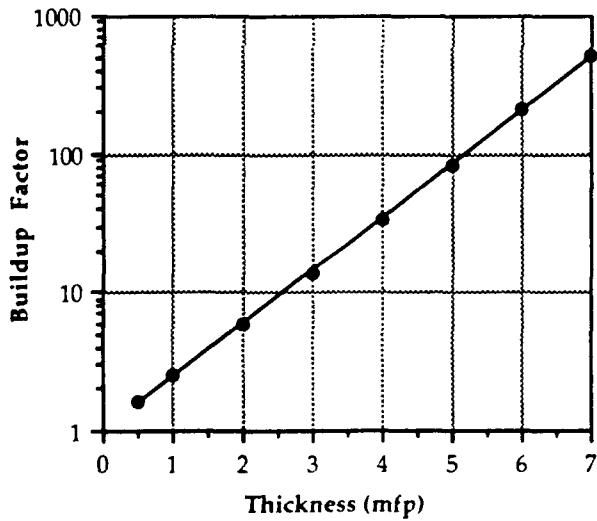
FIGURE 14. MODEL FITS TO NEUTRON BUILDUP FACTOR DATA FOR ALUMINUM, GEOMETRY A



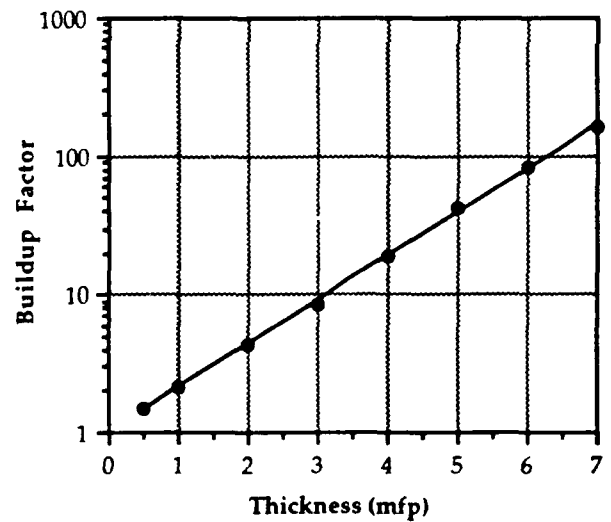
(a) $E_0 = 10^{-7}$ MeV



(b) $E_0 = 0.1$ MeV

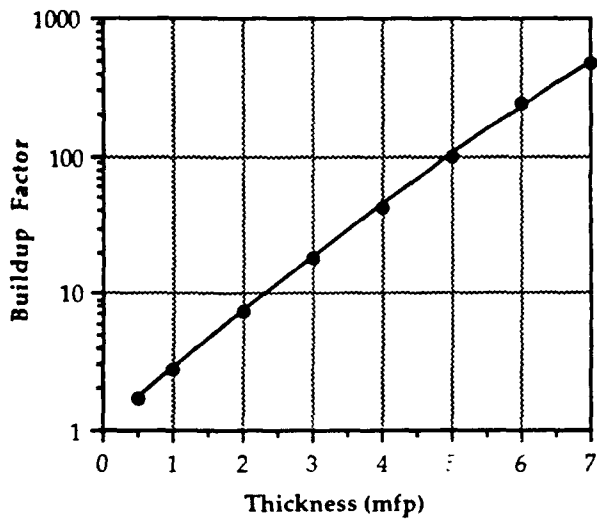


(c) $E_0 = 1.0$ MeV

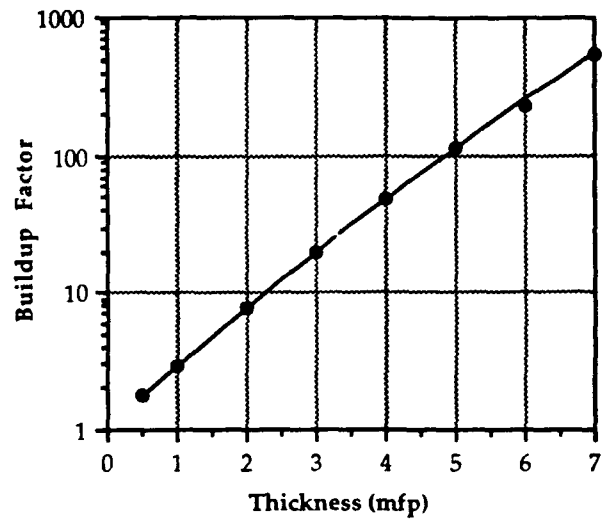


(d) $E_0 = 14$ MeV

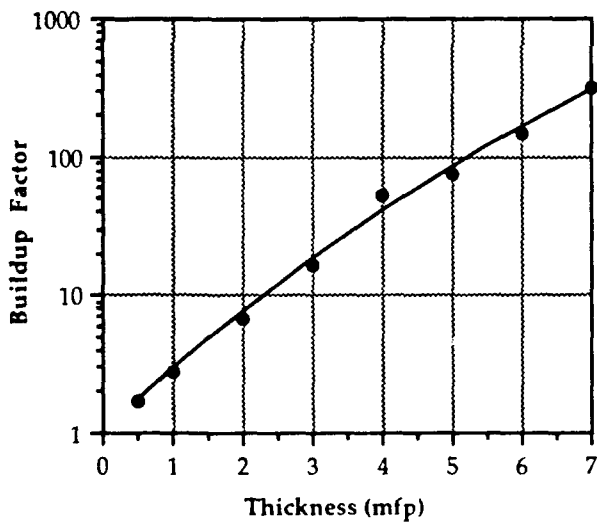
FIGURE 15. MODEL FITS TO NEUTRON BUILDUP FACTOR DATA FOR IRON, GEOMETRY A



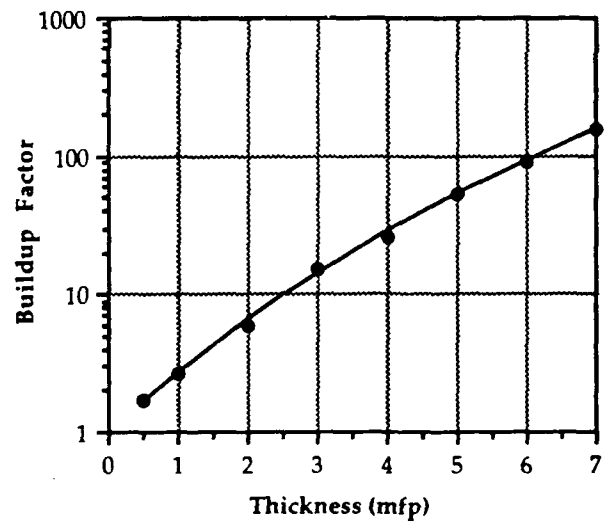
(a) $E_0 = 10^{-7}$ MeV



(b) $E_0 = 0.1$ MeV

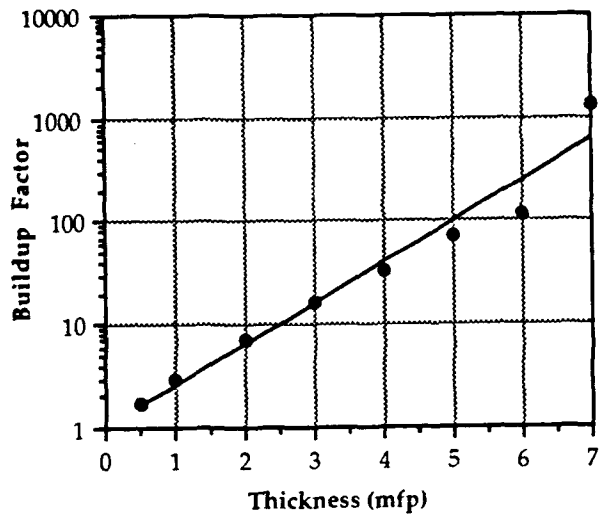


(c) $E_0 = 1.0$ MeV

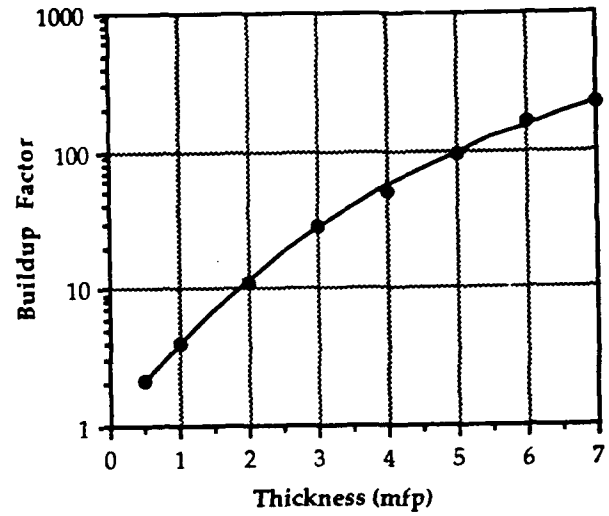


(d) $E_0 = 14$ MeV

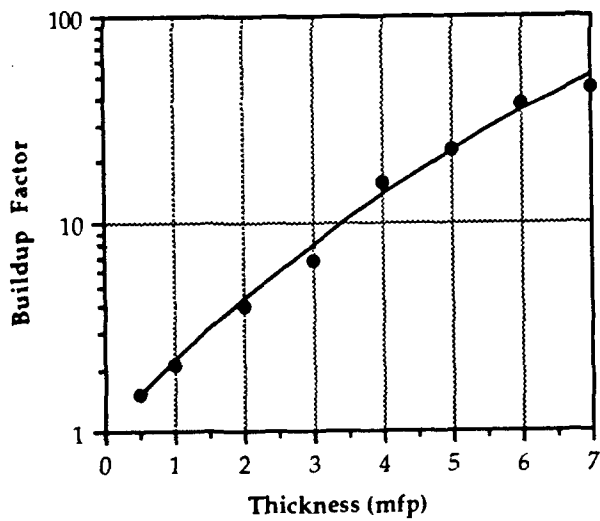
FIGURE 16. MODEL FITS TO NEUTRON BUILDUP FACTOR DATA FOR LEAD, GEOMETRY A



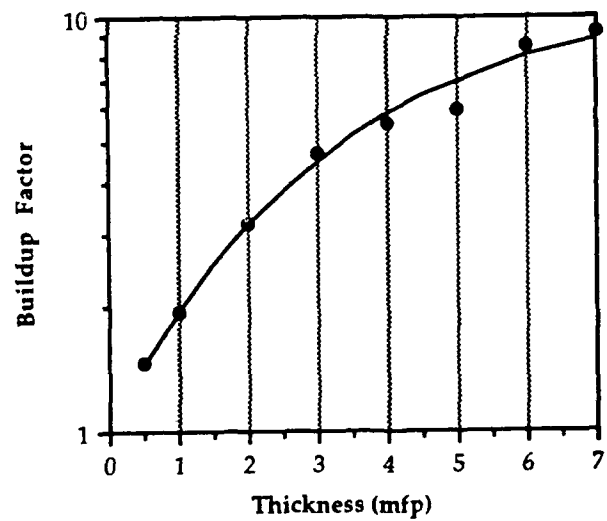
(a) $E_0 = 10^{-7}$ MeV



(b) $E_0 = 0.1$ MeV

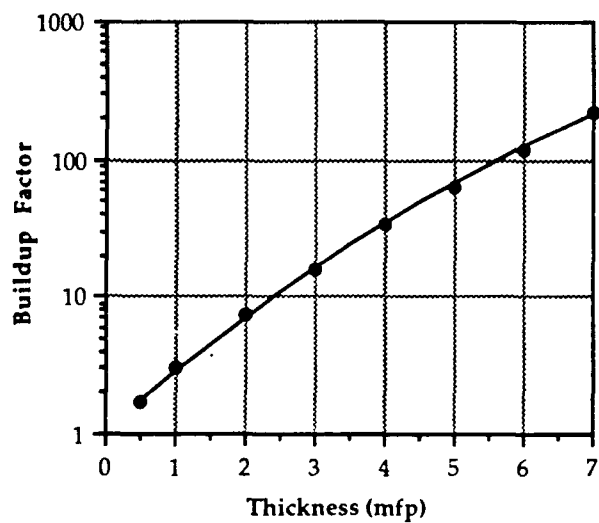


(c) $E_0 = 1.0$ MeV

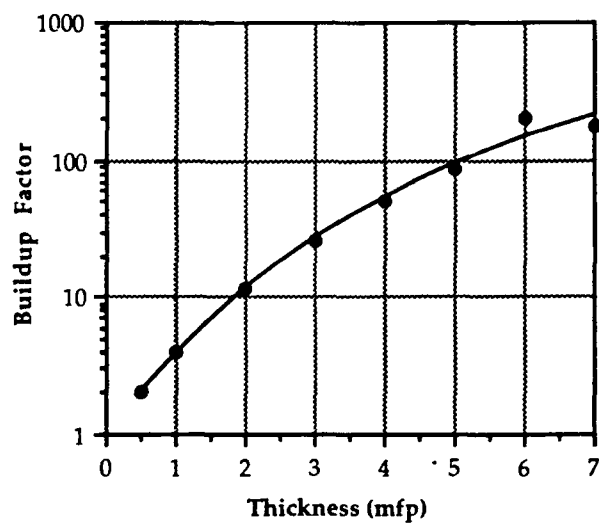


(d) $E_0 = 14$ MeV

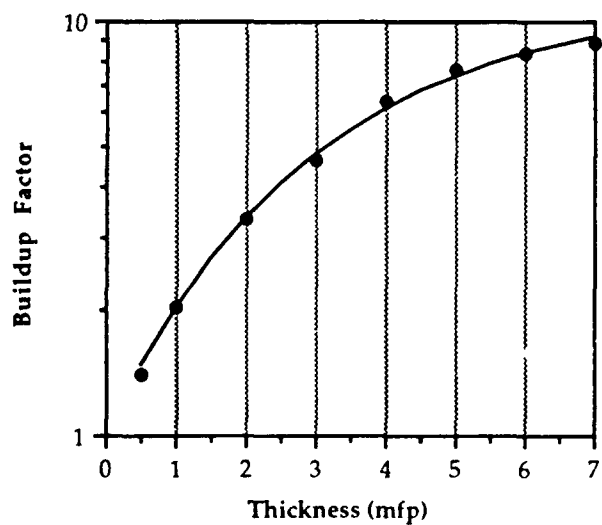
FIGURE 17. MODEL FITS TO NEUTRON BUILDUP FACTOR DATA FOR WATER, GEOMETRY A



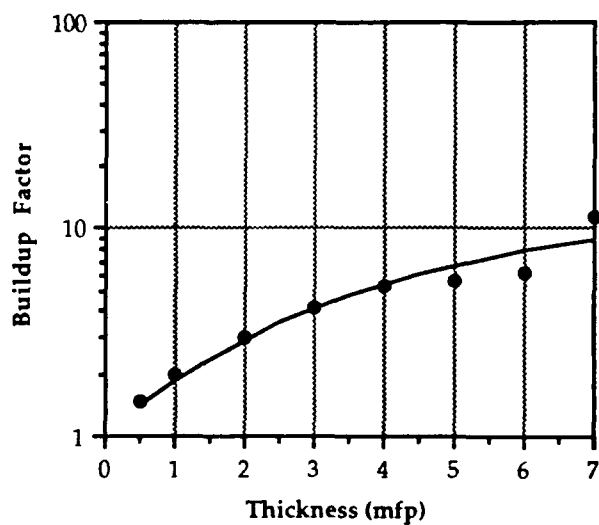
(a) $E_0 = 10^{-7}$ MeV



(b) $E_0 = 0.1$ MeV

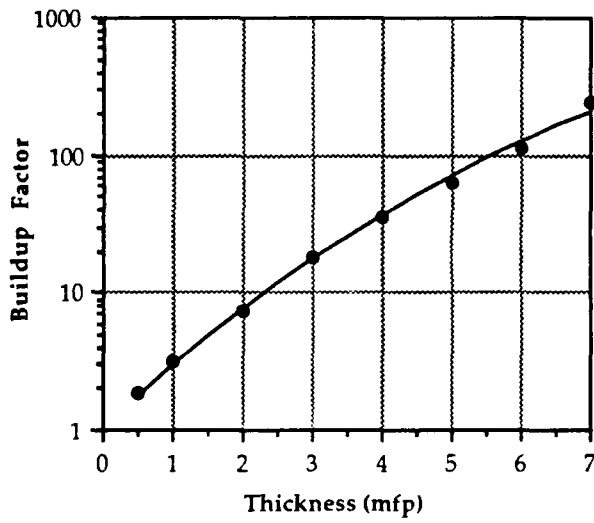


(c) $E_0 = 1.0$ MeV

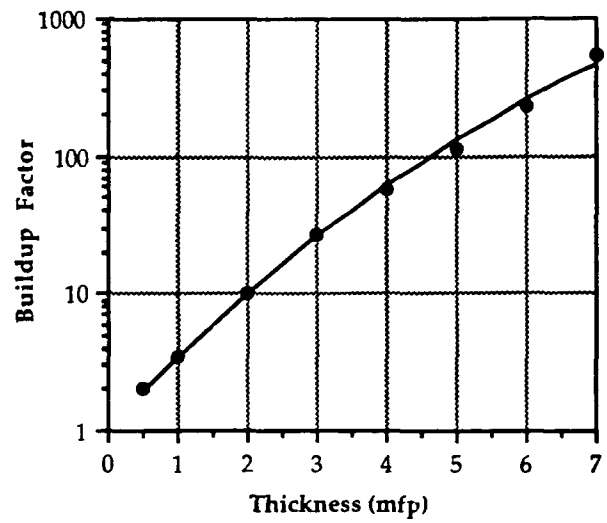


(d) $E_0 = 14$ MeV

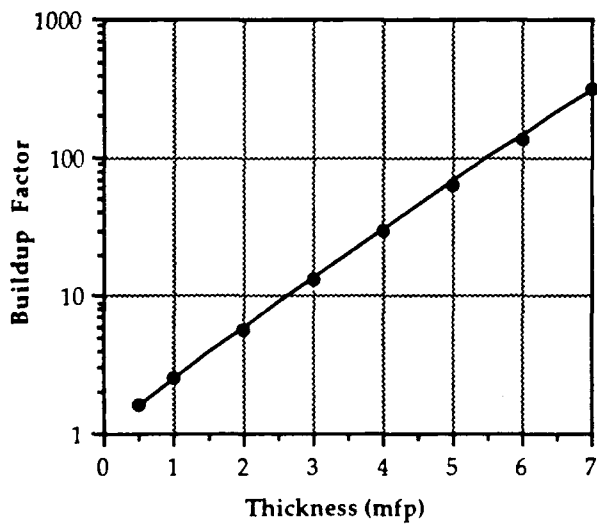
FIGURE 18. MODEL FITS TO NEUTRON BUILDUP FACTOR DATA FOR POLYETHYLENE, GEOMETRY A



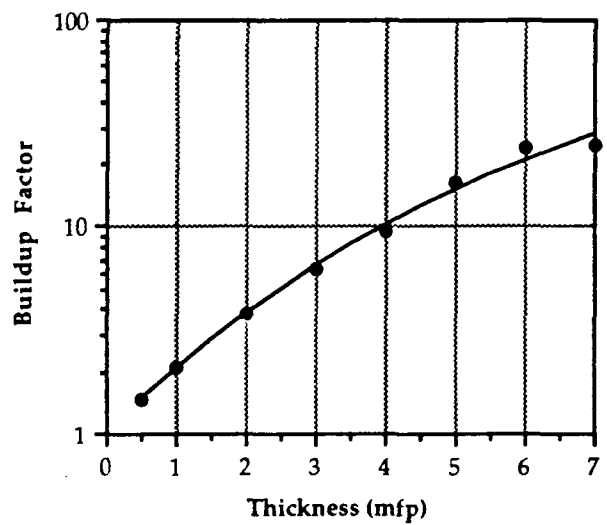
(a) $E_0 = 10^{-7}$ MeV



(b) $E_0 = 0.1$ MeV



(c) $E_0 = 1.0$ MeV



(d) $E_0 = 14$ MeV

FIGURE 19. MODEL FITS TO NEUTRON BUILDUP FACTOR DATA FOR CONCRETE, GEOMETRY A

TABLE 9. GAMMA-RAY BUILDUP FACTOR MODEL CONSTANTS AND LEAST-SQUARES FUNCTION VALUES FOR ALUMINUM, GEOMETRY A

E_0 (MeV)	α	β	E^2 [Eq. (25)]
0.1	2.8962	0.26795	0.00252
0.15	3.6771	0.21581	0.00242
0.2	3.7295	0.21295	0.00094
0.3	3.6681	0.21676	0.01885
0.4	4.1448	0.17225	0.01056
0.5	3.1913	0.23428	0.00225
0.6	3.7483	0.18360	0.02823
0.8	2.6846	0.26751	0.00122
1.0	2.4785	0.29992	0.00961
1.5	2.0324	0.30603	0.00069
2.0	2.1503	0.26785	0.00068
3.0	1.8797	0.27096	0.00103
4.0	1.4088	0.35725	0.00067
5.0	1.3623	0.33759	0.00142
6.0	1.4363	0.26846	0.00238
7.0	1.1856	0.31796	0.00080

TABLE 10. GAMMA-RAY BUILDUP FACTOR MODEL CONSTANTS AND LEAST-SQUARES FUNCTION VALUES FOR IRON, GEOMETRY A

E_0 (MeV)	α	β	E^2 [Eq. (25)]
0.1	0.74817	0.39040	0.00029
0.15	1.2664	0.39122	0.00028
0.2	1.9127	0.30201	0.00045
0.3	2.2859	0.28600	0.00030
0.4	2.8271	0.22713	0.00204
0.5	2.5499	0.28056	0.00486
0.6	4.5594	0.13020	0.03385
0.8	2.9603	0.20622	0.00150
1.0	2.8027	0.20508	0.00406
1.5	2.5014	0.22043	0.00370
2.0	1.9913	0.28161	0.00020
3.0	1.9565	0.25611	0.00259
4.0	1.4677	0.32540	0.00170
5.0	1.3848	0.29065	0.00021
6.0	1.5526	0.24439	0.00359
7.0	1.3903	0.23676	0.00023

TABLE 11. GAMMA-RAY BUILDUP FACTOR MODEL CONSTANTS AND LEAST-SQUARES FUNCTION VALUES FOR LEAD, GEOMETRY A

E_0 (MeV)	α	β	E^2 [Eq. (25)]
0.1	28122.	0.99861×10^{-5}	0.27880
0.15	1.0180	0.045595	0.00776
0.2	0.58877	0.071418	0.00084
0.3	0.68880	0.10557	0.00065
0.4	0.74957	0.14894	0.00112
0.5	0.96775	0.14993	0.00184
0.6	1.3939	0.12005	0.00379
0.8	0.90157	0.33901	0.00062
1.0	1.2188	0.25896	0.00233
1.5	1.3547	0.25944	0.00286
2.0	1.8395	0.17128	0.00292
3.0	1.4837	0.21944	0.00083
4.0	5.2344	0.040595	0.00345
5.0	1.9686	0.11324	0.00064
6.0	2.5172	0.080925	0.00028
7.0	2.1919	0.086542	0.00203

TABLE 12. GAMMA-RAY BUILDUP FACTOR MODEL CONSTANTS AND LEAST-SQUARES FUNCTION VALUES FOR WATER, GEOMETRY A

E_0 (MeV)	α	β	E^2 [Eq. (25)]
0.1	5.9135	0.17786	0.07237
0.2	5.3945	0.16557	0.00495
0.4	4.7587	0.16298	0.00439
0.6	3.5426	0.20497	0.00152
0.8	4.2179	0.14475	0.00319
1.0	4.1584	0.13978	0.00441
3.0	1.6889	0.32705	0.00637
5.0	1.9985	0.19195	0.00568
7.0	1.1522	0.33548	0.00015

TABLE 13. GAMMA-RAY BUILDUP FACTOR MODEL CONSTANTS AND LEAST-SQUARES FUNCTION VALUES FOR POLYETHYLENE, GEOMETRY A

E_0 (MeV)	α	β	E^2 [Eq. (25)]
0.1	9.2795	0.11251	0.00116
0.2	8.9009	0.095266	0.00125
0.4	5.2734	0.14796	0.00479
0.6	4.3754	0.16709	0.00051
0.8	3.7495	0.17971	0.00327
1.0	5.2524	0.10787	0.00853
3.0	1.9444	0.27952	0.00431
5.0	1.3687	0.33572	0.00093
7.0	1.6009	0.24609	0.00667

TABLE 14. GAMMA-RAY BUILDUP FACTOR MODEL CONSTANTS AND LEAST-SQUARES FUNCTION VALUES FOR CONCRETE, GEOMETRY A

E_0 (MeV)	α	β	E^2 [Eq. (25)]
0.1	2.7446	0.27817	0.00148
0.2	3.9973	0.19375	0.00110
0.4	3.9108	0.18217	0.00158
0.6	3.0014	0.24372	0.00155
0.8	2.5841	0.27820	0.00295
1.0	2.5027	0.27242	0.00253
3.0	1.9688	0.25214	0.00571
5.0	1.4335	0.30087	0.00254
7.0	1.5588	0.20786	0.00585

TABLE 15. NEUTRON BUILDUP FACTOR MODEL CONSTANTS AND LEAST-SQUARES FUNCTION VALUES FOR ALUMINUM, GEOMETRY A

E_0 (MeV)	α	β	E^2 [Eq. (25)]
10^{-7}	11.629	0.080388	0.00848
10^{-5}	19.786	0.053864	0.00264
10^{-3}	16.615	0.060263	0.00160
0.1	68.454	0.015026	0.00726
1.0	8.2200	0.12454	0.00129
10.0	11.116	0.075348	0.05729
14.0	9.1800	0.078672	0.00747

TABLE 16. NEUTRON BUILDUP FACTOR MODEL CONSTANTS AND LEAST-SQUARES FUNCTION VALUES FOR IRON, GEOMETRY A

E_0 (MeV)	α	β	E^2 [Eq. (25)]
10^{-7}	10.201	0.088922	0.00722
10^{-5}	21.037	0.049567	0.00152
10^{-3}	12.583	0.089226	0.00820
0.1	21.026	0.050671	0.00170
1.0	181.31	0.0049458	0.00197
10.0	34.805	0.024564	0.00355
14.0	184.65	0.0040040	0.00279

TABLE 17. NEUTRON BUILDUP FACTOR MODEL CONSTANTS AND LEAST-SQUARES FUNCTION VALUES FOR LEAD, GEOMETRY A

E_0 (MeV)	α	β	E^2 [Eq. (25)]
10^{-7}	20.744	0.050315	0.00175
10^{-5}	17.588	0.063265	0.01922
10^{-3}	18.155	0.060490	0.01322
0.1	21.194	0.050152	0.00129
1.0	12.264	0.089434	0.01911
10.0	11.928	0.081221	0.00464
14.0	9.2724	0.11128	0.00267

TABLE 18. NEUTRON BUILDUP FACTOR MODEL CONSTANTS AND LEAST-SQUARES FUNCTION VALUES FOR WATER, GEOMETRY A

E_0 (MeV)	α	β	E^2 [Eq. (25)]
10^{-7}	185.32	0.0049994	0.22271
10^{-5}	4.1957	0.22286	0.00424
10^{-3}	16.917	0.040197	0.00470
0.1	6.8747	0.21769	0.00198
1.0	7.1663	0.11286	0.01399
10.0	2.2659	0.42849	0.00543
14.0	2.4468	0.31352	0.00626

TABLE 19. NEUTRON BUILDUP FACTOR MODEL CONSTANTS AND LEAST-SQUARES FUNCTION VALUES FOR POLYETHYLENE, GEOMETRY A

E_0 (MeV)	α	β	E^2 [Eq. (25)]
10^{-7}	10.546	0.10125	0.00319
10^{-5}	6.4120	0.13450	0.01529
10^{-3}	11.823	0.059551	0.00146
0.1	6.7813	0.22173	0.02242
1.0	2.4444	0.33895	0.00098
10.0	2.2963	0.42277	0.00217
14.0	2.5669	0.26306	0.02852

TABLE 20. NEUTRON BUILDUP FACTOR MODEL CONSTANTS AND LEAST-SQUARES FUNCTION VALUES FOR CONCRETE, GEOMETRY A

E_0 (MeV)	α	β	E^2 [Eq. (25)]
10^{-7}	9.3174	0.12088	0.00944
10^{-5}	6.2911	0.14769	0.00240
10^{-3}	13.088	0.059824	0.00538
0.1	11.073	0.11505	0.00916
1.0	31.248	0.028788	0.00175
10.0	5.1856	0.16810	0.00333
14.0	5.0002	0.15602	0.00635

It is instructive to compare the model of Equation (27) for large slab thickness to infinite medium results, in order to assure that reasonable behavior is obtained. We recall that as $a \rightarrow \infty$, the model approaches e^a , so that the behavior for all a is smooth, monotonically increasing, and bounded. We compare in Table 21 gamma-ray buildup factors - calculated by extrapolating the model of Equation (27) to $a=40$ mfp - with infinite-medium values at 40 mfp source-detector separation taken from Trubey,¹⁰ for water. The model of Equation (27) gives values that are always lower than the equivalent infinite-medium results, as they should be. In general, these results also behave with energy in the proper manner, decreasing with increasing energy. Thus, we can conclude that the model behaves reasonably, is fairly accurate over the interval $0 \leq a \leq 7$ mfp, and can be used without concern for pathological behavior even at large a .

ENERGY AVERAGING PROCEDURE

The point-kernel formulation allows us to express dose equivalent in terms of dose equivalent due to uncollided radiation and a buildup factor. For a source with energy spectrum $S(E_0)$, the spectrum-averaged dose equivalent for a slab of thickness T can be written

$$\bar{H}(T) = \frac{\int_{\Delta E_0} B(E_0, a(E, T)) H_0(E_0) S(E_0) dE_0}{\int_{\Delta E_0} S(E_0) dE_0}, \quad (30a)$$

TABLE 21. BUILDUP FACTORS IN WATER FOR SOURCE-DETECTOR SEPARATION OF 40 MFP*

E_0 (MeV)	Total Buildup Factor, B	
	Trubey ¹⁰	Equation (27)
0.1	20,300	368
0.2	12,800	219
0.4	1,940	116
0.6	683	34.5
0.8	349	67.0
1.0	214	63.0
3.0	36.5	5.41
5.0	20.7	7.37

* Trubey results are for infinite media; Equation (27) results are for slab Geometry A.

where

$$a(E,T) = \alpha(E)T \quad (30b)$$

and ΔE_0 is the energy range over which $S(E_0)$ is defined. Since MREMS treats source spectra as embedded in the buildup factor model constants, we write the approximate form

$$\bar{H}(T) = \bar{B}(T) \bar{H}_0, \quad (31)$$

where \bar{B} is a spectrum-averaged buildup factor and \bar{H}_0 is a spectrum-averaged, pseudo-uncollided dose equivalent.

We now divide the source energy range into J contiguous intervals, the j^{th} interval having width $\Delta E_j = E_{0,j} - E_{0,j-1}$, and define the relative yield from interval j as

$$Y_j = \frac{[S(E_{0,j}) + S(E_{0,j-1})] \Delta E_j}{\sum_{p=1}^J [S(E_{0,p}) + S(E_{0,p-1})] \Delta E_p} \quad (32)$$

Then, we define

$$H_0 = \frac{\bar{h}_\phi e^{-\bar{\sigma}T}}{4\pi R^2} \quad (33)$$

where \bar{h}_ϕ and $\bar{\sigma}$ are parameters to be determined.

Next, we assume a model for \bar{B} of the same form as Equation (27) and thus write

$$\bar{B}(T) = e^{\bar{\alpha}(1 - e^{-\bar{\beta}T})} \quad (34)$$

Then, using Equations (33) and (34), Equation (31) becomes

$$\bar{H}(T) = \bar{h}_\phi e^{\bar{\alpha}(1 - e^{-\bar{\beta}T})} \frac{e^{-\bar{\sigma}T}}{4\pi R^2} \quad (35)$$

Then, we consider a set of slab thicknesses $\{T_n, n=1,2,\dots,N\}$ and calculate a corresponding set of spectrum-averaged dose equivalents $\{H_n, n=1,2,\dots,N\}$, from

$$H_n = \frac{\sum_{j=1}^J Y_j h_\phi(\bar{E}_{0,j}) e^{-\sigma(\bar{E}_{0,j}) T_n} B(\bar{E}_{0,j}, \alpha(\bar{E}_{0,j}) T_n)}{4\pi R_n^2} \quad (36)$$

By fitting the model of Equation (35) to the set of H_n using a least-squares procedure, we can obtain $\bar{\alpha}$, $\bar{\beta}$, $\bar{\sigma}$, and \bar{h}_ϕ . To simplify the fitting process, these parameters are evaluated iteratively as follows:

- (1) starting with an estimate of \bar{h}_ϕ and $\bar{\sigma}$, say $\bar{h}_\phi^{(0)}$ and $\bar{\sigma}^{(0)}$, evaluate $\bar{\alpha}$ and $\bar{\beta}$ as the solution to the system

$$\bar{\alpha} \sum_{n=1}^N (1 - e^{-\bar{\beta} \bar{\sigma}^{(0)} T_n})^2 - \sum_{n=1}^N (1 - e^{-\bar{\beta} \bar{\sigma}^{(0)} T_n}) \ln B_n = 0 \quad (37a)$$

$$\bar{\alpha} \sum_{n=1}^N (1 - e^{-\bar{\beta} \bar{\sigma}^{(0)} T_n}) \bar{\sigma}^{(0)} T_n e^{-\bar{\beta} \bar{\sigma}^{(0)} T_n} - \sum_{n=1}^N \bar{\sigma}^{(0)} T_n e^{-\bar{\beta} \bar{\sigma}^{(0)} T_n} \ln B_n = 0, \quad (37b)$$

where

$$B_n = \frac{H_n}{\bar{h}_\phi^{(0)} e^{-\bar{\sigma}^{(0)} T_n}} \quad (38)$$

- (2) using the estimates of $\bar{\alpha}$ and $\bar{\beta}$ from Equations (37), find improved values for \bar{h}_ϕ and $\bar{\sigma}$ from:

$$N \ln \bar{h}_\phi + \bar{\sigma} \sum T_n = \sum \ln \frac{H_n}{B_n^*}, \quad (39a)$$

$$\ln \bar{h}_\phi \sum T_n + \bar{\sigma} \sum T_n^2 = \sum T_n \ln \frac{H_n}{B_n^*}, \quad (39b)$$

where

$$B_n^* = e^{\bar{\alpha}(1 - e^{-\bar{\beta} \bar{\sigma}^{(0)} T_n})} \quad (40)$$

- (3) using the new \bar{h}_ϕ and $\bar{\sigma}$, repeat steps (1) and (2) until all parameters converge or until χ^2 is minimized.

The WBAR code, documented in Appendix A, calculates the spectrum-averaged constants, $\bar{\alpha}$, $\bar{\beta}$, $\bar{\sigma}$, and \bar{h}_ϕ .

CHAPTER 5

ALBEDO CALCULATIONS

Since the calculation of albedo was a separate task (Option 2, Item 0003), the albedo algorithms, results, and simplified models are described separately in this chapter. However, the albedo analysis follows closely the development for the transmission case, and so the nomenclature, conventions, and definitions are not repeated here.

ALGORITHMS

Albedo is typically defined as the ratio of the magnitudes of backscattered to incident currents. However, for purposes of the MREMS model, an albedo definition was chosen that employs the concept of an image source, as considered, e.g., by Eisenhauer.¹³ This image source geometry is shown in Figure 2 (see Chapter 2) for a typical case; the three specific albedo geometries considered in this report are shown in Figure 20.

In this geometry, the albedo factor, A , is defined as

$$A = \frac{4\pi r_1^2 H}{h_0(E_0)} \quad (41)$$

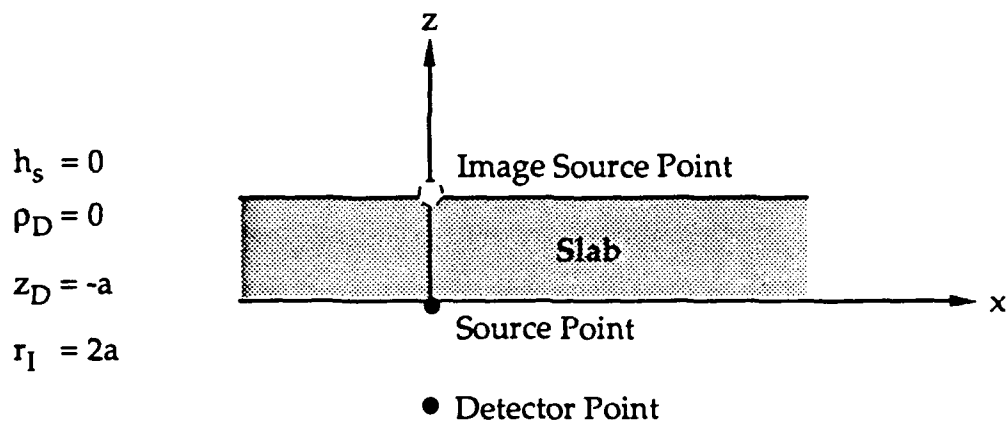
where H is total dose equivalent at the detector point due to the backscattered radiation from the actual source and r_1 is the physical distance, in cm, between the image source point and the detector point.

The albedo A can thus be determined by solving Equations (7) and (8) for $\Phi(\rho_D, z_D, E, \Omega)$, converting to dose equivalent, and multiplying by $4\pi r_1^2/h_0(E_0)$. This follows because the single- and multiple-scatter models for buildup factor were developed for the general case of arbitrary z_D . We do not allow geometries in which the source and detector points coincide (since the free-field dose would be undefined). Thus, for example, buildup factor Geometry A does not have an equivalent albedo Geometry A.

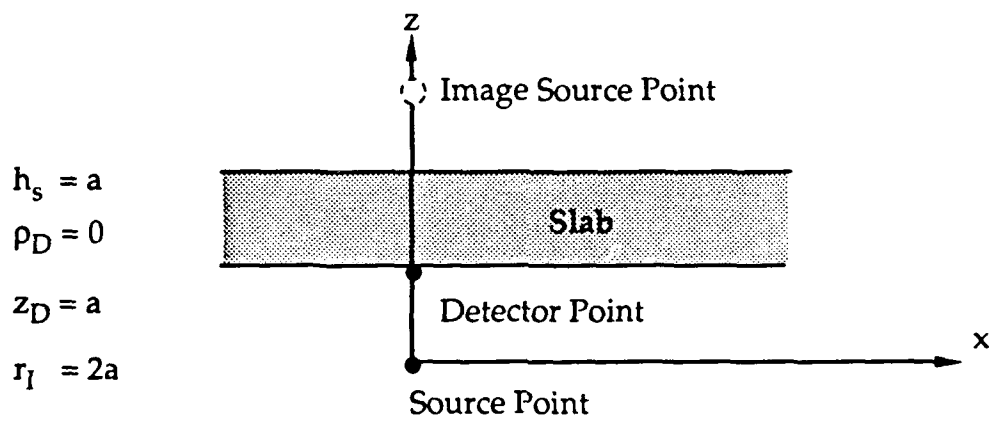
The single-scatter component of the total flux at the detector position can be expressed as

$$\Phi_1 = \frac{\sigma_s(E_0)}{2\pi} \int_0^1 \int_0^{2\pi} \int_0^\pi \frac{e^{-\sigma_0 \zeta/\mu_0} e^{-\sigma R}}{r^2} f(E_0 \rightarrow E, \mu_0 \rightarrow \mu) d\zeta d\phi_0 d\mu_0 \quad (42)$$

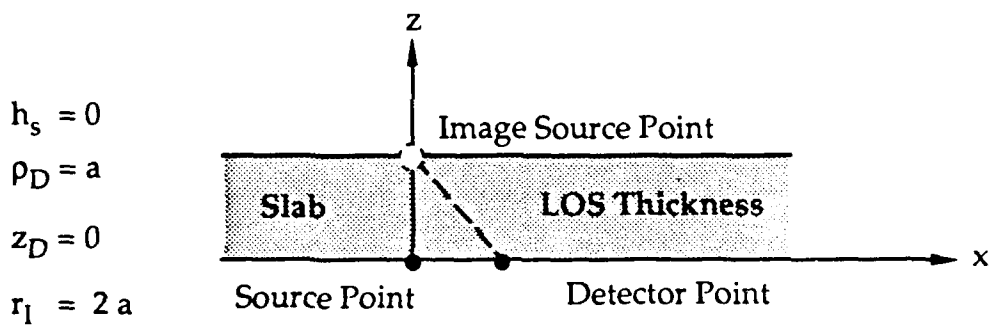
where, the appropriate form for f is used for each type of scatter.



(a) Albedo Geometry B



(b) Albedo Geometry C



(c) Albedo Geometry D

FIGURE 20. THE THREE ALBEDO FACTOR CONFIGURATIONS

The multiple-scatter model is exactly as described in Chapter 3. In Equation (42), the R and r are simply determined with respect to a detector on the near (source) side of the slab instead of the far (unexposed) side. Otherwise, the treatment is identical to that for the buildup factor.

The albedo algorithm can thus be summarized as follows:

- Determine r_1 and compute the quantity $4\pi r_1^2$.
- Compute Φ_{1i} by Equation (42), for each element, i , encountered along the LOS.
- Compute Φ_{ij} by Equation (21).
- Compute

$$H = \sum_{i=1}^m \left[h_{\phi}(E_i) \Phi_{1i} + \sum_{j=1}^J h_{\phi}(E_{ij}) \Phi_{ij} \right] \quad (43)$$

where J is the number of interaction types in element i that contribute to H .

- Compute A by Equation (41).

Note that A_1 is computed as

$$A_1 = \frac{4\pi r_1^2 \sum_{i=1}^m h_{\phi}(E_i) \Phi_{1i}}{h_{\phi}(E_0)} \quad (44)$$

SAMPLE RESULTS

The GBAS and NBAS codes compute albedo as well as buildup factors. Only albedo Geometries B, C, and D are considered, since for Geometry A the source point would coincide with the detector point. Tables 22 and 23 give gamma-ray and neutron albedos, respectively, for aluminum in Geometry B, for several source energies. More complete results for all six materials and for Geometries B, C, and D are given in Appendix D for gamma rays and in Appendix E for neutrons.

We note that most of the albedo results given in the appendices are less than unity, but some are larger. The definition that we use for albedo is the dose equivalent from reflected radiation divided by the dose equivalent that would be seen at the detector if the source were at the image source position (see Figure 20) and the slab were not present. The numerator involves radiation scattered from all points in the slab, while the denominator involves radiation transported only along the LOS between source and detector. Thus, using this definition, the only constraint on the value of the albedo is that it be positive (or zero in the case that the slab is completely absorbing), and values larger than unity are possible, especially for large slab thicknesses.

TABLE 22. GAMMA-RAY ALBEDO FACTORS FOR ALUMINUM, GEOMETRY B

(a) Single-scatter

LOS Thickness (mfp)	0.5	1.0	2.0	3.0	4.0	5.0	6.0	7.0
Energy (Mev)								
0.10	0.3342	0.4684	0.5829	0.6634	0.6612	0.6789	0.6910	0.7004
1.0	0.06125	0.08861	0.1158	0.1297	0.1383	0.1440	0.1482	0.1513
7.0	0.02272	0.03118	0.03891	0.04260	0.04476	0.04618	0.04716	0.04789

(b) Total scatter

Energy (Mev)								
0.10	0.4400	0.7011	0.9658	1.118	1.208	1.258	1.295	1.321
1.0	0.09436	0.1659	0.2497	0.3017	0.3353	0.3571	0.3754	0.3878
7.0	0.04327	0.06896	0.09723	0.1114	0.1213	0.1282	0.1325	0.1356

TABLE 23. NEUTRON ALBEDO FACTORS FOR ALUMINUM, GEOMETRY B

(a) Single-scatter

LOS Thickness (mfp)	0.5	1.0	3.0	5.0	7.0
Energy (Mev)					
10 ⁻⁷	0.4766E+00	0.6906E+00	0.9772E+00	0.1061E+01	0.1099E+01
0.10	0.4242E+00	0.5644E+00	0.7312E+00	0.7769E+00	0.7954E+00
1.0	0.4464E+00	0.6311E+00	0.8795E+00	0.9587E+00	0.9948E+00
14.0	0.3263E+00	0.4703E+00	0.6640E+00	0.7210E+00	0.7459E+00

(b) Total

Energy (Mev)					
10 ⁻⁷	0.6524E+00	0.1130E+01	0.2189E+01	0.2637E+01	0.2850E+01
0.10	0.8406E+00	0.1495E+01	0.3000E+01	0.3832E+01	0.4384E+01
1.0	0.6941E+00	0.1237E+01	0.2478E+01	0.2966E+01	0.3222E+01
14.0	0.4585E+00	0.8061E+00	0.1514E+01	0.1793E+01	0.1938E+01

SIMPLIFIED MODELS

Since there is no albedo Geometry A, Geometry B is chosen as the base geometry for the albedo models. With the definition of Equation (41), the albedo is zero for zero slab thickness, and generally increases as slab thickness increases. The model

$$A(a) = \alpha(E_0) [1 - e^{-\beta(E_0) a}] \quad (45)$$

has the correct general behavior and was fit to the gamma-ray albedo factors of Tables D-1 through D-6 in Appendix D and the neutron albedo factors of Tables E-1 through E-6 in Appendix E.

The Geometry B albedo factors and the model fits are plotted in Figures 21-26, for gamma rays, and in Figures 27-32, for neutrons. The model constants and least-squares function values are given in Tables 24 (gamma rays) and 25 (neutrons). In general, the simple, two-parameter model of Equation (45) fits the data quite well.

We employ a similar energy-averaging procedure as we did for buildup factors. We write the spectrum-averaged dose equivalent as

$$\bar{H}(T) = \frac{\bar{A}(T) h_0(E_0)}{(4\pi r^2)} \quad (46)$$

and assume

$$\bar{A}(T) = \bar{\alpha} (1 - e^{-\bar{\beta} \bar{\sigma} T}) \quad (47)$$

Then, we can calculate $\bar{\sigma}$, \bar{h}_0 , $\bar{\alpha}$, and $\bar{\beta}$ using a procedure similar to that described on p. 52, except in this case $\bar{\sigma}$ is set to unity. We assume an initial value $\bar{h}_0^{(0)}$ and solve the system

$$\bar{\alpha} \sum_{n=1}^N (1 - e^{-\bar{\beta} \bar{\sigma}^{(0)} T_n}) - \sum_{n=1}^N (1 - e^{-\bar{\beta} \bar{\sigma}^{(0)} T_n}) A_n = 0 \quad (48a)$$

$$\bar{\alpha} \sum_{n=1}^N (1 - e^{-\bar{\beta} \bar{\sigma}^{(0)} T_n}) \bar{\sigma}^{(0)} T_n e^{-\bar{\beta} \bar{\sigma}^{(0)} T_n} - \sum_{n=1}^N \bar{\sigma}^{(0)} T_n e^{-\bar{\beta} \bar{\sigma}^{(0)} T_n} A_n = 0, \quad (48b)$$

where

$$A_n = \frac{4\pi r_n^2 H_n}{\bar{h}_0^{(0)}}, \quad (49)$$

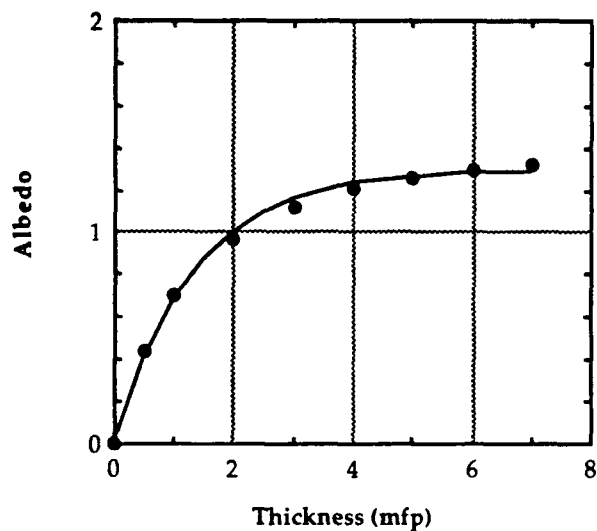
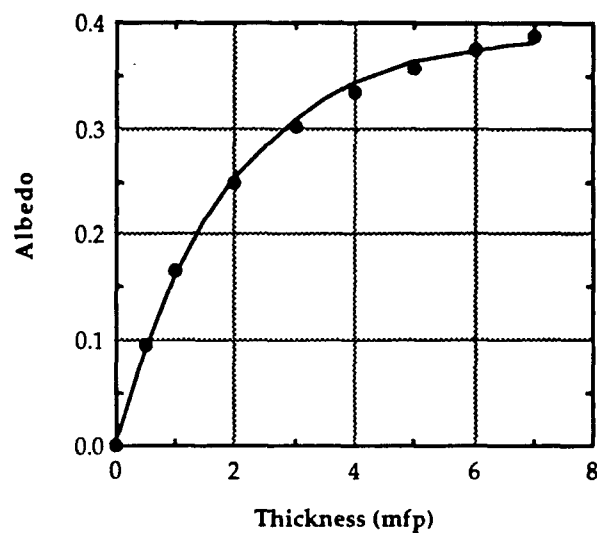
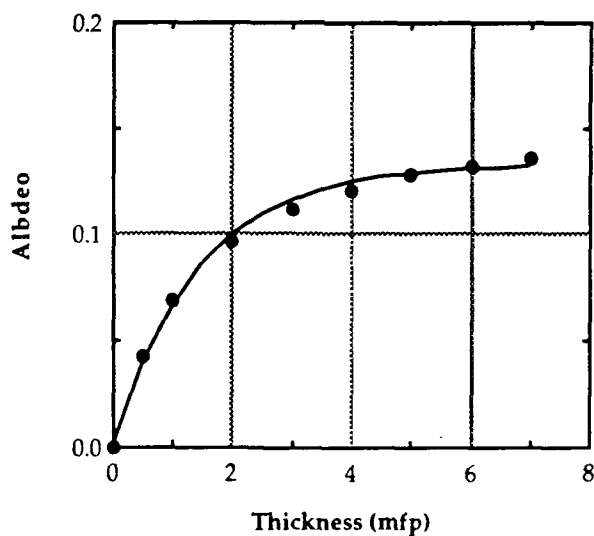
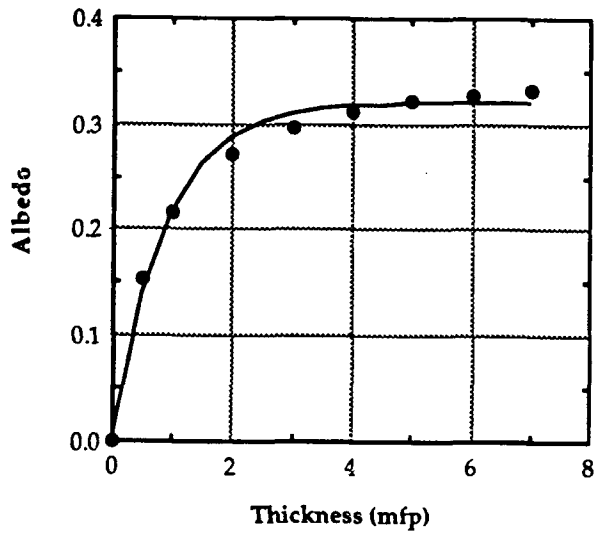
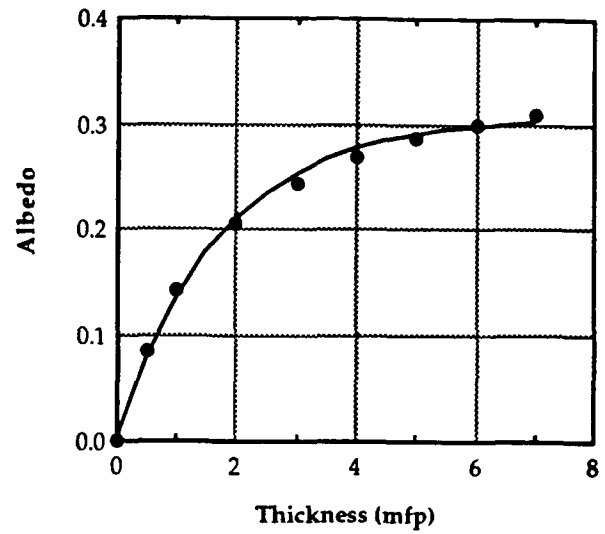

(a) $E_0 = 0.1$ MeV

(b) $E_0 = 1.0$ MeV

(c) $E_0 = 7.0$ MeV

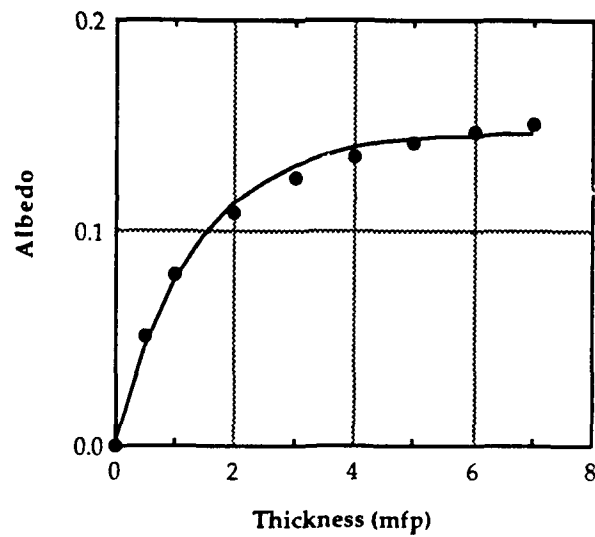
FIGURE 21. MODEL FITS TO GAMMA-RAY ALBEDO FACTOR DATA FOR ALUMINUM, GEOMETRY B



(a) $E_0 = 0.1$ MeV

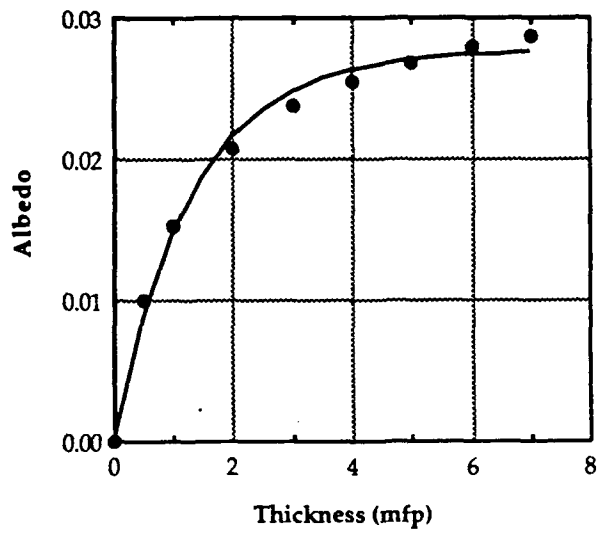


(b) $E_0 = 1.0$ MeV

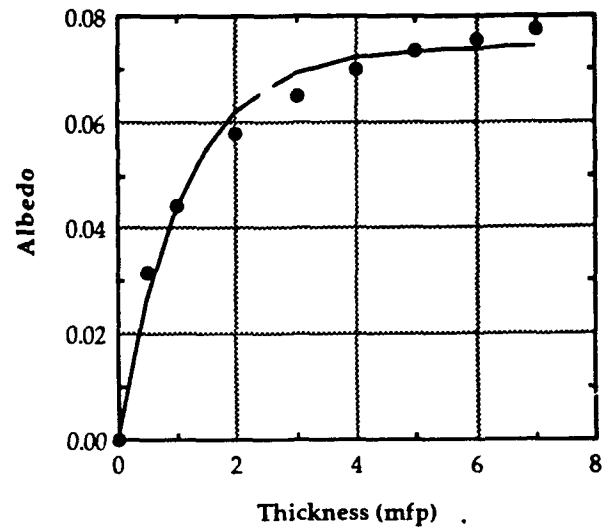


(c) $E_0 = 7.0$ MeV

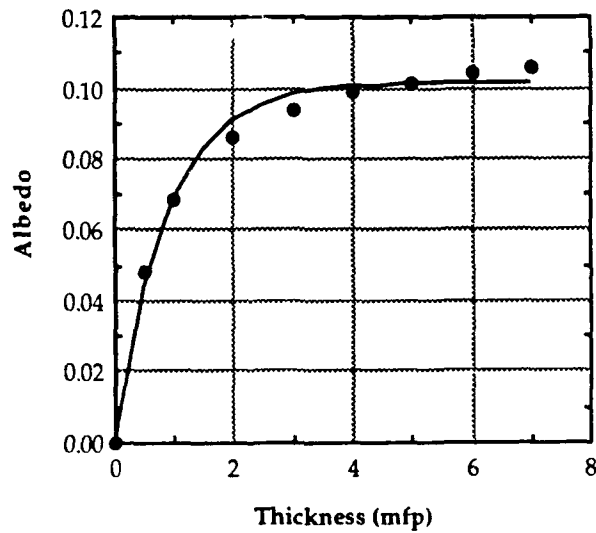
FIGURE 22. MODEL FITS TO GAMMA-RAY ALBEDO FACTOR DATA FOR IRON, GEOMETRY B



(a) $E_0 = 0.1$ MeV

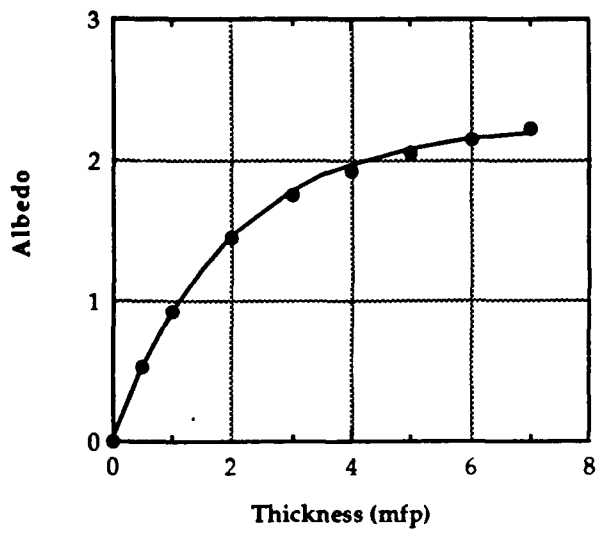


(b) $E_0 = 1.0$ MeV

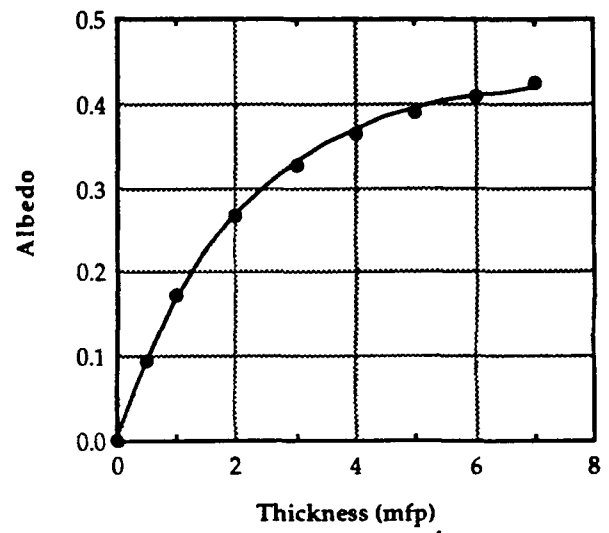


(c) $E_0 = 7.0$ MeV

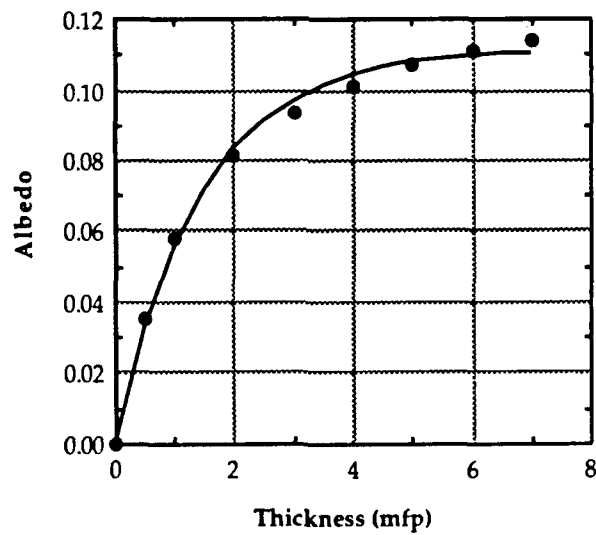
FIGURE 23. MODEL FITS TO GAMMA-RAY ALBEDO FACTOR DATA FOR LEAD, GEOMETRY B



(a) $E_0 = 0.1$ MeV

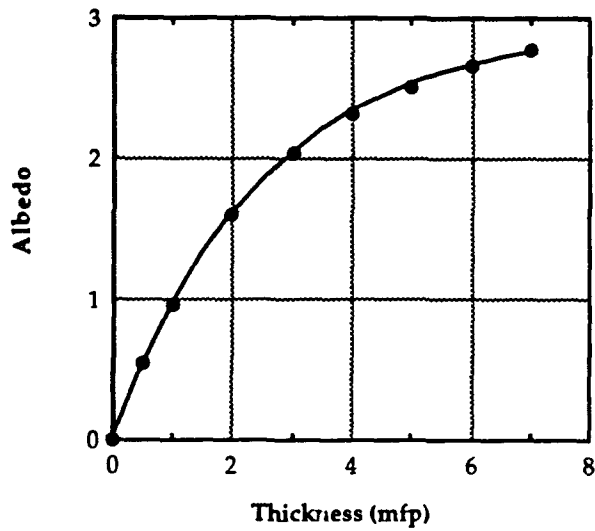


(b) $E_0 = 1.0$ MeV

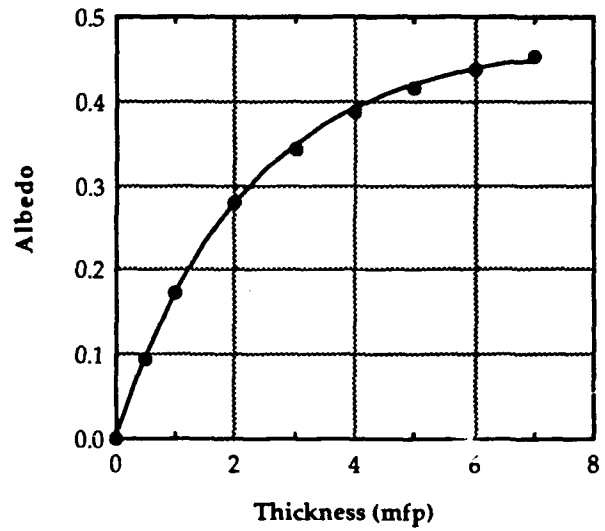


(c) $E_0 = 7.0$ MeV

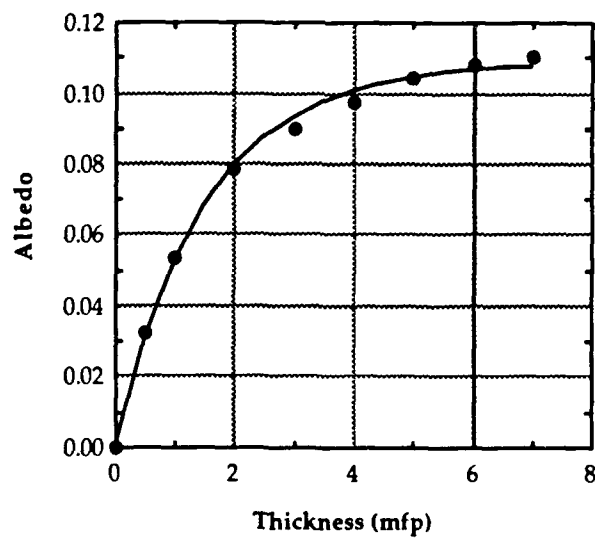
FIGURE 24. MODEL FITS TO GAMMA-RAY ALBEDO FACTOR DATA FOR WATER, GEOMETRY B



(a) $E_0 = 0.1$ MeV

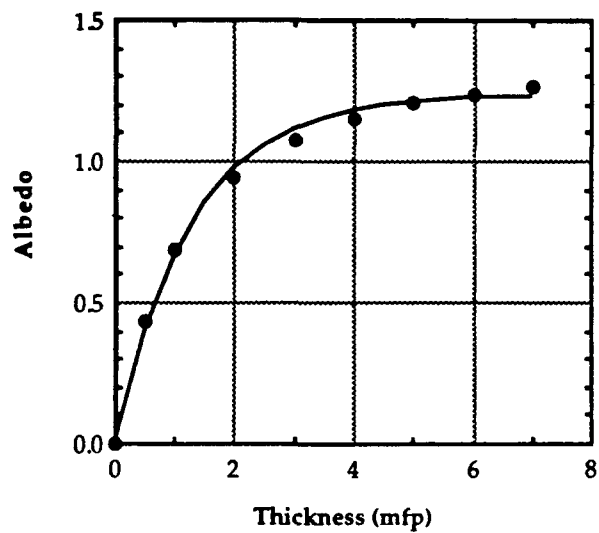


(b) $E_0 = 1.0$ MeV

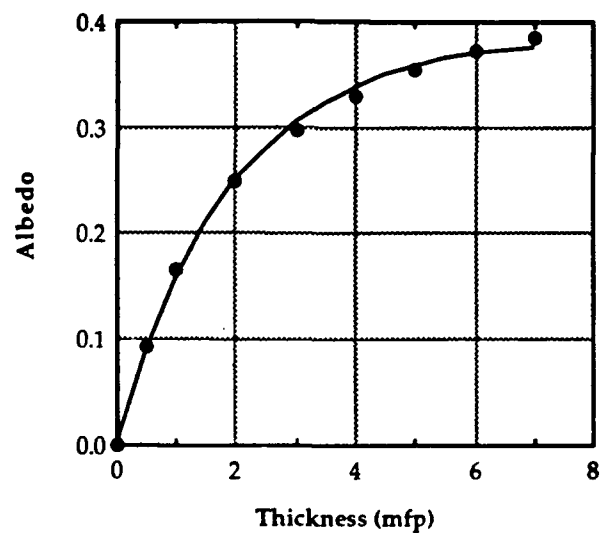


(c) $E_0 = 7.0$ MeV

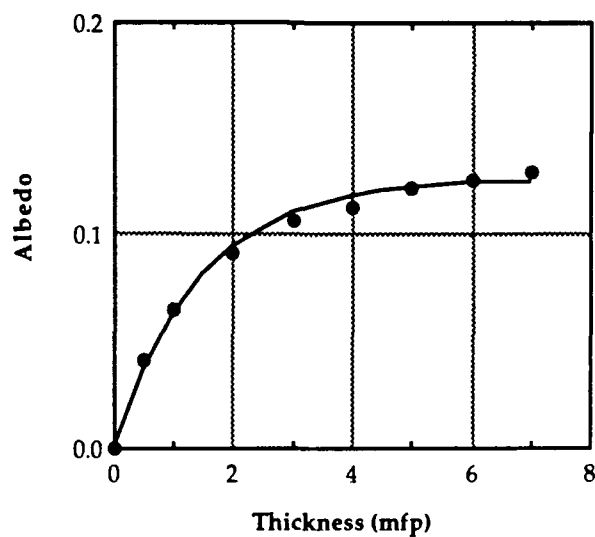
FIGURE 25. MODEL FITS TO GAMMA-RAY ALBEDO FACTOR DATA FOR POLYETHYLENE, GEOMETRY B



(a) $E_0 = 0.1$ MeV

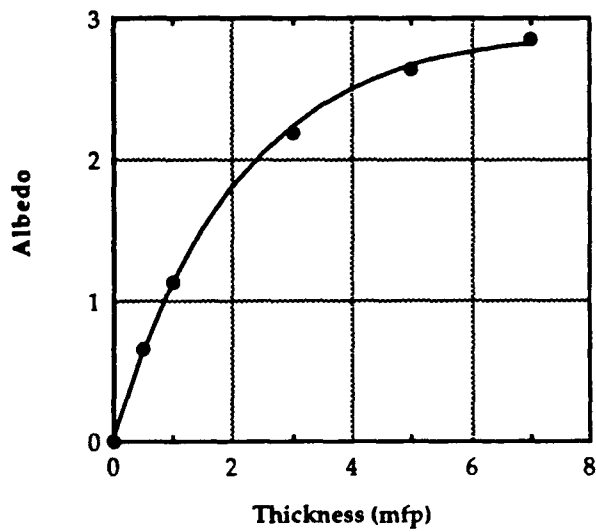


(b) $E_0 = 1.0$ MeV

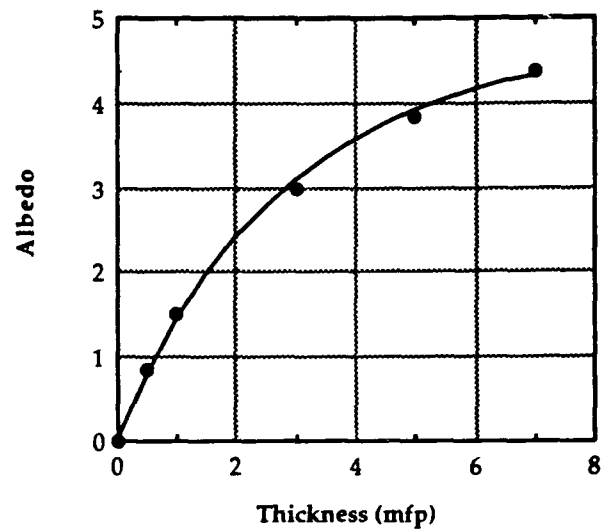


(c) $E_0 = 7.0$ MeV

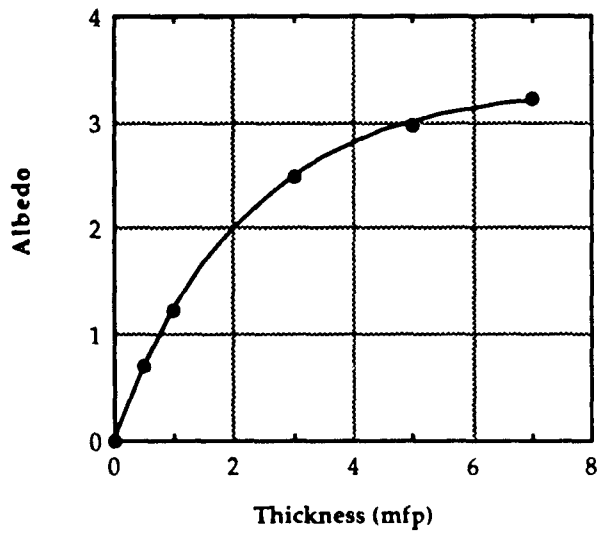
FIGURE 26. MODEL FITS TO GAMMA-RAY ALBEDO FACTOR DATA FOR CONCRETE, GEOMETRY B



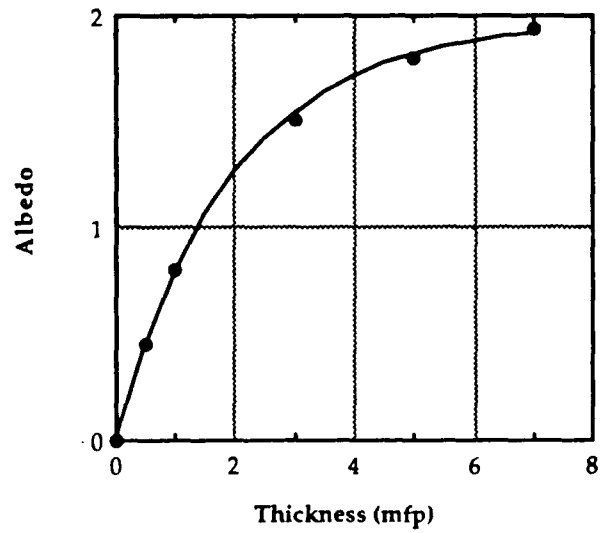
(a) $E_0 = 10^{-7}$ MeV



(b) $E_0 = 0.1$ MeV

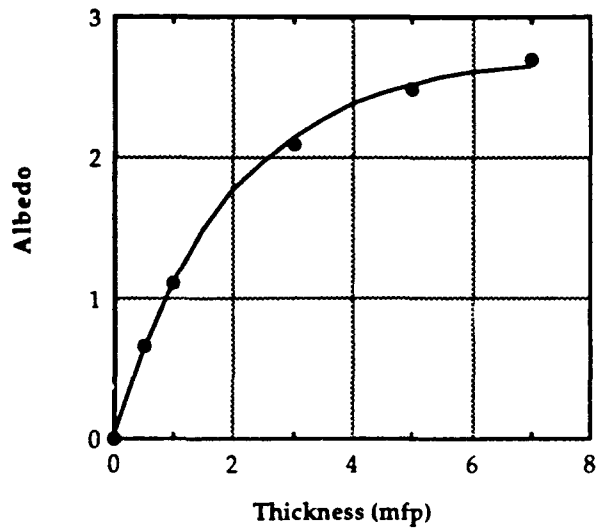


(c) $E_0 = 1.0$ MeV

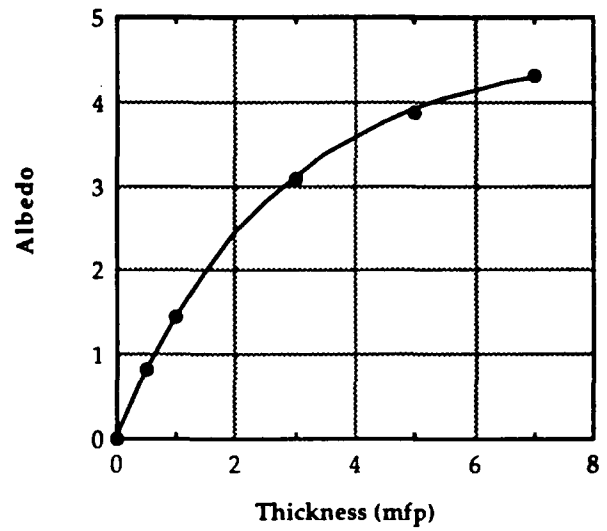


(d) $E_0 = 14$ MeV

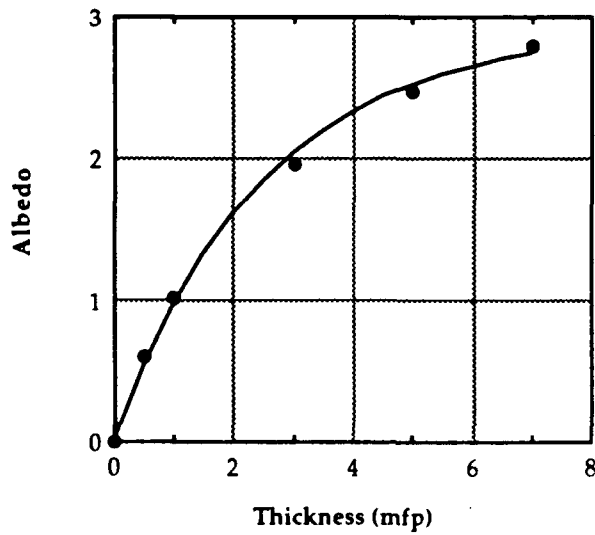
FIGURE 27. MODEL FITS TO NEUTRON ALBEDO FACTOR DATA FOR ALUMINUM, GEOMETRY B



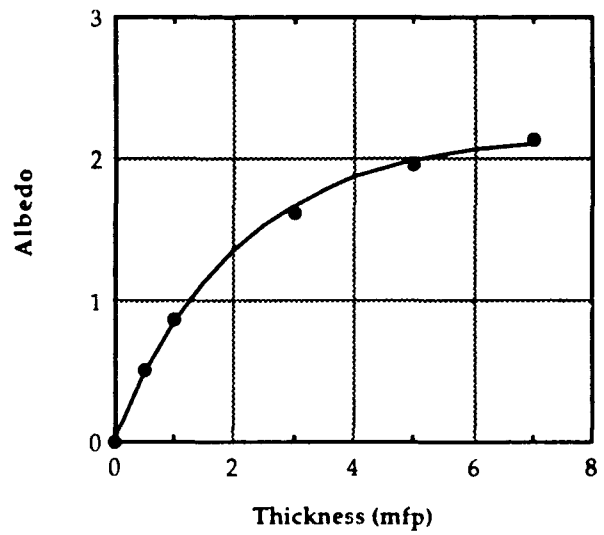
(a) $E_0 = 10^{-7}$ MeV



(b) $E_0 = 0.1$ MeV

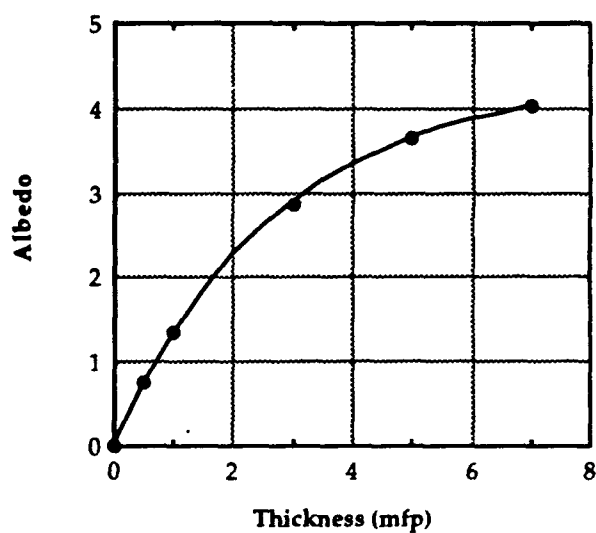


(c) $E_0 = 1.0$ MeV

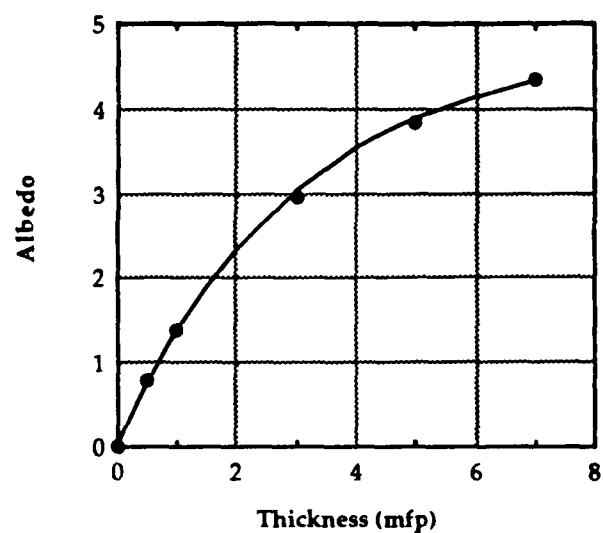


(d) $E_0 = 14$ MeV

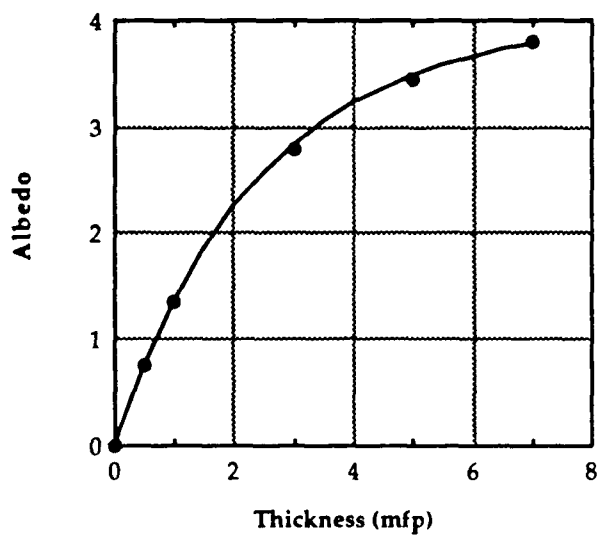
FIGURE 28. MODEL FITS TO NEUTRON ALBEDO FACTOR DATA FOR IRON, GEOMETRY B



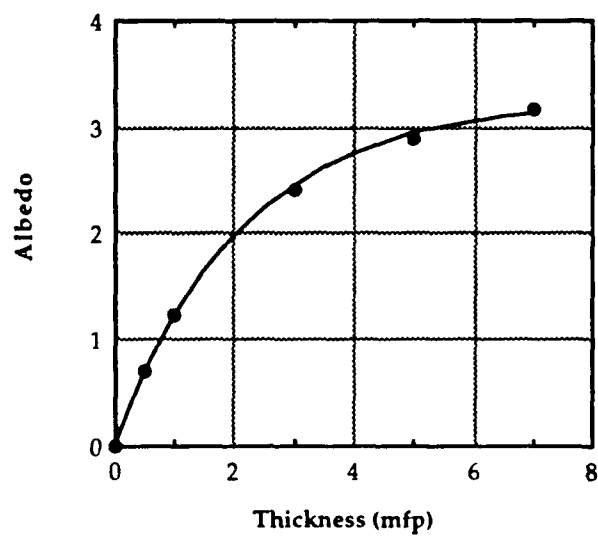
(a) $E_0 = 10^{-7}$ MeV



(b) $E_0 = 0.1$ MeV

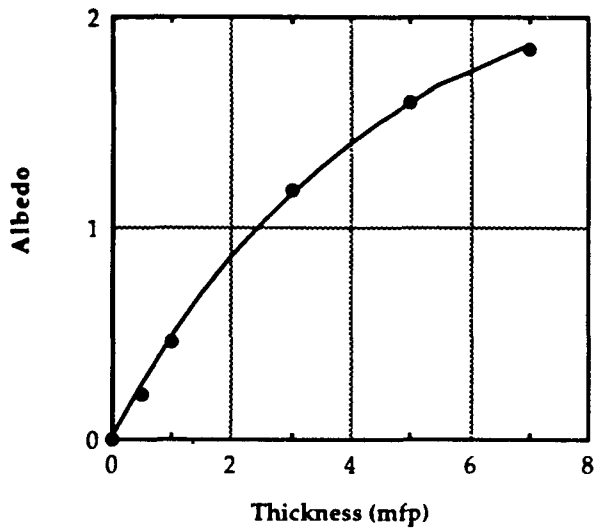


(c) $E_0 = 1.0$ MeV

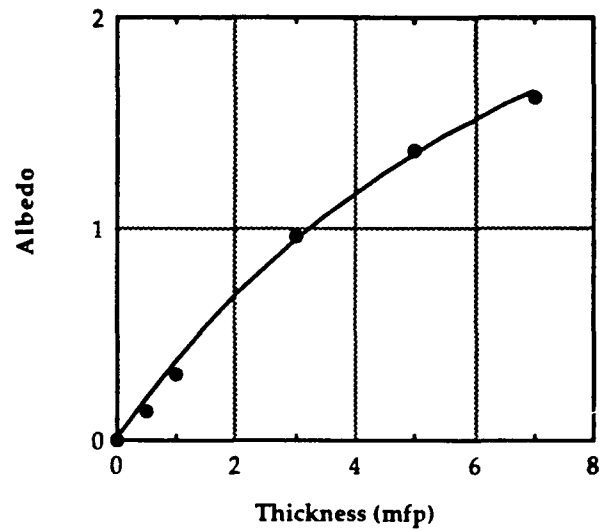


(d) $E_0 = 14$ MeV

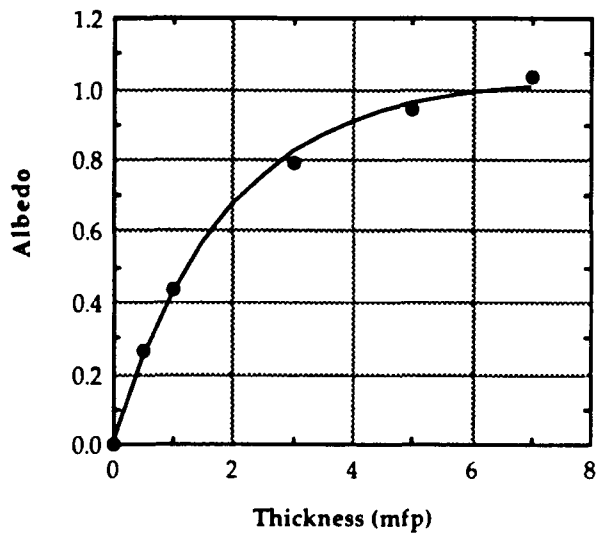
FIGURE 29. MODEL FITS TO NEUTRON ALBEDO FACTOR DATA FOR LEAD, GEOMETRY B



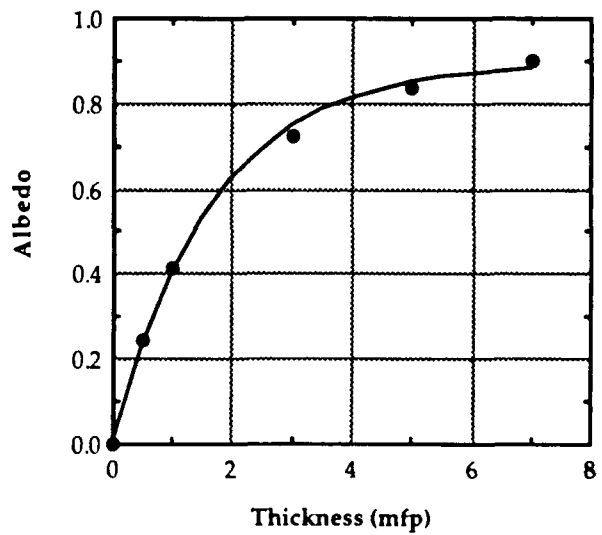
(a) $E_0 = 10^{-7}$ MeV



(b) $E_0 = 0.1$ MeV

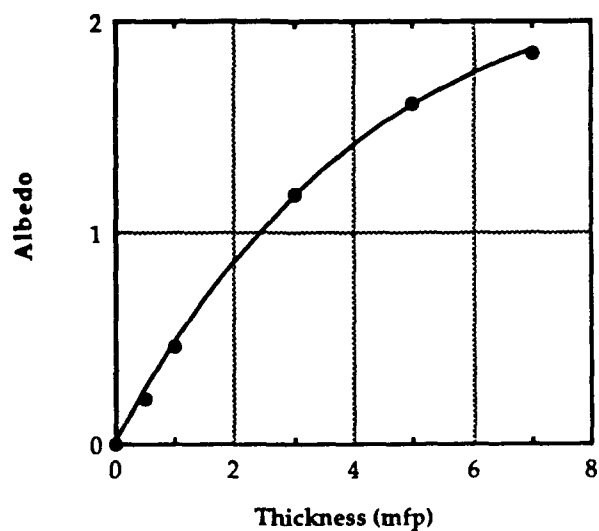


(c) $E_0 = 1.0$ MeV

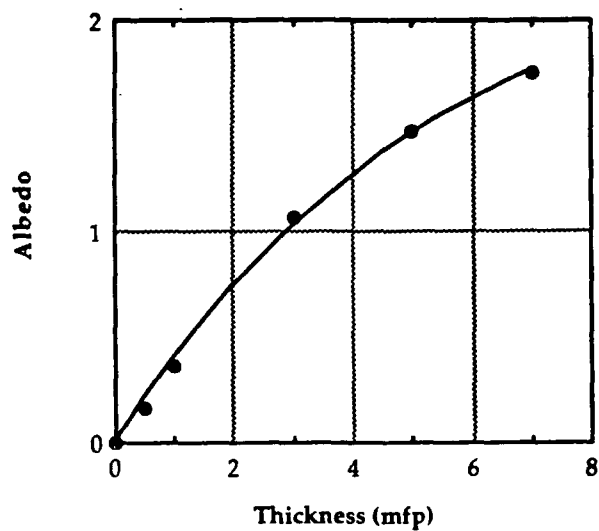


(d) $E_0 = 14$ MeV

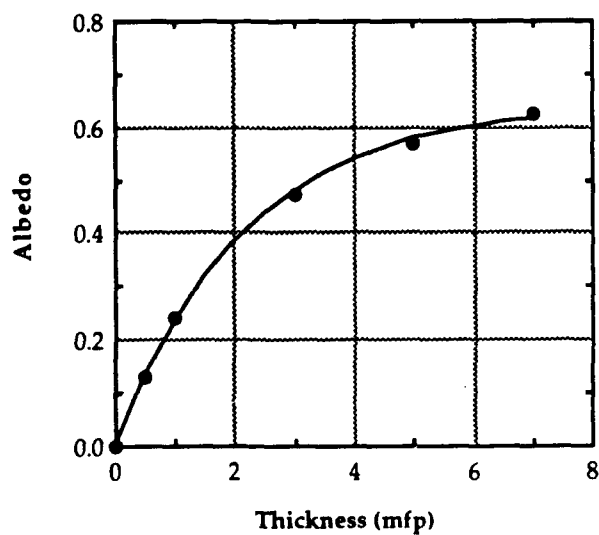
FIGURE 30. MODEL FITS TO NEUTRON ALBEDO FACTOR DATA FOR WATER, GEOMETRY B



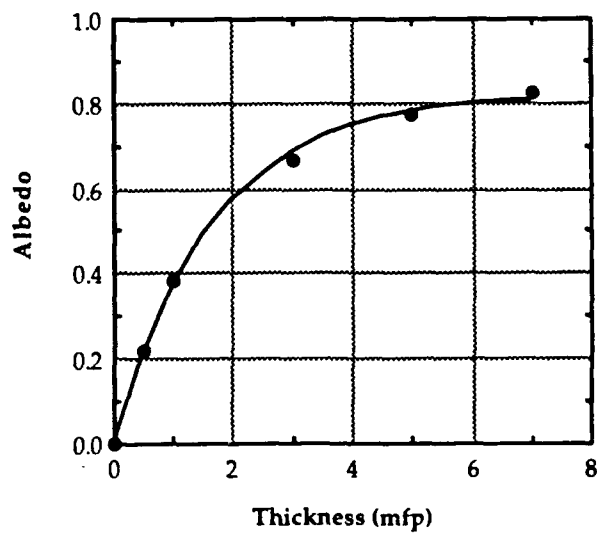
(a) $E_0 = 10^{-7}$ MeV



(b) $E_0 = 0.1$ MeV

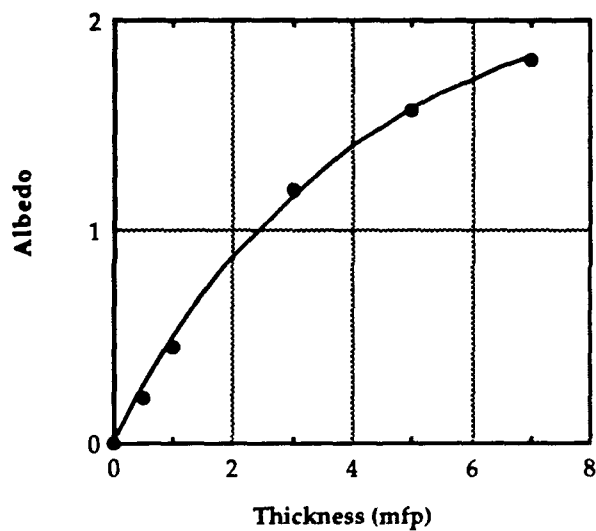


(c) $E_0 = 1.0$ MeV

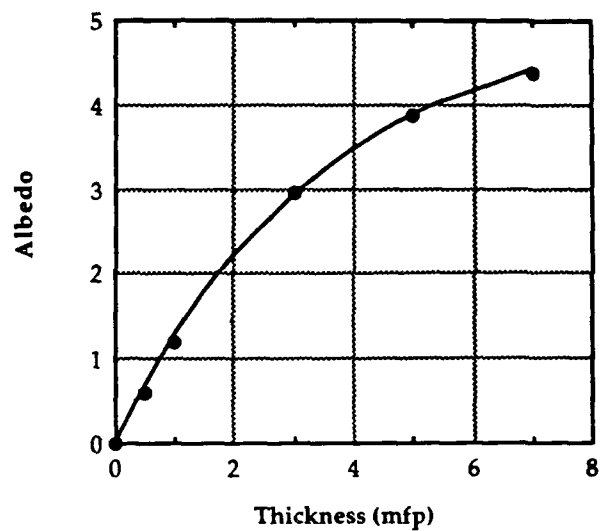


(d) $E_0 = 14$ MeV

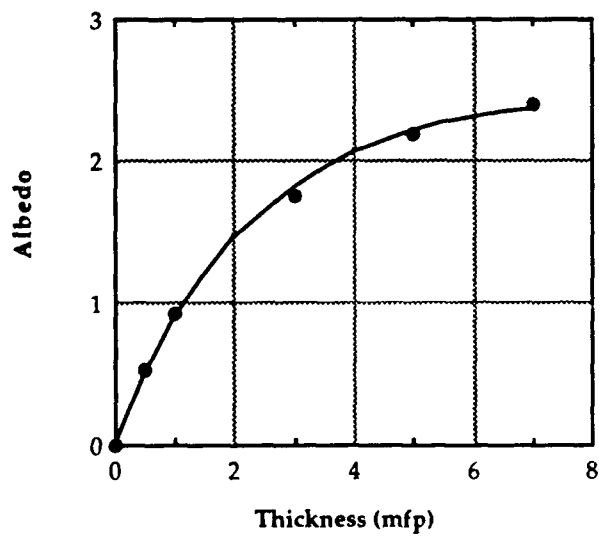
FIGURE 31. MODEL FITS TO NEUTRON ALBEDO FACTOR DATA FOR POLYETHYLENE, GEOMETRY B



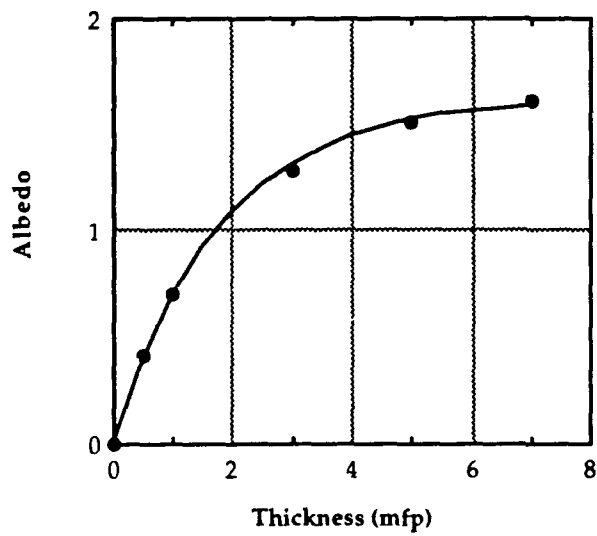
(a) $E_0 = 10^{-7}$ MeV



(b) $E_0 = 0.1$ MeV



(c) $E_0 = 1.0$ MeV



(d) $E_0 = 14$ MeV

FIGURE 32. MODEL FITS TO NEUTRON ALBEDO FACTOR DATA FOR CONCRETE, GEOMETRY B

NAVSWC TR 91-16

TABLE 24. GAMMA-RAY ALBEDO FACTOR MODEL CONSTANTS AND LEAST-SQUARES FUNCTION VALUES FOR GEOMETRY B

Material	E_0 (MeV)	α	β	E^2 [Eq. (25)]
Aluminum	0.1	1.295	0.7346	0.1061E-2
	1.0	0.3908	0.5152	0.4216E-4
	7.0	0.1328	0.6875	0.1369E-4
Iron	0.1	0.3196	1.139	0.1366E-3
	1.0	0.3062	0.5783	0.5910E-4
	7.0	0.1469	0.7397	0.2181E-4
Lead	0.1	0.0276	0.7588	0.1024E-5
	1.0	0.0740	0.8798	0.1247E-4
	7.0	0.1013	1.124	0.1537E-4
Water	0.1	2.246	0.5186	0.7135E-3
	1.0	0.4320	0.4828	0.2550E-4
	7.0	0.1113	0.6804	0.9265E-5
Polyethylene	0.1	2.929	0.3981	0.3054E-3
	1.0	0.4679	0.4506	0.1461E-4
	7.0	0.1086	0.6494	0.6465E-5
Concrete	0.1	1.234	0.7701	0.9084E-3
	1.0	0.3865	0.5153	0.5171E-4
	7.0	0.1261	0.6883	0.1432E-4

TABLE 25. NEUTRON ALBEDO FACTOR MODEL CONSTANTS AND LEAST-SQUARES FUNCTION VALUES FOR GEOMETRY B

Material	E_0 (MeV)	α	β	E^2 [Eq. (25)]
Aluminum	10^{-7}	2.925	0.4761	0.1313E-2
	0.1	4.700	0.3548	0.1039E-1
	1.0	3.333	0.4573	0.6196E-3
	14.0	1.967	0.5091	0.8338E-3
Iron	10^{-7}	2.725	0.5134	0.2059E-2
	0.1	4.631	0.3676	0.1178E-2
	1.0	2.905	0.4035	0.6142E-2
	14.0	2.177	0.4833	0.2161E-2
Lead	10^{-7}	4.351	0.3641	0.1373E-2
	0.1	4.790	0.3292	0.2503E-2
	1.0	3.994	0.4081	0.8449E-3
	14.0	3.256	0.4618	0.1888E-2
Water	10^{-7}	2.318	0.2313	0.7207E-3
	0.1	2.387	0.1666	0.2492E-2
	1.0	1.032	0.5290	0.7742E-3
	14.0	0.8922	0.6023	0.4135E-3
Polyethylene	10^{-7}	2.326	0.2313	0.8214E-3
	0.1	2.467	0.1792	0.1956E-2
	1.0	0.6437	0.4512	0.5056E-4
	14.0	0.8194	0.6036	0.2894E-3
Concrete	10^{-7}	2.198	0.2510	0.1309E-2
	0.1	5.109	0.2810	0.3695E-2
	1.0	2.476	0.4394	0.2980E-2
	14.0	1.623	0.5531	0.7514E-3

for $\bar{\alpha}$ and $\bar{\beta}$. Using these estimates, we find a new value for \bar{h}_ϕ is determined from

$$\bar{h}_\phi = \frac{1}{N} \sum_{n=1}^N \frac{4\pi r_n^2 H_n}{A_n} . \quad (50)$$

This procedure is repeated until all three parameters converge or X^2 is minimized.

CHAPTER 6

SAMPLE PROBLEM ANALYSIS

Six sample problems were analyzed, as required by Item 0004. In typical MREMS applications, the source and detector are separated by distances much greater than the slant thicknesses through the intervening slabs. Thus, a model that estimates the buildup factor at the surface of a slab due to a source on the other slab surface may or may not be adequate for use in MREMS, depending on how sensitive the buildup factor is to source-detector separation effects. In order to assess the effects of source-detector separation, four sample problems were considered; this led to the development of a correction factor model for source-detector separation. Also, it is important that the final buildup factor model be tested in realistic situations, and so two other sample problems were analyzed; these problems were selected to provide substantive tests of the developed models for single- and multiple-slab cases.

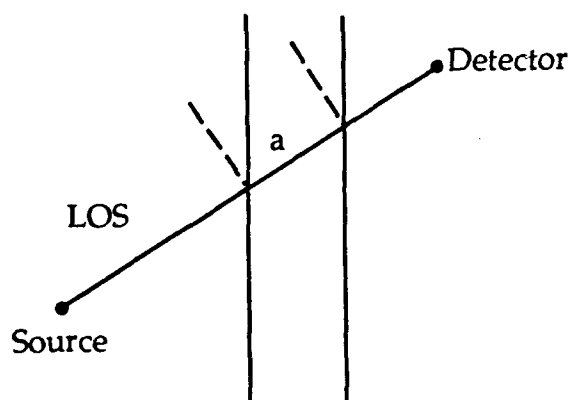
CORRECTION FOR SOURCE-DETECTOR SEPARATION

The model for G_M described in Chapter 4 is reasonably good for Geometry A, i.e., for the case when $h_s = h_D = \rho_D = 0$. In order to characterize what happens for nonzero h_s , h_D , and ρ_D , the four sample problems identified as Geometries E, F, G, and H and described in Table 26 were studied in detail. Buildup factors were determined for all four geometries and are given in Appendix F for gamma rays and Appendix G for neutrons; albedo factors were calculated for all geometries except E (for which the source and detector points would coincide) and are given in Appendices H and I.

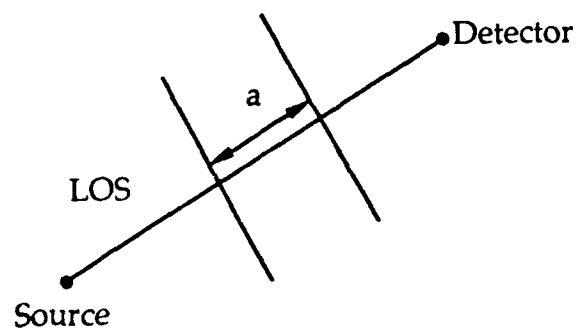
For a slab buildup model, MREMS would treat oblique incidence in the way shown in Figure 33. MREMS provides total source-detector separation and calculates slant thickness through walls encountered along the LOS; however, MREMS does not provide source-to-slab and slab-to-detector distances, h_s and h_D , respectively, and thus has no way to specify the location of the slab in Figure 33(b). Thus, a correction factor that accounts for total source-detector separation, but not for specific location of the intervening slab (i.e., not on h_s and h_D , individually), is sought.

TABLE 26. THE SAMPLE PROBLEM GEOMETRIES

Geometry	h_s	ρ_D	z_D	
(a) Buildup factors				
A	0	0	a	
B	0	0	2a	
C	a	0	2a	
D	0	a	a	
E	10a	0	21a	
F	0	0	11a	
G	10a	0	11a	
H	0	2a	2a	
(b) Albedo factors				
				r_1
B	0	0	-a	2a
C	a	0	a	2a
D	0	a	0	$\sqrt{2}a$
F	0	0	-10a	11a
G	10a	0	10a	11a
H	0	2a	-a	$2\sqrt{2}a$



(a) MREMS attenuation geometry



(b) MREMS buildup geometry

FIGURE 33. MREMS TREATMENT OF OBLIQUE INCIDENCE ON SLABS

Letting S be source-detector separation expressed in multiples of slab thickness, Geometries A, B, C, E, F, and G can be used to study the dependence of buildup and albedo factors on S , as shown schematically in Figure 34. Further analysis showed that there is usually a marked reduction in the buildup factors for h_D very close to 0, but not otherwise. Thus, to be conservative, Geometries C and G (for which $h_D = 0$) were excluded, and a model for g_M was fit to the data of Geometries A, B, F, and E as a function of source-detector separation.

Equation (23) decomposes the buildup factor into the product of two functions--one, G_M , for $h_s = h_D = \rho_D = 0$ (Geometry A) and one, g_M , for source-detector separation effects. In developing a model for g_M , the following notation is used:

$B(a,S)$ is buildup factor as a function of slab thickness and source-detector separation;

$B(a,1) = B_0$, for a given slab thickness, a , is the buildup factor for Geometry A; and

$$B(a,S) = B_0 g_M(S|a) , \quad (51)$$

where $g_M(S|a)$ is a correction factor as a function of S for given a .

Since no modification is needed for Geometry A, it is clear that $f_M(1|a) = 1$. It is also presumed that g_M varies monotonically and that as $S \rightarrow \infty$, B approaches a finite value, which is called $1+\delta$. Thus our model for g_M decreases monotonically from unity, at $S = 1$, and approaches the limit

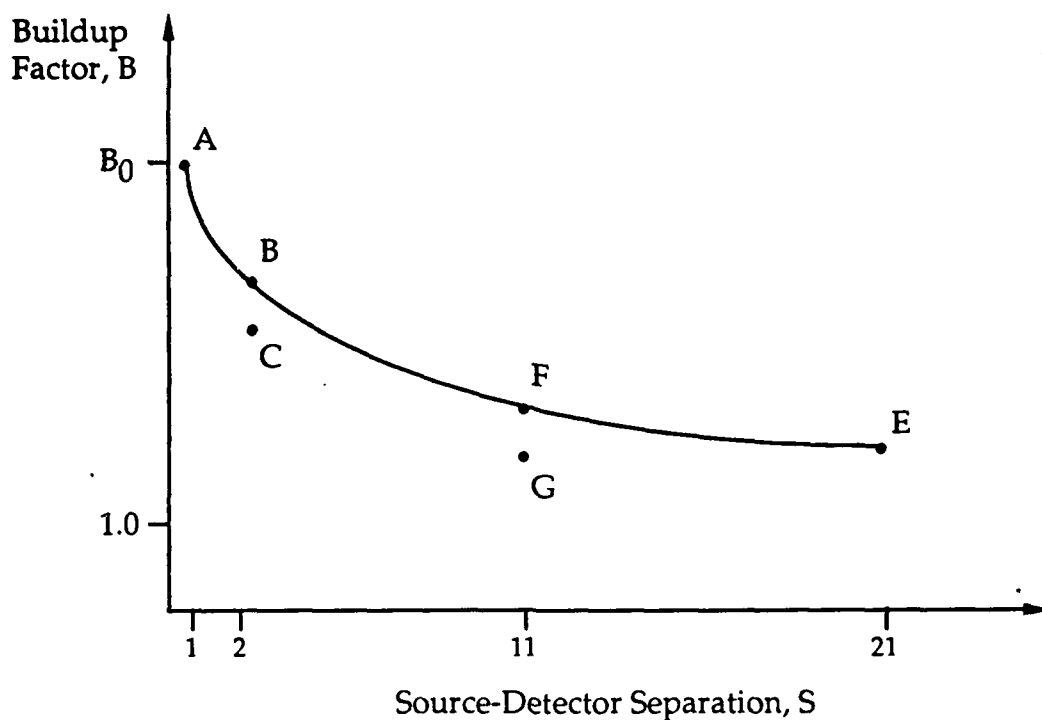
$$\lim_{S \rightarrow \infty} g_M(S|a) = \frac{1+\delta}{B_0} . \quad (52)$$

After considerable analysis, the following model for g_M was developed,

$$g_M(S|a) = \frac{1+\delta}{B_0} + \left[1 - \frac{1+\delta}{B_0} \right] e^{-\gamma[(S-1)a]^v} , \quad (53)$$

which exhibits the proper features:

- (1) As $S \rightarrow 1$, $g_M \rightarrow 1$;
- (2) As $S \rightarrow \infty$, $g_M \rightarrow \frac{1+\delta}{B_0}$;
- (3) g_M decreases monotonically.



* The letters near the dots identify the geometries

FIGURE 34. APPROXIMATE BEHAVIOR OF B VERSUS S

This model was fit to the buildup factor data of Geometries A, B, F, and E--which gives B as a function of S for S = 1, 2, 11, and 21, respectively--for each of the six materials. It was found that one set of values of the parameters γ and ν suffice for all slab thicknesses and all energies, for a given material. It was also found that δ was always very small and use of $\delta = 0$ in Equation (53), which simplifies the model, did not adversely affect the fit.

Thus, the two-parameter model

$$g_M(S|a) = \frac{1}{B_0} + \left[1 - \frac{1}{B_0}\right] e^{-\gamma[(S-1)a]^\nu}, \quad (54)$$

was selected as the correction factor for source-detector separation effects. The parameter values shown in Table 27 were obtained by a least-squares fit of the model of Equation (54) to the buildup factor data between Geometries A, B, F, and E. Also shown in Table 27 are the percent differences between the model for g_M given by Equation (54) and the calculated buildup factors. The gamma ray fits employed three source energies (0.1, 1.0, and 7.0 MeV) and the neutron fits four energies (10^{-7} , 0.1, 1.0, and 14.0 MeV); eight slab thicknesses were considered (0.5, 1, 2, 3, 4, 5, 6, and 7 m).

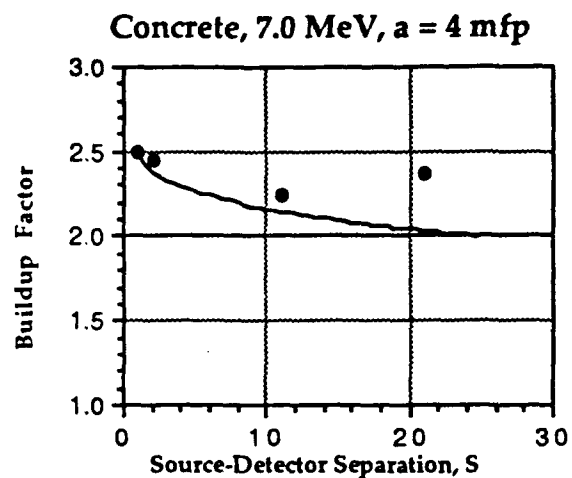
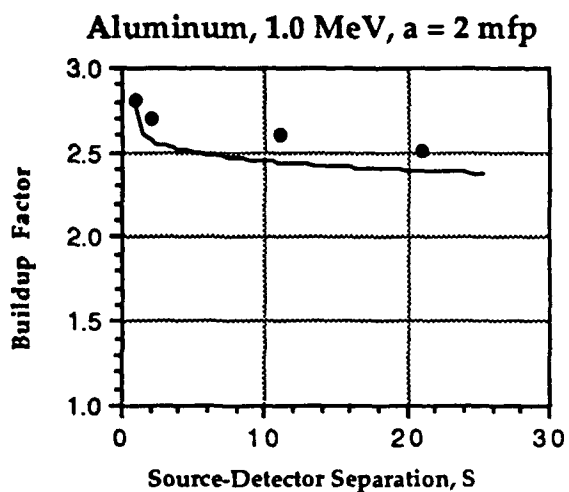
TABLE 27. THE PARAMETER VALUES FOR γ AND ν IN THE MODEL OF EQUATION (54) FOR g_M

	Material	γ	ν	% Difference
(a) Gamma Rays				
	Aluminum	0.1249	0.2060	9.9
	Iron	0.2057	0.0453	7.4
	Lead	0.1326	0.0381	4.4
	Water	0.0715	0.4700	17.1
	Polyethylene	0.1007	0.4000	12.6
	Concrete	0.0459	0.4800	8.5
(b) Neutrons				
	Aluminum	0.1060	0.3688	17.5
	Iron	0.0748	0.4186	9.9
	Lead	0.0704	0.4895	12.6
	Water	0.1314	0.2522	28.8
	Polyethylene	0.1534	0.1365	13.6
	Concrete	0.1007	0.3409	10.6

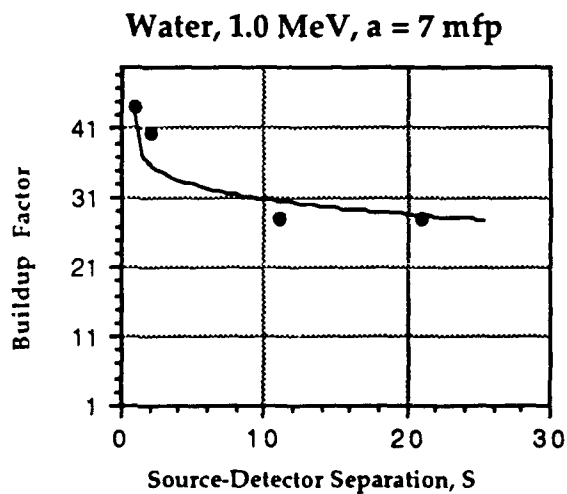
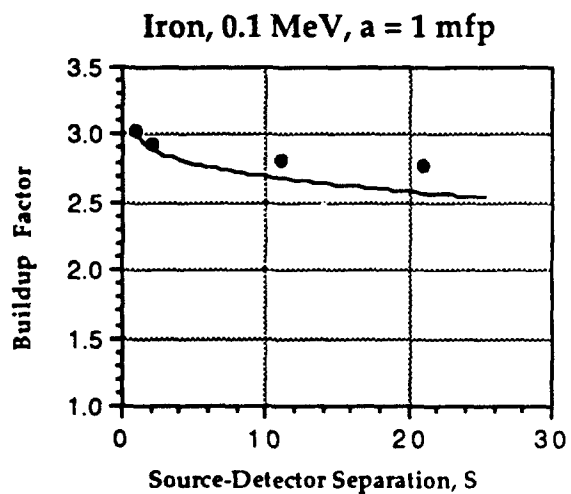
The model for g_M is a correction factor that reduces the buildup factor as the source-detector separation, S , increases. In Figure 35, the product $B_0 g_M$ is shown as a function of S for four typical cases, selected arbitrarily. Without the correction factor, g_M , the modeled behavior would be constant, at the value $B_0 = B(a, S=1)$. Calculated buildup factors for Geometries A, B, F, and E, as determined by the GBAS and NBAS codes, are shown as the data points. The solid lines show the model of Equation (51), with g_M given by Equation (54) and the values for γ and ν taken from Table 27. Note that the fits shown are obviously not the best fits to the data points shown, but rather are averages over ranges of source energy and slab thickness. For source-detector separations of 10 to 30 slab thicknesses, the buildup factors are typically reduced by about 10 to 40 %, and the model for g_M obviously improves the fit to the data, in general. These results indicate that the simple two-parameter model of Equation (54) is able to approximately account for source-detector separation effects over broad source energy and slab thickness ranges.

SINGLE SLABS

The analysis of four sample problems (Geometries E, F, G, and H) provided a means to construct a simple two-parameter model for "correcting" the Geometry A model, G_M , for source-detector separation effects. With the models for G_M and g_M complete, it is now possible to test the developed aggregate model, $G_M g_M$, to see how well it compares to actual results for arbitrary source-slab-detector arrangements.



(a) Gamma Ray



(b) Neutron

FIGURE 35. PLOTS OF $B_0 g_M(S|a)$ VERSUS S FOR FOUR CASES

First, we consider the single-slab problem identified as Sample Problem 5 in Table 28 and Figure 36. This problem was specified in physical units; thus, the slab thickness varies in optical units, depending on the slab material and the source type and energy. Source spectra were specified in simple step-wise forms over five energy intervals, as shown in Table 28.

The GBAS and NBAS codes were used to generate dose equivalents at each average source energy, for both gamma rays and neutrons, for each of the six materials. These results were averaged over the energy spectra shown in Table 28, and total dose equivalents were calculated. Then, the WBAR code was used to determine the spectrum-averaged model parameters, and the models for G_M and g_M were used to generate estimated buildup factors and uncollided dose equivalents, as follows:

$$G_M = e^{\bar{\alpha}} [1 - e^{-\bar{\alpha}T}] \quad (55a)$$

$$g_M = \frac{1}{B_0} + \left[1 - \frac{1}{B_0}\right] e^{-\gamma[(S-1)\bar{\sigma}T]^\gamma} \quad (55b)$$

$$B = G_M g_M \quad (55c)$$

TABLE 28. DESCRIPTION OF SAMPLE PROBLEM 5*

Interval, i	E_{i-1} (MeV)	E_i (MeV)	ΔE_i (MeV)	\bar{E}_i (MeV)	$S(E_i)$ (MeV ⁻¹)	$\sum_{j=1}^i S(E_j) \Delta E_j$
(a) Gamma Rays						
1	0	1	1	0.5	0.0401	0.0401
2	1	2	1	1.5	0.1785	0.2186
3	2	3	1	2.5	0.2942	0.5128
4	3	5	2	4.0	0.1952	0.9032
5	5	7	2	6.0	0.0484	1.0000
(b) Neutrons						
1	0	0.001	0.001	0.0005	0.1665	0.0002
2	0.001	1	0.999	0.4995	0.1335	0.1335
3	1	5	4	3.0	0.1000	0.5335
4	5	10	5	7.5	0.0665	0.8660
5	10	14	4	12.0	0.0335	1.0000

* $h_s = 30.48$ cm, $z_D = 304.8$ cm, $\rho_D = 0$, $T = 2.54$ cm

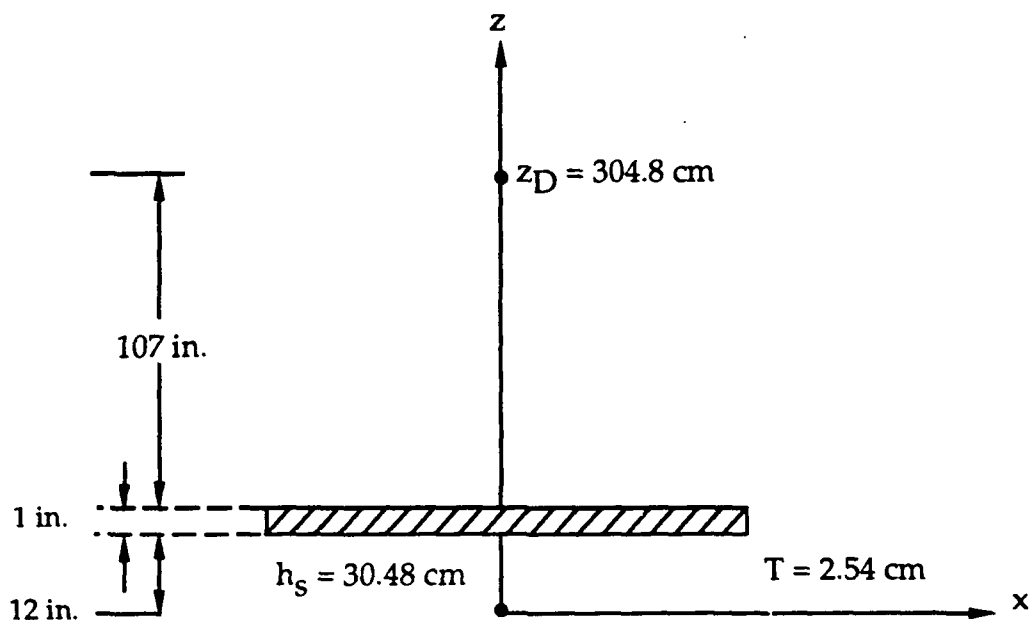


FIGURE 36. GEOMETRICAL ARRANGEMENT FOR SAMPLE PROBLEM 5

and

$$H_0 = \frac{\bar{h}_\phi e^{-\bar{\sigma}T}}{4\pi R^2}, \quad (55d)$$

where $S = R/T$, with $R = z_D = 304.8$ cm and $T = 2.54$ cm. Finally, dose equivalents at the detector point were estimated from the following

$$H = B H_0. \quad (56)$$

The constants obtained by the WBAR code for the spectra in Table 28 are given in Table 29. We note that $\bar{\sigma}$ and \bar{h}_ϕ are not really cross section and fluence-to-dose equivalent factors; rather they are parameters in the averaged model of Equation (34). (If \bar{h}_ϕ were simply the spectrum-averaged fluence-to-dose equivalent factor, it would not depend on the slab's material, as it does--to a small extent--in Table 29.) Also, it is noted that $\bar{\alpha}$ and β do not change substantially, regardless of the material, for gamma rays, whereas for neutrons the values for iron are noticeably different from those for the other materials. Again, this is a consequence of the fact that the model of Equation (34) was simply presumed to hold for slabs exposed to sources with distributed energies, and $\bar{\alpha}$ and β are empirical parameters whose values were determined to obtain the best overall fit. For a given material, as $\bar{\alpha}$ increases, β decreases, and the model is still well-behaved and fits the data quite well. A large value for $\bar{\alpha}$ generally results when there is little curvature to the $\ln B$ versus a curve--see, e.g., Figure 15 and Table 16, for iron exposed to neutrons.

TABLE 29. MODEL CONSTANTS OBTAINED BY THE WBAR CODE FOR THE SPECTRA OF TABLE 28

Material	$\bar{\alpha}$	$\bar{\beta}$	$\bar{\sigma}$ (cm ⁻¹)	\bar{h}_{ϕ} (mrem-cm ²)
(a) Gamma Rays				
Aluminum	1.895	0.1938	0.09004	0.003807
Iron	1.787	0.2384	0.2803	0.003714
Lead	2.439	0.1010	0.4926	0.003648
Water	2.570	0.1287	0.03628	0.003819
Polyethylene	2.483	0.1389	0.03469	0.003814
Concrete	2.176	0.1649	0.07882	0.003799
(b) Neutrons				
Aluminum	27.76	0.02658	0.1155	0.09515
Iron	383.7	0.002133	0.2254	0.08766
Lead	23.74	0.03537	0.1390	0.09540
Water	5.077	0.1020	0.1382	0.09020
Polyethylene	10.50	0.03454	0.1736	0.09408
Concrete	16.58	0.04533	0.1276	0.09161

The model results, using the parameter values in Table 29, are compared to the Monte Carlo results in Table 30. It is evident that the buildup factor models and the WBAR spectrum-averaging procedure work extremely well for single slabs which are perpendicular to the source-detector LOS. The dose equivalents obtained by the model are within a few percent of the Monte Carlo values for all cases except iron exposed to neutrons, for which the difference is only 13%.

INTERSECTING WALLS

We next considered Sample Problem 6, which is represented in Figure 37. The hemispherically domed cylinders of the geometry, shown in Figure 37(a), are treated in the slab approximation of Figure 37(b). The wall thicknesses shown are for steel, which is treated as 100% iron. Two cases are compared: (1), where the plenum of volume A is filled with air (treated as a vacuum); and (2), where the plenum is filled with water. The fission source is considered to be a point, with neutron and gamma-ray spectra as given in Table 31. The gamma-ray spectrum, representative of photon spectra from fission weapons, is taken from Glasstone and Dolan, pp. 360-1.¹⁴ The neutron spectrum is a discrete approximation to the ²³⁵U prompt neutron spectrum given by

$$S(E) = 0.453 e^{-1.036E} \sinh(\sqrt{2.29E}) , \quad (57)$$

TABLE 30. MODEL AND MONTE CARLO RESULTS FOR SAMPLE PROBLEM 5

		Dose Equivalent (units of 10^{-8} mrem)		% Difference
		Monte Carlo	Model	
(a)	Gamma Rays			
	Aluminum	0.2790	0.2768	0.8
	Iron	0.2086	0.1952	6.5
	Lead	0.1232	0.1150	6.6
	Water	0.2987	0.3057	2.3
	Polyethylene	0.2993	0.3062	2.3
	Concrete	0.2831	0.2822	0.3
(b)	Neutrons			
	Aluminum	7.378	7.065	4.2
	Iron	6.761	5.868	13.2
	Lead	7.243	7.009	3.2
	Water	6.150	6.198	0.8
	Polyethylene	5.933	5.870	1.1
	Concrete	7.035	6.769	3.8

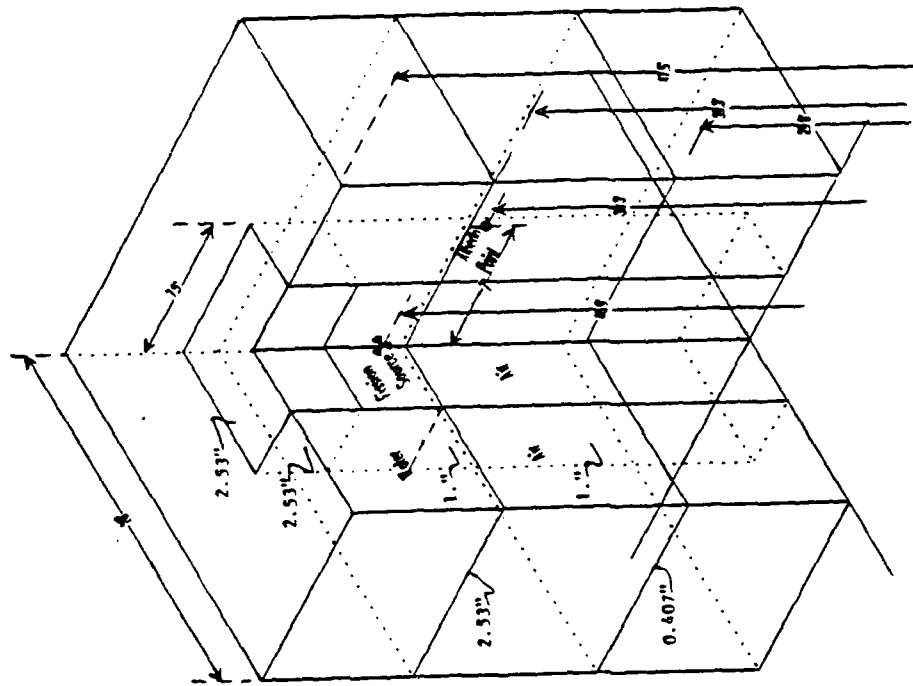
which is taken from Lamarsh.¹⁵ We show the gamma spectrum in Figure 38(a) and the neutron spectrum--as given by Equation (57) and its discrete approximation (see Table 31(b))--in Figure 38(b).

The LOS from source to detector intersects two of the iron slabs, as indicated in Figure 39(a); both are 2.53 in. or 6.4262-cm thick. The slant thicknesses, T_1 and T_2 , are 6.855 cm and 18.456 cm, respectively. When the plenum is filled with air (Sample Problem 6(a)), these are the only materials intersected by the LOS, and we treat this case as a single slab of total thickness $T = T_1 + T_2 = 25.311$ cm, as shown in Figure 39(b) with $T_3 = 0$. When the plenum is filled with water (Sample Problem 6(b)), the LOS also intersects $T_3 = 18.133$ cm of water. In Table 32, we give the spectrum averaged constants obtained from WBAR for the spectra of Table 31.

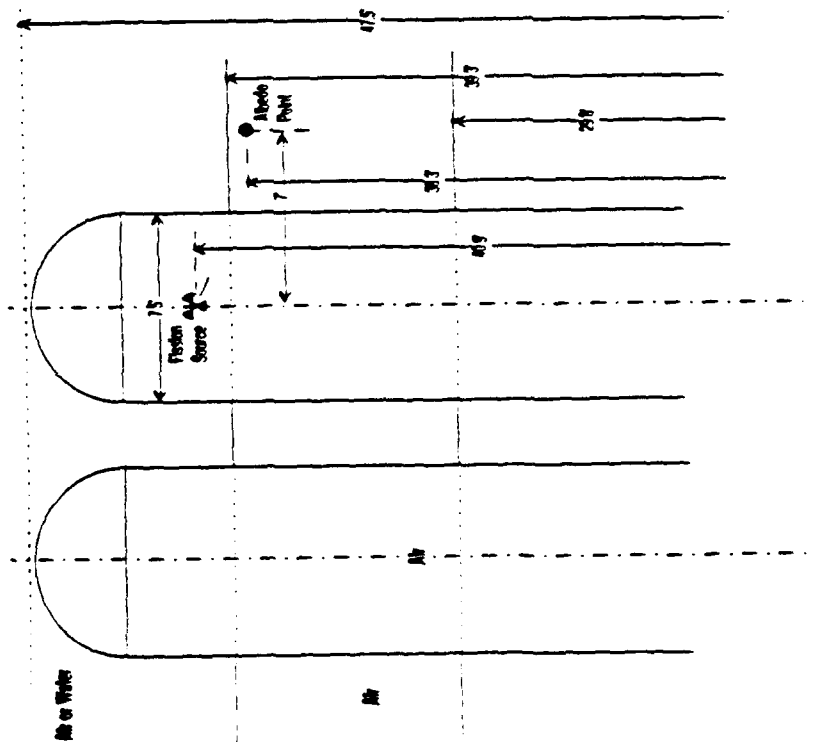
For Sample Problem 6(a), the single-slab procedure described on p. 79 was used with the following additional data

$$T = 25.311 \text{ cm}, \quad R = 227.60 \text{ cm}, \quad \gamma = 0.2057, \quad v = 0.0453$$

to obtain the model results shown in Table 33. Also shown in Table 33 are Monte Carlo results, obtained by averaging GBAS and NBAS code results for the problem described by Figure 37(b) over the spectra of Table 31. Note that the model results account for buildup



(b) Slab approximation



(a) Actual case

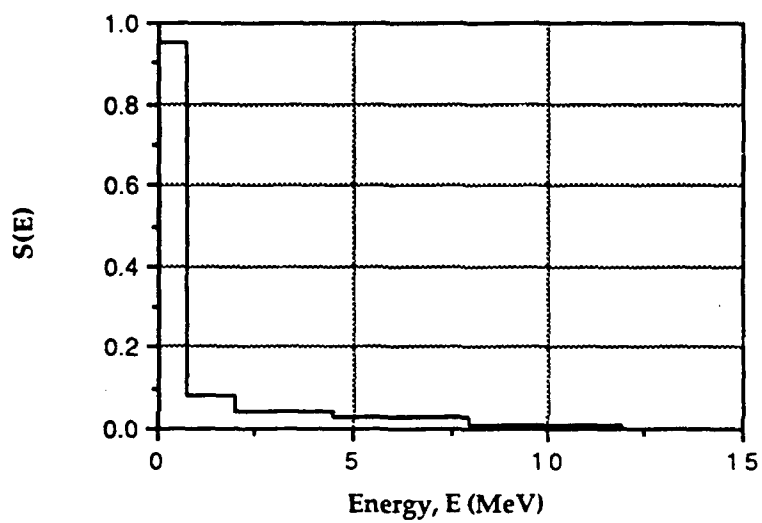
FIGURE 37. SAMPLE PROBLEM 6 DESCRIPTION

TABLE 31. ASSUMED SPECTRA FOR SAMPLE PROBLEM 6

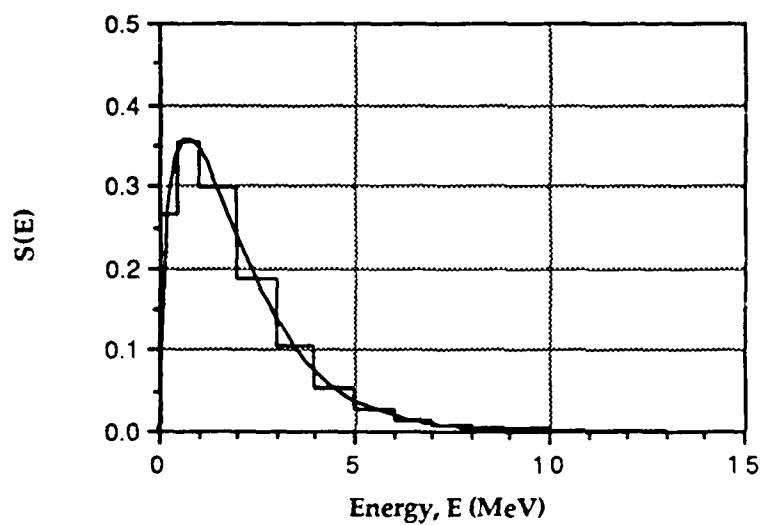
Interval, i	E_{i-1} (MeV)	E_i (MeV)	ΔE_i (MeV)	\bar{E}_i (MeV)	$S(E_i)$ (MeV ⁻¹)	$\sum_{j=1}^i S(E_j) \Delta E_j$
(a) Gamma Rays						
	0.01	0.51	0.50	0.26	0.946	0.473
	0.51	0.75	0.24	0.63	0.946	0.700
	0.75	1.25	0.50	1.00	0.080	0.740
	1.25	2.00	0.76	1.625	0.080	0.800
	2.00	3.00	1.00	2.5	0.036	0.836
	3.00	4.50	1.50	3.75	0.036	0.890
	4.50	6.00	1.50	5.25	0.025	0.928
	6.00	8.00	2.00	7.00	0.026	0.980
	8.00	10.00	2.00	9.00	0.005	0.990
	10.00	12.00	2.00	11.00	0.005	1.000
(b) Neutrons						
	0.0	0.5	0.5	0.25	0.2656	0.1328
	0.5	1.0	0.5	0.75	0.3540	0.3098
	1.0	2.0	1.0	1.5	0.2963	0.6061
	2.0	3.0	1.0	2.5	0.1857	0.7918
	3.0	4.0	1.0	3.5	0.1032	0.8950
	4.0	5.0	1.0	4.5	0.0538	0.9488
	5.0	6.0	1.0	5.5	0.0269	0.9757
	6.0	7.0	1.0	6.5	0.0130	0.9887
	7.0	8.0	1.0	7.5	0.0060	0.9947
	8.0	10.0	2.0	9.0	0.0022	0.9991
	10.0	13.0	3.0	11.5	0.0003	1.0000

only in the two slabs encountered along the LOS, whereas the Monte Carlo results account for interactions with all modeled surfaces; thus it is expected that the model results would be somewhat smaller than the Monte Carlo results, as is the case. Also, the model results implicitly assume that the intersected iron slabs extend infinitely at constant thickness, which is not the case, as shown in Figure 39(a).

For Sample Problem 6(b), we have to develop a methodology for using the single-slab buildup factor models for the case when slabs of different materials are encountered along the LOS. Since there is no *a priori* convention, we looked at two different methodologies. The objective of this project was to develop single-slab, not multiple-slab, models and so neither of the two methodologies described below may be optimum for treating multiple-slab cases. However, they do allow an initial look at how our single-slab models perform when applied to multiple slab cases.

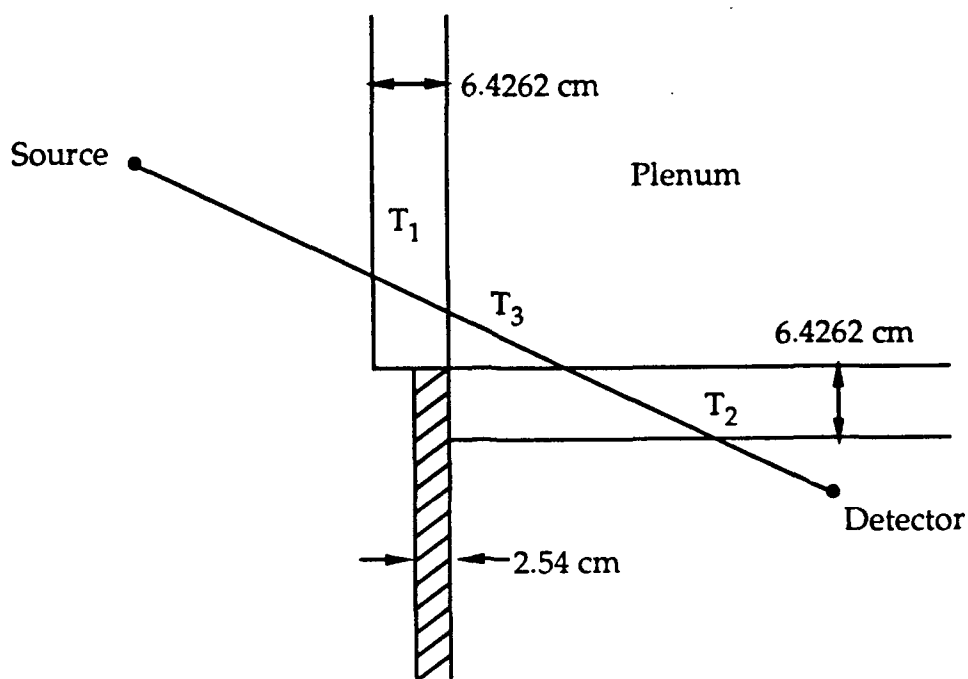


(a) Gamma rays

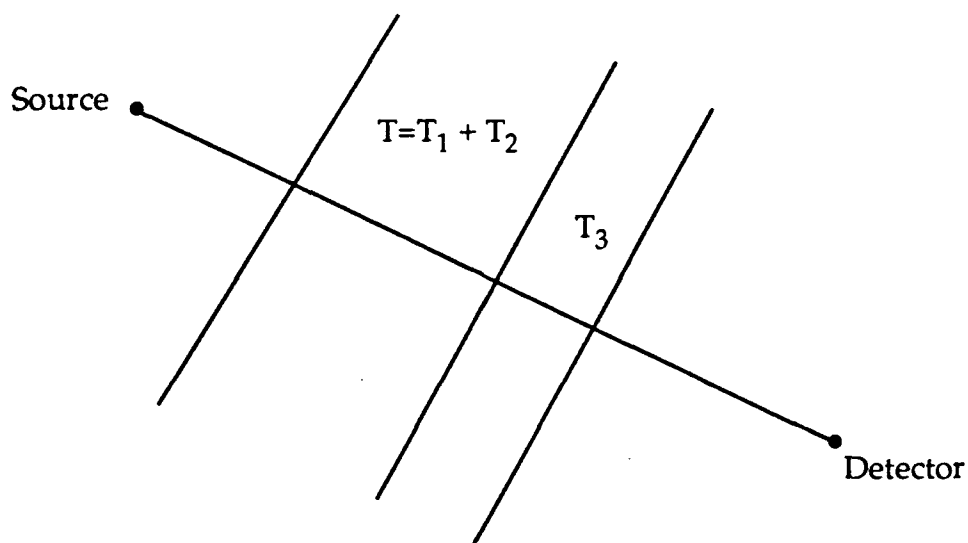


(b) Neutrons

FIGURE 38. ENERGY SPECTRA FOR SAMPLE PROBLEM 6



(a) Intersection of LOS with two iron walls and the plenum



(b) As treated for modeling purposes

(not to scale)

FIGURE 39. SCHEMATIC OF THE LOCAL GEOMETRY ALONG THE LOS FOR SAMPLE PROBLEM 6

NAVSWC TR 91-16

TABLE 32. MODEL CONSTANTS OBTAINED BY THE WBAR CODE FOR SAMPLE PROBLEM 6

	Material	$\bar{\alpha}$	$\bar{\beta}$	$\bar{\sigma}$ (cm ⁻¹)	\bar{h}_{ϕ} (mrem-cm ²)
(a) Gamma Rays					
	Iron	4.172	0.05595	0.2732	0.001891
	Water	1.024x10 ⁷	1.752x10 ⁻⁸	0.02958	0.001824
(b) Neutrons					
	Iron	139.1	0.005838	0.1362	0.1238
	Water	13.70	0.03136	0.1853	0.1370

TABLE 33. MODEL AND MONTE CARLO RESULTS FOR SAMPLE PROBLEM 6(a).

	Dose Equivalent (mrem)		% Difference
	Monte Carlo	Model	
Gamma Rays	1.647x10 ⁻¹¹	0.9223x10 ⁻¹¹	44.0
Neutrons	1.476x10 ⁻⁷	0.7326x10 ⁻⁷	50.4

In the first methodology, called Model A, we employ the following procedure:

1. Given the dimensions T , T_3 , and R and the model constants $\bar{\alpha}_1$, $\bar{\beta}_1$, $\bar{\sigma}_1$, $\bar{h}_{\phi 1}$, γ_1 , and v_1 , for iron and $\bar{\alpha}_2$, $\bar{\beta}_2$, $\bar{\sigma}_2$, $\bar{h}_{\phi 2}$, γ_2 , and v_2 for water we compute

$$a_1 = \bar{\sigma}_1 T , \quad (58a)$$

$$a_2 = \bar{\sigma}_2 T_3 , \quad (58b)$$

$$a = a_1 + a_2 , \quad (58c)$$

$$S = \frac{R}{T + T_3} , \quad (58d)$$

$$\hat{h}_{\phi} = \frac{a_1 \bar{h}_{\phi 1} + a_2 \bar{h}_{\phi 2}}{a} , \quad (58e)$$

and

$$\hat{H}_0 = \frac{\hat{h}_{\phi} e^{-a}}{4\pi R^2} . \quad (58f)$$

2. Then we develop new model constants

$$\hat{\alpha} = \exp\left[\frac{a_1 \ln \bar{\alpha}_1 + a_2 \ln \bar{\alpha}_2}{a}\right] , \quad (59a)$$

$$\hat{\beta} = \frac{a_1 \bar{\beta}_1 + a_2 \bar{\beta}_2}{a} , \quad (59b)$$

$$\hat{\gamma} = \frac{a_1 \gamma_1 + a_2 \gamma_2}{a} , \quad (59c)$$

and

$$\hat{v} = \frac{a_1 v_1 + a_2 v_2}{a} . \quad (59d)$$

The averaging of $\ln \bar{\alpha}$ instead of $\bar{\alpha}$ results from the fact that the exponent in G_M has $\bar{\alpha}$ as a linear factor and β in an exponential.

3. Then, we evaluate H as follows

$$G_M = e^{\hat{\alpha} [1 - e^{-\hat{\beta} a}]} = B_0 \quad (60a)$$

$$g_M = \frac{1}{B_0} + \left[1 - \frac{1}{B_0}\right] e^{-\hat{\gamma} [(S-1) a]^{\hat{\nu}}} \quad (60b)$$

$$\hat{B} = G_M f_M \quad (60c)$$

and

$$H = \hat{B} \hat{H}_0 . \quad (60d)$$

The Model B procedure utilizes Equations (58a through f), and then proceeds as follows:

$$b_{01} = \bar{\alpha}_1 (1 - e^{-\bar{\beta}_1 a_1}) , \quad (61a)$$

$$b_{02} = \bar{\alpha}_2 (1 - e^{-\bar{\beta}_2 a_2}) , \quad (61b)$$

$$g_1 = e^{-b_{01}} + (1 - e^{-b_{01}}) e^{-\gamma_1 [(S-1) a]^{\nu_1}} , \quad (61c)$$

$$g_2 = e^{-b_{02}} + (1 - e^{-b_{02}}) e^{-\gamma_2 [(S-1) a]^{\nu_2}} , \quad (61d)$$

$$\hat{B} = \exp \left\{ \frac{1}{2} (b_{01} + \ln g_1) (1 + e^{-\bar{\beta}_2 a_2}) + (b_{02} + \ln g_2) (1 + e^{-\bar{\beta}_1 a_1}) \right\} , \quad (61e)$$

and finally

$$H = \hat{B} \hat{H}_0 . \quad (61f)$$

The two models are compared to the Monte Carlo results in Table 34. We note that the $\bar{\alpha}_2$ constant obtained by WBAR for water exposed to gamma rays is abnormally large and the β_2 constant is correspondingly small (see Table 32). This is a consequence of the spectrum pre-averaging procedure used in WBAR, wherein the best mathematical fit of the assumed model is obtained. We can obtain the same value for G_M at $a = 7$ mfp using more reasonable values (e.g., $\bar{\alpha}_2 = 1000$ and $\beta_2 = 0.0001795$), and thus, we also show in Table 34 the dose equivalent obtained assuming these values.

TABLE 34. MODEL AND MONTE CARLO RESULTS FOR SAMPLE PROBLEM 6(b)

	Dose Equivalent (mrem)		
	Monte Carlo	Model A	Model B
Gamma Rays	1.401×10^{-11}	6.228×10^{-11}	0.5816×10^{-11}
Gamma Rays	1.401×10^{-11}	0.9881×10^{-11}	0.5448×10^{-11}
Neutrons	8.954×10^{-8}	2.994×10^{-8}	0.8110×10^{-8}

* Calculated assuming $\alpha = 1.024 \times 10^7$ and $\beta = 1.752 \times 10^{-8}$, for water.

** Calculated assuming $\alpha = 1,000$ and $\beta = 0.0001752$, for water.

We note that there are three major assumptions inherent in this comparison. The first assumption is that the solution to the idealized problem shown in Figure 39(b) is reasonably close to the solution of the actual problem shown in Figure 39(a). The second assumption is that the dose equivalent due to multiple slabs of different materials, as shown in Figure 39(b), can be determined from the model constants for the individual slabs, such as $\bar{\alpha}_1$, $\bar{\alpha}_2$, etc. We have shown two ways (Models A and B) of using those constants, but both are empirical, not rigorous. The third assumption is that the WBAR preaveraging procedure is valid even for multiple slabs. This is not clear since the WBAR code assumes the source spectrum for each slab, whereas the actual spectrum seen by the second slab is a modified version of the source spectrum.

The first assumption is suspect for several reasons. Essentially, we have assumed that the two iron walls intersected by the LOS extend infinitely at constant thickness whereas, in reality, they change thickness. The first wall changes from 6.2462 cm to 2.54 cm just below the intersection of the LOS, and the second changes to zero thickness just to the left of the intersection of the LOS. The idealized problem of Figure 39(b) does not account for any of the water in the plenum above a level of 6.314 cm, the height of the first point of the intersection of the LOS with the water. The actual dose equivalent at the detector point certainly is dependent on the volume of water in the plenum, but the idealized problem in no direct way accounts for that. Also, the modeled problem in essence assumes the water extends indefinitely to the left, which is not actually the case. These points can perhaps be appreciated by realizing that the problem shown in Figure 40 would also be modeled as shown in Figure 39(b); however, the dose equivalents for the problems of Figure 39(a) and Figure 40 would be expected to be quite different.

Given these points, and the fact that the buildup models do not account for albedo from any of the other walls shown in Figure 37, it is certainly encouraging that Model A gives dose equivalents that are within a factor of five of the Monte Carlo results (for both gamma rays and neutrons) and the Model B results are a factor of 2.4 times smaller (for gamma rays) and 11 times smaller (for neutrons) than the Monte Carlo results.

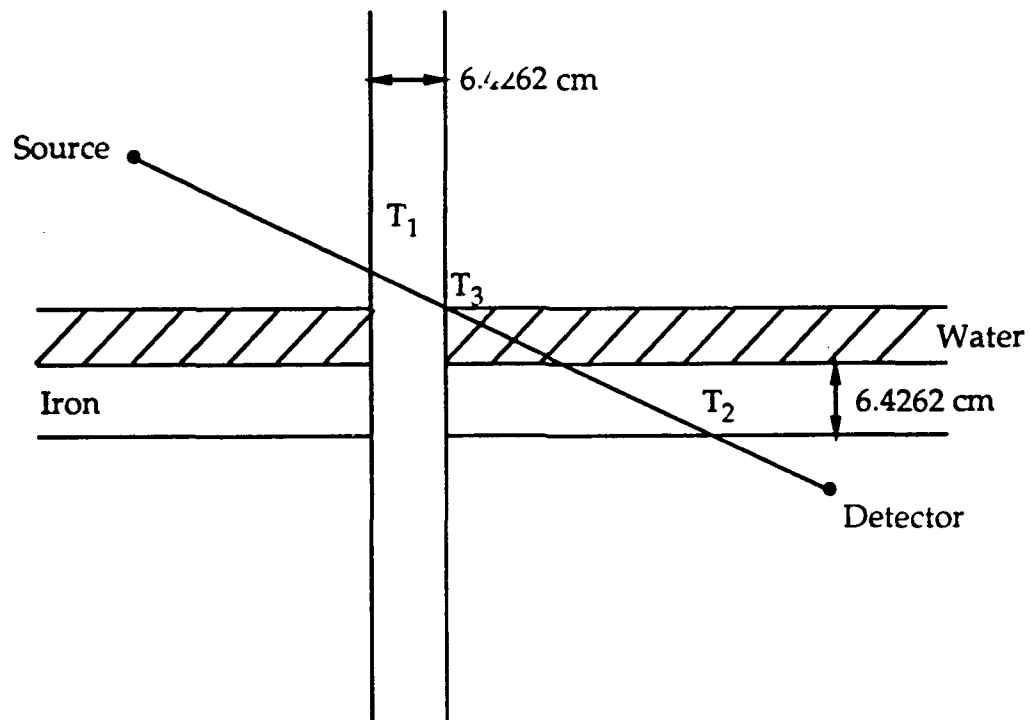


FIGURE 40. A HYPOTHETICAL PROBLEM WHICH WOULD BE MODELED AS SHOWN IN FIGURE 39(b)

CHAPTER 7

SUMMARY AND CONCLUSIONS

Dose equivalent buildup and albedo factors were calculated for uniform semi-infinite slabs, for both gamma-ray and neutron point sources. A single-scatter solution was constructed and the multiple-scatter contribution was determined by a Monte Carlo procedure. Two codes, GBAS for gamma-ray sources and NBAS for neutron sources, were constructed that utilize the single-scatter and Monte Carlo multiple-scatter models to estimate dose equivalent and dose equivalent buildup or albedo factor at an arbitrary point due to a monoenergetic point source located outside a uniform slab medium.

The dose equivalent buildup factor is defined as

$$B = \frac{H}{H_0} , \quad (62)$$

where H is dose equivalent at the detector point and H_0 is the uncollided contribution to the dose equivalent and is defined by

$$H_0 = \frac{S_0 h_\phi e^{-a}}{4\pi R^2} , \quad (63)$$

with S_0 the source strength, h_ϕ a fluence-to-dose equivalent conversion factor, a the slab thickness in mean free paths at the source energy, and R the source-detector separation. Here

$$a = \sigma T , \quad (64)$$

with σ the total macroscopic cross section of the slab material at the source energy and T the slab thickness in physical units.

The albedo factor is defined as

$$A = \frac{4\pi r_f^2 H}{h_\phi} , \quad (65)$$

where r_1 is image source-detector separation (the image source is a source point reflected about the slab mid-plane).

The slab buildup factors were fit to the following simplified parametric models

$$B = G_M(a) g_M(S|a), \quad (66)$$

where

$$G_M(a) = e^{\alpha[1-e^{-\beta a}]} \quad (67a)$$

and

$$g_M(S|a) = \frac{1}{B_0} + \left(1 - \frac{1}{B_0}\right) e^{-\gamma[(S-1)\sigma T]^\nu} \quad (67b)$$

In Equations (67a and b), α , β , γ , and ν are model parameters, B_0 is the buildup factor for the case $R = T$ (i.e., geometry A), and S is source-detector separation expressed in units of slab thickness, viz.

$$S = \frac{R}{T} \quad (68)$$

The parameters α and β are functions of source energy, whereas γ and ν are not. Also, for modeling purposes,

$$G_M(a) \equiv B_0 \quad (69)$$

The simplified model for albedo is

$$A = \alpha[1 - e^{-\beta a}] \quad (70)$$

where again α and β are model constants that are functions of source energy and a is slab thickness in mfp.

Models were also developed that can be used to estimate buildup and albedo factors and, from them, dose equivalents, for arbitrary gamma-ray and neutron spectra. The WBAR code was written to determine the model parameters for this energy-averaged model, for arbitrary spectra defined over suitable energy intervals. This model was shown to give reasonable results for single slabs.

The primary conclusions of the work carried out under this project can be summarized as:

- The developed single-scatter model provides an accurate and efficient method for estimating flux, fluence, and dose equivalent due to single scatters in slabs.
- The GBAS and NBAS codes can be used to estimate buildup and albedo factors for slabs composed of any of the six materials of interest (aluminum, iron, lead, water, polyethylene, and concrete) exposed to monoenergetic point sources of gamma rays and neutrons, respectively.
- The simple two-parameter models of Equations (67a) and (70) for buildup and albedo factors, respectively, fit the Monte Carlo results generated by GBAS and NBAS, for geometry A, extremely well over the ranges of source energy and slab thickness studied.
- The two-parameter model of Equation (67b) can be used to approximately correct the buildup factor model G_M for source-detector separation effects.
- The models of Equations (67a and b) are completely consistent with the MREMS code and thus may be used in place of the infinite media buildup factors currently used in MREMS.
- A model that can be applied to single slabs exposed to distributed-energy sources was developed and coded into the WBAR code.
- The models were demonstrated by considering 12 single-slab problems (one for each of the six slab materials, for both gamma-ray and neutron sources) for arbitrary source spectra; the results indicate that dose equivalent can generally be predicted by the simplified models to within a few percent (the largest percent difference from Monte Carlo results was 13.2%).
- Dose equivalents for complex intersecting arrangements of walls can be estimated to within an order of magnitude of Monte Carlo results, using various procedures for combining the single-slab models developed in this research.

REFERENCES

1. N.M. Schaeffer, Reactor Shielding for Nuclear Engineers, TID-25951, U.S. Atomic Energy Commission, 1973.
2. W.L. Dunn and C.E. Siewert, "The Searchlight Problem in Radiation Transport: Some Analytical and Computational Results," Z. angew. Math. Phys., Vol. 34, p. 627, 1983.
3. C.E. Siewert, "On the Singular Components of the Solution to the Searchlight Problem in Radiative Transfer," J. Quant. Spectrosc. Radiat. Transfer, Vol. 33, No. 6, p. 551, 1985.
4. C.E. Siewert and W.L. Dunn, "The Searchlight Problem in Radiative Transfer," J. Quant. Spectrosc. Radiat. Transfer, Vol. 41, No. 6, p. 467, 1989.
5. J.H. Hubbell, Photon Cross Sections, Attenuation Coefficients, and Energy Absorption Coefficients from 10 keV to 100 GeV, NSRDS-NBS-29, U.S. Department of Commerce, 1969.
6. J.H. Hubbell, H.A. Gimm, and I. Overbo, "Pair, Triplet, and Total Atomic Cross Sections, and Mass Attenuation Coefficients for 1 MeV-100 GeV Photons in Elements $Z = 1$ to 100," J. Phys. Chem. Ref. Data, Vol. 9, No. 4, p. 1023, 1980.
7. W.L. Dunn, A.M. Yacout, and F. O'Foghludha, Investigation of Shape and Composition Factors in Gamma-Ray Shielding, DNA-TR-86-129, Defense Nuclear Agency, 1986.
8. L.L. Carter and E.D. Cashwell, Particle-Transport Simulation with the Monte Carlo Method, TID-26607, U.S. Energy Research and Development Administration, 1975.
9. Los Alamos Monte Carlo Group, MCNP - A General Monte Carlo Code for Neutron and Photon Transport, LA-7396-M, Revised, Los Alamos National Laboratory, 1981.
10. D.K. Trubey, New Gamma-Ray Buildup Factor Data for Point Kernel Calculations: ANS-6.4.3 Standard Reference Data, ORNL/RSIC-49, Oak Ridge National Laboratory, 1988.

REFERENCES (Cont.)

11. W.L. Dunn and T.S. Dunn, "An Asymmetric Model for XPS Analysis," Surf. Interface Anal., Vol. 4, No. 3, p. 77, 1982.
12. P.R. Bevington, Data Reduction and Error Analysis for the Physical Sciences, McGraw-Hill, New York, 1969.
13. C. Eisenhauer, "An Image Source Technique for Calculating Reflection of Gamma-Rays or Neutrons," Health Phys., Vol. 11, p. 1145, 1965.
14. S. Glasstone and P.J. Dolan, Eds., The Effects of Nuclear Weapons, Third Edition, U.S. Department of Defense and U.S. Department of Energy, 1977.
15. J.R. Lamarsh, Introduction to Nuclear Reactor Theory, Addison-Wesley Publishing Co., Inc., Reading, MA, 1966.

NOMENCLATURE

ALPHABETICAL LISTING

<u>Symbol</u>	<u>Description</u>	<u>Units</u>
a	Slab thickness	mfp ¹
A	Albedo factor = $\frac{4\pi r_f^2 (H_1 + H_n)}{h_0}$	
A ₁	Single-scatter albedo factor = $\frac{4\pi r_f^2 H_1}{h_0}$	
B	Dose equivalent buildup factor	
B ₁	Single-scatter buildup factor = $1 + \frac{H_1}{H_0}$	
c	The ratio of scatter to total cross sections, σ_s/σ	
D	Absorbed dose	mrads
E	Radiation energy	MeV
E ₀	Source radiation energy	MeV
f (E' → E, Ω' → Ω)	Probability density function for scattering from energy E' and direction Ω' to energy E and direction Ω	
F	Fluence	cm ⁻²
g _M	Correction factor for source-detector separation	
G _M	Buildup factor model for geometry A	
h _D	Detector-to-slab distance	cm or mfp
h _φ	Fluence-to-dose equivalent conversion factor	mrem-cm ²
h _s	Source-to-slab distance	cm or mfp

¹ mean free path

NAVSWC TR 91-16

NOMENCLATURE (Cont.)

<u>Symbol</u>	<u>Description</u>	<u>Units</u>
H	Dose equivalent	mrem
H ₀	Dose equivalent at detector point due to uncollided radiation	mrem
H ₁	Dose equivalent at detector point due to once-scattered radiation	mrem
H _n	Dose equivalent at detector point due to multiply scattered radiation	mrem
L _{max}	Maximum track length to escape the slab	cm
μ	$\cos \theta$, the z-direction cosine of Ω	
ω	Vector specifying the projection of Ω into the x-y plane	
Ω	Solid angle unit vector, specifying direction of radiation propagation	ster
p	Path length from slab entry point to interaction point	cm or mfp
ϕ	Azimuthal angle between x-axis and projection of Ω into x-y plane	rad
Φ	Flux	cm ⁻² -sec ⁻¹
Φ_1	Single-scatter flux, due to an isotropic point source	cm ⁻² -sec ⁻¹
Φ_{10}	Single-scatter flux, due to a beam incident on a slab in direction Ω_0	cm ⁻² -sec ⁻¹
Ψ	Angular flux	cm ⁻² -sec ⁻¹ -ster ⁻¹
q	Path length from interaction point to slab exit point	cm or mfp
Q	Quality factor	mrem/mrad
r	Distance from an interaction in the slab to the detector	cm or mfp
r ₁	Image source to detector distance	cm
R	Source-detector separation = $[x_D^2 + y_D^2 + z_D^2]$	cm
ρ, τ, z	Cylindrical coordinates	
ρ_d, τ_d, z_d	Cylindrical coordinates of the point that a radiation particle exits the slab	

NAVSWC TR 91-16

NOMENCLATURE (Cont.)

<u>Symbol</u>	<u>Description</u>	<u>Units</u>
ρ_D, τ_D, z_D	Cylindrical coordinates of detector point	
S	Source-detector separation expressed in multiples of slab thickness	
S_0	Source strength	sec^{-1}
σ	Macroscopic total cross section	cm^{-1}
σ_s	Macroscopic scatter cross section	cm^{-1}
T	Slab thickness	cm
θ	Polar angle between z-axis and Ω	rad
w_i	Weight fraction of element i	
x, y, z	Cartesian coordinates	
x_D, y_D, z_D	Cartesian coordinates of detector point	
ξ	Pseudo random number, uniformly distributed on the unit interval	
Z	Atomic number	

LETTERS AND SYMBOLS LISTING

<u>Symbol</u>	<u>Description</u>	<u>Units</u>
a	Slab thickness	mfp^1
A	Albedo factor = $\frac{4\pi r_f^2 (H_1 + H_n)}{h_0}$	
A_1	Single-scatter albedo factor = $\frac{4\pi r_f^2 H_1}{h_0}$	
B	Dose equivalent buildup factor	
B_1	Single-scatter buildup factor = $1 + \frac{H_1}{H_0}$	
c	The ratio of scatter to total cross sections, σ_s/σ	

¹ mean free path

NOMENCLATURE (Cont.)

<u>Symbol</u>	<u>Description</u>	<u>Units</u>
D	Absorbed dose	mrads
E	Radiation energy	MeV
E ₀	Source radiation energy	MeV
f (E' → E, Ω' → Ω)	Probability density function for scattering from energy E' and direction Ω' to energy E and direction Ω	
F	Fluence	cm ⁻²
g _M	Correction factor for source-detector separation	
G _M	Buildup factor model for geometry A	
h _D	Detector-to-slab distance	cm or mfp
h _φ	Fluence-to-dose equivalent conversion factor	mrem-cm ²
h _s	Source-to-slab distance	cm or mfp
H	Dose equivalent	mrems
H ₀	Dose equivalent at detector point due to uncollided radiation	mrems
H ₁	Dose equivalent at detector point due to once-scattered radiation	mrems
H _n	Dose equivalent at detector point due to multiply scattered radiation	mrems
L _{max}	Maximum track length to escape the slab	cm
p	Path length from slab entry point to interaction point	cm or mfp
q	Path length from interaction point to slab exit point	cm or mfp
Q	Quality factor	mrem/mrad
r	Distance from an interaction in the slab to the detector	cm or mfp
r _I	Image source to detector distance	cm
R	Source-detector separation = $[x_D^2 + y_D^2 + z_D^2]$	cm
S	Source-detector separation expressed in multiples of slab thickness	
S ₀	Source strength	sec ⁻¹

NAVSWC TR 91-16
NOMENCLATURE (Cont.)

<u>Symbol</u>	<u>Description</u>	<u>Units</u>
T	Slab thickness	cm
w_i	Weight fraction of element i	
x,y,z	Cartesian coordinates	
x_D,y_D,z_D	Cartesian coordinates of detector point	
Z	Atomic number	
μ	$\cos \theta$, the z-direction cosine of Ω	
ω	Vector specifying the projection of Ω into the x-y plane	
Ω	Solid angle unit vector, specifying direction of radiation propagation	ster
ϕ	Azimuthal angle between x-axis and projection of Ω into x-y plane	rad
Φ	Flux	$\text{cm}^{-2}\text{-sec}^{-1}$
Φ_1	Single-scatter flux, due to an isotropic point source	$\text{cm}^{-2}\text{-sec}^{-1}$
Φ_{10}	Single-scatter flux, due to a beam incident on a slab in direction Ω_0	$\text{cm}^{-2}\text{-sec}^{-1}$
Ψ	Angular flux	$\text{cm}^{-2}\text{-sec}^{-1}\text{-ster}^{-1}$
ρ,τ,z	Cylindrical coordinates	
ρ_d,τ_d,z_d	Cylindrical coordinates of the point that a radiation particle exits the slab	
ρ_D,τ_D,z_D	Cylindrical coordinates of detector point	
σ	Macroscopic total cross section	cm^{-1}
σ_s	Macroscopic scatter cross section	cm^{-1}
θ	Polar angle between z-axis and Ω	rad
ξ	Pseudo random number, uniformly distributed on the unit interval	

APPENDIX A
COMPUTER CODE DOCUMENTATION

15 PAGES

REFERENCED IN CHAPTER 1, INTRODUCTION, CHAPTER 3, SAMPLE RESULTS,
AND CHAPTER 4, ENERGY AVERAGING PROCEDURE

GBAS CODE

General:

GBAS is a program to compute photon dose buildup and albedo factors for infinite slabs. The code is written in standard FORTRAN 77. All subprograms used by the code are supplied except for the three subroutines DOSTIM, DOSDAT, and GETARG, and the function IARGC, which are part of the Microway NDP FORTRAN Library and are machine dependent. Most FORTRAN compilers supply equivalent routines. Quantum has similar routines for the VAX-11 VMS and assembly routines for IBM PC/compatible DOS computers. These routines can be removed from the code without affecting the transport calculations.

DOSTIM is used to monitor the CPU time used by the code. If DOSTIM is removed, the CPU time write statement may also be removed (if it is kept, the program will print zero CPU time). DOSDAT is used to obtain the date from the machine code, and can be removed without further modifications. IARGC and GETARG are used to get user input file names from the command line. The current version of the code reads these names in two ways: from the command line or via a console dialog. In the command line mode, the user starts the program by typing:

RUN GBAS <input file> <output file>

where <input file> and <output file> are appropriate file names. If either or both of the file names are missing from the command line, the program enters the dialog mode and requests the missing name from the user. Thus, removing IARGC and GETARG will simply put the program in the dialog mode permanently.

Input:

GBAS requires three standard ASCII input files; a user input file, a cross section file, and a quadrature file. The user-input file name is supplied by the user, the cross section file name is GAMMA.LIB. The quadrature file contains the nodes and weights for the Gauss-Legendre quadrature. Its name is identified by the code according to the requested number of nodes. The user input file contains a description of the case or cases he desires to run. Each case is described by the following lines:

- Case Title (up to 80 characters): brief title of the case.
- Geometry (4 real numbers): a , h_s , p_D , z_D ; i.e., slab thickness, source-to-slab distance, detector radial distance from z-axis, and detector z-coordinate. If the slab thickness is input as a negative number, the code assumes all dimensions are in mean free path at the source photon energy, otherwise all dimensions are assumed to be in inches.
- Slab Composition (1 integer and 1 real number): number of elements and density (in gm/cc).

NAVSWC TR 91-16

- Slab Elements Description (1 integer and 1 real number): element index, as described in GAMMA.LIB, and weight fraction. Repeat for each element.
- Detector Composition (1 integer and 1 real number): number of elements and density (in gm/cc).
- Detector Elements Description (1 integer and 1 real number); element index, as described in GAMMA.LIB, and weight fraction. Repeat for each element.
- Quadrature Orders for the Single-Scatter Integral (3 integer numbers): number of z-nodes, number of θ -nodes, and number of ϕ -nodes.
- Control Parameters (3 integer numbers): multiple scatter control (0: no multiple scatter), Rayleigh scatter control (0: suppress Rayleigh scatter), and track sampling control (0: allow photon to escape, 1: force photon interactions within the slab).
- Monte Carlo Parameters, if multiple scatter control is not zero (3 integers and 2 real numbers): number of histories, random number generator seed, maximum number of scatters allowed per history, weight for history termination, and photon termination energy (MeV).
- Source Energy (1 real number): source photon energy in MeV (between 0.01 and 20 MeV).

A sample input file is shown in Figure A-1. Notice that no specific formats are required; commas (or other acceptable delimiters) are used to separate the input entries in a record. Note also that any number of cases can be stacked; the code terminates when it reaches the end of the file.

Output:

Output from the GBAS code is stored in a standard ASCII file (name supplied by the user) on the current (default) disk drive and directory. The first part of the output file (for every input case) is a detailed printout of the user input. The GBAS code checks the input for invalid data. If invalid data are encountered, a message is printed immediately following the input where the error was detected; the same message is also displayed at the user terminal and the program is terminated. In the second part of the output, the results of the calculations are presented. The calculated fluxes and the cross sections at the source energy are printed, in addition to the calculated doses and dose buildup factors. At the end of each case the program prints the CPU time and elapsed time used to complete the calculations. Figure A-2 shows the output file generated by the input file of Figure A-1.

```

IRON-0.1MEV- 0.5MFP
-.5,0.0,0.0,5.5
1,7.86
26,1.
2,1.
1,0.1119457
8,0.8885126
10,10,10
1,0,1
100,555,30,.000001,.01
0.1

```

FIGURE A-1. SAMPLE GBAS CODE INPUT FILE

NBAS CODE

General:

NBAS is a program to compute neutron dose buildup and albedo factors for infinite slabs. The code is written in standard FORTRAN 77. All subprograms used by the code are supplied except for the three subroutines DOSTIM, DOSDAT, and GETARG, and the function IARGC, which are part of the Microway NDP FORTRAN Library and are machine dependent. These routines can be removed from the code without disabling the transport calculations; their purpose and use are as described for the GBAS code.

In the command line mode, the user starts the program by typing:

```
RUN NBAS <input file> <output file>
```

where <input file> and <output file> are appropriate file names. If either or both of the file names are missing from the command line, the program enters the dialog mode and requests the missing name from the user.

GBAS V1.0
TUS-10/24/1989
13:03:55
IRON-0.1MEV- 0.5MFP

PAGE 1

INPUT FROM: IRONF.TST
OUTPUT TO: IRONF.OUT

GEOMETRY:

SLAB THICKNESS (MFP): -.5000
SOURCE-TO-SLAB DISTANCE (MFP): .0000
DETECTOR COORDINATES (MFP): .0000 , .0000 , 5.500

DETECTOR LOCATION RELATIVE TO SOURCE:

RADIAL DISTANCE (MFP) LOS ANGLE (RAD.) SOURCE DISTANCE (MFP)
.0000 .0000 5.500

SLAB COMPOSITION:

NUMBER OF ELEMENTS: 01 DENSITY (GM/CC): 7.860

ELEMENT	INDEX	WEIGHT FRACTION
01	26	1.000

DETECTOR COMPOSITION:

NUMBER OF ELEMENTS: 02 DENSITY (GM/CC): 1.000

ELEMENT	INDEX	WEIGHT FRACTION
01	01	.1119
02	08	.8881

QUADRATURES:

NUMBER OF TRACK NODES: 010
NUMBER OF POLAR ANGLE NODES: 010
NUMBER OF AZIMUTHAL ANGLE NODES: 010

CONTROL PARAMETERS:

MULTIPLE SCATTER CONTROL: 1 0=NO
RAYLEIGH SCATTER CONTROL: 0 0=NO
TRACK SAMPLING CONTROL: 1 0=ALLOW ESCAPE, 1=NO ESCAPE

MONTE CARLO PARAMETERS (MULTIPLE SCATTER):

NUMBER OF HISTORIES: 00000100
RANDOM NUMBER SEED: 00000555
MAXIMUM NUMBER OF SCATTERS/HISTORY: 00000030
HISTORY TERMINATION WEIGHT: .1000E-05
HISTORY TERMINATION ENERGY: .1000E-01

SOURCE ENERGY (MEV): .1000

FIGURE A-2. SAMPLE GBAS CODE OUTPUT FILE

NAVSWC TR 91-16

GBAS V1.0
TUS-10/24/1989
13:03:55
IRON-0.1MEV- 0.5MFP

PAGE 2

SLAB CROSS SECTION EDIT (1/CM):					
ENERGY MEV	COMPTON	RAYLEIGH	PAIR	TOTAL	AVG. ENERGY LOSS
.100	1.083	.0000	.0000	2.700	.2557E-02

LOS MEAN FREE PATH: .5000

AVERAGE NUMBER OF SCATTERS/HISTORY: 6.140

FLUX EDIT:				
UNCOLLIDED	SINGLE SCATTER	HIGH ORDER SCATTER	TOTAL SCATTER	SINGLE/TOTAL
.1163E-01	.1901E-02	.2617E-03	.2163E-02	.8790
		+/- 8.61%	+/- 1.04%	

DOSE EQUIVALENT EDIT (MREM/HR):				
UNCOLLIDED	SINGLE SCATTER	HIGH ORDER SCATTER	TOTAL SCATTER	SINGLE/TOTAL
.1715E-05	.2557E-06	.3217E-07	.2879E-06	.8882
		+/- 8.89%	+/- .99%	

BUILDUP EDIT:			
SINGLE SCATTER	HIGH ORDER SCATTER	TOTAL SCATTER	SINGLE/TOTAL
1.149	1.019	1.168	.9839
	+/- .16%	+/- .14%	

TOTAL CPU, INCLUDING I/O=	30.260000	SEC.
TOTAL CPU, EXCLUDING I/O=	27.740000	SEC.

FIGURE A-2. SAMPLE GBAS CODE OUTPUT FILE (Cont.)

Input:

NBAS requires a binary direct access cross section file and two standard ASCII input files: a user input file, and a quadrature file. The name of the cross section file, which is produced by the XSDBASE code supplied the NBAS code, is NEUTRON.LIB, the user-input file name is supplied by the user. Quadrature files contain the nodes and weights of a Gauss-Legendre quadrature. Their names are identified by the code according to the requested number of nodes. The user input file contains a description of the case or cases he desires to run. Each case is described by the following lines:

- Case Title (up to 80 characters): brief title of the case.
- Geometry (4 real numbers): a , h_s , ρ_D , z_D ; i.e., slab thickness, source-to-slab distance, detector radial distance from z-axis, and detector z-coordinate. If the slab thickness is input as a negative number, the code assumes that all dimensions are in mean free paths at the source photon energy, otherwise all dimensions are assumed to be in inches.
- Slab Composition: 1 integer and 1 real number: number of elements and density (in gm/cc).
- Slab Elements Description (1 integer and 2 real numbers): element index, as described in NEUTRON.LIB, weight fraction, and atomic weight (amu). Repeat for all elements.
- Quadrature Orders for the Single-Scatter Integral (3 integer numbers): number of z-nodes, number of θ -nodes, and number of ϕ -nodes.
- Control Parameters (3 integer numbers): multiple scatter control (0: no multiple scatter), track sampling control (0: allow neutron to escape, 1: force neutron interactions within the slab).
- Monte Carlo Parameters, if multiple scatter control is not zero (3 integers and 2 real numbers): number of histories, random number generator seed, maximum number of scatters allowed per history, weight for history termination, and photon termination energy (MeV).
- Source Energy (1 real number): source photon energy in MeV.

A sample input file is shown in Figure A-3. Notice that no specific formats are required; commas (or other acceptable delimiters) are used to separate the input entries in a record. Multiple cases are run by stacking input; the code terminates when it reaches the end of the file.

```

IRON-1.e-7MEV- 0.5MFP
-0.5,0.0,0.0,-5.5
1,7.86
26,1.0,55.847
10,10,10
1,1
1000,555,30,.000001,1.E-8
1.e-7

```

FIGURE A-3. SAMPLE NBAS CODE INPUT FILE

Output:

Output from the NBAS code is stored in a standard ASCII file (name supplied by the user) on the current (default) disk drive and directory. The first part of the output file (for every input case) is a detailed printout of the user input. The NBAS code checks the input for invalid data. If invalid data are encountered, a message is printed immediately following the input where the error was detected; the same message is also displayed at the user terminal and the program is terminated. In the second part of the output, the results of the calculations are presented. The calculated fluxes and the cross sections at the source energy are also printed, in addition to the calculated doses and dose buildup factors. At the end of each case the program prints the CPU time and elapsed time used to complete the calculations. Figure A-4 shows the output file generated by the input file of Figure A-3.

WBAR CODE

General:

WBAR is a program to compute spectrum-averaged buildup or albedo model parameters as well as averaged total cross section and flux-to-dose conversion factors. Unlike the GBAS and NBAS codes, all subprograms used by the code are supplied. File names for input and output are supplied by the user in the dialog mode only.

NBAS-V1.0
TUS-10/24/1989
16:59:55
IRON-1.e-7MEV- 0.5MFP

PAGE 1

INPUT FROM: IRONB_N.TST
OUTPUT TO: IRONB_N.OU3

GEOMETRY:
SLAB THICKNESS (MFP): -.5000
SOURCE-TO-SLAB DISTANCE (MFP): .0000
DETECTOR COORDINATES (MFP): .0000 , .0000 , -5.500

DETECTOR LOCATION RELATIVE TO SOURCE:
RADIAL DISTANCE (MFP) LOS ANGLE (RAD.) SOURCE DISTANCE (MFP)
.0000 3.142 5.500

THIS CASE IS A REFLECTION CASE:

IMAGE DETECTOR Z-COORDINATE (MFP): 6.000
IMAGE DETECTOR-TO-SOURCE DISTANCE (MFP): 6.000

SLAB COMPOSITION:
NUMBER OF ELEMENTS: 1 DENSITY (GM/CC): 7.860

ELEMENT	INDEX	AMU	WEIGHT FRACTION
1	26	55.85	1.000

QUADRATURES:
NUMBER OF TRACK NODES: 10
NUMBER OF POLAR ANGLE NODES: 10
NUMBER OF AZIMUTHAL ANGLE NODES: 10

CONTROL PARAMETERS:
MULTIPLE SCATTER CONTROL: 1 0=NO
TRACK SAMPLE CONTROL: 1 0=ALLOW ESCAPE, 1=NO ESCAPE

MONTE CARLO PARAMETERS (MULTIPLE SCATTER):
NUMBER OF HISTORIES: 1000
RANDOM NUMBER SEED: 555
MAXIMUM NUMBER OF SCATTERS/HISTORY: 30
HISTORY TERMINATION WEIGHT: .1000E-05
HISTORY TERMINATION ENERGY (MEV): .1000E-07

SOURCE ENERGY (MEV): .1000E-06

FIGURE A-4. SAMPLE NBAS CODE OUTPUT FILE

NAVSWC TR 91-16

NBAS-V1.0
TUS-10/24/1989
16:59:55
IRON-1.e-7MEV- 0.5MFP

PAGE 2

SLAB CROSS SECTION EDIT (1/CM)

SOURCE ENERGY MEV	ELASTIC	INELASTIC	ABSORPTION	TOTAL
.1000E-06	.9663	.0000	.1092	1.075

LOS MEAN FREE PATH: .5000

AVERAGE NUMBER OF SCATTERS/HISTORY: 10.97

FLUX EDIT:

SINGLE SCATTER	HIGH ORDER SCATTER	TOTAL SCATTER	SINGLE/TOTAL
.7200E-03	.4365E-03	.1157E-02	.6226
	+/- 2.73%	+/- 1.03%	

DOSE EQUIVALENT EDIT (MREM/HR):

SINGLE SCATTER	HIGH ORDER SCATTER	TOTAL SCATTER	SINGLE/TOTAL
.3160E-05	.1914E-05	.5074E-05	.6229
	+/- 2.73%	+/- 1.03%	

ALBEDO EDIT (MREM*CM*CM/HR):

SINGLE SCATTER	HIGH ORDER SCATTER	TOTAL SCATTER	SINGLE/TOTAL
.1236E-02	.7485E-03	.1985E-02	.6229
	+/- 2.73%	+/- 1.03%	

TOTAL CPU, INCLUDING I/O=	329.99000	SEC.
TOTAL CPU, EXCLUDING I/O=	306.21000	SEC.

FIGURE A-4. SAMPLE NBAS CODE OUTPUT FILE (Cont.)

Input:

In addition to an ASCII user input file, WBAR requires the GAMMA.LIB and NEUTRON.LIB cross section files described for the GBAS and NBAS codes. The user input file contains a description of the case or cases he wishes to run. Each case is described by the following lines:

1. Case Title (up to 80 characters): brief title of the case.
2. Options (4 integers): spectrum type (0: gamma source, 1: neutron source); spectrum yield input method (0: input in this file, 1: calculated using the user supplied function SPECTR(E) to evaluate the density, S(E), at energy E); case factor type (0: buildup, 1: albedo); type of run (0: no fitting, just print spectrum averaged doses, 1: fit to $e^{\alpha(1-e^{-\beta a})}$ for buildup or $\alpha(1-e^{-\beta a})$ for albedo).
3. Slab Composition (1 integer, 1 real number): number of elements and density (in gm/cc).
4. Description of Slab Elements
 - Gamma spectrum (1 integer, 1 real number): element index as described in GAMMA.LIB and weight fraction;
 - Neutron spectrum (1 integer, 2 real numbers): element index as described in NEUTRON.LIB, weight fraction, and element atomic mass (amu).

Repeat for each element.
5. Spectrum Description (1 integer, 1 real number): number of energy intervals, energy of the left boundary of the first interval (in MeV).
6. Spectrum Energy Intervals (real numbers*): interval average energy. Repeat for all intervals.
7. Spectrum Yield, if yield option is 0 (real numbers): spectrum yield in each interval, use positive values for average number of particles per unit energy between the interval boundaries and negative values for total number of particles in the interval.
8. Buildup/Albedo Calculation Number of Points (2 integers): number of points in buildup/albedo calculation table and number of slab thicknesses to use in fitting spectrum model parameters.
9. Buildup/Albedo Calculation Model Parameters (3 real numbers): energy (in MeV), α , and β . Repeat for number of table points.

* One or more real numbers per input line as appropriate for a record of 80 bytes.

10. Model Fitting Slab Thickness (real numbers): slab thicknesses (in mfp) to use in fitting spectrum model parameters. Repeat for number of data points.

A sample input file is shown in Figure A-5. Notice that no specific formats are required; commas (or other delimiters) are used to separate the input entries in a record. Note also that any number of cases can be stacked; the code terminates when it reaches the end of file.

Output:

Output from the WBAR code is stored in a standard ASCII file (name supplied by the user) on the current (default) disk drive and directory. The first part of the output file (for every input case) is a detailed printout of the user input. The WBAR code checks the input for invalid data. If invalid data are encountered, a message is printed immediately following the input where the error was detected; the same message is also displayed at the user terminal and the program is terminated. In the second part of the output, the results of the calculations are presented. The calculated buildup or albedo factors from the spectrum model and from the spectrum averaging for every energy interval are printed, in addition to the averaged flux-to-dose conversion factor, the averaged total cross section, and $\bar{\alpha}$ and β . Figure A-6 shows a sample output file that was generated by the input file of Figure A-5.

```
POLY AVERAGE BUILDUP FACTORS FOR SAMPLE PROBLEM SPECTRUM, GAMMA .
0,0,0,1
2,0.9500
1,0.1438
6,0.8562
5,0.01
0.5,1.5,2.5,4.0,6.0
-.053,-0.236,-.389,-.258,-.064
9,8
0.10,9.2795,-0.11251
0.20,8.9009,-0.095266
0.40,5.2734,-0.14796
0.60,4.3754,-0.16709
0.80,3.7495,-0.17971
1.00,5.2524,-0.10787
3.00,1.9444,-0.27952
5.00,1.3687,-0.33572
7.00,1.6009,-0.24609
.5,1.,2.,3.,4.,5.,6.,7.
```

FIGURE A-5. SAMPLE WBAR CODE INPUT FILE

POLY AVERAGE BUILDUP FACTORS FOR SAMPLE PROBLEM SPECTRUM, GAMMA.

INPUT FROM: POLYG.IN
OUTPUT TO: TPOLY2.OUT

****INPUT EDIT****

OPTIONS:

SOURCE TYPE= 0 , 0=GAMMA, 1=NEUTRON
SOURCE YIELD= 0 , 0=INPUT, 1=USE SPECTR FUNCTION
FACTOR TYPE= 0 , 0=BUILDUP, 1=ALBEDO
RUN TYPE= 1 , 1=EXP(G) OR G MODEL FITTING, 0=NO MODEL FITTING

SLAB COMPOSITION:

NUMBER OF ELEMENTS: 02 DENSITY (GM/CC): 0.9500

ELEMENT	INDEX	WEIGHT FRACTION
01	01	0.1438
02	06	0.8562

SOURCE SPECTRUM:

NUMBER OF ENERGY INTERVALS= 5
FIRST INTERVAL LEFT BOUNDARY (MEV)= 0.1000E-01

ENERGY(MEV)	FRACTIONAL YIELD
0.5000	0.5300E-01
1.500	0.2360
2.500	0.3890
4.000	0.2580
6.000	0.6400E-01

DOSE CALCULATION MODEL PARAMETERS:

ENERGY(MEV)	ALPHA	BETA
0.1000	9.280	-0.1125
0.2000	8.901	-0.9527E-01
0.4000	5.273	-0.1480
0.6000	4.375	-0.1671
0.8000	3.750	-0.1797
1.000	5.252	-0.1079
3.000	1.944	-0.2795
5.000	1.369	-0.3357
7.000	1.601	-0.2461

DATA FOR FITTING OR SPECTRUM DOSE CALCULATIONS:

DATA POINT	SLAB THICKNESS (MFP)
1	0.5000
2	1.000
3	2.000
4	3.000
5	4.000
6	5.000
7	6.000
8	7.000

****OUTPUT EDIT****

SPECTRUM AVERAGEC MODEL PARAMETERS:

ALPHA= 2.483 BETA=-0.1389 CHI-SQUARE= 0.8572E-09

AVERAGED TOTAL ATTENUATION CROSS SECTION (1/CM)= 0.3469E-01
AVERAGE FLUX-TO-DOSE CONVERSION FACTOR (MREM/HR)= 0.3814E-02

FIGURE A-6. SAMPLE WBAR CODE OUTPUT FILE

POLY AVERAGE BUILDUP FACTORS FOR SAMPLE PROBLEM SPECTRUM, GAMMA.

SLAB THICKNESS (MFP)	BUILDUP/ALBEDO ACTUAL	BUILDUP/ALBEDO MODEL FIT	ERROR%
0.1831	1.038	1.064	2.6
0.3099	1.095	1.110	1.4
0.3662	1.121	1.131	0.9
0.4091	1.140	1.147	0.6
0.5311	1.196	1.193	-0.2
0.6198	1.237	1.227	-0.8
0.6609	1.256	1.243	-1.0
0.7323	1.289	1.272	-1.4
0.8183	1.329	1.306	-1.7
1.062	1.443	1.406	-2.5
1.098	1.460	1.421	-2.6
1.240	1.525	1.481	-2.9
1.322	1.564	1.517	-3.0
1.465	1.631	1.580	-3.1
1.637	1.711	1.657	-3.2
1.831	1.802	1.747	-3.1
1.859	1.815	1.760	-3.0
2.124	1.939	1.886	-2.7
2.197	1.973	1.922	-2.6
2.455	2.093	2.049	-2.1
2.479	2.104	2.062	-2.0
2.563	2.144	2.104	-1.8
2.644	2.181	2.145	-1.6
3.099	2.394	2.384	-0.4
3.186	2.435	2.431	-0.2
3.273	2.476	2.478	0.1
3.719	2.688	2.723	1.3
3.966	2.807	2.863	2.0
4.091	2.868	2.935	2.3
4.249	2.946	3.025	2.7
4.339	2.991	3.077	2.9
4.910	3.285	3.414	3.9
5.287	3.490	3.640	4.3
5.311	3.503	3.654	4.3
5.728	3.743	3.907	4.4
6.373	4.147	4.300	3.7
6.609	4.307	4.445	3.2
7.435	4.926	4.949	0.5
7.931	5.352	5.249	-1.9
9.253	6.735	6.028	-10.5

FIGURE A-6. SAMPLE WBAR CODE OUTPUT FILE (Cont.)

POLY AVERAGE BUILDUP FACTORS FOR SAMPLE PROBLEM SPECTRUM, GAMMA.

THICKNESS (CM)	ACTUAL DOSE MREM*CM**2/HR	MODEL DOSE MREM*CM**2/HR	%ERROR
5.277	0.3295E-02	0.3380E-02	-2.59
8.933	0.3063E-02	0.3106E-02	-1.41
10.55	0.2963E-02	0.2991E-02	-0.94
11.79	0.2889E-02	0.2906E-02	-0.61
15.31	0.2682E-02	0.2676E-02	0.25
17.87	0.2539E-02	0.2519E-02	0.78
19.05	0.2474E-02	0.2449E-02	1.00
21.11	0.2364E-02	0.2332E-02	1.36
23.59	0.2236E-02	0.2197E-02	1.74
30.62	0.1902E-02	0.1854E-02	2.54
31.66	0.1856E-02	0.1807E-02	2.63
35.73	0.1684E-02	0.1636E-02	2.90
38.10	0.1590E-02	0.1543E-02	3.01
42.22	0.1438E-02	0.1393E-02	3.13
47.17	0.1270E-02	0.1230E-02	3.16
52.77	0.1102E-02	0.1068E-02	3.07
53.60	0.1078E-02	0.1046E-02	3.04
61.23	0.8838E-03	0.8599E-03	2.71
63.33	0.8362E-03	0.8146E-03	2.59
70.76	0.6855E-03	0.6713E-03	2.08
71.46	0.6727E-03	0.6591E-03	2.03
73.88	0.6300E-03	0.6185E-03	1.84
76.20	0.5915E-03	0.5818E-03	1.64
89.33	0.4118E-03	0.4100E-03	0.43
91.85	0.3838E-03	0.3831E-03	0.18
94.35	0.3578E-03	0.3580E-03	-0.07
107.2	0.2487E-03	0.2520E-03	-1.33
114.3	0.2030E-03	0.2070E-03	-1.99
117.9	0.1829E-03	0.1871E-03	-2.32
122.5	0.1605E-03	0.1648E-03	-2.69
125.1	0.1489E-03	0.1532E-03	-2.90
141.5	0.9239E-04	0.9602E-04	-3.93
152.4	0.6729E-04	0.7018E-04	-4.30
153.1	0.6598E-04	0.6883E-04	-4.31
165.1	0.4645E-04	0.4848E-04	-4.37
183.7	0.2701E-04	0.2800E-04	-3.69
190.5	0.2214E-04	0.2285E-04	-3.20
214.3	0.1109E-04	0.1114E-04	-0.46
228.6	0.7337E-05	0.7196E-05	1.92
266.7	0.2462E-05	0.2204E-05	10.50

FIGURE A-6. SAMPLE WBAR CODE OUTPUT FILE (Cont.)

APPENDIX B

GAMMA-RAY BUILDUP FACTOR TABLES, GEOMETRIES A-D

19 PAGES

REFERENCED IN CHAPTER 1, INTRODUCTION, AND
CHAPTER 3, SAMPLE RESULTS

NAVSWC TR 91-16

TABLE B-1. GAMMA-RAY BUILDUP FACTORS FOR ALUMINUM, GEOMETRY A
($h_s = 0$, $\rho_D = 0$, $z_D = a$)

(a) Single-scatter

Thickness, a (mfp)	0.5	1.0	2.0	3.0	4.0	5.0	6.0	7.0
Energy (Mev)								
0.10	1.356	1.614	2.005	2.304	2.548	2.753	2.930	3.085
0.15	1.361	1.635	2.064	2.400	2.678	2.915	3.121	3.303
0.20	1.353	1.628	2.064	2.408	2.695	2.941	3.155	3.344
0.30	1.337	1.605	2.033	2.374	2.659	2.902	3.115	3.303
0.40	1.323	1.582	1.998	2.328	2.603	2.839	3.045	3.227
0.50	1.312	1.563	1.964	2.283	2.549	2.775	2.973	3.148
0.60	1.303	1.546	1.935	2.242	2.498	2.716	2.906	3.074
0.80	1.288	1.518	1.884	2.172	2.411	2.614	2.791	2.947
1.0	1.277	1.496	1.844	2.115	2.340	2.530	2.696	2.843
1.5	1.256	1.457	1.770	2.012	2.212	2.382	2.529	2.660
2.0	1.241	1.428	1.716	1.940	2.123	2.280	2.416	2.537
3.0	1.216	1.381	1.635	1.832	1.996	2.135	2.257	2.365
4.0	1.196	1.344	1.572	1.752	1.901	2.029	2.141	2.241
5.0	1.179	1.312	1.521	1.687	1.826	1.946	2.051	2.146
6.0	1.163	1.285	1.478	1.633	1.764	1.877	1.978	2.068
7.0	1.150	1.262	1.441	1.587	1.710	1.819	1.915	2.002

(b) Total

Energy (Mev)								
0.10	1.492	2.075	3.393	4.994	6.275	8.262	9.846	12.44
0.15	1.496	2.105	3.685	5.685	8.253	10.55	15.69	17.31
0.20	1.480	2.088	3.639	5.902	8.207	11.16	15.50	17.81
0.30	1.452	2.019	3.514	5.365	8.000	15.31	13.15	16.36
0.40	1.426	1.966	3.392	5.421	7.756	9.416	17.45	17.18
0.50	1.412	1.946	3.145	4.936	7.059	9.866	11.18	12.38
0.60	1.397	1.888	3.119	5.241	6.555	8.012	17.00	13.02
0.80	1.373	1.825	2.967	4.392	6.244	7.213	8.583	9.417
1.0	1.355	1.781	2.814	5.111	5.475	6.774	8.698	8.012
1.5	1.332	1.695	2.614	3.405	4.188	4.683	5.527	6.183
2.0	1.312	1.653	2.408	3.209	4.308	4.816	5.710	6.041
3.0	1.289	1.565	2.193	2.866	3.353	4.011	4.808	4.783
4.0	1.262	1.521	2.078	2.528	2.958	3.148	3.345	3.797
5.0	1.231	1.450	1.994	2.349	2.801	2.942	3.496	3.312
6.0	1.211	1.418	1.856	2.225	2.627	2.686	3.014	3.640
7.0	1.196	1.403	1.743	2.103	2.338	2.427	2.829	2.912

NAVSWC TR 91-16

TABLE B-2. GAMMA-RAY BUILDUP FACTORS FOR IRON, GEOMETRY A ($h_s = 0$, $\rho_D = 0$, $z_D = a$)

(a) Single-scatter

Thickness, a (mfp)	0.5	1.0	2.0	3.0	4.0	5.0	6.0	7.0
Energy (Mev)								
0.10	1.149	1.248	1.388	1.489	1.569	1.634	1.689	1.736
0.15	1.236	1.402	1.648	1.831	1.977	2.099	2.202	2.292
0.20	1.280	1.485	1.797	2.035	2.229	2.391	2.531	2.653
0.30	1.305	1.540	1.908	2.195	2.432	2.633	2.808	2.962
0.40	1.306	1.546	1.926	2.226	2.474	2.686	2.870	3.033
0.50	1.301	1.539	1.918	2.217	2.465	2.678	2.862	3.026
0.60	1.295	1.529	1.902	2.196	2.440	2.648	2.830	2.991
0.80	1.283	1.508	1.864	2.145	2.378	2.576	2.748	2.901
1.0	1.273	1.489	1.830	2.097	2.318	2.506	2.669	2.814
1.5	1.254	1.453	1.763	2.006	2.205	2.375	2.524	2.655
2.0	1.239	1.424	1.712	1.938	2.125	2.286	2.426	2.551
3.0	1.211	1.373	1.628	1.831	2.002	2.151	2.282	2.400
4.0	1.188	1.331	1.559	1.745	1.904	2.043	2.168	2.280
5.0	1.167	1.295	1.502	1.674	1.823	1.956	2.076	2.186
6.0	1.150	1.265	1.453	1.613	1.755	1.882	1.999	2.107
7.0	1.135	1.239	1.412	1.561	1.696	1.819	1.933	2.039

(b) Total

Energy (Mev)								
0.10	1.165	1.292	1.494	1.657	1.779	1.891	2.019	2.000
0.15	1.280	1.534	1.964	2.353	2.750	2.933	3.182	3.272
0.20	1.348	1.678	2.340	3.168	3.737	4.365	5.046	5.403
0.30	1.387	1.807	2.699	3.701	4.691	5.654	6.462	7.375
0.40	1.391	1.806	2.759	4.236	5.251	6.474	8.813	9.427
0.50	1.384	1.829	3.151	4.610	5.029	6.718	7.574	9.675
0.60	1.374	1.786	2.789	5.402	5.352	7.033	15.43	14.50
0.80	1.357	1.759	2.781	3.832	4.958	7.098	8.336	9.417
1.0	1.345	1.731	2.628	3.646	4.428	6.469	6.665	8.976
1.5	1.321	1.691	2.454	3.437	4.360	5.024	5.739	7.876
2.0	1.306	1.625	2.369	3.045	3.875	4.557	5.135	5.461
3.0	1.270	1.558	2.197	2.671	3.533	4.415	4.831	4.785
4.0	1.239	1.474	1.988	2.432	2.986	3.504	3.515	3.545
5.0	1.214	1.429	1.856	2.212	2.606	2.816	3.187	3.343
6.0	1.192	1.394	1.779	2.104	2.713	3.307	3.366	3.312
7.0	1.178	1.352	1.690	2.016	2.350	2.667	2.803	3.139

TABLE B-3. GAMMA-RAY BUILDUP FACTORS FOR LEAD, GEOMETRY A ($h_s = 0$, $\rho_D = 0$, $z_D = a$)

(a) Single-scatter

Thickness, a (mfp)	0.5	1.0	2.0	3.0	4.0	5.0	6.0	7.0
Energy (Mev)								
0.10	1.013	1.032	1.102	1.273	1.711	2.842	5.791	13.53
0.15	1.019	1.031	1.047	1.059	1.067	1.074	1.080	1.085
0.20	1.031	1.050	1.078	1.098	1.113	1.126	1.137	1.146
0.30	1.060	1.099	1.155	1.195	1.227	1.252	1.274	1.293
0.40	1.089	1.147	1.232	1.294	1.342	1.382	1.417	1.446
0.50	1.113	1.189	1.300	1.381	1.446	1.500	1.546	1.585
0.60	1.132	1.222	1.355	1.454	1.533	1.599	1.655	1.704
0.80	1.157	1.268	1.434	1.559	1.660	1.744	1.816	1.879
1.0	1.172	1.295	1.481	1.623	1.738	1.835	1.918	1.990
1.5	1.186	1.322	1.534	1.702	1.841	1.961	2.066	2.160
2.0	1.182	1.317	1.535	1.712	1.865	1.998	2.118	2.225
3.0	1.160	1.279	1.483	1.659	1.817	1.961	2.093	2.217
4.0	1.137	1.240	1.422	1.586	1.738	1.881	2.017	2.147
5.0	1.118	1.207	1.368	1.520	1.665	1.806	1.944	2.078
6.0	1.103	1.181	1.324	1.463	1.602	1.744	1.878	2.018
7.0	1.091	1.159	1.287	1.415	1.546	1.680	1.819	1.961

(b) Total

Energy (Mev)								
0.10	1.013	1.032	1.106	1.292	1.776	3.055	6.493	15.69
0.15	1.019	1.032	1.051	1.069	1.094	1.140	1.251	1.562
0.20	1.031	1.053	1.083	1.106	1.129	1.160	1.207	1.331
0.30	1.062	1.106	1.169	1.220	1.257	1.294	1.353	1.462
0.40	1.094	1.159	1.262	1.336	1.415	1.484	1.506	1.596
0.50	1.121	1.207	1.349	1.472	1.576	1.623	1.757	1.806
0.60	1.169	1.252	1.430	1.575	1.662	1.812	1.914	2.304
0.80	1.173	1.322	1.570	1.774	1.919	2.039	2.150	2.361
1.0	1.191	1.348	1.644	1.879	2.059	2.638	2.641	2.706
1.5	1.213	1.396	1.731	2.070	2.326	2.553	3.237	2.992
2.0	1.209	1.387	1.740	2.175	2.362	2.668	3.443	3.731
3.0	1.186	1.342	1.651	1.994	2.506	2.672	3.017	3.142
4.0	1.158	1.293	1.575	1.836	2.177	2.485	2.878	3.949
5.0	1.136	1.257	1.496	1.751	2.074	2.432	2.540	2.918
6.0	1.118	1.215	1.427	1.705	2.035	2.318	2.690	2.913
7.0	1.107	1.189	1.412	1.583	1.881	2.375	2.445	2.619

NAVSWC TR 91-16

TABLE B-4. GAMMA-RAY BUILDUP FACTORS FOR WATER, GEOMETRY A
($h_s = 0$, $\rho_D = 0$, $z_D = a$)

(a) Single-scatter

Thickness, a (mfp)	0.5	1.0	2.0	3.0	4.0	5.0	6.0	7.0
Energy (Mev)								
0.10	1.404	1.705	2.168	2.529	2.828	3.083	3.306	3.503
0.20	1.361	1.644	2.094	2.452	2.750	3.007	3.231	3.430
0.40	1.325	1.585	2.004	2.337	2.615	2.853	3.060	3.244
0.60	1.303	1.547	1.937	2.246	2.503	2.722	2.913	3.081
0.80	1.288	1.519	1.886	2.175	2.413	2.617	2.794	2.951
1.0	1.277	1.497	1.845	2.117	2.342	2.533	2.699	2.846
3.0	1.219	1.384	1.637	1.832	1.991	2.126	2.244	2.347
5.0	1.185	1.322	1.532	1.694	1.827	1.941	2.039	2.126
7.0	1.160	1.278	1.459	1.602	1.719	1.820	1.908	1.986

(b) Total

Energy (Mev)								
0.10	1.625	2.513	5.413	10.26	18.03	58.93	41.15	58.53
0.20	1.501	2.168	4.265	7.759	14.44	19.43	29.79	44.69
0.40	1.432	2.001	3.642	5.894	8.871	14.04	21.36	26.74
0.60	1.396	1.885	3.273	5.153	7.545	9.754	11.40	15.43
0.80	1.375	1.842	3.088	4.397	6.409	8.378	12.62	15.42
1.0	1.360	1.789	2.971	4.129	5.750	7.650	9.862	14.75
3.0	1.292	1.583	2.202	2.853	3.447	3.858	4.970	4.046
5.0	1.239	1.482	1.994	2.368	2.663	3.248	4.450	4.259
7.0	1.204	1.396	1.728	2.108	2.309	2.577	2.727	2.820

TABLE B-5. GAMMA-RAY BUILDUP FACTORS FOR POLYETHYLENE, GEOMETRY
A ($h_s = 0$, $\rho_D = 0$, $z_D = a$)

(a) Single-scatter

Thickness, a (mfp)	0.5	1.0	2.0	3.0	4.0	5.0	6.0	7.0
Energy (Mev)								
0.10	1.410	1.716	2.188	2.557	2.864	3.126	3.355	3.558
0.20	1.362	1.645	2.097	2.456	2.757	3.014	3.240	3.440
0.40	1.325	1.586	2.004	2.338	2.616	2.854	3.062	3.245
0.60	1.304	1.547	1.938	2.247	2.503	2.722	2.913	3.082
0.80	1.288	1.519	1.886	2.175	2.414	2.617	2.795	2.951
1.0	1.277	1.497	1.845	2.117	2.342	2.533	2.699	2.846
3.0	1.219	1.385	1.637	1.831	1.989	2.123	2.239	2.341
5.0	1.187	1.325	1.535	1.696	1.828	1.939	2.035	2.120
7.0	1.163	1.283	1.465	1.606	1.722	1.821	1.906	1.982

(b) Total

Energy (Mev)

0.10	1.433	2.569	6.335	14.41	30.69	53.38	95.24	155.5
0.20	1.501	2.190	4.606	8.911	17.26	29.60	50.63	72.42
0.40	1.433	1.992	3.778	6.455	10.32	18.30	21.69	28.57
0.60	1.398	1.914	3.412	5.664	8.472	12.24	16.22	19.82
0.80	1.374	1.846	3.112	4.870	7.050	8.260	12.80	14.48
1.0	1.361	1.804	2.928	4.382	5.806	7.892	11.73	18.64
3.0	1.284	1.601	2.417	2.819	3.512	4.687	5.195	4.947
5.0	1.239	1.480	2.012	2.422	2.639	2.918	3.338	3.536
7.0	1.215	1.412	1.773	2.240	2.784	3.201	3.944	3.276

TABLE B-6. GAMMA-RAY BUILDUP FACTORS FOR CONCRETE, GEOMETRY A
 $(h_s = 0, \rho_D = 0, z_D = a)$

(a) Single-scatter

Thickness, a (mfp)	0.5	1.0	2.0	3.0	4.0	5.0	6.0	7.0
Energy (Mev)								
0.10	1.350	1.604	1.987	2.280	2.518	2.718	2.891	3.042
0.20	1.352	1.626	2.058	2.401	2.686	2.929	3.142	3.329
0.40	1.323	1.582	1.996	2.326	2.601	2.837	3.042	3.223
0.60	1.303	1.546	1.934	2.242	2.497	2.715	2.905	3.073
0.80	1.288	1.518	1.884	2.172	2.410	2.614	2.791	2.947
1.0	1.276	1.496	1.843	2.115	2.340	2.530	2.697	2.843
3.0	1.217	1.382	1.635	1.832	1.994	2.132	2.253	2.360
5.0	1.180	1.315	1.524	1.689	1.828	1.946	2.051	2.144
7.0	1.152	1.265	1.445	1.590	1.713	1.819	1.914	1.998

(b) Total

Energy (MeV)								
0.10	1.480	2.045	3.257	4.694	6.068	7.559	9.281	11.00
0.20	1.478	2.087	3.712	5.843	8.225	12.01	15.30	20.24
0.40	1.425	1.967	3.374	5.330	7.327	9.650	13.72	17.30
0.60	1.398	1.875	3.043	4.943	6.808	7.931	10.25	11.46
0.80	1.371	1.828	2.932	4.365	5.537	7.733	8.219	8.583
1.0	1.357	1.777	2.771	4.010	5.354	6.827	7.894	7.747
3.0	1.277	1.572	2.191	3.108	3.221	4.018	4.232	5.663
5.0	1.230	1.460	1.894	2.254	2.771	3.077	3.615	3.269
7.0	1.200	1.387	1.734	2.034	2.503	2.600	2.689	3.712

TABLE B-7. GAMMA-RAY BUILDUP FACTORS FOR ALUMINUM, GEOMETRY B
($h_s = 0$, $\rho_D = 0$, $z_D = 2a$)

(a) Single-scatter

Thickness, a (mfp)	0.5	1.0	2.0	3.0	4.0	5.0	6.0	7.0
Energy (Mev)								
0.10	1.337	1.566	1.895	2.133	2.319	2.470	2.596	2.703
1.0	1.274	1.486	1.808	2.052	2.248	2.410	2.548	2.667
7.0	1.153	1.267	1.447	1.593	1.718	1.827	1.924	2.011

(b) Total

Energy (Mev)								
0.10	1.481	2.000	3.050	4.201	5.282	6.676	7.941	9.255
1.0	1.361	1.772	2.708	3.678	4.820	5.883	7.235	7.835
7.0	1.202	1.389	1.716	2.028	2.244	2.436	2.752	3.085

TABLE B-8. GAMMA-RAY BUILDUP FACTORS FOR IRON, GEOMETRY B ($h_s = 0$,
 $\rho_D = 0$, $z_D = 2a$)

(a) Single-scatter

Thickness, a (mfp)	0.5	1.0	2.0	3.0	4.0	5.0	6.0	7.0
Energy (Mev)								
0.10	1.144	1.230	1.351	1.430	1.489	1.534	1.571	1.602
1.0	1.271	1.486	1.797	2.037	2.229	2.389	2.525	2.642
7.0	1.137	1.243	1.414	1.562	1.695	1.816	1.928	2.032

(b) Total

Energy (Mev)								
0.10	1.161	1.273	1.445	1.573	1.673	1.763	1.842	1.909
1.0	1.348	1.756	2.538	3.461	4.253	5.232	6.054	7.014
7.0	1.180	1.354	1.666	1.965	2.353	2.810	3.473	3.767

NAVSWC TR 91-16

TABLE B-9. GAMMA-RAY BUILDUP FACTORS FOR LEAD, GEOMETRY B ($h_s = 0$, $\rho_D = 0$, $z_D = 2a$)

(a) Single-scatter

Thickness, a (mfp)	0.5	1.0	2.0	3.0	4.0	5.0	6.0	7.0
Energy (Mev)								
0.10	1.012	1.028	1.089	1.245	1.651	2.716	5.524	12.94
1.0	1.172	1.292	1.469	1.600	1.703	1.789	1.861	1.923
7.0	1.092	1.160	1.285	1.411	1.539	1.670	1.803	1.941

(b) Total build-up

Energy (Mev)								
0.10	1.012	1.028	1.093	1.262	1.712	2.924	6.176	14.99
1.0	1.193	1.347	1.620	1.856	2.032	2.208	2.343	2.437
7.0	1.107	1.192	1.367	1.600	1.813	2.079	2.406	2.806

TABLE B-10. GAMMA-RAY BUILDUP FACTORS FOR WATER, GEOMETRY B ($h_s = 0$, $\rho_D = 0$, $z_D = 2a$)

(a) Single-scatter

Thickness, a (mfp)	0.5	1.0	2.0	3.0	4.0	5.0	6.0	7.0
Energy (Mev)								
0.10	1.381	1.646	2.033	2.322	2.552	2.742	2.904	3.044
1.0	1.275	1.486	1.809	2.054	2.249	2.412	2.550	2.669
7.0	1.163	1.283	1.468	1.612	1.732	1.835	1.925	2.005

(b) Total

Energy (Mev)								
0.10	1.599	2.463	5.056	8.992	14.59	22.80	30.31	44.23
1.0	1.363	1.796	2.792	3.991	5.065	6.438	7.196	8.413
7.0	1.214	1.414	1.772	2.095	2.366	2.601	2.854	3.020

NAVSWC TR 91-16

TABLE B-11. GAMMA-RAY BUILDUP FACTORS FOR POLYETHYLENE,
GEOMETRY B ($h_s = 0$, $\rho_D = 0$, $z_D = 2a$)

(a) Single-scatter

Thickness, a (mfp)	0.5	1.0	2.0	3.0	4.0	5.0	6.0	7.0
Energy (Mev)								
0.10	1.387	1.655	2.050	2.345	2.581	2.777	2.944	3.089
1.0	1.275	1.486	1.809	2.054	2.250	2.412	2.550	2.669
7.0	1.167	1.289	1.475	1.619	1.737	1.838	1.926	2.005

(b) Total

Energy (Mev)								
0.10	1.623	2.537	6.023	12.78	24.64	43.44	70.05	102.1
1.0	1.364	1.798	2.842	4.020	5.470	7.142	8.031	9.383
7.0	1.217	1.426	1.747	2.120	2.361	2.667	2.828	2.790

TABLE B-12. GAMMA-RAY BUILDUP FACTORS FOR CONCRETE, GEOMETRY B
($h_s = 0$, $\rho_D = 0$, $z_D = 2a$)

(a) Single-scatter

Thickness, a (mfp)	0.5	1.0	2.0	3.0	4.0	5.0	6.0	7.0
Energy (Mev)								
0.10	1.332	1.557	1.879	2.112	2.294	2.441	2.563	2.667
1.0	1.274	1.486	1.808	2.052	2.248	2.410	2.548	2.667
7.0	1.155	1.270	1.452	1.598	1.721	1.829	1.924	2.010

(b) Total

Energy (Mev)								
0.10	1.469	1.971	3.016	4.077	5.156	6.521	7.959	9.304
1.0	1.362	1.777	2.698	3.709	4.691	5.818	6.393	7.891
7.0	1.205	1.394	1.735	2.087	2.453	2.757	3.318	3.906

TABLE B-13. GAMMA-RAY BUILDUP FACTORS FOR ALUMINUM, GEOMETRY C
($h_s = a$, $\rho_D = 0$, $z_D = 2a$)

(a) Single-scatter

Thickness, a (mfp)	0.5	1.0	2.0	3.0	4.0	5.0	6.0	7.0
Energy (Mev)								
0.10	1.327	1.547	1.869	2.109	2.300	2.458	2.593	2.710
1.0	1.262	1.465	1.782	2.029	2.231	2.402	2.550	2.680
7.0	1.142	1.248	1.416	1.550	1.663	1.761	1.846	1.923

(b) Total

Energy (Mev)								
0.10	1.466	1.918	3.605	4.240	5.247	4.906	6.289	6.955
1.0	1.331	1.689	2.456	4.069	4.016	6.524	7.308	7.527
7.0	1.183	1.345	1.677	1.818	2.113	1.991	2.056	2.739

TABLE B-14. GAMMA-RAY BUILDUP FACTORS FOR IRON, GEOMETRY C ($h_s = a$,
 $\rho_D = 0$, $z_D = 2a$)

(a) Single-scatter

Thickness, a (mfp)	0.5	1.0	2.0	3.0	4.0	5.0	6.0	7.0
Energy (Mev)								
0.10	1.135	1.221	1.342	1.429	1.498	1.553	1.600	1.640
1.0	1.259	1.459	1.771	2.014	2.213	2.382	2.527	2.655
7.0	1.127	1.225	1.388	1.528	1.652	1.765	1.868	1.964

(b) Total

Energy (Mev)								
0.10	1.149	1.253	1.420	1.566	1.702	1.813	1.901	1.925
1.0	1.321	1.626	2.491	3.055	3.824	5.794	22.64	7.483
7.0	1.162	1.301	1.710	2.028	4.400	2.960	3.208	4.450

NAVSWC TR 91-16

TABLE B-15. GAMMA-RAY BUILDUP FACTORS FOR LEAD, GEOMETRY C ($h_s = a$, $\rho_D = 0$, $z_D = 2a$)

(a) Single-scatter

Thickness, a (mfp)	0.5	1.0	2.0	3.0	4.0	5.0	6.0	7.0
Energy (Mev)								
0.10	1.014	1.033	1.110	1.298	1.778	3.013	6.223	14.60
1.0	1.164	1.281	1.456	1.587	1.692	1.779	1.853	1.917
7.0	1.085	1.149	1.271	1.392	1.513	1.637	1.763	1.892

(b) Total

Energy (Mev)								
0.10	1.014	1.034	1.116	1.322	1.863	3.307	7.143	17.53
1.0	1.176	1.322	1.591	1.749	2.336	2.134	2.123	2.108
7.0	1.096	1.175	1.319	1.754	1.827	1.831	1.894	2.113

TABLE B-16. GAMMA-RAY BUILDUP FACTORS FOR WATER, GEOMETRY C ($h_s = a$, $\rho_D = 0$, $z_D = 2a$)

(a) Single-scatter

Thickness, a (mfp)	0.5	1.0	2.0	3.0	4.0	5.0	6.0	7.0
Energy (Mev)								
0.10	1.373	1.629	2.006	2.289	2.515	2.704	2.866	3.006
1.0	1.263	1.466	1.783	2.030	2.233	2.404	2.552	2.682
7.0	1.152	1.263	1.433	1.563	1.669	1.758	1.835	1.901

(b) Total

Energy (Mev)								
0.10	1.597	2.382	4.807	8.430	13.91	21.55	27.95	27.10
1.0	1.377	1.740	2.735	3.342	4.674	6.387	6.827	7.381
7.0	1.192	1.416	1.657	2.255	2.568	2.707	2.435	2.307

NAVSWC TR 91-16

TABLE B-17. GAMMA-RAY BUILDUP FACTORS FOR POLYETHYLENE,
GEOMETRY C ($h_s = a$, $\rho_D = 0$, $z_D = 2a$)

(a) Single-scatter

Thickness, a (mfp)	0.5	1.0	2.0	3.0	4.0	5.0	6.0	7.0
Energy (Mev)								
0.10	1.378	1.640	2.024	2.311	2.543	2.736	2.901	3.044
1.0	1.263	1.466	1.783	2.030	2.233	2.404	2.552	2.682
7.0	1.155	1.268	1.438	1.567	1.671	1.758	1.831	1.895

(b) Total

Energy (Mev)								
0.10	1.635	2.495	5.662	11.67	25.59	33.22	107.30	73.10
1.0	1.346	1.759	2.701	3.899	4.937	4.824	5.553	6.102
7.0	1.202	1.408	1.777	7.769	2.072	2.049	2.035	2.054

TABLE B-18. GAMMA-RAY BUILDUP FACTORS FOR CONCRETE, GEOMETRY C
($h_s = a$, $\rho_D = 0$, $z_D = 2a$)

(a) Single-scatter

Thickness, a (mfp)	0.5	1.0	2.0	3.0	4.0	5.0	6.0	7.0
Energy (Mev)								
0.10	1.321	1.538	1.854	2.088	2.276	2.431	2.563	2.678
1.0	1.262	1.465	1.782	2.029	2.231	2.402	2.550	2.680
7.0	1.144	1.251	1.420	1.553	1.665	1.760	1.844	1.918

(b) Total

Energy (Mev)								
0.10	1.454	1.893	3.055	4.702	5.054	5.986	10.01	8.283
1.0	1.332	1.670	2.641	3.693	4.713	5.670	5.207	7.478
7.0	1.184	1.335	1.567	1.768	2.067	2.182	2.754	2.490

NAVSVC TR 91-16

TABLE B-19. GAMMA-RAY BUILDUP FACTORS FOR ALUMINUM, GEOMETRY D
($h_s = 0$, $\rho_D = a$, $z_D = a$)

(a) Single-scatter

LOS Thickness (mfp)	0.5	1.0	2.0	3.0	4.0	5.0	6.0	7.0
Energy (Mev)								
0.10	1.323	1.564	1.932	2.217	2.451	2.650	2.822	2.973
0.20	1.323	1.579	1.992	2.322	2.599	2.837	3.045	3.231
0.60	1.283	1.514	1.889	2.190	2.441	2.656	2.844	3.010
1.0	1.261	1.473	1.811	2.079	2.300	2.488	2.652	2.796
3.0	1.208	1.370	1.620	1.814	1.974	2.111	2.229	2.334
5.0	1.173	1.305	1.510	1.673	1.808	1.925	2.027	2.118
7.0	1.145	1.256	1.432	1.574	1.695	1.800	1.893	1.977

(b) Total

Energy (Mev)								
0.10	1.433	1.907	3.006	4.228	5.672	7.170	8.346	23.04
0.20	1.435	1.896	3.046	5.335	6.068	11.39	10.17	11.71
0.60	1.363	1.791	2.842	4.155	6.648	7.746	7.659	7.045
1.0	1.326	1.674	2.514	3.244	4.881	5.885	8.792	6.203
3.0	1.254	1.503	2.187	3.249	4.141	4.135	3.935	4.440
5.0	1.237	1.432	1.824	2.285	2.653	2.798	2.452	2.566
7.0	1.190	1.380	1.671	1.836	2.291	2.251	3.770	2.245

NAVSWC TR 91-16

TABLE B-20. GAMMA-RAY BUILDUP FACTORS FOR IRON, GEOMETRY D ($h_s = 0$,
 $\rho_D = a$, $z_D = a$)

(a) Single-scatter

LOS Thickness (mfp)	0.5	1.0	2.0	3.0	4.0	5.0	6.0	7.0
Energy (Mev)								
0.10	1.136	1.228	1.362	1.460	1.538	1.602	1.657	1.704
0.20	1.256	1.449	1.747	1.978	2.167	2.327	2.465	2.586
0.60	1.275	1.499	1.859	2.147	2.387	2.593	2.773	2.931
1.0	1.258	1.466	1.799	2.062	2.280	2.465	2.626	2.768
3.0	1.203	1.362	1.613	1.813	1.981	2.126	2.255	2.369
5.0	1.161	1.287	1.491	1.660	1.806	1.936	2.054	2.160
7.0	1.130	1.232	1.403	1.550	1.682	1.802	1.914	2.018

(b) Total

Energy (Mev)								
0.10	1.149	1.264	1.441	1.617	1.694	1.772	1.794	1.826
0.20	1.314	1.606	2.162	2.855	3.449	4.242	4.246	4.445
0.60	1.350	1.702	2.479	3.878	6.839	5.734	5.608	6.094
1.0	1.326	1.708	2.482	3.007	4.485	6.693	7.966	11.28
3.0	1.253	1.502	2.026	2.687	2.981	3.045	3.093	3.537
5.0	1.208	1.383	1.797	2.493	3.027	2.650	4.007	3.143
7.0	1.166	1.326	1.658	1.832	2.264	2.847	2.602	2.529

NAVSWC TR 91-16

TABLE B-21. GAMMA-RAY BUILDUP FACTORS FOR LEAD, GEOMETRY D ($h_s = 0$,
 $\rho_D = a$, $z_D = a$)

(a) Single-scatter

LOS Thickness (mfp)	0.5	1.0	2.0	3.0	4.0	5.0	6.0	7.0
Energy (Mev)								
0.10	1.012	1.029	1.094	1.257	1.674	2.753	5.571	12.96
0.20	1.028	1.047	1.074	1.094	1.109	1.122	1.132	1.141
0.60	1.125	1.214	1.344	1.442	1.519	1.583	1.638	1.685
1.0	1.165	1.285	1.469	1.608	1.721	1.815	1.896	1.967
3.0	1.154	1.272	1.473	1.646	1.802	1.943	2.074	2.195
5.0	1.114	1.202	1.361	1.511	1.654	1.793	1.929	2.061
7.0	1.087	1.154	1.281	1.408	1.537	1.670	1.806	1.948

(b) Total

Energy (Mev)								
0.10	1.012	1.029	1.098	1.272	1.729	2.927	6.143	14.76
0.20	1.029	1.049	1.078	1.102	1.123	1.153	1.197	1.300
0.60	1.136	1.238	1.425	1.538	1.716	1.727	1.805	1.903
1.0	1.185	1.344	1.607	1.797	1.970	2.472	2.149	2.239
3.0	1.175	1.328	1.624	1.901	2.719	2.448	3.214	3.149
5.0	1.128	1.249	1.499	1.708	2.073	2.030	2.439	2.590
7.0	1.099	1.183	1.360	1.676	1.942	2.028	3.021	3.553

NAVSWC TR 91-16

TABLE B-22. GAMMA-RAY BUILDUP FACTORS FOR WATER, GEOMETRY D
($h_s = 0$, $\rho_D = a$, $z_D = a$)

(a) Single-scatter

LOS Thickness (mfp)	0.5	1.0	2.0	3.0	4.0	5.0	6.0	7.0
Energy (Mev)								
0.10	1.367	1.646	2.083	2.427	2.713	2.959	3.174	3.364
0.20	1.330	1.593	2.019	2.362	2.650	2.899	3.117	3.312
0.60	1.283	1.515	1.892	2.193	2.445	2.661	2.850	3.017
1.0	1.261	1.473	1.812	2.080	2.302	2.490	2.654	2.799
3.0	1.211	1.373	1.622	1.813	1.969	2.101	2.215	2.315
5.0	1.180	1.314	1.520	1.679	1.809	1.919	2.014	2.097
7.0	1.155	1.271	1.450	1.588	1.703	1.800	1.884	1.958

(b) Total

Energy (MeV)								
0.10	1.520	2.241	4.478	7.948	13.65	21.31	32.12	117.3
0.20	1.455	2.042	3.951	6.410	11.66	14.63	19.94	24.10
0.60	1.375	1.852	3.207	4.848	6.184	10.04	7.769	20.28
1.0	1.329	1.717	2.507	4.105	4.879	6.586	6.730	8.174
3.0	1.348	1.528	2.076	2.576	2.977	3.341	3.957	5.816
5.0	1.223	1.537	2.018	2.173	2.987	3.033	2.737	2.590
7.0	1.202	1.365	1.852	2.088	2.322	2.481	2.404	2.268

NAVSWC TR 91-16

TABLE B-23. GAMMA-RAY BUILDUP FACTORS FOR POLYETHYLENE,
GEOMETRY D ($h_s = 0$, $\rho_D = a$, $z_D = a$)

(a) Single-scatter

LOS Thickness (mfp)	0.5	1.0	2.0	3.0	4.0	5.0	6.0	7.0
Energy (Mev)								
0.10	1.372	1.656	2.102	2.453	2.747	2.999	3.220	3.416
0.20	1.330	1.595	2.022	2.366	2.656	2.906	3.125	3.321
0.60	1.283	1.515	1.892	2.194	2.446	2.662	2.851	3.018
1.0	1.261	1.473	1.812	2.080	2.302	2.491	2.654	2.799
3.0	1.212	1.374	1.622	1.813	1.968	2.098	2.211	2.309
5.0	1.102	1.317	1.524	1.681	1.809	1.917	2.010	2.091
7.0	1.159	1.276	1.455	1.593	1.705	1.800	1.882	1.953

(b) Total

Energy (MeV)								
0.10	1.533	2.257	4.926	10.91	18.91	37.74	91.23	138.1
0.20	1.447	2.052	3.979	7.952	11.60	22.86	51.6	61.12
0.60	1.370	1.815	3.095	5.216	7.128	11.78	11.63	14.65
1.0	1.328	1.702	2.643	3.650	6.644	7.190	7.212	9.924
3.0	1.269	1.599	1.969	2.493	3.396	2.991	2.946	3.344
5.0	1.233	1.447	1.857	2.104	4.204	2.988	3.982	2.821
7.0	1.196	1.442	1.730	2.289	2.102	7.348	2.294	2.196

NAVSWC TR 91-16

TABLE B-24. GAMMA-RAY BUILDUP FACTORS FOR CONCRETE, GEOMETRY D
($h_s = 0$, $\rho_D = a$, $z_D = a$)

(a) Single-scatter

LOS Thickness (mfp)	0.5	1.0	2.0	3.0	4.0	5.0	6.0	7.0
Energy (Mev)								
0.10	1.318	1.554	1.915	2.194	2.423	2.617	2.785	2.932
0.20	1.322	1.577	1.987	2.315	2.590	2.827	3.034	3.218
0.60	1.282	1.514	1.889	2.189	2.440	2.655	2.843	3.009
1.0	1.261	1.473	1.811	2.079	2.300	2.488	2.652	2.796
3.0	1.209	1.371	1.620	1.814	1.973	2.108	2.225	2.328
5.0	1.174	1.307	1.513	1.675	1.810	1.925	2.026	2.116
7.0	1.147	1.259	1.436	1.578	1.697	1.800	1.891	1.973

(b) Total

Energy (MeV)								
0.10	1.415	1.888	3.007	4.145	4.956	5.935	7.581	7.206
0.20	1.434	1.911	3.114	4.860	7.305	8.627	10.09	14.62
0.60	1.364	1.824	2.847	3.997	6.810	6.863	9.540	11.83
1.0	1.347	1.740	2.531	4.454	6.333	5.972	8.294	13.24
3.0	1.251	1.572	2.101	2.456	3.741	4.452	4.060	4.133
5.0	1.235	1.420	1.865	2.291	2.257	2.318	2.364	2.382
7.0	1.194	1.427	1.747	2.027	2.370	2.178	2.191	2.295

APPENDIX C

NEUTRON BUILDUP FACTOR TABLES, GEOMETRIES A-D

16 PAGES

REFERENCED IN CHAPTER 1, INTRODUCTION, AND
CHAPTER 3, SAMPLE RESULTS

TABLE C-1. NEUTRON BUILDUP FACTORS FOR ALUMINUM, GEOMETRY A
($h_s = 0$, $\rho_D = 0$, $z_D = a$)

(a) Single-scatter

Thickness, a (mfp)	0.5	1.0	2.0	3.0	4.0	5.0	6.0	7.0
Energy (Mev)								
10 ⁻⁷	1.427	1.723	2.139	2.432	2.655	2.833	3.003	3.128
10 ⁻⁵	1.465	1.788	2.242	2.562	2.806	3.002	3.163	3.299
10 ⁻³	1.456	1.775	2.225	2.544	2.788	2.984	3.146	3.283
0.1	1.327	1.478	1.651	1.752	1.819	1.866	1.901	1.926
1.0	1.407	1.649	1.924	2.060	2.132	2.172	2.196	2.213
10.0	1.355	1.572	1.833	1.989	2.093	2.168	2.224	2.268
14.0	1.299	1.487	1.722	1.867	1.967	2.041	2.097	2.141

(b) Total

Energy (Mev)								
10 ⁻⁷	1.647	2.550	5.458	12.43	25.61	39.58	96.60	146.3
10 ⁻⁵	1.736	2.832	7.903	18.97	43.43	103.6	257.6	490.6
10 ⁻³	1.708	2.810	6.860	15.39	36.08	75.05	148.6	304.9
0.1	1.819	3.146	8.125	20.29	51.50	128.9	363.1	990.5
1.0	1.693	2.697	6.154	12.79	25.85	44.13	72.35	125.4
10.0	1.571	2.395	5.268	10.87	18.67	27.05	38.76	134.8
14.0	1.462	2.065	4.121	7.118	11.03	17.30	35.20	49.26

TABLE C-2. NEUTRON BUILDUP FACTORS FOR IRON, GEOMETRY A ($h_s = 0$, $\rho_D = 0$, $z_D = a$)

(a) Single-scatter

Thickness, a (mfp)	0.5	1.0	2.0	3.0	4.0	5.0	6.0	7.0
Energy (Mev)								
10 ⁻⁷	1.417	1.704	2.105	2.386	2.599	2.769	2.908	3.026
10 ⁻⁵	1.461	1.778	2.222	2.534	2.770	2.959	3.115	3.247
10 ⁻³	1.459	1.776	2.220	2.531	2.770	2.961	3.120	3.252
0.1	1.448	1.726	2.068	2.268	2.395	2.480	2.548	2.617
1.0	1.493	1.959	3.015	4.497	6.828	10.73	17.46	29.44
10.0	1.403	1.679	2.070	2.368	2.643	2.950	3.357	3.986
14.0	1.338	1.564	1.875	2.098	2.288	2.479	2.705	3.010

(b) Total

Energy (Mev)								
10 ⁻⁷	1.624	2.486	5.933	10.29	20.55	34.43	73.37	115.5
10 ⁻⁵	1.729	2.855	7.182	18.65	42.33	97.67	237.9	470.8
10 ⁻³	1.715	2.833	7.149	19.55	41.18	89.14	196.7	353.2
0.1	1.781	3.033	7.492	19.29	47.73	105.8	248.1	543.6
1.0	1.634	2.533	5.941	13.82	33.20	80.71	205.7	501.6
10.0	1.607	2.490	5.333	12.14	24.38	55.54	110.6	263.2
14.0	1.499	2.163	4.262	8.475	18.60	42.20	81.81	157.6

NAVSWC TR 91-16

TABLE C-3. NEUTRON BUILDUP FACTORS FOR LEAD, GEOMETRY A ($h_s = 0$,
 $\rho_D = 0$, $z_D = a$)

(a) Single-scatter

Thickness, a (mfp)	0.5	1.0	2.0	3.0	4.0	5.0	6.0	7.0
Energy (Mev)								
10 ⁻⁷	1.459	1.773	2.211	2.517	2.748	2.933	3.085	3.213
10 ⁻⁵	1.464	1.782	2.224	2.533	2.768	2.954	3.109	3.239
10 ⁻³	1.462	1.780	2.221	2.530	2.765	2.952	3.106	3.235
0.1	1.466	1.784	2.228	2.536	2.772	2.958	3.111	3.242
1.0	1.417	1.659	1.936	2.092	2.193	2.265	2.318	2.358
10.0	1.398	1.651	1.979	2.190	2.342	2.459	2.552	2.627
14.0	1.429	1.718	2.115	2.391	2.600	2.766	2.902	3.019

(b) Total

Energy (Mev)								
10 ⁻⁷	1.736	2.806	7.532	18.29	41.59	98.50	237.2	463.2
10 ⁻⁵	1.737	2.887	7.816	19.00	47.64	159.4	249.5	495.6
10 ⁻³	1.733	2.862	7.807	18.43	46.56	145.7	246.9	488.3
0.1	1.749	2.884	7.630	19.45	48.46	114.2	232.0	528.0
1.0	1.711	2.741	6.902	16.63	53.21	76.59	146.8	314.7
10.0	1.636	2.564	5.702	14.82	24.86	52.95	104.3	173.9
14.0	1.672	2.639	6.047	15.30	26.37	53.25	90.14	152.3

TABLE C-4. NEUTRON BUILDUP FACTORS FOR WATER, GEOMETRY A ($h_s = 0$, $\rho_D = 0$, $z_D = a$)

(a) Single-scatter

Thickness, a (mfp)	0.5	1.0	2.0	3.0	4.0	5.0	6.0	7.0
Energy (Mev)								
10^{-7}	1.466	1.833	2.409	2.863	3.246	3.585	3.872	4.154
10^{-5}	1.424	1.800	2.485	3.099	3.652	4.154	4.610	5.026
10^{-3}	1.336	1.646	2.209	2.713	3.168	3.581	3.959	4.306
0.1	1.661	2.175	2.910	3.397	3.734	3.978	4.159	4.299
1.0	1.385	1.726	2.371	3.031	3.755	4.580	5.549	6.709
10.0	1.375	1.634	2.000	2.264	2.473	2.646	2.791	2.920
14.0	1.314	1.535	1.854	2.087	2.270	2.418	2.540	2.644

(b) Total

Energy (Mev)								
10^{-7}	1.723	2.905	6.997	16.44	33.13	71.77	119.4	1351.
10^{-5}	1.598	2.317	4.552	8.291	11.83	15.26	21.03	30.21
10^{-3}	1.416	1.982	3.705	6.715	12.53	19.94	42.70	60.04
0.1	2.089	3.964	11.25	27.94	50.31	94.26	158.1	215.0
1.0	1.526	2.114	4.001	6.703	15.81	22.83	38.02	44.19
10.0	1.550	2.198	3.937	4.947	6.620	6.718	7.621	9.629
14.0	1.462	1.953	3.201	4.712	5.483	5.952	8.546	9.209

TABLE C-5. NEUTRON BUILDUP FACTORS FOR POLYETHYLENE, GEOMETRY A
($h_s = 0$, $\rho_D = 0$, $z_D = a$)

(a) Single-scatter

Thickness, a (mfp)	0.5	1.0	2.0	3.0	4.0	5.0	6.0	7.0
Energy (Mev)								
10 ⁻⁷	1.467	1.835	2.412	2.865	3.248	3.587	3.897	4.190
10 ⁻⁵	1.430	1.806	2.486	3.093	3.640	4.136	4.586	4.996
10 ⁻³	1.338	1.649	2.210	2.711	3.162	3.571	3.954	4.288
0.1	1.658	2.169	2.902	3.388	3.725	3.970	4.152	4.292
1.0	1.301	1.529	1.866	2.111	2.299	2.450	2.573	2.676
10.0	1.357	1.590	1.901	2.110	2.386	2.534	2.656	2.760
14.0	1.309	1.518	1.803	1.998	2.144	2.257	2.348	2.421

(b) Total

Energy (Mev)								
10 ⁻⁷	1.704	2.982	7.547	16.10	33.67	62.83	116.2	216.3
10 ⁻⁵	1.632	2.361	4.871	7.316	16.81	20.61	31.58	55.98
10 ⁻³	1.416	1.969	3.708	6.721	12.34	20.02	34.22	60.32
0.1	2.050	4.031	11.55	26.16	50.22	85.77	199.2	179.3
1.0	1.417	2.035	3.314	4.610	6.370	7.610	8.392	8.870
10.0	1.543	2.267	3.738	4.859	6.899	7.625	7.849	9.087
14.0	1.461	1.982	2.971	4.183	5.275	5.649	6.067	11.51

TABLE C-6. NEUTRON BUILDUP FACTORS FOR CONCRETE, GEOMETRY A
($h_s = 0$, $\rho_D = 0$, $z_D = a$)

(a) Single-scatter

Thickness, a (mfp)	0.5	1.0	2.0	3.0	4.0	5.0	6.0	7.0
Energy (Mev)								
10 ⁻⁷	1.490	1.876	2.477	2.944	3.335	3.678	3.990	4.285
10 ⁻⁵	1.444	1.796	2.366	2.829	3.222	3.564	3.866	4.136
10 ⁻³	1.399	1.715	2.220	2.628	2.974	3.274	3.539	3.776
0.1	1.550	1.949	2.514	2.898	3.176	3.383	3.541	3.663
1.0	1.492	1.942	2.858	3.912	5.233	6.988	9.423	12.91
10.0	1.362	1.613	1.969	2.232	2.448	2.638	2.812	2.977
14.0	1.319	1.539	1.848	2.068	2.240	2.380	2.501	2.606

(b) Total

Energy (Mev)								
10 ⁻⁷	1.857	3.248	7.417	18.38	34.72	63.82	115.1	237.4
10 ⁻⁵	1.619	2.500	5.042	9.537	16.11	24.72	42.86	58.02
10 ⁻³	1.625	2.303	4.531	8.105	15.88	26.94	52.83	93.30
0.1	2.019	3.495	10.37	26.66	56.71	114.6	229.6	525.0
1.0	1.634	2.563	5.732	13.50	29.33	63.73	137.3	315.0
10.0	1.540	2.231	4.561	7.897	12.68	17.80	30.27	35.76
14.0	1.461	2.101	3.779	6.309	9.449	16.16	23.67	25.09

NAVSWC TR 91-16

TABLE C-7. NEUTRON BUILDUP FACTORS FOR ALUMINUM, GEOMETRY B
($h_s = 0$, $\rho_D = 0$, $z_D = 2a$)

(a) Single-scatter

Thickness, a (mfp)	0.5	1.0	2.0	3.0	4.0	5.0	6.0	7.0
Energy (Mev)								
10 ⁻⁷	1.404	1.657	1.987	2.208	2.372	2.501	2.608	2.698
0.1	1.332	1.470	1.611	1.684	1.729	1.761	1.784	1.801
1.0	1.392	1.601	1.810	1.896	1.932	1.947	1.955	1.960
14.0	1.284	1.445	1.628	1.731	1.798	1.844	1.879	1.906

(b) Total

Energy (Mev)								
10 ⁻⁷	1.640	2.483	5.210	10.05	18.58	32.63	56.98	90.60
0.1	1.837	2.992	7.303	17.40	43.56	112.6	294.3	760.5
1.0	1.714	2.676	5.730	10.71	18.20	31.73	51.97	77.07
14.0	1.455	2.040	3.717	6.211	9.593	13.05	18.16	24.57

TABLE C-8. NEUTRON BUILDUP FACTORS FOR IRON, GEOMETRY B ($h_s = 0$,
 $\rho_D = 0$, $z_D = 2a$)

(a) Single-scatter

Thickness, a (mfp)	0.5	1.0	2.0	3.0	4.0	5.0	6.0	7.0
Energy (Mev)								
10 ⁻⁷	1.392	1.636	1.952	2.161	2.317	2.440	2.540	2.625
0.1	1.425	1.665	1.931	2.069	2.148	2.197	2.235	2.276
1.0	1.453	1.836	2.658	3.816	5.685	8.901	14.62	25.01
14.0	1.319	1.512	1.756	1.922	2.065	2.214	2.401	2.668

(b) Total

Energy (Mev)								
10 ⁻⁷	1.617	2.415	4.831	9.028	16.43	28.02	45.37	74.17
0.1	1.774	2.920	7.077	16.37	40.33	90.50	209.0	449.2
1.0	1.599	2.400	5.350	12.23	28.67	68.28	168.9	405.6
14.0	1.488	2.099	3.937	7.407	14.62	29.35	62.41	127.1

TABLE C-9. NEUTRON BUILDUP FACTORS FOR LEAD, GEOMETRY B ($h_s = 0$, $\rho_D = 0$, $z_D = 2a$)

(a) Single-scatter

Thickness, a (mfp)	0.5	1.0	2.0	3.0	4.0	5.0	6.0	7.0
Energy (Mev)								
10 ⁻⁷	1.431	1.698	2.041	2.268	2.436	2.568	2.677	2.768
0.1	1.437	1.707	2.054	2.283	2.452	2.585	2.694	2.786
1.0	1.395	1.602	1.820	1.932	1.999	2.043	2.073	2.095
14.0	1.404	1.649	1.959	2.162	2.311	2.429	2.526	2.609

(b) Total

Energy (Mev)								
10 ⁻⁷	1.718	2.771	6.857	16.24	37.83	83.04	170.6	346.5
0.1	1.739	2.821	7.136	17.57	41.94	88.59	188.40	361.4
1.0	1.711	2.722	6.416	14.09	28.96	56.51	109.6	198.5
14.0	1.667	2.580	5.718	11.38	21.29	36.83	65.39	101.5

 TABLE C-10. NEUTRON BUILDUP FACTORS FOR WATER, GEOMETRY B ($h_s = 0$, $\rho_D = 0$, $z_D = 2a$)

(a) Single-scatter

Thickness, a (mfp)	0.5	1.0	2.0	3.0	4.0	5.0	6.0	7.0
Energy (Mev)								
10 ⁻⁷	1.528	1.932	2.544	3.010	3.395	3.730	4.032	4.314
0.1	1.675	2.178	2.857	3.273	3.541	3.723	3.852	3.946
1.0	1.380	1.699	2.284	2.875	3.525	4.271	5.155	6.223
14.0	1.314	1.525	1.820	2.030	2.193	2.325	2.435	2.528

(b) Total

Energy (Mev)								
10 ⁻⁷	1.789	2.922	6.883	15.02	29.76	55.82	103.3	181.8
0.1	2.111	3.997	10.87	24.36	44.27	74.48	119.2	177.9
1.0	1.483	2.114	3.970	6.854	11.37	17.29	26.60	40.49
14.0	1.460	1.982	3.061	4.215	5.153	6.336	7.358	8.281

TABLE C-11. NEUTRON BUILDUP FACTORS FOR POLYETHYLENE, GEOMETRY B
($h_s = 0$, $\rho_D = 0$, $z_D = 2a$)

(a) Single-scatter

Thickness, a (mfp)	0.5	1.0	2.0	3.0	4.0	5.0	6.0	7.0
Energy (Mev)								
10 ⁻⁷	1.528	1.931	2.543	3.009	3.394	3.728	4.030	4.312
0.1	1.671	2.170	2.845	3.260	3.528	3.709	3.838	3.933
1.0	1.311	1.539	1.871	2.110	2.292	2.437	2.556	2.656
14.0	1.313	1.516	1.786	1.968	2.102	2.206	2.290	2.358

(b) Total

Energy (Mev)								
10 ⁻⁷	1.789	2.398	6.867	14.93	29.88	56.70	100.8	179.6
0.1	2.101	3.993	11.22	23.80	44.38	75.59	117.6	176.5
1.0	1.432	1.976	3.275	4.705	5.884	7.163	7.944	8.802
14.0	1.470	1.984	3.014	3.938	4.657	5.306	5.890	6.140

TABLE C-12. NEUTRON BUILDUP FACTORS FOR CONCRETE, GEOMETRY B
($h_s = 0$, $\rho_D = 0$, $z_D = 2a$)

(a) Single-scatter

Thickness, a (mfp)	0.5	1.0	2.0	3.0	4.0	5.0	6.0	7.0
Energy (Mev)								
10 ⁻⁷	1.504	1.892	2.486	2.945	3.329	3.667	3.977	4.270
0.1	1.541	1.912	2.407	2.723	2.936	3.084	3.191	3.268
1.0	1.461	1.845	2.589	3.435	4.510	5.970	8.039	11.06
14.0	1.306	1.498	1.750	1.920	2.048	2.153	2.242	2.322

(b) Total

Energy (Mev)								
10 ⁻⁷	1.762	2.900	7.002	14.68	28.93	55.98	104.7	200.0
0.1	1.940	3.550	10.21	24.78	51.44	98.50	170.5	290.9
1.0	1.611	2.436	5.317	11.45	24.87	54.61	118.8	261.7
14.0	1.454	2.007	3.449	5.443	7.975	11.83	15.98	21.33

TABLE C-13. NEUTRON BUILDUP FACTORS FOR ALUMINUM, GEOMETRY C
($h_s = a$, $\rho_D = 0$, $z_D = 2a$)

(a) Single-scatter

Thickness, a (mfp)	0.5	1.0	3.0	5.0	7.0
Energy (Mev)					
10 ⁻⁷	1.379	1.609	2.066	2.268	2.377
0.1	1.276	1.400	1.608	1.671	1.688
1.0	1.355	1.539	1.798	1.846	1.855
14.0	1.263	1.406	1.646	1.721	1.746

(b) Total

Energy (Mev)					
10 ⁻⁷	1.686	2.468	9.519	62.55	110.8
0.1	1.731	2.908	20.49	137.9	801.3
1.0	1.647	2.410	10.39	37.99	72.07
14.0	1.445	1.930	5.109	11.42	14.95

TABLE C-14. NEUTRON BUILDUP FACTORS FOR IRON, GEOMETRY C ($h_s = a$,
 $\rho_D = 0$, $z_D = 2a$)

(a) Single-scatter

Thickness, a (mfp)	0.5	1.0	3.0	5.0	7.0
Energy (Mev)					
10 ⁻⁷	1.370	1.592	2.030	2.220	2.321
0.1	1.393	1.604	1.947	2.044	2.099
1.0	1.470	1.903	4.213	9.863	27.01
14.0	1.299	1.474	1.820	2.036	2.366

(b) Total

Energy (Mev)					
10 ⁻⁷	1.671	2.464	8.175	26.00	47.78
0.1	1.715	2.821	18.42	92.57	545.9
1.0	1.624	2.484	13.79	73.59	562.3
14.0	1.457	2.057	7.684	28.53	125.6

NAVSWC TR 91-16

TABLE C-15. NEUTRON BUILDUP FACTORS FOR LEAD, GEOMETRY C ($h_s = a$,
 $\rho_D = 0$, $z_D = 2a$)

(a) Single-scatter

Thickness, a (mfp)	0.5	1.0	3.0	5.0	7.0
Energy (Mev)					
10 ⁻⁷	1.407	1.650	2.128	2.335	2.444
0.1	1.413	1.660	2.144	2.354	2.464
1.0	1.362	1.540	1.829	1.935	1.980
14.0	1.380	1.603	2.035	2.219	2.316

(b) Total

Energy (Mev)					
10 ⁻⁷	1.696	2.636	15.51	65.88	288.1
0.1	1.686	2.682	19.03	81.27	203.0
1.0	1.705	2.632	12.22	41.68	227.4
14.0	1.642	2.495	9.908	38.52	49.41

TABLE C-16. NEUTRON BUILDUP FACTORS FOR WATER, GEOMETRY C ($h_s = a$,
 $\rho_D = 0$, $z_D = 2a$)

(a) Single-scatter

Thickness, a (mfp)	0.5	1.0	3.0	5.0	7.0
Energy (Mev)					
10 ⁻⁷	1.462	1.790	2.589	3.070	3.428
0.1	1.605	2.042	2.963	3.323	3.478
1.0	1.352	1.645	2.663	3.750	5.139
14.0	1.280	1.462	1.872	2.088	2.219

(b) Total

Energy (Mev)					
10 ⁻⁷	1.710	5.431	12.63	40.21	189.7
0.1	1.955	3.692	18.03	53.56	49.12
1.0	1.447	2.077	6.470	9.961	14.30
14.0	1.414	1.933	3.067	3.723	3.426

NAVSWC TR 91-16

TABLE C-17. NEUTRON BUILDUP FACTORS FOR POLYETHYLENE, GEOMETRY C
($h_s = a$, $\rho_D = 0$, $z_D = 2a$)

(a) Single-scatter

Thickness, a (mfp)	0.5	1.0	3.0	5.0	7.0
Energy (Mev)					
10 ⁻⁷	1.462	1.790	2.589	3.069	3.427
0.1	1.602	2.036	2.952	3.313	3.469
1.0	1.269	1.459	1.900	2.121	2.245
14.0	1.276	1.446	1.801	1.963	2.047

(b) Total

Energy (Mev)					
10 ⁻⁷	1.707	2.556	12.52	38.90	175.5
0.1	1.934	3.727	17.22	41.04	175.4
1.0	1.378	1.797	3.816	4.126	4.754
14.0	1.433	1.764	3.355	13.28	3.076

TABLE C-18. NEUTRON BUILDUP FACTORS FOR CONCRETE, GEOMETRY C
($h_s = a$, $\rho_D = 0$, $z_D = 2a$)

(a) Single-scatter

Thickness, a (mfp)	0.5	1.0	3.0	5.0	7.0
Energy (Mev)					
10 ⁻⁷	1.444	1.769	2.581	3.077	3.464
0.1	1.496	1.824	2.519	2.814	2.949
1.0	1.460	1.851	3.298	5.002	7.513
14.0	1.284	1.457	1.815	1.987	2.093

(b) Total

Energy (Mev)					
10 ⁻⁷	1.681	2.666	13.24	48.83	100.7
0.1	2.291	3.290	23.81	76.20	333.3
1.0	1.605	2.457	12.25	47.06	249.0
14.0	1.430	1.912	4.556	10.06	11.33

TABLE C-19. NEUTRON BUILDUP FACTORS FOR ALUMINUM, GEOMETRY D
($h_s = 0$, $\rho_D = a$, $z_D = a$)

(a) Single-scatter

LOS Thickness (mfp)	0.5	1.0	3.0	5.0	7.0
Energy (Mev)					
10 ⁻⁷	1.386	1.665	2.362	2.778	3.074
0.1	1.303	1.456	1.768	1.919	2.011
1.0	1.369	1.600	2.038	2.202	2.291
14.0	1.271	1.451	1.842	2.044	2.175

(b) Total

Energy (Mev)					
10 ⁻⁷	1.546	2.287	8.604	26.78	80.63
0.1	1.675	2.673	14.57	93.03	617.4
1.0	1.582	2.323	8.818	29.41	144.1
14.0	1.394	1.886	6.187	10.97	31.68

TABLE C-20. NEUTRON BUILDUP FACTORS FOR IRON, GEOMETRY D ($h_s = 0$,
 $\rho_D = a$, $z_D = a$)

(a) Single-scatter

LOS Thickness (mfp)	0.5	1.0	3.0	5.0	7.0
Energy (Mev)					
10 ⁻⁷	1.378	1.650	2.329	2.737	3.026
0.1	1.407	1.674	2.228	2.474	2.641
1.0	1.445	1.881	4.412	11.28	34.76
14.0	1.306	1.521	2.057	2.464	3.039

(b) Total

Energy (Mev)					
10 ⁻⁷	1.630	2.258	8.307	24.97	64.54
0.1	1.638	2.527	13.93	73.89	401.0
1.0	1.547	2.305	11.62	62.05	291.8
14.0	1.416	1.973	7.029	27.58	121.5

TABLE C-21. NEUTRON BUILDUP FACTORS FOR LEAD, GEOMETRY D ($h_s = 0$, $\rho_D = a$, $z_D = a$)

(a) Single-scatter

LOS Thickness (mfp)	0.5	1.0	3.0	5.0	7.0
Energy (Mev)					
10 ⁻⁷	1.416	1.713	2.450	2.887	3.196
0.1	1.422	1.723	2.471	2.917	3.231
1.0	1.381	1.617	2.079	2.292	2.426
14.0	1.390	1.663	2.334	2.732	3.013

(b) Total

Energy (Mev)					
10 ⁻⁷	1.601	2.436	11.73	75.45	251.8
0.1	1.632	2.507	13.37	70.29	966.9
1.0	1.594	2.455	12.56	48.30	210.8
14.0	1.583	2.396	9.932	36.95	66.35

TABLE C-22. NEUTRON BUILDUP FACTORS FOR WATER, GEOMETRY D ($h_s = 0$, $\rho_D = a$, $z_D = a$)

(a) Single-scatter

LOS Thickness (mfp)	0.5	1.0	3.0	5.0	7.0
Energy (Mev)					
10 ⁻⁷	1.470	1.858	3.019	3.878	4.604
0.1	1.631	2.133	3.393	4.059	4.472
1.0	1.364	1.694	2.984	4.519	6.622
14.0	1.299	1.517	2.086	2.448	2.710

(b) Total

Energy (Mev)					
10 ⁻⁷	1.646	2.743	13.13	45.55	124.8
0.1	1.950	3.460	17.79	73.34	291.9
1.0	1.449	2.018	6.214	15.96	27.46
14.0	1.394	1.878	3.625	6.819	7.273

NAVSWC TR 91-16

TABLE C-23. NEUTRON BUILDUP FACTORS FOR POLYETHYLENE, GEOMETRY D
($h_s = 0$, $\rho_D = a$, $z_D = a$)

(a) Single-scatter

LOS Thickness (mfp)	0.5	1.0	3.0	5.0	7.0
Energy (Mev)					
10 ⁻⁷	1.470	1.858	3.018	3.877	4.601
0.1	1.627	2.126	3.381	4.046	4.459
1.0	1.296	1.526	2.142	2.524	2.796
14.0	1.298	1.508	2.026	2.330	2.538

(b) Total

Energy (Mev)					
10 ⁻⁷	1.649	2.761	12.35	44.40	121.1
0.1	1.933	3.461	18.65	72.69	200.4
1.0	1.377	1.829	4.377	6.156	5.482
14.0	1.408	1.918	7.976	7.873	5.114

TABLE C-24. NEUTRON BUILDUP FACTORS FOR CONCRETE, GEOMETRY D
($h_s = 0$, $\rho_D = a$, $z_D = a$)

(a) Single-scatter

LOS Thickness (mfp)	0.5	1.0	3.0	5.0	7.0
Energy (Mev)					
10 ⁻⁷	1.471	1.852	2.957	3.769	4.470
0.1	1.512	1.898	2.872	3.417	3.764
1.0	1.444	1.858	3.688	6.547	12.12
14.0	1.290	1.499	2.022	2.346	2.591

(b) Total

Energy (Mev)					
10 ⁻⁷	1.672	2.600	22.78	43.20	155.3
0.1	1.773	3.113	18.36	93.55	545.9
1.0	1.551	2.306	10.65	50.18	217.5
14.0	1.436	1.833	5.667	15.42	37.20

APPENDIX D

GAMMA-RAY ALBEDO FACTOR TABLES, GEOMETRIES B-D

13 PAGES

REFERENCED IN CHAPTER 1, INTRODUCTION, AND
CHAPTER 5, SAMPLE RESULTS

TABLE D-1. GAMMA-RAY ALBEDO FACTORS FOR ALUMINUM, GEOMETRY B ($h_s=0$, $\rho_D=0$, $z_D=-a$)

(a) Single-scatter		0.5	1.0	2.0	3.0	4.0	5.0	6.0	7.0
Thickness (mfp)									
Energy (Mev)									
0.10	0.3342E+00	0.4684E+00	0.5829E+00	0.6334E+00	0.6612E+00	0.6789E+00	0.6910E+00	0.7004E+00	
1.0	0.6125E-01	0.8861E-01	0.1158E+00	0.1297E+00	0.1383E+00	0.1440E+00	0.1482E+00	0.1513E+00	
7.0	0.2272E-01	0.3118E-01	0.3891E-01	0.4260E-01	0.4476E-01	0.4618E-01	0.4716E-01	0.4789E-01	

(b) Total scatter		0.5	1.0	2.0	3.0	4.0	5.0	6.0	7.0
Thickness (mfp)									
Energy (Mev)									
0.10	0.4400E+00	0.7011E+00	0.9658E+00	0.1118E+01	0.1208E+01	0.1258E+01	0.1295E+01	0.1321E+01	
1.0	0.9436E-01	0.1659E+00	0.2497E+00	0.3017E+00	0.3353E+00	0.3571E+00	0.3754E+00	0.3878E+00	
7.0	0.4327E-01	0.6896E-01	0.9723E-01	0.1114E+00	0.1213E+00	0.1282E+00	0.1325E+00	0.1356E+00	

TABLE D-2. GAMMA-RAY ALBEDO FACTORS FOR IRON, GEOMETRY B ($h_s=0$, $\rho_D=0$, $z_D=-a$)

(a) Single-scatter		0.5	1.0	2.0	3.0	4.0	5.0	6.0	7.0
Thickness (mfp)									
Energy (Mev)									
0.10	0.1405E+00	0.1917E+00	0.2344E+00	0.2534E+00	0.2638E+00	0.2705E+00	0.2751E+00	0.2783E+00	
1.0	0.5943E-01	0.8551E-01	0.1114E+00	0.1247E+00	0.1330E+00	0.1384E+00	0.1425E+00	0.1454E+00	
7.0	0.3105E-01	0.4277E-01	0.5329E-01	0.5819E-01	0.6103E-01	0.6285E-01	0.6412E-01	0.6503E-01	

(b) Total scatter		0.5	1.0	2.0	3.0	4.0	5.0	6.0	7.0
Thickness (mfp)									
Energy (Mev)									
0.10	0.1540E+00	0.2169E+00	0.2724E+00	0.2974E+00	0.3116E+00	0.3209E+00	0.3272E+00	0.3318E+00	
1.0	0.8642E-01	0.1425E+00	0.2063E+00	0.2440E+00	0.2697E+00	0.2868E+00	0.2999E+00	0.3089E+00	
7.0	0.5136E-01	0.8008E-01	0.1099E+00	0.1263E+00	0.1354E+00	0.1424E+00	0.1475E+00	0.1515E+00	

TABLE D-3. GAMMA-RAY ALBEDO FACTORS FOR LEAD, GEOMETRY B ($h_s=0$, $\rho_D=0$, $z_D=-a$)

(a) Single-scatter		0.5	1.0	2.0	3.0	4.0	5.0	6.0	7.0
Thickness (mfp)									
Energy (Mev)									
(b) Total scatter	0.10	0.9912E-02	0.1504E-01	0.2015E-01	0.2262E-01	0.2405E-01	0.2498E-01	0.2565E-01	0.2614E-01
	1.0	0.2830E-01	0.3838E-01	0.4843E-01	0.5364E-01	0.5691E-01	0.5918E-01	0.6078E-01	0.6200E-01
	7.0	0.4110E-01	0.5540E-01	0.6762E-01	0.7302E-01	0.7603E-01	0.7798E-01	0.7922E-01	0.8014E-01
Energy (Mev)									
(b) Total scatter	0.10	0.1001E-01	0.1532E-01	0.2083E-01	0.2368E-01	0.2548E-01	0.2680E-01	0.2784E-01	0.2865E-01
	1.0	0.3147E-01	0.4440E-01	0.5780E-01	0.6499E-01	0.6981E-01	0.7338E-01	0.7553E-01	0.7754E-01
	7.0	0.4859E-01	0.6839E-01	0.8583E-01	0.9380E-01	0.9888E-01	0.1011E+00	0.1039E+00	0.1056E+00

TABLE D-4. GAMMA-RAY ALBEDO FACTORS FOR WATER, GEOMETRY B ($h_s=0$, $\rho_D=0$, $z_D=-a$)

(a) Single-scatter		0.5	1.0	2.0	3.0	4.0	5.0	6.0	7.0
Thickness (mfp)									
Energy (Mev)									
(b) Total scatter	0.10	0.3791E+00	0.5357E+00	0.6699E+00	0.7292E+00	0.7621E+00	0.7829E+00	0.7970E+00	0.8071E+00
	1.0	0.6137E-01	0.8886E-01	0.1161E+00	0.1301E+00	0.1387E+00	0.1445E+00	0.1486E+00	0.1517E+00
	7.0	0.1731E-01	0.2382E-01	0.2991E-01	0.3290E-01	0.3467E-01	0.3587E-01	0.3671E-01	0.3733E-01
Energy (Mev)									
(b) Total scatter	0.10	0.5370E+00	0.9270E+00	0.1461E+01	0.1752E+01	0.1930E+01	0.2059E+01	0.2155E+01	0.2222E+01
	1.0	0.9507E-01	0.1722E+00	0.2680E+00	0.3262E+00	0.3648E+00	0.3895E+00	0.4088E+00	0.4241E+00
	7.0	0.3533E-01	0.5775E-01	0.8120E-01	0.9364E-01	0.1009E+00	0.1071E+00	0.1109E+00	0.1139E+00

TABLE D-5. GAMMA-RAY ALBEDO FACTORS FOR POLYETHYLENE, GEOMETRY B ($h_s=0$, $\rho_D=0$, $\rho_D=-a$)

(a) Single-scatter		0.5	1.0	2.0	3.0	4.0	5.0	6.0	7.0
Thickess (mfp)									
Energy (Mev)									
0.10	0.3842E+00	0.5434E+00	0.6800E+00	0.7403E+00	0.7735E+00	0.7947E+00	0.8092E+00	0.8197E+00	0.8197E+00
1.0	0.6139E-01	0.8886E-01	0.1161E+00	0.1301E+00	0.1386E+00	0.1445E+00	0.1487E+00	0.1518E+00	0.1518E+00
7.0	0.1554E-01	0.2143E-01	0.2703E-01	0.2981E-01	0.3149E-01	0.3260E-01	0.3339E-01	0.3399E-01	0.3399E-01
(b) Total scatter									
Energy (Mev)									
0.10	0.5530E+00	0.9708E+00	0.1608E+01	0.2038E+01	0.2323E+01	0.2508E+01	0.2657E+01	0.2773E+01	0.2773E+01
1.0	0.9569E-01	0.1734E+00	0.2809E+00	0.3428E+00	0.3879E+00	0.4150E+00	0.4374E+00	0.4529E+00	0.4529E+00
7.0	0.3267E-01	0.5394E-01	0.7862E-01	0.9011E-01	0.9762E-01	0.1039E+00	0.1076E+00	0.1104E+00	0.1104E+00

TABLE D-6. GAMMA-RAY ALBEDO FACTORS FOR CONCRETE, GEOMETRY B ($h_s=0$, $\rho_D=0$, $\rho_D=-a$)

(a) Single-scatter		0.5	1.0	2.0	3.0	4.0	5.0	6.0	7.0
Thickess (mfp)									
Energy (Mev)									
0.10	0.3289E+00	0.4609E+00	0.5734E+00	0.6226E+00	0.6501E+00	0.6673E+00	0.6796E+00	0.6879E+00	0.6879E+00
1.0	0.6115E-01	0.8850E-01	0.1156E+00	0.1295E+00	0.1381E+00	0.1438E+00	0.1479E+00	0.1511E+00	0.1511E+00
7.0	0.2158E-01	0.2961E-01	0.3699E-01	0.4053E-01	0.4259E-01	0.4395E-01	0.4493E-01	0.4562E-01	0.4562E-01
(b) Total scatter									
Energy (Mev)									
0.10	0.4303E+00	0.6842E+00	0.9481E+00	0.1076E+01	0.1154E+01	0.1206E+01	0.1237E+01	0.1263E+01	0.1263E+01
1.0	0.9321E-01	0.1650E+00	0.2484E+00	0.2967E+00	0.3291E+00	0.3551E+00	0.3717E+00	0.3837E+00	0.3837E+00
7.0	0.4142E-01	0.6551E-01	0.9198E-01	0.1070E+00	0.1136E+00	0.1219E+00	0.1257E+00	0.1294E+00	0.1294E+00

TABLE D-7. GAMMA-RAY ALBEDO FACTORS FOR ALUMINUM, GEOMETRY C ($h_s=a$, $\rho_D=0$, $z_D=a$)

(a) Single-scatter									
Thickness (mfp)	0.5	1.0	2.0	3.0	4.0	5.0	6.0	7.0	
Energy (Mev)									
0.10	0.3158E+00	0.4333E+00	0.5248E+00	0.5584E+00	0.5722E+00	0.5773E+00	0.5775E+00	0.5753E+00	
1.0	0.5365E-01	0.7361E-01	0.9042E-01	0.9731E-01	0.1005E+00	0.1019E+00	0.1023E+00	0.1020E+00	
7.0	0.1678E-01	0.2057E-01	0.2272E-01	0.2306E-01	0.2283E-01	0.2237E-01	0.2178E-01	0.2113E-01	
(b) Total scatter									
Energy (Mev)									
0.10	0.4195E+00	0.6191E+00	0.8372E+00	0.1002E+01	0.1085E+01	0.1064E+01	0.1045E+01	0.1224E+01	
1.0	0.8554E-01	0.1274E+00	0.2611E+00	0.1815E+00	0.2351E+00	0.1895E+00	0.2303E+00	0.1938E+00	
7.0	0.3103E-01	0.5555E-01	0.5347E-01	0.7209E-01	0.6863E-01	0.8781E-01	0.7013E-01	0.8795E-01	

TABLE D-8. GAMMA-RAY ALBEDO FACTORS FOR IRON, GEOMETRY C ($h_s=a$, $\rho_D=0$, $z_D=a$)

(a) Single-scatter									
Thickness (mfp)	0.5	1.0	2.0	3.0	4.0	5.0	6.0	7.0	
Energy (Mev)									
0.10	0.1216E+00	0.1580E+00	0.1836E+00	0.1922E+00	0.1948E+00	0.1950E+00	0.1937E+00	0.1916E+00	
1.0	0.5073E-01	0.6873E-01	0.8374E-01	0.8991E-01	0.9267E-01	0.9377E-01	0.9399E-01	0.9360E-01	
7.0	0.2425E-01	0.3039E-01	0.3415E-01	0.3495E-01	0.3486E-01	0.3436E-01	0.3370E-01	0.3290E-01	
(b) Total scatter									
Energy (Mev)									
0.10	0.1316E+00	0.1759E+00	0.2032E+00	0.2176E+00	0.2138E+00	0.2139E+00	0.2120E+00	0.2110E+00	
1.0	0.7094E-01	0.1096E+00	0.1231E+00	0.1501E+00	0.1485E+00	0.2293E+00	0.2163E+00	0.2037E+00	
7.0	0.4264E-01	0.6757E-01	0.6455E-01	0.6745E-01	0.6484E-01	0.4968E-01	0.5126E-01	0.4707E-01	

TABLE D-9. GAMMA-RAY ALBEDO FACTORS FOR LEAD, GEOMETRY C ($h_s=a$, $\rho_D=0$, $z_D=a$)

(a) Single-scatter		0.5	1.0	2.0	3.0	4.0	5.0	6.0	7.0
Thickess (mfp)									
Energy (Mev)									
0.10	0.1199E-01	0.2050E-01	0.3206E-01	0.3984E-01	0.4557E-01	0.5007E-01	0.5375E-01	0.5678E-01	
1.0	0.1615E-01	0.1888E-01	0.2018E-01	0.1997E-01	0.1931E-01	0.1848E-01	0.1757E-01	0.1665E-01	
7.0	0.3035E-01	0.3666E-01	0.3983E-01	0.4002E-01	0.3939E-01	0.3842E-01	0.3726E-01	0.3606E-01	
(b) Total scatter									
Energy (Mev)									
0.10	0.1212E-01	0.2092E-01	0.3317E-01	0.4169E-01	0.4825E-01	0.5400E-01	0.5737E-01	0.6137E-01	
1.0	0.1721E-01	0.2033E-01	0.2095E-01	0.2223E-01	0.2022E-01	0.2009E-01	0.1871E-01	0.1757E-01	
7.0	0.3619E-01	0.4484E-01	0.5423E-01	0.5435E-01	0.6141E-01	0.5022E-01	0.6239E-01	0.6176E-01	

TABLE D-10. GAMMA-RAY ALBEDO FACTORS FOR WATER, GEOMETRY C ($h_s=a$, $\rho_D=0$, $z_D=a$)

(a) Single-scatter		0.5	1.0	2.0	3.0	4.0	5.0	6.0	7.0
Thickess (mfp)									
Energy (Mev)									
0.10	0.3670E+00	0.5115E+00	0.6269E+00	0.6703E+00	0.6894E+00	0.6969E+00	0.6982E+00	0.6959E+00	
1.0	0.5389E-01	0.7400E-01	0.9093E-01	0.9793E-01	0.1012E+00	0.1025E+00	0.1030E+00	0.1027E+00	
7.0	0.1226E-01	0.1489E-01	0.1633E-01	0.1649E-01	0.1625E-01	0.1585E-01	0.1537E-01	0.1485E-01	
(b) Total scatter									
Energy (Mev)									
0.10	0.5175E+00	0.9129E+00	0.1443E+01	0.1588E+01	0.1908E+01	0.1831E+01	0.2112E+01	0.2102E+01	
1.0	0.8339E-01	0.1434E+00	0.1797E+00	0.3268E+00	0.2239E+00	0.2421E+00	0.2418E+00	0.2705E+00	
7.0	0.2448E-01	0.3632E-01	0.3956E-01	0.4901E-01	0.2877E-01	0.2798E-01	0.2797E-01	0.2715E-01	

TABLE D-11. GAMMA-RAY ALBEDO FACTORS FOR POLYETHYLENE, GEOMETRY C ($h_s=a$, $\rho_D=0$, $z_D=a$)

(a) Single-scatter		0.5	1.0	2.0	3.0	4.0	5.0	6.0	7.0
Thickness (mfp)									
Energy (Mev)									
0.10	0.3729E+00	0.5209E+00	0.6395E+00	0.6846E+00	0.7037E+00	0.7115E+00	0.7131E+00	0.7110E+00	0.7110E+00
1.0	0.5392E-01	0.7403E-01	0.9099E-01	0.9793E-01	0.1012E+00	0.1026E+00	0.1030E+00	0.1028E+00	0.1028E+00
7.0	0.1084E-01	0.1314E-01	0.1440E-01	0.1453E-01	0.1431E-01	0.1393E-01	0.1349E-01	0.1301E-01	0.1301E-01

(b) Total scatter		0.5	1.0	2.0	3.0	4.0	5.0	6.0	7.0
Energy (Mev)									
0.10	0.5479E+00	0.9391E+00	0.1447E+01	0.2025E+01	0.1955E+01	0.2143E+01	0.2219E+01	0.2358E+01	0.2358E+01
1.0	0.8035E-01	0.1509E+00	0.2167E+00	0.2455E+00	0.2552E+00	0.3847E+00	0.2815E+00	0.3597E+00	0.3597E+00
7.0	0.2298E-01	0.2711E-01	0.3914E-01	0.2977E-01	0.3870E-01	0.3139E-01	0.3242E-01	0.3674E-01	0.3674E-01

TABLE D-12. GAMMA-RAY ALBEDO FACTORS FOR CONCRETE, GEOMETRY C ($h_s=a$, $\rho_D=0$, $z_D=a$)

(a) Single-scatter		0.5	1.0	2.0	3.0	4.0	5.0	6.0	7.0
Thickness (mfp)									
Energy (Mev)									
0.10	0.3103E+00	0.4252E+00	0.5138E+00	0.5469E+00	0.5604E+00	0.5653E+00	0.5655E+00	0.5629E+00	0.5629E+00
1.0	0.5354E-01	0.7347E-01	0.9022E-01	0.9716E-01	0.1003E+00	0.1017E+00	0.1020E+00	0.1018E+00	0.1018E+00
7.0	0.1580E-01	0.1932E-01	0.2131E-01	0.2159E-01	0.2135E-01	0.2090E-01	0.2034E-01	0.1971E-01	0.1971E-01

(b) Total scatter		0.5	1.0	2.0	3.0	4.0	5.0	6.0	7.0
Energy (Mev)									
0.10	0.4024E+00	0.6360E+00	0.8023E+00	0.9447E+00	0.1055E+01	0.1173E+01	0.1146E+01	0.1068E+01	0.1068E+01
1.0	0.8441E-01	0.1392E+00	0.1752E+00	0.1990E+00	0.2468E+00	0.2155E+00	0.2811E+00	0.2674E+00	0.2674E+00
7.0	0.3101E-01	0.3751E-01	0.4072E-01	0.4433E-01	0.4463E-01	0.5000E-01	0.4586E-01	0.6269E-01	0.6269E-01

TABLE D-13. GAMMA-RAY ALBEDO FACTORS FOR ALUMINUM, GEOMETRY D ($h_s=0$, $\rho_D=a$, $z_D=0$)

(a) Single-scatter

LOS Thickness (mfp)	0.5	1.0	2.0	3.0	4.0	5.0	6.0	7.0
Energy (Mev)								
0.10	0.2760E+00	0.3274E+00	0.2566E+00	0.1616E+00	0.9376E-01	0.5213E-01	0.2824E-01	0.1502E-01
0.20	0.2413E+00	0.2967E+00	0.2428E+00	0.1571E+00	0.9283E-01	0.5231E-01	0.2862E-01	0.1535E-01
0.60	0.1767E+00	0.2222E+00	0.1866E+00	0.1224E+00	0.7294E-01	0.4130E-01	0.2267E-01	0.1219E-01
1.0	0.1529E+00	0.1923E+00	0.1615E+00	0.1058E+00	0.6288E-01	0.3553E-01	0.1947E-01	0.1045E-01
3.0	0.1125E+00	0.1397E+00	0.1155E+00	0.7497E-01	0.4430E-01	0.2494E-01	0.1362E-01	0.7288E-02
5.0	0.9260E-01	0.1138E+00	0.9376E-01	0.6103E-01	0.3619E-01	0.2044E-01	0.1120E-01	0.6008E-02
7.0	0.7794E-01	0.9541E-01	0.7895E-01	0.5171E-01	0.3087E-01	0.1753E-01	0.9652E-02	0.5206E-02

(b) Total

Energy (Mev)								
0.10	0.3711E+00	0.4640E+00	0.5473E+00	0.3631E+00	0.2468E+00	0.1173E+00	0.6399E-01	0.9365E-01
0.20	0.3032E+00	0.4430E+00	0.4445E+00	0.3595E+00	0.2142E+00	0.1430E+00	0.6936E-01	0.4549E-01
0.60	0.2144E+00	0.3091E+00	0.3175E+00	0.2647E+00	0.1536E+00	0.1017E+00	0.6932E-01	0.3785E-01
1.0	0.1838E+00	0.2542E+00	0.3069E+00	0.2123E+00	0.1527E+00	0.9117E-01	0.4735E-01	0.4117E+00
3.0	0.1363E+00	0.2189E+00	0.1850E+00	0.1125E+00	0.1026E+00	0.8488E-01	0.2076E-01	0.1034E-01
5.0	0.1095E+00	0.1626E+00	0.1335E+00	0.9603E-01	0.6773E-01	0.3324E-01	0.1650E-01	0.8423E-02
7.0	0.9588E-01	0.1224E+00	0.1151E+00	0.7046E-01	0.6265E-01	0.2578E-01	0.1253E-01	0.6731E-02

TABLE D-14. GAMMA-RAY ALBEDO FACTORS FOR IRON, GEOMETRY D ($h_s=0$, $\rho_D=a$, $z_D=0$)

(a) Single-scatter									
LOS Thickness	0.0	1.0	2.0	3.0	4.0	5.0	6.0	7.0	
(mfp)									
Energy (Mev)									
0.10	0.1136E+00	0.1290E+00	0.9675E-01	0.5963E-01	0.3415E-01	0.1881E-01	0.1011E-01	0.5341E-02	
0.20	0.1881E+00	0.2241E+00	0.1782E+00	0.1135E+00	0.6646E-01	0.3718E-01	0.2021E-01	0.1079E-01	
0.60	0.1711E+00	0.2135E+00	0.1787E+00	0.1171E+00	0.6971E-01	0.3947E-01	0.2167E-01	0.1164E-01	
1.0	0.1504E+00	0.1887E+00	0.1582E+00	0.1036E+00	0.6164E-01	0.3484E-01	0.1909E-01	0.1024E-01	
3.0	0.1113E+00	0.1382E+00	0.1149E+00	0.7505E-01	0.4466E-01	0.2530E-01	0.1388E-01	0.7471E-02	
5.0	0.8945E-01	0.1099E+00	0.9139E-01	0.6023E-01	0.3621E-01	0.2071E-01	0.1147E-01	0.6223E-02	
7.0	0.7342E-01	0.8985E-01	0.7505E-01	0.4995E-01	0.3035E-01	0.1755E-01	0.9824E-02	0.5381E-02	
(b) Total									
Energy (Mev)									
0.10	0.1229E+00	0.1449E+00	0.1141E+00	0.7135E-01	0.4364E-01	0.2284E-01	0.1279E-01	0.6954E-02	
0.20	0.2159E+00	0.2880E+00	0.2510E+00	0.1824E+00	0.1063E+00	0.5694E-01	0.2967E-01	0.1621E-01	
0.60	0.2341E+00	0.3399E+00	0.2710E+00	0.1921E+00	0.1259E+00	0.8212E-01	0.6032E-01	0.2310E-01	
1.0	0.1770E+00	0.2557E+00	0.2591E+00	0.1725E+00	0.1284E+00	0.6765E-01	0.4108E-01	0.2903E-01	
3.0	0.1325E+00	0.1908E+00	0.1691E+00	0.1140E+00	0.6828E-01	0.5795E-01	0.2045E-01	0.1389E-01	
5.0	0.1064E+00	0.1410E+00	0.1290E+00	0.9206E-01	0.7144E-01	0.2885E-01	0.1410E-01	0.8588E-02	
7.0	0.9132E-01	0.1245E+00	0.1087E+00	0.7442E-01	0.6667E-01	0.2221E-01	0.1348E-01	0.7842E-02	

TABLE D-15. GAMMA-RAY ALBEDO FACTORS FOR LEAD, GEOMETRY D ($h_s=0$, $\rho_D=a$, $z_D=0$)

(a) Single-scatter								
LOS Thickness	0.5	1.0	2.0	3.0	4.0	5.0	6.0	7.0
		(mfp)						
Energy (Mev)								
0.10	0.9508E-02	0.1461E-01	0.1875E-01	0.1963E-01	0.1947E-01	0.1902E-01	0.1853E-01	0.1806E-01
0.20	0.2010E-01	0.2278E-01	0.1738E-01	0.1082E-01	0.6211E-02	0.3411E-02	0.1827E-02	0.9593E-03
0.60	0.7358E-01	0.8720E-01	0.6922E-01	0.4372E-01	0.2528E-01	0.1395E-01	0.7473E-02	0.3929E-02
1.0	0.9164E-01	0.1108E+00	0.8965E-01	0.5729E-01	0.3338E-01	0.1853E-01	0.1000E-01	0.5290E-02
3.0	0.8826E-01	0.1062E+00	0.8845E-01	0.5889E-01	0.3572E-01	0.2060E-01	0.1150E-01	0.6278E-02
5.0	0.6899E-01	0.8166E-01	0.6837E-01	0.4648E-01	0.2887E-01	0.1704E-01	0.9720E-02	0.5428E-02
7.0	0.5549E-01	0.6478E-01	0.5406E-01	0.3718E-01	0.2347E-01	0.1411E-01	0.8216E-02	0.4676E-02
(b) Total								
Energy (Mev)								
0.10	0.9574E-02	0.1497E-01	0.1946E-01	0.2050E-01	0.2055E-01	0.2045E-01	0.2022E-01	0.2009E-01
0.20	0.2041E-01	0.2326E-01	0.1813E-01	0.1146E-01	0.6729E-02	0.3804E-02	0.2166E-02	0.1265E-02
0.60	0.8714E-01	0.9266E-01	0.7666E-01	0.4787E-01	0.2856E-01	0.1610E-01	0.8971E-02	0.4718E-02
1.0	0.9630E-01	0.1215E+00	0.1190E+00	0.6944E-01	0.4503E-01	0.2203E-01	0.1234E-01	0.7664E-02
3.0	0.9483E-01	0.1345E+00	0.1136E+00	0.8962E-01	0.5372E-01	0.2635E-01	0.1398E-01	0.8935E-02
5.0	0.7598E-01	0.9186E-01	0.8008E-01	0.5983E-01	0.4221E-01	0.1973E-01	0.1275E-01	0.7562E-02
7.0	0.6084E-01	0.7223E-01	0.7265E-01	0.4350E-01	0.2769E-01	0.1755E-01	0.9754E-02	0.5141E-02

TABLE D-16. GAMMA-RAY ALBEDO FACTORS FOR WATER, GEOMETRY D ($h_s=0$, $\rho_D=a$, $z_D=0$)

(a) Single-scatter								
LOS Thickness	0.5	1.0	2.0	3.0	4.0	5.0	6.0	7.0
(mfp)								
Energy (Mev)								
0.10	0.3148E+00	0.3787E+00	0.3004E+00	0.1916E+00	0.1120E+00	0.6257E-01	0.3396E-01	0.1818E-01
0.20	0.2469E+00	0.3046E+00	0.2513E+00	0.1624E+00	0.9617E-01	0.5423E-01	0.2968E-01	0.1596E-01
0.60	0.1771E+00	0.2228E+00	0.1884E+00	0.1228E+00	0.7316E-01	0.4145E-01	0.2273E-01	0.1223E-01
1.0	0.1531E+00	0.1927E+00	0.1627E+00	0.1059E+00	0.6300E-01	0.3557E-01	0.1948E-01	0.1046E-01
3.0	0.1130E+00	0.1401E+00	0.1157E+00	0.7476E-01	0.4406E-01	0.2472E-01	0.1343E-01	0.7182E-02
5.0	0.9449E-01	0.1160E+00	0.9481E-01	0.6137E-01	0.3614E-01	0.2027E-01	0.1100E-01	0.5888E-02
7.0	0.8124E-01	0.9941E-01	0.8108E-01	0.5274E-01	0.3114E-01	0.1750E-01	0.9522E-02	0.5106E-02
(b) Total								
Energy (Mev)								
0.10	0.4104E+00	0.6434E+00	0.6889E+00	0.6217E+00	0.6370E+00	0.3345E+00	0.1966E+00	0.1310E+00
0.20	0.3158E+00	0.4816E+00	0.5331E+00	0.4257E+00	0.2875E+00	0.2478E+00	0.1314E+00	0.7839E-01
0.60	0.2195E+00	0.3103E+00	0.3289E+00	0.2564E+00	0.1709E+00	0.1252E+00	0.7083E-01	0.3689E-01
1.0	0.1842E+00	0.2583E+00	0.2824E+00	0.2124E+00	0.1521E+00	0.8398E-01	0.5095E-01	0.2806E-01
3.0	0.1329E+00	0.1789E+00	0.1806E+00	0.1275E+00	0.7884E-01	0.4547E-01	0.2510E-01	0.1515E-01
5.0	0.1099E+00	0.1672E+00	0.1407E+00	0.8390E-01	0.5192E-01	0.2595E-01	0.1990E-01	0.1458E-01
7.0	0.9643E-01	0.1351E+00	0.1219E+00	0.7715E-01	0.3755E-01	0.2408E-01	0.1076E-01	0.6151E-02

TABLE D-17. GAMMA-RAY ALBEDO FACTORS FOR POLYETHYLENE, GEOMETRY D ($h_s=0$, $\rho_D=a$, $z_D=0$)

(a) Single-scatter								
LOS Thickness	0.5	1.0	2.0	3.0	4.0	5.0	6.0	7.0
(mfp)								
Energy (Mev)								
0.10	0.3194E+00	0.3847E+00	0.3069E+00	0.1953E+00	0.1142E+00	0.6390E-01	0.3480E-01	0.1859E-01
0.20	0.2475E+00	0.3056E+00	0.2513E+00	0.1631E+00	0.9656E-01	0.5447E-01	0.2985E-01	0.1603E-01
0.60	0.1772E+00	0.2228E+00	0.1872E+00	0.1228E+00	0.7319E-01	0.4147E-01	0.2276E-01	0.1223E-01
1.0	0.1531E+00	0.1925E+00	0.1618E+00	0.1059E+00	0.6299E-01	0.3558E-01	0.1950E-01	0.1046E-01
3.0	0.1131E+00	0.1402E+00	0.1155E+00	0.7464E-01	0.4393E-01	0.2463E-01	0.1340E-01	0.7142E-02
5.0	0.9506E-01	0.1167E+00	0.9538E-01	0.6145E-01	0.3611E-01	0.2021E-01	0.1098E-01	0.5853E-02
7.0	0.8245E-01	0.1008E+00	0.8233E-01	0.5308E-01	0.3121E-01	0.1749E-01	0.9517E-02	0.5078E-02
(b) Total								
Energy (Mev)								
0.10	0.4208E+00	0.7786E+00	0.7941E+00	0.7769E+00	0.6065E+00	0.5480E+00	0.3230E+00	0.4367E+00
0.20	0.3147E+00	0.4783E+00	0.5430E+00	0.5096E+00	0.3784E+00	0.2590E+00	0.2936E+00	0.1167E+00
0.60	0.2136E+00	0.3083E+00	0.3752E+00	0.2963E+00	0.2555E+00	0.1550E+00	0.8392E-01	0.4635E-01
1.0	0.1842E+00	0.2598E+00	0.2931E+00	0.2186E+00	0.1551E+00	0.8834E-01	0.4574E-01	0.2788E-01
3.0	0.1328E+00	0.1836E+00	0.2021E+00	0.1185E+00	0.9271E-01	0.4884E-01	0.2476E-01	0.1250E-01
5.0	0.1712E+00	0.1513E+00	0.1409E+00	0.9022E-01	0.7036E-01	0.3431E-01	0.1443E-01	0.8015E-02
7.0	0.9511E-01	0.1310E+00	0.1060E+00	0.8195E-01	0.5111E-01	0.4712E-01	0.1935E-01	0.9021E-02

TABLE D-18. GAMMA-RAY ALBEDO FACTORS FOR CONCRETE, GEOMETRY D ($h_s=0$, $\rho_D=a$, $z_D=0$)

(a) Single-scatter								
LOS Thickness	0.5	1.0	2.0	3.0	4.0	5.0	6.0	7.0
(mfp)								
Energy (Mev)								
0.10	0.2715E+00	0.3219E+00	0.2519E+00	0.1584E+00	0.9188E-01	0.5104E-01	0.2762E-01	0.1470E-01
0.20	0.2404E+00	0.2950E+00	0.2415E+00	0.1561E+00	0.9221E-01	0.5196E-01	0.2843E-01	0.1525E-01
0.60	0.1765E+00	0.2220E+00	0.1863E+00	0.1223E+00	0.7281E-01	0.4126E-01	0.2264E-01	0.1218E-01
1.0	0.1527E+00	0.1922E+00	0.1612E+00	0.1056E+00	0.6283E-01	0.3549E-01	0.1944E-01	0.1043E-01
3.0	0.1127E+00	0.1397E+00	0.1154E+00	0.7490E-01	0.4424E-01	0.2488E-01	0.1356E-01	0.7255E-02
5.0	0.9294E-01	0.1142E+00	0.9414E-01	0.6114E-01	0.3623E-01	0.2043E-01	0.1118E-01	0.5995E-02
7.0	0.7866E-01	0.9621E-01	0.7949E-01	0.5194E-01	0.3094E-01	0.1753E-01	0.9633E-02	0.5186E-02
(b) Total								
Energy (Mev)								
0.10	0.3563E+00	0.4529E+00	0.5081E+00	0.3199E+00	0.2170E+00	0.1143E+00	0.6029E-01	0.3595E-01
0.20	0.2988E+00	0.4414E+00	0.4308E+00	0.4038E+00	0.2157E+00	0.1517E+00	0.8100E-01	0.4245E-01
0.60	0.2114E+00	0.3144E+00	0.3037E+00	0.2590E+00	0.1707E+00	0.1316E+00	0.5316E-01	0.2948E-01
1.0	0.1806E+00	0.2570E+00	0.2611E+00	0.2466E+00	0.1247E+00	0.8188E+00	0.4503E-01	0.4026E+00
3.0	0.1311E+00	0.1794E+00	0.1688E+00	0.1491E+00	0.9475E-01	0.5649E-01	0.2132E-01	0.1669E-01
5.0	0.1181E+00	0.1491E+00	0.1310E+00	0.8492E-01	0.5785E-01	0.2832E-01	0.1651E-01	0.8048E-02
7.0	0.9825E-01	0.1348E+00	0.1112E+00	0.7738E-01	0.4578E-01	0.2538E-01	0.1373E-01	0.8743E-02

APPENDIX E

NEUTRON ALBEDO FACTOR TABLES, GEOMETRIES B-D

10 PAGES

REFERENCED IN CHAPTER 1, INTRODUCTION, AND
CHAPTER 5, SAMPLE RESULTS

NAVSWC TR 91-16

TABLE E-1. NEUTRON ALBEDO FACTORS FOR ALUMINUM, GEOMETRY B ($h_s=0$, $\rho_D=0$, $z_D=-a$)

(a) Single-scatter

Thickness (mfp)	0.5	1.0	3.0	5.0	7.0
Energy (Mev)					
10 ⁻⁷	0.4766E+00	0.6906E+00	0.9772E+00	0.1061E+01	0.1099E+01
0.10	0.4242E+00	0.5644E+00	0.7312E+00	0.7769E+00	0.7954E+00
1.0	0.4464E+00	0.6311E+00	0.8795E+00	0.9587E+00	0.9948E+00
14.0	0.3263E+00	0.4703E+00	0.6640E+00	0.7210E+00	0.7459E+00

(b) Total

Energy (Mev)					
10 ⁻⁷	0.6524E+00	0.1130E+01	0.2189E+01	0.2637E+01	0.2850E+01
0.10	0.8406E+00	0.1495E+01	0.3000E+01	0.3832E+01	0.4384E+01
1.0	0.6941E+00	0.1237E+01	0.2478E+01	0.2966E+01	0.3222E+01
14.0	0.4585E+00	0.8061E+00	0.1514E+01	0.1793E+01	0.1938E+01

TABLE E-2. NEUTRON ALBEDO FACTORS FOR IRON, GEOMETRY B ($h_s=0$, $\rho_D=0$, $z_D=-a$)

(a) Single-scatter

Thickness (mfp)	0.5	1.0	3.0	5.0	7.0
Energy (Mev)					
10 ⁻⁷	0.4797E+00	0.6944E+00	0.9803E+00	0.1064E+01	0.1101E+01
0.10	0.5356E+00	0.7665E+00	0.1070E+01	0.1159E+01	0.1198E+01
1.0	0.4987E+00	0.7436E+00	0.1109E+01	0.1224E+01	0.1278E+01
14.0	0.3797E+00	0.5486E+00	0.7753E+00	0.8423E+00	0.8718E+00

(b) Total

Energy (Mev)					
10 ⁻⁷	0.6509E+00	0.1120E+01	0.2103E+01	0.2483E+01	0.2693E+01
0.10	0.8054E+00	0.1446E+01	0.3079E+01	0.3860E+01	0.4308E+01
1.0	0.6042E+00	0.1020E+01	0.1969E+01	0.2477E+01	0.2790E+01
14.0	0.5069E+00	0.8645E+00	0.1618E+01	0.1963E+01	0.2139E+01

NAVSWC TR 91-16

TABLE E-3. NEUTRON ALBEDO FACTORS FOR LEAD, GEOMETRY B ($h_s=0$, $\rho_D=0$, $z_D=-a$)

(a) Single-scatter

Thickness (mfp)	0.5	1.0	3.0	5.0	7.0
Energy (Mev)					
10 ⁻⁷	0.5389E+00	0.7793E+00	0.1098E+01	0.1191E+01	0.1232E+01
0.10	0.5467E+00	0.7902E+00	0.1113E+01	0.1207E+01	0.1249E+01
1.0	0.5185E+00	0.7452E+00	0.1037E+01	0.1118E+01	0.1152E+01
14.0	0.5028E+00	0.7257E+00	0.1021E+01	0.1108E+01	0.1147E+01

(b) Total

Energy (Mev)					
10 ⁻⁷	0.7590E+00	0.1358E+01	0.2853E+01	0.3636E+01	0.4031E+01
0.10	0.7729E+00	0.1387E+01	0.2963E+01	0.3841E+01	0.4344E+01
1.0	0.7591E+00	0.1359E+01	0.2801E+01	0.3450E+01	0.3790E+01
14.0	0.7028E+00	0.1231E+01	0.2411E+01	0.2895E+01	0.3168E+01

TABLE E-4. NEUTRON ALBEDO FACTORS FOR WATER, GEOMETRY B ($h_s=0$, $\rho_D=0$, $z_D=-a$)

(a) Single-scatter

Thickness (mfp)	0.5	1.0	3.0	5.0	7.0
Energy (Mev)					
10 ⁻⁷	0.1163E+00	0.1763E+00	0.2765E+00	0.3129E+00	0.3293E+00
0.10	0.6700E-01	0.9674E-01	0.1366E+00	0.1484E+00	0.1537E+00
1.0	0.2199E+00	0.3249E+00	0.4740E+00	0.5209E+00	0.5426E+00
14.0	0.1742E+00	0.2515E+00	0.3576E+00	0.3900E+00	0.4045E+00

(b) Total

Energy (Mev)					
10 ⁻⁷	0.2181E+00	0.4613E+00	0.1181E+01	0.1597E+01	0.1848E+01
0.10	0.1385E+00	0.3172E+00	0.9708E+00	0.1377E+01	0.1620E+01
1.0	0.2638E+00	0.4387E+00	0.7936E+00	0.9450E+00	0.1031E+01
14.0	0.2456E+00	0.4147E+00	0.7244E+00	0.8381E+00	0.8984E+00

TABLE E-5. NEUTRON ALBEDO FACTORS FOR POLYETHYLENE, GEOMETRY B
($h_s=0$, $\rho_D=0$, $z_D=-a$)

(a) Single-scatter

Thickness (mfp)	0.5	1.0	3.0	5.0	7.0
Energy (Mev)					
10 ⁻⁷	0.1170E+00	0.1772E+00	0.2779E+00	0.3144E+00	0.3309E+00
0.10	0.8002E-01	0.1155E+00	0.1633E+00	0.1776E+00	0.1839E+00
1.0	0.9167E-01	0.1331E+00	0.1905E+00	0.2082E+00	0.2164E+00
14.0	0.1521E+00	0.2201E+00	0.3136E+00	0.3420E+00	0.3548E+00

(b) Total

Energy (Mev)					
10 ⁻⁷	0.2172E+00	0.4610E+00	0.1186E+01	0.1604E+01	0.1853E+01
0.10	0.1636E+00	0.3625E+00	0.1065E+01	0.1468E+01	0.1749E+01
1.0	0.1326E+00	0.2403E+00	0.4721E+00	0.5706E+00	0.6228E+00
14.0	0.2230E+00	0.3819E+00	0.6675E+00	0.7706E+00	0.8238E+00

TABLE E-6. NEUTRON ALBEDO FACTORS FOR CONCRETE, GEOMETRY B ($h_s=0$,
 $\rho_D=0$, $z_D=-a$)

(a) Single-scatter

Thickness (mfp)	0.5	1.0	3.0	5.0	7.0
Energy (Mev)					
10 ⁻⁷	0.1157E+00	0.1707E+00	0.2584E+00	0.2930E+00	0.3118E+00
0.10	0.3628E+00	0.5234E+00	0.7364E+00	0.7987E+00	0.8261E+00
1.0	0.4368E+00	0.6525E+00	0.9620E+00	0.1059E+01	0.1106E+01
14.0	0.3067E+00	0.4447E+00	0.6320E+00	0.6884E+00	0.7136E+00

(b) Total

Energy (Mev)					
10 ⁻⁷	0.2189E+00	0.4587E+00	0.1199E+01	0.1573E+01	0.1807E+01
0.10	0.6032E+00	0.1202E+01	0.2967E+01	0.3870E+01	0.4367E+01
1.0	0.5370E+00	0.9191E+00	0.1757E+01	0.2180E+01	0.2400E+01
14.0	0.4131E+00	0.7040E+00	0.1287E+01	0.1505E+01	0.1614E+01

TABLE E-7. NEUTRON ALBEDO FACTORS FOR ALUMINUM, GEOMETRY C ($h_s=a$, $\rho_D=0$, $z_D=a$)

(a) Single-scatter

Thickness (mfp)	0.5	1.0	3.0	5.0	7.0
Energy (Mev)					
10 ⁻⁷	0.4352E+00	0.6108E+00	0.7597E+00	0.7225E+00	0.6536E+00
0.10	0.2720E+00	0.3017E+00	0.2412E+00	0.1674E+00	0.1130E+00
1.0	0.3707E+00	0.4900E+00	0.5743E+00	0.5337E+00	0.4716E+00
14.0	0.2919E+00	0.4031E+00	0.4887E+00	0.4576E+00	0.4088E+00

(b) Total

Energy (Mev)					
10 ⁻⁷	0.6113E+00	0.1011E+01	0.1752E+01	0.2950E+01	0.3228E+01
0.10	0.6607E+00	0.1206E+01	0.2645E+01	0.3113E+01	0.4424E+01
1.0	0.5832E+00	0.1043E+01	0.2058E+01	0.1910E+01	0.2011E+01
14.0	0.4048E+00	0.6727E+00	0.1157E+01	0.1319E+01	0.1349E+01

TABLE E-8. NEUTRON ALBEDO FACTORS FOR IRON, GEOMETRY C ($h_s=a$, $\rho_D=0$, $z_D=a$)

(a) Single-scatter

Thickness (mfp)	0.5	1.0	3.0	5.0	7.0
Energy (Mev)					
10 ⁻⁷	0.4370E+00	0.6125E+00	0.7606E+00	0.7231E+00	0.6543E+00
0.10	0.4735E+00	0.6453E+00	0.7674E+00	0.7126E+00	0.6309E+00
1.0	0.5048E+00	0.7819E+00	0.1247E+01	0.1364E+01	0.1373E+01
14.0	0.3459E+00	0.4825E+00	0.5957E+00	0.5634E+00	0.5064E+00

(b) Total

Energy (Mev)					
10 ⁻⁷	0.5928E+00	0.9440E+00	0.1952E+01	0.2272E+01	0.2241E+01
0.10	0.7313E+00	0.1254E+01	0.2620E+01	0.3876E+01	0.3806E+01
1.0	0.6247E+00	0.1154E+01	0.2254E+01	0.2851E+01	0.3133E+01
14.0	0.4673E+00	0.8043E+00	0.1349E+01	0.1557E+01	0.1880E+01

NAVSWC TR 91-16

TABLE E-9. NEUTRON ALBEDO FACTORS FOR LEAD, GEOMETRY C ($h_s=a$, $\rho_D=0$, $z_D=a$)

(a) Single-scatter

Thickness (mfp)	0.5	1.0	3.0	5.0	7.0
Energy (Mev)					
10 ⁻⁷	0.4939E+00	0.6917E+00	0.8553E+00	0.8108E+00	0.7315E+00
0.10	0.5009E+00	0.7012E+00	0.8670E+00	0.8213E+00	0.7403E+00
1.0	0.4649E+00	0.6362E+00	0.7316E+00	0.6554E+00	0.5624E+00
14.0	0.4586E+00	0.6398E+00	0.7868E+00	0.7433E+00	0.6690E+00

(b) Total

Energy (Mev)					
10 ⁻⁷	0.7079E+00	0.1243E+01	0.2641E+01	0.3922E+01	0.3517E+01
0.10	0.7278E+00	0.1299E+01	0.2704E+01	0.3551E+01	0.4071E+01
1.0	0.7100E+00	0.1190E+01	0.2680E+01	0.2594E+01	0.2426E+01
14.0	0.6585E+00	0.1086E+01	0.1882E+01	0.2487E+01	0.2788E+01

TABLE E-10. NEUTRON ALBEDO FACTORS FOR WATER, GEOMETRY C ($h_s=a$, $\rho_D=0$, $z_D=a$)

(a) Single-scatter

Thickness (mfp)	0.5	1.0	3.0	5.0	7.0
Energy (Mev)					
10 ⁻⁷	0.8831E-01	0.1216E+00	0.1423E+00	0.1266E+00	0.1079E+00
0.10	0.6062E-01	0.8431E-01	0.1034E+00	0.9739E-01	0.8742E-01
1.0	0.2117E+00	0.3121E+00	0.4295E+00	0.4330E+00	0.4101E+00
14.0	0.1546E+00	0.2130E+00	0.2583E+00	0.2419E+00	0.2158E+00

(b) Total

Energy (Mev)					
10 ⁻⁷	0.2024E+00	0.3629E+00	0.6892E+00	0.1124E+01	0.9376E+00
0.10	0.1232E+00	0.2966E+00	0.7518E+00	0.7759E+00	0.8947E+00
1.0	0.2643E+00	0.4602E+00	0.7369E+00	0.8874E+00	0.8924E+00
14.0	0.2256E+00	0.3646E+00	0.4906E+00	0.5461E+00	0.4738E+00

TABLE E-11. NEUTRON ALBEDO FACTORS FOR POLYETHYLENE, GEOMETRY C
($h_s=a$, $\rho_D=0$, $z_D=a$)

(a) Single-scatter

Thickness (mfp)	0.5	1.0	3.0	5.0	7.0
Energy (Mev)					
10 ⁻⁷	0.8900E-01	0.1226E+00	0.1435E+00	0.1279E+00	0.1090E+00
0.10	0.7217E-01	0.1002E+00	0.1227E+00	0.1155E+00	0.1035E+00
1.0	0.8166E-01	0.1134E+00	0.1395E+00	0.1315E+00	0.1180E+00
14.0	0.1331E+00	0.1828E+00	0.2180E+00	0.2014E+00	0.1777E+00

(b) Total

Energy (Mev)					
10 ⁻⁷	0.2027E+00	0.3659E+00	0.6668E+00	0.1217E+01	0.8920E+00
0.10	0.1449E+00	0.2887E+00	0.7651E+00	0.1051E+01	0.1291E+01
1.0	0.1092E+00	0.1854E+00	0.3539E+00	0.3500E+00	0.4826E+00
14.0	0.1893E+00	0.2834E+00	0.4392E+00	0.4096E+00	0.3592E+00

TABLE E-12. NEUTRON ALBEDO FACTORS FOR CONCRETE, GEOMETRY C ($h_s=a$,
 $\rho_D=0$, $z_D=a$)

(a) Single-scatter

Thickness (mfp)	0.5	1.0	3.0	5.0	7.0
Energy (Mev)					
10 ⁻⁷	0.9412E-01	0.1338E+00	0.1772E+00	0.1730E+00	0.1571E+00
0.10	0.3274E+00	0.4535E+00	0.5467E+00	0.5081E+00	0.4504E+00
1.0	0.4388E+00	0.6687E+00	0.9693E+00	0.1006E+01	0.9799E+00
14.0	0.2762E+00	0.3844E+00	0.4709E+00	0.4433E+00	0.3975E+00

(b) Total

Energy (Mev)					
10 ⁻⁷	0.1680E+00	0.3743E+00	0.1005E+01	0.1373E+01	0.1376E+01
0.10	0.5361E+00	0.1093E+01	0.2810E+01	0.2877E+01	0.3869E+01
1.0	0.5538E+00	0.9906E+00	0.1781E+01	0.2352E+01	0.2631E+01
14.0	0.3734E+00	0.6110E+00	0.1103E+01	0.1119E+01	0.1383E+01

TABLE E-13. NEUTRON ALBEDO FACTORS FOR ALUMINUM, GEOMETRY D
($h_s=0$, $\rho_D=a$, $z_D=0$)

(a) Single-scatter

LOS Thickness (mfp)	0.5	1.0	3.0	5.0	7.0
Energy (Mev)					
10 ⁻⁷	0.5827E+00	0.7357E+00	0.4129E+00	0.1415E+00	0.4227E-01
0.10	0.5098E+00	0.5930E+00	0.3012E+00	0.9674E-01	0.2705E-01
1.0	0.5626E+00	0.6911E+00	0.3687E+00	0.1226E+00	0.3581E-01
14.0	0.4073E+00	0.5061E+00	0.2733E+00	0.9155E-01	0.2683E-01

(b) Total

Energy (Mev)					
10 ⁻⁷	0.6905E+00	0.1025E+01	0.1204E+01	0.4662E+00	0.2460E+00
0.10	0.8150E+00	0.1181E+01	0.1341E+01	0.1147E+01	0.8343E+00
1.0	0.7155E+00	0.1030E+01	0.8933E+00	0.4336E+00	0.2039E+00
14.0	0.4860E+00	0.6940E+00	0.5683E+00	0.2758E+00	0.9320E-01

TABLE E-14. NEUTRON ALBEDO FACTORS FOR IRON, GEOMETRY D ($h_s=0$, $\rho_D=a$, $z_D=0$)

(a) Single-scatter

LOS Thickness (mfp)	0.5	1.0	3.0	5.0	7.0
Energy (Mev)					
10 ⁻⁷	0.5540E+00	0.6971E+00	0.3882E+00	0.1327E+00	0.3955E-01
0.10	0.6279E+00	0.7776E+00	0.4178E+00	0.1397E+00	0.4101E-01
1.0	0.6104E+00	0.8242E+00	0.6053E+00	0.2987E+00	0.1494E+00
14.0	0.4510E+00	0.5655E+00	0.3135E+00	0.1081E+00	0.3306E-01

(b) Total

Energy (Mev)					
10 ⁻⁷	0.6714E+00	0.1053E+01	0.8829E+00	0.4408E+00	0.1860E+00
0.10	0.7878E+00	0.1224E+01	0.1296E+01	0.8837E+00	0.6430E+00
1.0	0.6818E+00	0.1022E+01	0.1137E+01	0.8600E+00	0.5570E+00
14.0	0.5318E+00	0.7675E+00	0.6414E+00	0.4013E+00	0.1983E+00

NAVSWC TR 91-16

TABLE E-15. NEUTRON ALBEDO FACTORS FOR LEAD, GEOMETRY D ($h_s=0$, $\rho_D=a$, $z_D=0$)

(a) Single-scatter

LOS Thickness (mfp)	0.5	1.0	3.0	5.0	7.0
Energy (Mev)					
10 ⁻⁷	0.6316E+00	0.7959E+00	0.4453E+00	0.1526E+00	0.4562E-01
0.10	0.6395E+00	0.8058E+00	0.4509E+00	0.1546E+00	0.4622E-01
1.0	0.5943E+00	0.7284E+00	0.3785E+00	0.1243E+00	0.3601E-01
14.0	0.5899E+00	0.7412E+00	0.4128E+00	0.1412E+00	0.4222E-01

(b) Total

Energy (Mev)					
10 ⁻⁷	0.7746E+00	0.1133E+01	0.1234E+01	0.7226E+00	0.5219E+00
0.10	0.7994E+00	0.1159E+01	0.1252E+01	0.1054E+01	0.6136E+00
1.0	0.7739E+00	0.1106E+01	0.1034E+01	0.6691E+00	0.3771E+00
14.0	0.7329E+00	0.1040E+01	0.9771E+00	0.4988E+00	0.2979E+00

TABLE E-16. NEUTRON ALBEDO FACTORS FOR WATER, GEOMETRY D ($h_s=0$, $\rho_D=a$, $z_D=0$)

(a) Single-scatter

LOS Thickness (mfp)	0.5	1.0	3.0	5.0	7.0
Energy (Mev)					
10 ⁻⁷	0.3636E+00	0.4684E+00	0.2686E+00	0.9174E-01	0.2717E-01
0.10	0.3071E+00	0.3902E+00	0.2053E+00	0.6440E-01	0.1777E-01
1.0	0.3501E+00	0.4644E+00	0.3014E+00	0.1179E+00	0.4052E-01
14.0	0.2838E+00	0.3543E+00	0.1942E+00	0.6583E-01	0.1951E-01

(b) Total

Energy (Mev)					
10 ⁻⁷	0.4453E+00	0.7910E+00	0.8500E+00	0.5879E+00	0.2787E+00
0.10	0.4413E+00	0.8495E+00	0.1220E+01	0.7592E+00	0.2768E+00
1.0	0.3956E+00	0.5653E+00	0.5602E+00	0.3063E+00	0.1297E+00
14.0	0.3360E+00	0.5099E+00	0.3299E+00	0.1228E+00	0.4172E-01

TABLE E-17. NEUTRON ALBEDO FACTORS FOR POLYETHYLENE, GEOMETRY D
($h_s=0$, $\rho_D=a$, $z_D=0$)

(a) Single-scatter

LOS Thickness (mfp)	0.5	1.0	3.0	5.0	7.0
Energy (Mev)					
10 ⁻⁷	0.3639E+00	0.4692E+00	0.2690E+00	0.9186E-01	0.2722E-01
0.10	0.3184E+00	0.4045E+00	0.2141E+00	0.6753E-01	0.1873E-01
1.0	0.2029E+00	0.2565E+00	0.1408E+00	0.4701E-01	0.1372E-01
14.0	0.2682E+00	0.3326E+00	0.1783E+00	0.5932E-01	0.1729E-01

(b) Total

Energy (Mev)					
10 ⁻⁷	0.4470E+00	0.7826E+00	0.8548E+00	0.5583E+00	0.2843E+00
0.10	0.4599E+00	0.8013E+00	0.1098E+01	0.8015E+00	0.2845E+00
1.0	0.2492E+00	0.3674E+00	0.3009E+00	0.1086E+00	0.1063E+00
14.0	0.3339E+00	0.4772E+00	0.2989E+00	0.1419E+00	0.2670E-01

TABLE E-18. NEUTRON ALBEDO FACTORS FOR CONCRETE, GEOMETRY D ($h_s=0$,
 $\rho_D=a$, $z_D=0$)

(a) Single-scatter

LOS Thickness (mfp)	0.5	1.0	3.0	5.0	7.0
Energy (Mev)					
10 ⁻⁷	0.3000E+00	0.3770E+00	0.2034E+00	0.6763E-01	0.1986E-01
0.10	0.5237E+00	0.6595E+00	0.3607E+00	0.1203E+00	0.3503E-01
1.0	0.5882E+00	0.7918E+00	0.5469E+00	0.2317E+00	0.8920E-01
14.0	0.4033E+00	0.5081E+00	0.2839E+00	0.9722E-01	0.2905E-01

(b) Total

Energy (Mev)					
10 ⁻⁷	0.3889E+00	0.6095E+00	0.7984E+00	0.5652E+00	0.7748E+00
0.10	0.6918E+00	0.1164E+01	0.1331E+01	0.1056E+01	0.5312E+00
1.0	0.6617E+00	0.1010E+01	0.1036E+01	0.6803E+00	0.4407E+00
14.0	0.4727E+00	0.6734E+00	0.5202E+00	0.3378E+00	0.1115E+00

APPENDIX F

GAMMA-RAY BUILDUP FACTOR TABLES, GEOMETRIES E-H

22 PAGES

REFERENCED IN CHAPTER 1, INTRODUCTION, AND
CHAPTER 6, SAMPLE PROBLEM ANALYSIS

NAVSWC TR 91-16

TABLE F-1. GAMMA-RAY BUILDUP FACTORS FOR ALUMINUM, GEOMETRY E
($h_s = 10a$, $p_D = 0$, $z_D = 21a$)

(a) Single-scatter

Thickness, a (mfp)	0.5	1.0	2.0	3.0	4.0	5.0	6.0	7.0
Energy (Mev)								
0.10	1.291	1.494	1.790	2.009	2.183	2.326	2.446	2.549
0.20	1.295	1.519	1.864	2.129	2.345	2.526	2.680	2.814
0.60	1.265	1.476	1.811	2.074	2.290	2.473	2.630	2.768
1.0	1.248	1.445	1.757	2.001	2.201	2.370	2.515	2.642
3.0	1.204	1.362	1.608	1.801	1.960	2.095	2.213	2.317
5.0	1.171	1.303	1.512	1.678	1.817	1.938	2.044	2.139
7.0	1.145	1.258	1.439	1.587	1.713	1.824	1.923	2.012

(b) Total

Energy (Mev)								
0.10	1.428	1.876	2.780	3.703	4.591	5.516	6.436	7.397
0.20	1.425	1.925	3.077	4.368	5.802	7.524	9.454	11.22
0.60	1.357	1.774	2.728	3.802	5.064	6.232	7.720	9.084
1.0	1.326	1.699	2.516	3.457	4.361	5.415	6.570	7.480
3.0	1.263	1.535	2.073	2.614	3.173	3.676	4.003	4.347
5.0	1.222	1.438	1.870	2.279	2.730	3.135	3.529	3.946
7.0	1.187	1.365	1.705	2.018	2.331	2.650	3.005	3.280

NAVSWC TR 91-16

TABLE F-2. GAMMA-RAY BUILDUP FACTORS FOR IRON, GEOMETRY E ($h_s = 10a$,
 $\rho_D = 0$, $z_D = 21a$)

(a) Single-scatter

Thickness, a (mfp)	0.5	1.0	2.0	3.0	4.0	5.0	6.0	7.0
Energy (Mev)								
0.10	1.122	1.202	1.313	1.392	1.453	1.502	1.543	1.577
0.20	1.235	1.405	1.660	1.851	2.004	2.131	2.237	2.329
0.60	1.258	1.463	1.786	2.040	2.248	2.424	2.575	2.707
1.0	1.245	1.439	1.747	1.988	2.185	2.351	2.495	2.620
3.0	1.198	1.353	1.600	1.796	1.962	2.105	2.231	2.343
5.0	1.159	1.284	1.488	1.658	1.805	1.937	2.055	2.163
7.0	1.129	1.231	1.404	1.553	1.687	1.810	1.923	2.029

(b) Total

Energy (Mev)								
0.10	1.138	1.238	1.389	1.506	1.605	1.686	1.755	1.814
0.20	1.294	1.563	2.064	2.551	3.005	3.457	3.874	4.250
0.60	1.334	1.693	2.475	3.309	4.178	5.135	6.049	7.216
1.0	1.314	1.652	2.382	3.205	4.040	4.981	5.931	6.975
3.0	1.252	1.507	2.034	2.558	3.116	3.686	4.178	4.619
5.0	1.204	1.403	1.797	2.192	2.592	2.988	3.435	3.997
7.0	1.166	1.322	1.632	1.962	2.307	2.682	3.185	3.683

TABLE F-3. GAMMA-RAY BUILDUP FACTORS FOR LEAD, GEOMETRY E ($h_s = 10a$,
 $\rho_D = 0$, $z_D = 21a$)

(a) Single-scatter

Thickness, a (mfp)	0.5	1.0	2.0	3.0	4.0	5.0	6.0	7.0
Energy (Mev)								
0.10	1.011	1.027	1.091	1.256	1.688	2.824	5.817	13.71
0.20	1.026	1.043	1.067	1.084	1.097	1.108	1.116	1.123
0.60	1.119	1.203	1.327	1.417	1.489	1.548	1.597	1.639
1.0	1.159	1.275	1.451	1.584	1.691	1.780	1.856	1.922
3.0	1.150	1.266	1.463	1.633	1.784	1.922	2.048	2.165
5.0	1.111	1.198	1.356	1.502	1.642	1.777	1.908	2.036
7.0	1.085	1.152	1.278	1.402	1.528	1.657	1.788	1.924

(b) Total

Energy (Mev)								
0.10	1.011	1.028	1.097	1.282	1.781	3.136	6.798	16.73
0.20	1.027	1.045	1.071	1.092	1.112	1.141	1.195	1.324
0.60	1.129	1.230	1.393	1.530	1.639	1.736	1.844	1.950
1.0	1.177	1.327	1.593	1.809	2.023	2.219	2.429	2.574
3.0	1.172	1.327	1.635	1.966	2.341	2.682	3.061	3.436
5.0	1.127	1.239	1.471	1.751	2.035	2.334	2.756	3.134
7.0	1.097	1.181	1.360	1.566	1.813	2.054	2.369	2.742

NAVSWC TR 91-16

TABLE F-4. GAMMA-RAY BUILDUP FACTORS FOR WATER, GEOMETRY E
($h_s = 10a$, $\rho_D = 0$, $z_D = 21a$)

(a) Single-scatter

Thickness, a (mfp)	0.5	1.0	2.0	3.0	4.0	5.0	6.0	7.0
Energy (Mev)								
0.10	1.330	1.565	1.913	2.172	2.380	2.552	2.697	2.823
0.20	1.302	1.531	1.886	2.160	2.384	2.571	2.731	2.871
0.60	1.265	1.477	1.813	2.077	2.294	2.477	2.635	2.773
1.0	1.248	1.446	1.758	2.002	2.203	2.372	2.517	2.645
3.0	1.206	1.365	1.612	1.802	1.958	2.090	2.203	2.304
5.0	1.179	1.314	1.525	1.688	1.823	1.938	2.039	2.127
7.0	1.156	1.275	1.461	1.607	1.729	1.834	1.926	2.007

(b) Total

Energy (Mev)								
0.10	1.546	2.305	4.436	7.358	11.15	15.83	21.48	28.02
0.20	1.449	2.029	3.616	5.783	8.555	11.82	15.84	21.01
0.60	1.361	1.799	2.857	4.093	5.537	7.099	8.751	10.73
1.0	1.330	1.715	2.593	3.584	4.565	5.775	6.943	8.319
3.0	1.266	1.545	2.106	2.653	3.163	3.592	3.972	4.195
5.0	1.228	1.449	1.888	2.299	2.701	3.152	3.490	3.799
7.0	1.200	1.387	1.728	2.069	2.378	2.689	2.876	3.034

TABLE F-5. GAMMA-RAY BUILDUP FACTORS FOR POLYETHYLENE,
GEOMETRY E ($h_s = 10a$, $\rho_D = 0$, $z_D = 21a$)

(a) Single-scatter

Thickness, a (mfp)	0.5	1.0	2.0	3.0	4.0	5.0	6.0	7.0
Energy (Mev)								
0.10	1.335	1.574	1.928	2.193	2.405	2.580	2.729	2.858
0.20	1.302	1.533	1.889	2.164	2.388	2.576	2.737	2.877
0.60	1.265	1.477	1.813	2.077	2.294	2.477	2.635	2.773
1.0	1.248	1.446	1.758	2.002	2.203	2.372	2.517	2.645
3.0	1.207	1.366	1.613	1.802	1.957	2.088	2.200	2.299
5.0	1.181	1.318	1.529	1.692	1.825	1.939	2.037	2.124
7.0	1.160	1.281	1.468	1.613	1.734	1.837	1.927	2.007

(b) Total

Energy (Mev)								
0.10	1.566	2.418	5.338	10.56	18.40	29.74	46.15	67.65
0.20	1.452	2.061	3.921	6.835	10.99	16.81	24.39	34.83
0.60	1.361	1.805	2.924	4.366	6.098	8.097	10.29	13.00
1.0	1.329	1.718	2.637	3.682	4.805	5.972	7.083	8.678
3.0	1.268	1.552	2.123	2.668	3.221	3.762	4.277	4.707
5.0	1.230	1.460	1.897	2.294	2.685	3.043	3.348	3.546
7.0	1.204	1.396	1.756	2.104	2.459	2.813	3.048	3.264

NAVSWC TR 91-16

TABLE F-6. GAMMA-RAY BUILDUP FACTORS FOR CONCRETE, GEOMETRY E
($h_s = 10a$, $\rho_D = 0$, $z_D = 21a$)

(a) Single-scatter

Thickness, a (mfp)	0.5	1.0	2.0	3.0	4.0	5.0	6.0	7.0
Energy (Mev)								
0.10	1.286	1.486	1.776	1.991	2.161	2.301	2.419	2.520
0.20	1.294	1.517	1.860	2.124	2.338	2.518	2.671	2.804
0.60	1.265	1.476	1.811	2.074	2.290	2.472	2.630	2.767
1.0	1.248	1.445	1.757	2.001	2.201	2.370	2.515	2.643
3.0	1.204	1.363	1.609	1.801	1.959	2.094	2.210	2.313
5.0	1.173	1.306	1.515	1.681	1.820	1.939	2.045	2.138
7.0	1.148	1.261	1.444	1.591	1.717	1.826	1.923	2.011

(b) Total

Energy (Mev)								
0.10	1.416	1.848	2.700	3.567	4.372	5.325	6.164	6.913
0.20	1.422	1.919	3.039	4.306	5.744	7.292	9.075	10.62
0.60	1.357	1.775	2.719	3.785	5.087	6.363	7.754	9.004
1.0	1.327	1.698	2.513	3.399	4.372	5.431	6.330	7.341
3.0	1.264	1.535	2.083	2.644	3.166	3.745	4.272	4.917
5.0	1.222	1.436	1.866	2.267	2.661	3.034	3.355	3.563
7.0	1.190	1.367	1.712	2.047	2.373	2.704	3.151	3.505

TABLE F-7. GAMMA-RAY BUILDUP FACTORS FOR ALUMINUM, GEOMETRY F
 $(h_s = 0, \rho_D = 0, z_D = 11a)$

(a) Single-scatter

Thickness, a (mfp)	0.5	1.0	2.0	3.0	4.0	5.0	6.0	7.0
Energy (Mev)								
0.10	1.345	1.542	1.807	1.990	2.127	2.235	2.324	2.398
0.20	1.359	1.583	1.898	2.121	2.292	2.430	2.544	2.640
0.60	1.322	1.539	1.847	2.066	2.234	2.367	2.476	2.568
1.0	1.297	1.499	1.786	1.989	2.144	2.268	2.371	2.456
3.0	1.232	1.391	1.619	1.786	1.919	2.029	2.122	2.202
5.0	1.191	1.322	1.517	1.667	1.789	1.892	1.981	2.059
7.0	1.160	1.271	1.442	1.578	1.692	1.790	1.876	1.953

(b) Total

Energy (Mev)								
0.10	1.509	1.965	2.799	3.569	4.265	4.995	5.676	6.387
0.20	1.521	2.044	3.143	4.285	5.502	6.885	8.254	9.510
0.60	1.446	1.906	2.845	3.787	4.762	5.655	6.635	7.481
1.0	1.408	1.817	2.613	3.402	4.128	4.835	5.507	6.067
3.0	1.317	1.614	2.122	2.554	2.970	3.351	3.624	3.925
5.0	1.262	1.489	1.880	2.228	2.558	2.893	3.219	3.532
7.0	1.219	1.403	1.714	1.985	2.248	2.496	2.732	2.926

NAVSWC TR 91-16

TABLE F-8. GAMMA-RAY BUILDUP FACTORS FOR IRON, GEOMETRY F ($h_s = 0$, $\rho_D = 0$, $z_D = 11a$)

(a) Single-scatter

Thickness, a (mfp)	0.5	1.0	2.0	3.0	4.0	5.0	6.0	7.0
Energy (Mev)								
0.10	1.149	1.227	1.322	1.380	1.420	1.450	1.473	1.492
0.20	1.290	1.461	1.687	1.838	1.948	2.034	2.102	2.159
0.60	1.315	1.525	1.821	2.031	2.190	2.317	2.421	2.509
1.0	1.294	1.493	1.775	1.975	2.128	2.250	2.351	2.436
3.0	1.226	1.382	1.611	1.783	1.923	2.040	2.141	2.229
5.0	1.178	1.302	1.494	1.648	1.779	1.893	1.993	2.084
7.0	1.143	1.244	1.408	1.546	1.668	1.778	1.879	1.971

(b) Total

Energy (Mev)								
0.10	1.169	1.268	1.399	1.486	1.550	1.600	1.642	1.674
0.20	1.370	1.654	2.120	2.517	2.866	3.179	3.466	3.734
0.60	1.422	1.818	2.574	3.305	3.993	4.699	5.313	5.990
1.0	1.393	1.767	2.477	3.174	3.791	4.431	5.033	5.624
3.0	1.304	1.581	2.077	2.529	2.965	3.380	3.728	4.032
5.0	1.241	1.451	1.825	2.166	2.482	2.808	3.133	3.490
7.0	1.194	1.359	1.649	1.933	2.222	2.537	2.872	3.159

TABLE F-9. GAMMA-RAY BUILDUP FACTORS FOR LEAD, GEOMETRY F ($h_s = 0$, $\rho_D = 0$, $z_D = 11a$)

(a) Single-scatter

Thickness, a (mfp)	0.5	1.0	2.0	3.0	4.0	5.0	6.0	7.0
Energy (Mev)								
0.10	1.012	1.026	1.083	1.229	1.614	2.635	5.343	12.53
0.20	1.033	1.049	1.069	1.081	1.089	1.095	1.100	1.103
0.60	1.145	1.226	1.333	1.404	1.456	1.496	1.528	1.555
1.0	1.188	1.303	1.460	1.570	1.652	1.718	1.771	1.816
3.0	1.171	1.286	1.471	1.625	1.759	1.877	1.983	2.080
5.0	1.126	1.211	1.361	1.498	1.628	1.750	1.868	1.981
7.0	1.096	1.160	1.281	1.400	1.519	1.640	1.763	1.888

(b) Total

Energy (Mev)								
0.10	1.012	1.027	1.088	1.249	1.686	2.873	6.100	14.86
0.20	1.034	1.051	1.073	1.087	1.101	1.121	1.161	1.261
0.60	1.160	1.261	1.405	1.512	1.592	1.656	1.715	1.768
1.0	1.215	1.370	1.611	1.800	1.957	2.085	2.231	2.313
3.0	1.203	1.362	1.661	1.964	2.264	2.581	2.883	3.128
5.0	1.148	1.261	1.488	1.743	2.003	2.269	2.580	2.905
7.0	1.113	1.196	1.368	1.566	1.794	2.042	2.350	2.711

NAVSWC TR 91-16

TABLE F-10. GAMMA-RAY BUILDUP FACTORS FOR WATER, GEOMETRY F
($h_s = 0$, $\rho_D = 0$, $z_D = 11a$)

(a) Single-scatter

Thickness, a (mfp)	0.5	1.0	2.0	3.0	4.0	5.0	6.0	7.0
Energy (Mev)								
0.10	1.388	1.615	1.928	2.150	2.322	2.462	2.579	2.680
0.20	1.366	1.596	1.920	2.152	2.332	2.477	2.597	2.699
0.60	1.322	1.540	1.849	2.069	2.237	2.371	2.481	2.572
1.0	1.297	1.499	1.787	1.990	2.146	2.270	2.372	2.458
3.0	1.235	1.394	1.622	1.787	1.917	2.023	2.112	2.189
5.0	1.198	1.333	1.530	1.677	1.794	1.892	1.975	2.048
7.0	1.171	1.288	1.464	1.598	1.707	1.799	1.879	1.948

(b) Total

Energy (Mev)								
0.10	1.639	2.404	4.449	7.129	10.58	14.49	19.20	24.63
0.20	1.545	2.159	3.691	5.698	7.970	10.66	14.08	17.74
0.60	1.451	1.931	2.973	4.060	5.199	6.268	7.462	8.738
1.0	1.411	1.836	2.697	3.519	4.264	5.112	5.811	6.527
3.0	1.322	1.623	2.146	2.585	2.967	3.297	3.583	3.855
5.0	1.271	1.505	1.908	2.248	2.552	2.869	3.108	3.322
7.0	1.232	1.426	1.746	2.032	2.283	2.546	2.711	2.876

TABLE F-11. GAMMA-RAY BUILDUP FACTORS FOR POLYETHYLENE,
GEOMETRY F ($h_s = 0$, $\rho_D = 0$, $z_D = 11a$)

(a) Single-scatter

Thickness, a (mfp)	0.5	1.0	2.0	3.0	4.0	5.0	6.0	7.0
Energy (Mev)								
0.10	1.393	1.624	1.943	2.170	2.347	2.491	2.613	2.7170
0.20	1.366	1.597	1.923	2.156	2.336	2.482	2.603	2.7060
0.60	1.322	1.540	1.849	2.070	2.237	2.371	2.481	2.5730
1.0	1.297	1.499	1.787	1.990	2.146	2.270	2.372	2.4580
3.0	1.236	1.396	1.623	1.787	1.916	2.021	2.109	2.1840
5.0	1.201	1.336	1.533	1.679	1.796	1.892	1.974	2.0450
7.0	1.175	1.294	1.470	1.604	1.712	1.802	1.880	1.9480

(b) Total

Energy (Mev)								
0.10	1.664	2.518	5.338	10.25	17.49	28.05	41.90	60.08
0.20	1.547	2.186	3.970	6.698	10.52	15.42	21.47	29.97
0.60	1.452	1.941	3.062	4.326	5.680	7.084	8.491	9.899
1.0	1.411	1.844	2.748	3.633	4.504	5.247	5.933	6.695
3.0	1.324	1.632	2.162	2.602	3.000	3.362	3.698	3.966
5.0	1.274	1.515	1.918	2.244	2.566	2.845	3.073	3.242
7.0	1.238	1.436	1.764	2.046	2.331	2.608	2.807	2.968

TABLE F-12. GAMMA-RAY BUILDUP FACTORS FOR CONCRETE, GEOMETRY F
 $(h_s = 0, \rho_D = 0, z_D = 11a)$

(a) Single-scatter

Thickness, a (mfp)	0.5	1.0	2.0	3.0	4.0	5.0	6.0	7.0
Energy (Mev)								
0.10	1.340	1.533	1.793	1.972	2.105	2.211	2.297	2.369
0.20	1.358	1.581	1.894	2.115	2.285	2.422	2.535	2.630
0.60	1.322	1.538	1.847	2.066	2.233	2.366	2.475	2.567
1.0	1.297	1.499	1.786	1.989	2.144	2.268	2.371	2.456
3.0	1.233	1.392	1.620	1.786	1.918	2.027	2.119	2.198
5.0	1.193	1.324	1.520	1.670	1.791	1.893	1.982	2.059
7.0	1.162	1.274	1.447	1.583	1.696	1.792	1.877	1.952

(b) Total

Energy (Mev)								
0.10	1.496	1.933	2.726	3.453	4.100	4.786	5.406	5.998
0.20	1.517	2.033	3.106	4.235	5.439	6.643	7.936	9.147
0.60	1.445	1.904	2.834	3.776	4.769	5.710	6.670	7.486
1.0	1.407	1.816	2.608	3.368	4.113	4.850	5.523	6.192
3.0	1.318	1.612	2.120	2.565	2.968	3.364	3.734	4.149
5.0	1.263	1.490	1.883	2.230	2.525	2.814	3.073	3.295
7.0	1.221	1.405	1.720	1.999	2.250	2.511	2.813	3.031

TABLE F-13. GAMMA-RAY BUILDUP FACTORS FOR ALUMINUM, GEOMETRY G
 $(h_s = 10a, \rho_D = 0, z_D = 11a)$

(a) Single-scatter

Thickness, a (mfp)	0.5	1.0	2.0	3.0	4.0	5.0	6.0	7.0
Energy (Mev)								
0.10	1.306	1.473	1.689	1.828	1.927	1.999	2.053	2.093
0.20	1.316	1.504	1.756	1.926	2.049	2.142	2.213	2.268
0.60	1.269	1.443	1.684	1.850	1.971	2.062	2.132	2.186
1.0	1.240	1.396	1.612	1.758	1.863	1.940	1.997	2.039
3.0	1.169	1.276	1.417	1.505	1.562	1.598	1.620	1.630
5.0	1.129	1.210	1.313	1.376	1.414	1.435	1.445	1.447
7.0	1.102	1.165	1.247	1.296	1.325	1.341	1.349	1.349

(b) Total

Energy (Mev)								
0.10	1.482	1.779	2.575	3.612	4.098	4.021	4.650	5.193
0.20	1.464	1.881	2.571	3.246	4.582	3.844	3.381	3.344
0.60	1.581	1.824	2.766	3.787	3.564	3.655	3.234	3.095
1.0	1.494	1.849	2.156	3.059	2.551	2.793	2.950	3.401
3.0	1.216	1.394	1.585	1.781	1.771	1.741	1.729	1.727
5.0	1.160	1.328	1.621	1.562	1.563	1.482	1.472	1.467
7.0	1.134	1.251	1.369	1.399	1.376	1.377	1.369	1.366

NAVSWC TR 91-16

TABLE F-14. GAMMA-RAY BUILDUP FACTORS FOR IRON, GEOMETRY G
($h_s = 10a$, $\rho_D = 0$, $z_D = 11a$)

(a) Single-scatter

Thickness, a (mfp)	0.5	1.0	2.0	3.0	4.0	5.0	6.0	7.0
Energy (Mev)								
0.10	1.126	1.192	1.273	1.323	1.357	1.380	1.397	1.408
0.20	1.246	1.389	1.576	1.698	1.784	1.847	1.894	1.929
0.60	1.262	1.430	1.662	1.822	1.938	2.024	2.091	2.141
1.0	1.236	1.390	1.603	1.747	1.849	1.925	1.980	2.021
3.0	1.166	1.273	1.419	1.516	1.583	1.630	1.662	1.683
5.0	1.123	1.203	1.315	1.393	1.449	1.490	1.519	1.541
7.0	1.094	1.156	1.247	1.314	1.366	1.407	1.440	1.466

(b) Total

Energy (Mev)								
0.10	1.141	1.225	1.339	1.470	1.476	1.469	1.461	1.457
0.20	1.319	1.554	1.796	2.234	2.380	2.184	2.155	2.077
0.60	1.338	1.718	2.433	2.897	3.533	3.748	3.499	3.597
1.0	1.301	1.642	2.144	2.962	3.722	4.464	4.716	4.658
3.0	1.226	1.370	1.644	1.758	2.244	2.829	2.584	2.189
5.0	1.168	1.326	1.506	1.603	1.812	1.706	1.732	1.884
7.0	1.126	1.224	1.383	1.433	1.523	1.653	2.550	2.454

TABLE F-15. GAMMA-RAY BUILDUP FACTORS FOR LEAD, GEOMETRY G
($h_s = 10a$, $\rho_D = 0$, $z_D = 11a$)

(a) Single-scatter

Thickness, a (mfp)	0.5	1.0	2.0	3.0	4.0	5.0	6.0	7.0
Energy (Mev)								
0.10	1.018	1.045	1.150	1.407	2.048	3.669	7.792	18.34
0.20	1.026	1.040	1.057	1.067	1.073	1.077	1.080	1.081
0.60	1.113	1.177	1.256	1.303	1.334	1.353	1.365	1.372
1.0	1.144	1.230	1.341	1.409	1.453	1.482	1.500	1.511
3.0	1.124	1.206	1.330	1.425	1.501	1.564	1.616	1.660
5.0	1.087	1.147	1.247	1.333	1.411	1.482	1.549	1.612
7.0	1.065	1.109	1.188	1.264	1.340	1.415	1.492	1.570

(b) Total

Energy (Mev)								
0.10	1.019	1.047	1.163	1.459	2.224	4.200	9.812	23.35
0.20	1.027	1.042	1.062	1.075	1.089	1.112	1.147	1.322
0.60	1.125	1.243	1.322	1.342	1.365	1.398	1.420	1.468
1.0	1.167	1.279	1.483	1.564	1.496	1.524	2.023	1.692
3.0	1.147	1.289	1.527	1.542	1.857	1.891	1.961	1.876
5.0	1.101	1.189	1.296	1.559	1.548	1.598	1.662	1.701
7.0	1.085	1.122	1.244	1.496	1.730	1.924	1.682	1.749

NAVSWC TR 91-16

Table F-16. Gamma-ray buildup factors for Water, Geometry G ($h_s = 10a$, $\rho_D = 0$, $z_D = 11a$)

(a) Single-scatter

Thickness, a (mfp)	0.5	1.0	2.0	3.0	4.0	5.0	6.0	7.0
Energy (Mev)								
0.10	1.350	1.543	1.793	1.958	2.075	2.161	2.227	2.277
0.20	1.323	1.516	1.776	1.951	2.078	2.174	2.248	2.305
0.60	1.270	1.444	1.686	1.852	1.974	2.066	2.136	2.189
1.0	1.240	1.396	1.612	1.759	1.864	1.941	1.998	2.040
3.0	1.171	1.277	1.415	1.499	1.550	1.581	1.597	1.603
5.0	1.133	1.213	1.311	1.364	1.392	1.403	1.404	1.396
7.0	1.107	1.170	1.244	1.280	1.296	1.299	1.293	1.282

(b) Total

Energy (Mev)								
0.10	1.602	2.235	3.908	6.005	6.88	9.832	11.59	22.43
0.20	1.514	2.148	3.480	5.068	14.74	9.160	72.53	12.52
0.60	1.376	1.795	2.351	4.339	3.384	4.498	3.838	4.677
1.0	1.332	1.618	2.432	3.573	3.887	5.772	4.575	3.937
3.0	1.225	1.485	1.727	1.809	1.761	1.981	1.824	1.769
5.0	1.169	1.308	1.421	1.843	1.825	2.265	2.507	2.379
7.0	1.154	1.228	1.320	1.383	1.367	1.355	1.341	1.321

TABLE F-17. GAMMA-RAY BUILDUP FACTORS FOR POLYETHYLENE,
GEOMETRY G ($h_s = 10a$, $\rho_D = 0$, $z_D = 11a$)

(a) Single-scatter

Thickness, a (mfp)	0.5	1.0	2.0	3.0	4.0	5.0	6.0	7.0
Energy (Mev)								
0.10	1.355	1.551	1.806	1.974	2.093	2.182	2.249	2.300
0.20	1.324	1.517	1.778	1.954	2.082	2.178	2.252	2.310
0.60	1.270	1.444	1.686	1.853	1.974	2.066	2.136	2.190
1.0	1.240	1.396	1.613	1.759	1.864	1.941	1.998	2.040
3.0	1.171	1.278	1.415	1.497	1.547	1.576	1.590	1.595
5.0	1.134	1.214	1.310	1.360	1.385	1.393	1.391	1.381
7.0	1.109	1.171	1.242	1.275	1.286	1.285	1.276	1.262

(b) Total

Energy (Mev)								
0.10	1.635	2.376	4.209	7.894	13.18	15.49	40.38	35.85
0.20	1.483	1.976	3.449	4.929	7.469	18.46	51.43	81.21
0.60	1.369	1.883	3.301	4.063	3.903	3.275	13.37	9.727
1.0	1.334	1.712	2.728	3.210	3.167	3.369	3.675	2.952
3.0	1.260	1.492	1.687	2.042	2.055	2.356	2.658	2.180
5.0	1.176	1.347	1.563	2.238	2.210	1.761	1.709	1.662
7.0	1.149	1.257	1.315	1.360	1.727	1.742	1.670	1.585

Table F-18. Gamma-ray buildup factors for **Concrete**, Geometry G ($h_s = 10a$, $\rho_D = 0$, $z_D = 11a$)

(a) Single-scatter

Thickness, a (mfp)	0.5	1.0	2.0	3.0	4.0	5.0	6.0	7.0
Energy (Mev)								
0.10	1.301	1.465	1.677	1.814	1.910	1.981	2.033	2.073
0.20	1.314	1.502	1.753	1.922	2.044	2.136	2.207	2.261
0.60	1.269	1.443	1.684	1.850	1.971	2.062	2.132	2.185
1.0	1.240	1.396	1.612	1.758	1.863	1.940	1.997	2.039
3.0	1.169	1.276	1.417	1.503	1.559	1.593	1.613	1.622
5.0	1.130	1.211	1.313	1.374	1.410	1.430	1.438	1.438
7.0	1.103	1.166	1.246	1.293	1.319	1.333	1.337	1.335

(b) Total

Energy (Mev)								
0.10	1.443	1.809	2.428	2.844	3.124	3.756	3.794	3.215
0.20	1.455	1.859	2.451	3.157	3.651	4.352	5.343	3.439
0.60	1.592	1.737	2.757	2.903	3.392	3.082	4.732	3.819
1.0	1.508	1.746	2.348	2.725	2.694	4.688	5.357	13.94
3.0	1.307	1.517	1.657	1.842	1.842	1.853	2.010	2.194
5.0	1.186	1.363	1.449	1.519	1.679	1.563	1.499	1.500
7.0	1.155	1.247	1.306	1.392	1.399	1.418	1.374	1.369

NAVSWC TR 91-16

TABLE F-19. GAMMA-RAY BUILDUP FACTORS FOR ALUMINUM, GEOMETRY H
($h_s = 0$, $\rho_D = 2a$, $z_D = 2a$)

LOS Thickness (mfp)	0.5	1.0	2.0	3.0	4.0	5.0	6.0	7.0
Energy (Mev)								
0.10	1.306	1.520	1.847	2.117	2.369	2.623	2.892	3.187
1.0	1.259	1.461	1.780	2.042	2.276	2.503	2.732	2.974
7.0	1.149	1.262	1.442	1.592	1.726	1.851	1.972	2.091

(b) Total

Energy (Mev)								
0.10	1.418	1.862	2.833	3.961	5.291	6.937	8.902	11.86
1.0	1.329	1.703	2.539	3.482	4.684	6.139	7.872	10.48
7.0	1.191	1.370	1.698	2.032	2.357	2.692	3.036	3.473

TABLE F-20. GAMMA-RAY BUILDUP FACTORS FOR IRON, GEOMETRY H ($h_s = 0$,
 $\rho_D = 2a$, $z_D = 2a$)

LOS Thickness (mfp)	0.5	1.0	2.0	3.0	4.0	5.0	6.0	7.0
Energy (Mev)								
0.10	1.131	1.214	1.332	1.425	1.510	1.594	1.685	1.784
1.0	1.256	1.455	1.769	2.026	2.257	2.480	2.705	2.944
7.0	1.133	1.236	1.408	1.561	1.703	1.841	1.978	2.116

(b) Total

Energy (Mev)								
0.10	1.145	1.250	1.412	1.551	1.685	1.827	1.984	2.146
1.0	1.320	1.665	2.415	3.250	4.244	5.427	6.685	8.215
7.0	1.171	1.331	1.647	1.982	2.332	2.776	3.123	3.738

NAVSWC TR 91-16

TABLE F-21. GAMMA-RAY BUILDUP FACTORS FOR LEAD, GEOMETRY H ($h_s = 0$, $\rho_D = 2a$, $z_D = 2a$)

LOS Thickness (mfp)	0.5	1.0	2.0	3.0	4.0	5.0	6.0	7.0
Energy (Mev)								
0.10	1.011	1.025	1.083	1.230	1.617	2.635	5.323	12.43
1.0	1.166	1.283	1.459	1.598	1.721	1.837	1.954	2.076
7.0	1.089	1.156	1.282	1.411	1.545	1.688	1.806	2.009

(b) Total

Energy (Mev)								
0.10	1.011	1.026	1.086	1.245	1.669	2.809	5.873	14.17
1.0	1.184	1.337	1.605	1.847	2.080	2.334	2.629	2.779
7.0	1.102	1.185	1.362	1.576	1.824	2.135	2.474	3.110

TABLE F-22. GAMMA-RAY BUILDUP FACTORS FOR WATER, GEOMETRY H ($h_s = 0$, $\rho_D = 2a$, $z_D = 2a$)

LOS Thickness (mfp)	0.5	1.0	2.0	3.0	4.0	5.0	6.0	7.0
Energy (Mev)								
0.10	1.346	1.594	1.980	2.307	2.615	2.927	3.257	3.620
1.0	1.259	1.461	1.781	2.043	2.278	2.505	2.735	2.977
7.0	1.160	1.279	1.463	1.611	1.740	1.859	1.972	2.082

(b) Total

Energy (Mev)								
0.10	1.506	2.169	4.197	7.405	12.32	19.61	31.30	47.59
1.0	1.332	1.714	2.589	3.606	4.940	6.339	8.263	11.18
7.0	1.203	1.392	1.738	2.050	2.406	2.777	3.124	3.668

NAVSWC TR 91-16

TABLE F-23. GAMMA-RAY BUILDUP FACTORS FOR POLYETHYLENE,
GEOMETRY H ($h_s = 0$, $\rho_D = 2a$, $z_D = 2a$)

LOS Thickness (mfp)	0.5	1.0	2.0	3.0	4.0	5.0	6.0	7.0
Energy (Mev)								
0.10	1.351	1.603	1.997	2.331	2.647	2.966	3.305	3.677
1.0	1.259	1.461	1.782	2.043	2.278	2.505	2.735	2.977
7.0	1.164	1.284	1.469	1.617	1.745	1.862	1.972	2.080

(b) Total

Energy (Mev)								
0.10	1.519	2.236	4.721	9.641	18.71	34.67	60.61	106.6
1.0	1.332	1.715	2.645	3.780	5.069	6.821	8.922	11.38
7.0	1.207	1.406	1.751	2.097	2.420	2.856	3.347	3.883

TABLE F-24. GAMMA-RAY BUILDUP FACTORS FOR CONCRETE, GEOMETRY H
($h_s = 0$, $\rho_D = 2a$, $z_D = 2a$)

LOS Thickness (mfp)	0.5	1.0	2.0	3.0	4.0	5.0	6.0	7.0
Energy (Mev)								
0.10	1.302	1.512	1.832	2.096	2.343	2.591	2.853	3.142
1.0	1.259	1.461	1.780	2.042	2.276	2.503	2.732	2.974
7.0	1.151	1.265	1.446	1.596	1.729	1.853	1.972	2.089

(b) Total

Energy (Mev)								
0.10	1.408	1.840	2.763	3.808	5.071	6.628	8.609	11.23
1.0	1.330	1.703	2.544	3.524	4.661	6.088	7.766	9.989
7.0	1.193	1.373	1.709	2.050	2.407	2.658	3.069	3.394

APPENDIX G

NEUTRON BUILDUP FACTOR TABLES, GEOMETRIES E-H

19 PAGES

REFERENCED IN CHAPTER 1, INTRODUCTION, AND
CHAPTER 6, SAMPLE PROBLEM ANALYSIS

NAVSWC TR 91-16

TABLE G-1. NEUTRON BUILDUP FACTORS FOR ALUMINUM, GEOMETRY E
($h_s = 10a$, $\rho_D = 0$, $z_D = 21a$)

(a) Single-scatter

Thickness, a (mfp)	0.5	1.0	2.0	3.0	4.0	5.0	6.0	7.0
Energy (Mev)								
10 ⁻⁷	1.341	1.563	1.853	2.040	2.173	2.274	2.353	2.416
10 ⁻⁵	1.370	1.610	1.924	2.126	2.269	2.378	2.463	2.531
10 ⁻³	1.363	1.601	1.913	2.116	2.261	2.371	2.457	2.527
0.1	1.269	1.398	1.548	1.637	1.696	1.739	1.771	1.796
1.0	1.329	1.521	1.734	1.837	1.891	1.922	1.942	1.959
10.0	1.283	1.444	1.625	1.721	1.778	1.815	1.841	1.858
14.0	1.238	1.379	1.543	1.634	1.692	1.730	1.757	1.776

(b) Total

Energy (Mev)								
10 ⁻⁷	1.583	2.365	4.675	8.322	14.45	23.94	39.10	62.21
10 ⁻⁵	1.672	2.664	6.296	13.90	29.96	61.26	119.7	232.0
10 ⁻³	1.644	2.577	5.721	11.65	23.07	42.81	80.30	141.1
0.1	1.735	2.838	7.151	17.89	44.62	113.5	291.4	736.7
1.0	1.634	2.484	4.948	8.676	14.35	22.47	34.35	52.72
10.0	1.519	2.196	4.046	6.572	9.523	13.42	17.98	23.20
14.0	1.407	1.909	3.231	4.999	7.029	9.584	12.51	16.11

NAVSWC TR 91-16

TABLE G-2. NEUTRON BUILDUP FACTORS FOR IRON, GEOMETRY E ($h_s = 10a$,
 $\rho_D = 0$, $z_D = 21a$)

(a) Single-scatter

Thickness, a (mfp)	0.5	1.0	2.0	3.0	4.0	5.0	6.0	7.0
Energy (Mev)								
10 ⁻⁷	1.332	1.545	1.822	2.000	2.126	2.221	2.295	2.355
10 ⁻⁵	1.366	1.602	1.906	2.101	2.239	2.343	2.423	2.488
10 ⁻³	1.365	1.600	1.906	2.103	2.242	2.348	2.431	2.498
0.1	1.356	1.564	1.801	1.926	2.001	2.050	2.089	2.133
1.0	1.399	1.768	2.581	3.671	5.287	7.825	11.96	18.90
10.0	1.321	1.527	1.801	1.998	2.179	2.387	2.681	3.162
14.0	1.269	1.437	1.651	1.793	1.909	2.026	2.170	2.377

(b) Total

Energy (Mev)								
10 ⁻⁷	1.559	2.286	4.347	7.508	12.65	20.36	31.73	49.30
10 ⁻⁵	1.661	2.640	6.140	13.43	28.70	58.05	113.5	216.2
10 ⁻³	1.656	2.626	6.030	12.95	26.46	50.97	92.95	160.4
0.1	1.703	2.764	6.628	15.22	35.05	77.06	163.8	338.2
1.0	1.566	2.383	5.331	11.99	27.15	61.29	142.3	330.4
10.0	1.545	2.265	4.519	8.736	17.67	35.68	72.70	157.5
14.0	1.440	1.991	3.602	6.470	12.28	23.75	47.60	96.03

NAVSWC TR 91-16

TABLE G-3. NEUTRON BUILDUP FACTORS FOR LEAD, GEOMETRY E ($h_s = 10a$,
 $\rho_D = 0$, $z_D = 21a$)

(a) Single-scatter

Thickness, a (mfp)	0.5	1.0	2.0	3.0	4.0	5.0	6.0	7.0
Energy (Mev)								
10 ⁻⁷	1.364	1.597	1.897	2.089	2.223	2.324	2.403	2.466
10 ⁻⁵	1.368	1.603	1.906	2.098	2.234	2.335	2.414	2.478
10 ⁻³	1.367	1.602	1.904	2.097	2.232	2.334	2.413	2.477
0.1	1.369	1.605	1.908	2.101	2.236	2.337	2.416	2.480
1.0	1.332	1.514	1.712	1.823	1.896	1.949	1.989	2.021
10.0	1.316	1.504	1.729	1.861	1.948	2.010	2.056	2.092
14.0	1.341	1.555	1.827	1.998	2.118	2.208	2.278	2.334

(b) Total

Energy (Mev)								
10 ⁻⁷	1.661	2.652	6.145	13.65	29.55	60.65	119.8	226.0
10 ⁻⁵	1.672	2.675	6.420	14.39	31.75	66.43	135.4	258.5
10 ⁻³	1.668	2.666	6.343	14.01	30.46	63.22	127.9	246.4
0.1	1.677	2.708	6.539	15.22	32.30	65.81	127.3	244.2
1.0	1.643	2.558	5.659	11.67	22.60	42.74	76.17	128.8
10.0	1.570	2.335	4.681	8.763	15.82	26.90	42.97	67.14
14.0	1.603	2.426	4.992	9.245	15.96	26.76	41.74	63.25

NAVSWC TR 91-16

TABLE G-4. NEUTRON BUILDUP FACTORS FOR WATER, GEOMETRY E ($h_s = 10a$,
 $\rho_D = 0$, $z_D = 21a$)

(a) Single-scatter

Thickness, a (mfp)	0.5	1.0	2.0	3.0	4.0	5.0	6.0	7.0
Energy (Mev)								
10 ⁻⁷	1.410	1.734	2.242	2.641	2.976	3.271	3.538	3.786
10 ⁻⁵	1.409	1.774	2.423	2.983	3.470	3.895	4.268	4.596
10 ⁻³	1.320	1.610	2.129	2.581	2.979	3.332	3.647	3.929
0.1	1.588	2.038	2.671	3.086	3.373	3.580	3.737	3.858
1.0	1.335	1.625	2.154	2.674	3.219	3.821	4.506	5.306
10.0	1.338	1.575	1.914	2.159	2.351	2.507	2.639	2.752
14.0	1.274	1.465	1.740	1.942	2.102	2.234	2.345	2.439

(b) Total

Energy (Mev)								
10 ⁻⁷	1.670	2.712	6.244	12.65	23.97	43.62	75.47	132.7
10 ⁻⁵	1.601	2.291	4.146	6.742	10.38	15.46	22.17	29.80
10 ⁻³	1.397	1.927	3.482	6.054	9.910	15.98	25.10	38.88
0.1	2.005	3.755	9.916	20.17	35.11	55.69	83.52	121.2
1.0	1.445	2.029	3.678	6.031	9.454	13.80	20.20	27.88
10.0	1.521	2.100	3.271	4.372	5.314	6.261	7.224	8.160
14.0	1.413	1.865	2.781	3.698	4.534	5.394	6.458	7.514

NAVSWC TR 91-16

TABLE G-5. NEUTRON BUILDUP FACTORS FOR POLYETHYLENE, GEOMETRY E
($h_s = 10a$, $\rho_D = 0$, $z_D = 21a$)

(a) Single-scatter

Thickness, a (mfp)	0.5	1.0	2.0	3.0	4.0	5.0	6.0	7.0
Energy (Mev)								
10 ⁻⁷	1.410	1.733	2.241	2.640	2.975	3.269	3.535	3.783
10 ⁻⁵	1.411	1.774	2.416	2.969	3.449	3.868	4.235	4.558
10 ⁻³	1.320	1.610	2.125	2.573	2.966	3.314	3.625	3.903
0.1	1.584	2.030	2.658	3.070	3.355	3.562	3.718	3.838
1.0	1.279	1.490	1.807	2.040	2.222	2.370	2.493	2.597
10.0	1.327	1.551	1.869	2.099	2.281	2.430	2.555	2.663
14.0	1.275	1.462	1.723	1.904	2.040	2.144	2.226	2.292

(b) Total

Energy (Mev)								
10 ⁻⁷	1.669	2.711	6.252	12.72	23.91	43.38	75.27	131.2
10 ⁻⁵	1.624	2.339	4.233	6.844	10.43	15.52	22.13	30.80
10 ⁻³	1.400	1.938	3.488	6.023	9.805	15.66	24.45	37.48
0.1	2.002	3.780	9.878	20.24	35.40	56.88	85.85	122.7
1.0	1.397	1.883	2.994	4.133	5.229	6.352	7.444	8.652
10.0	1.516	2.068	3.148	4.116	5.036	5.694	6.125	6.449
14.0	1.420	1.863	2.708	3.470	4.076	4.653	5.339	6.097

TABLE G-6. NEUTRON BUILDUP FACTORS FOR CONCRETE, GEOMETRY E
 ($h_s = 10a$, $\rho_D = 0$, $z_D = 21a$)

Thickness, a (mfp)	0.5	1.0	2.0	3.0	4.0	5.0	6.0	7.0
Energy (Mev)								
10 ⁻⁷	1.432	1.774	2.314	2.743	3.106	3.428	3.725	4.007
10 ⁻⁵	1.389	1.690	2.165	2.538	2.845	3.103	3.325	3.516
10 ⁻³	1.342	1.606	2.017	2.339	2.604	2.829	3.024	3.195
0.1	1.463	1.790	2.242	2.545	2.758	2.915	3.031	3.118
1.0	1.399	1.748	2.417	3.134	3.970	5.001	6.328	8.098
10.0	1.293	1.486	1.746	1.926	2.067	2.185	2.287	2.380
14.0	1.258	1.426	1.649	1.798	1.908	1.996	2.069	2.133

(b) Total

Energy (Mev)								
10 ⁻⁷	1.693	2.751	6.365	13.32	24.82	44.41	78.45	137.8
10 ⁻⁵	1.601	2.394	4.560	7.610	11.68	17.02	23.42	31.14
10 ⁻³	1.509	2.177	4.047	6.936	11.24	17.78	27.31	41.56
0.1	1.901	3.439	9.437	20.62	40.10	71.65	122.3	189.9
1.0	1.569	2.386	5.150	10.59	21.84	44.98	90.92	188.2
10.0	1.486	2.092	3.634	5.559	7.897	10.54	13.44	17.02
14.0	1.406	1.888	3.081	4.520	6.314	8.522	10.90	14.14

NAVSWC TR 91-16

TABLE G-7. NEUTRON BUILDUP FACTORS FOR ALUMINUM, GEOMETRY F
($h_s = 0$, $\rho_D = 0$, $z_D = 11a$)

Thickness, a (mfp)	0.5	1.0	2.0	3.0	4.0	5.0	6.0	7.0
Energy (Mev)								
10 ⁻⁷	1.397	1.587	1.821	1.976	2.093	2.188	2.267	2.335
0.1	1.353	1.459	1.542	1.575	1.593	1.604	1.612	1.617
1.0	1.390	1.535	1.655	1.696	1.710	1.715	1.720	1.725
14.0	1.283	1.401	1.522	1.585	1.626	1.655	1.677	1.695

(b) Total

Energy (Mev)								
10 ⁻⁷	1.672	2.410	4.529	7.946	13.67	22.63	36.39	57.67
0.1	1.908	2.924	6.429	14.99	36.71	93.26	239.5	610.1
1.0	1.759	2.603	4.828	8.095	12.81	19.90	29.92	45.08
14.0	1.483	1.979	3.210	4.734	6.490	8.528	10.78	13.66

TABLE G-8. NEUTRON BUILDUP FACTORS FOR IRON, GEOMETRY F ($h_s = 0$,
 $\rho_D = 0$, $z_D = 11a$)

Thickness, a (mfp)	0.5	1.0	2.0	3.0	4.0	5.0	6.0	7.0
Energy (Mev)								
10 ⁻⁷	1.383	1.564	1.787	1.935	2.046	2.135	2.210	2.275
0.1	1.413	1.582	1.755	1.839	1.883	1.910	1.932	1.961
1.0	1.432	1.720	2.374	3.384	5.104	8.156	13.70	23.92
14.0	1.314	1.457	1.627	1.744	1.851	1.972	2.133	2.372

(b) Total

Energy (Mev)								
10 ⁻⁷	1.642	2.326	4.215	7.155	11.81	18.90	29.57	46.20
0.1	1.817	2.808	6.193	13.75	31.27	69.23	149.5	314.7
1.0	1.612	2.317	4.878	10.77	24.74	57.60	134.4	315.2
14.0	1.510	2.027	3.473	6.058	11.25	21.50	43.28	88.80

NAVSWC TR 91-16

TABLE G-9. NEUTRON BUILDUP FACTORS FOR LEAD, GEOMETRY F ($h_s = 0$, $\rho_D = 0$, $z_D = 11a$)

Thickness, a (mfp)	0.5	1.0	2.0	3.0	4.0	5.0	6.0	7.0
Energy (Mev)								
10 ⁻⁷	1.420	1.618	1.859	2.019	2.139	2.236	2.317	2.386
0.1	1.426	1.625	1.869	2.030	2.151	2.249	2.330	2.400
1.0	1.386	1.538	1.686	1.757	1.796	1.820	1.834	1.844
14.0	1.394	1.574	1.790	1.931	2.038	2.124	2.196	2.258

(b) Total

Energy (Mev)								
10 ⁻⁷	1.759	2.697	5.982	12.99	27.71	56.49	112.3	211.7
0.1	1.777	2.758	6.320	14.12	30.55	62.12	120.1	222.3
1.0	1.747	2.639	5.514	11.03	21.18	38.95	69.14	116.3
14.0	1.696	2.490	4.889	8.883	15.29	25.10	39.54	60.27

TABLE G-10. NEUTRON BUILDUP FACTORS FOR WATER, GEOMETRY F ($h_s = 0$, $\rho_D = 0$, $z_D = 11a$)

Thickness, a (mfp)	0.5	1.0	2.0	3.0	4.0	5.0	6.0	7.0
Energy (Mev)								
10 ⁻⁷	1.538	1.881	2.347	2.675	2.936	3.159	3.361	3.552
0.1	1.788	2.265	2.777	3.023	3.156	3.235	3.287	3.322
1.0	1.396	1.680	2.177	2.676	3.231	3.880	4.661	5.617
14.0	1.334	1.520	1.755	1.912	2.030	2.123	2.199	2.262

(b) Total

Energy (Mev)								
10 ⁻⁷	1.892	3.037	6.505	12.52	22.96	40.41	70.59	121.5
0.1	2.402	4.494	10.74	20.15	32.83	50.09	71.77	100.6
1.0	1.530	2.138	3.783	6.091	9.410	13.66	19.91	28.17
14.0	1.517	1.988	2.820	3.561	4.227	4.855	5.504	6.268

NAVSWC TR 91-16

TABLE G-11. NEUTRON BUILDUP FACTORS FOR POLYETHYLENE, GEOMETRY F
($h_s = 0$, $\rho_D = 0$, $z_D = 11a$)

Thickness, a (mfp)	0.5	1.0	2.0	3.0	4.0	5.0	6.0	7.0
Energy (Mev)								
10 ⁻⁷	1.539	1.881	2.347	2.675	2.935	3.157	3.359	3.550
0.1	1.781	2.253	2.762	3.009	3.143	3.223	3.276	3.311
1.0	1.334	1.548	1.833	2.020	2.155	2.257	2.338	2.403
14.0	1.335	1.513	1.725	1.858	1.952	2.023	2.079	2.124

(b) Total

Energy (Mev)								
10 ⁻⁷	1.893	3.043	6.524	12.52	22.80	40.33	70.46	120.9
0.1	2.392	4.463	10.77	20.16	33.26	50.72	73.09	100.3
1.0	1.497	2.040	3.091	3.997	4.813	5.520	6.210	6.7920
14.0	1.529	1.994	2.732	3.300	3.724	4.041	4.352	4.6510

TABLE G-12. NEUTRON BUILDUP FACTORS FOR CONCRETE, GEOMETRY F
($h_s = 0$, $\rho_D = 0$, $z_D = 11a$)

Thickness, a (mfp)	0.5	1.0	2.0	3.0	4.0	5.0	6.0	7.0
Energy (Mev)								
10 ⁻⁷	1.558	1.911	2.386	2.719	2.987	3.221	3.439	3.650
0.1	1.580	1.897	2.263	2.465	2.588	2.667	2.720	2.756
1.0	1.459	1.766	2.339	2.999	3.861	5.063	6.805	9.389
14.0	1.309	1.459	1.641	1.760	1.852	1.928	1.996	2.060

(b) Total

Energy (Mev)								
10 ⁻⁷	1.906	3.065	6.590	12.96	23.27	41.16	72.19	131.0
0.1	2.091	3.677	9.363	19.90	38.22	66.99	112.9	178.0
1.0	1.646	2.381	4.819	9.804	20.47	43.08	90.14	188.6
14.0	1.483	1.955	3.054	4.348	5.940	7.801	9.931	12.60

NAVSWC TR 91-16

TABLE G-13. NEUTRON BUILDUP FACTORS FOR ALUMINUM, GEOMETRY G
($h_s = 10a$, $p_D = 0$, $z_D = 11a$)

Thickness, a (mfp)	0.5	1.0	2.0	3.0	4.0	5.0	6.0	7.0
Energy (Mev)								
10 ⁻⁷	1.274	1.343	1.350	1.304	1.247	1.194	1.149	1.114
10 ⁻⁵	1.297	1.372	1.380	1.328	1.266	1.209	1.161	1.122
10 ⁻³	1.292	1.367	1.375	1.325	1.264	1.207	1.160	1.121
0.1	1.168	1.174	1.122	1.074	1.043	1.024	1.013	1.007
1.0	1.237	1.259	1.200	1.130	1.079	1.046	1.026	1.014
10.0	1.214	1.249	1.228	1.182	1.139	1.104	1.077	1.056
14.0	1.181	1.213	1.198	1.160	1.123	1.093	1.069	1.051

(b) Total

Energy (Mev)								
10 ⁻⁷	1.841	2.086	3.208	5.185	11.48	25.88	42.91	68.29
10 ⁻⁵	1.615	2.720	6.175	11.02	13.22	27.76	85.01	169.0
10 ⁻³	1.622	2.354	4.972	8.793	16.01	44.98	40.17	82.46
0.1	1.681	2.404	7.801	18.74	63.56	123.8	340.3	762.7
1.0	1.483	1.978	4.213	5.340	7.575	6.473	7.603	8.655
10.0	1.465	1.871	2.806	4.904	6.080	18.47	25.28	6.130
14.0	1.354	1.731	2.574	3.817	5.600	9.184	7.485	8.352

NAVSWC TR 91-16

TABLE G-14. NEUTRON BUILDUP FACTORS FOR IRON, GEOMETRY G ($h_s = 10a$, $\rho_D = 0$, $z_D = 11a$)

Thickness, a (mfp)	0.5	1.0	2.0	3.0	4.0	5.0	6.0	7.0
Energy (Mev)								
10 ⁻⁷	1.266	1.332	1.338	1.292	1.237	1.186	1.143	1.109
10 ⁻⁵	1.294	1.367	1.373	1.322	1.261	1.204	1.157	1.119
10 ⁻³	1.293	1.366	1.373	1.323	1.262	1.206	1.158	1.121
0.1	1.267	1.312	1.274	1.201	1.137	1.091	1.063	1.048
1.0	1.417	1.649	1.995	2.349	2.810	3.485	4.560	6.402
10.0	1.256	1.320	1.336	1.323	1.336	1.421	1.660	2.230
14.0	1.212	1.261	1.266	1.241	1.221	1.217	1.239	1.298

(b) Total

Energy (Mev)								
10 ⁻⁷	1.563	2.013	3.213	5.182	9.556	9.274	20.05	32.25
10 ⁻⁵	1.560	2.561	8.022	8.829	16.27	32.63	201.2	74.33
10 ⁻³	1.611	2.361	5.725	10.06	15.37	88.61	76.54	65.40
0.1	1.603	2.629	7.060	16.61	34.32	69.33	170.2	342.8
1.0	1.673	2.315	4.647	11.43	24.13	51.32	113.9	326.5
10.0	1.476	2.261	6.034	6.628	15.15	56.46	53.72	106.3
14.0	1.375	1.894	2.756	5.929	11.31	15.59	29.79	43.58

NAVSWC TR 91-16

TABLE G-15. NEUTRON BUILDUP FACTORS FOR LEAD, GEOMETRY G ($h_s = 10a$,
 $\rho_D = 0$, $z_D = 11a$)

Thickness, a (mfp)	0.5	1.0	2.0	3.0	4.0	5.0	6.0	7.0
Energy (Mev)								
10^{-7}	1.293	1.364	1.370	1.320	1.259	1.203	1.156	1.119
10^{-5}	1.295	1.367	1.373	1.322	1.260	1.204	1.157	1.119
10^{-3}	1.294	1.367	1.372	1.321	1.260	1.204	1.156	1.119
0.1	1.296	1.368	1.374	1.322	1.261	1.204	1.157	1.119
1.0	1.234	1.269	1.238	1.179	1.126	1.087	1.059	1.039
10.0	1.244	1.292	1.281	1.233	1.183	1.140	1.106	1.079
14.0	1.271	1.334	1.336	1.289	1.233	1.183	1.141	1.107

(b) Total

Energy (Mev)								
10^{-7}	1.601	2.862	4.661	10.30	17.15	45.22	214.7	120.9
10^{-5}	1.603	2.689	6.571	10.60	193.00	35.42	132.1	343.6
10^{-3}	1.599	2.684	6.715	10.85	182.50	39.70	267.2	334.8
0.1	1.646	2.270	4.701	14.55	57.64	152.9	101.9	192.8
1.0	1.590	2.345	4.402	8.118	8.34	24.43	59.22	194.9
10.0	1.457	1.990	3.402	5.221	18.04	17.51	34.20	27.55
14.0	1.545	2.223	3.641	7.322	11.95	27.05	76.26	231.7

NAVSWC TR 91-16

TABLE G-16. NEUTRON BUILDUP FACTORS FOR WATER, GEOMETRY G
($h_s = 10a$, $\rho_D = 0$, $z_D = 11a$)

Thickness, a (mfp)	0.5	1.0	2.0	3.0	4.0	5.0	6.0	7.0
Energy (Mev)								
10 ⁻⁷	1.202	1.252	1.242	1.199	1.158	1.125	1.101	1.083
10 ⁻⁵	1.215	1.344	1.455	1.459	1.414	1.353	1.289	1.232
10 ⁻³	1.146	1.228	1.294	1.292	1.262	1.222	1.181	1.145
0.1	1.391	1.499	1.447	1.319	1.210	1.134	1.084	1.052
1.0	1.221	1.311	1.374	1.376	1.356	1.328	1.298	1.268
10.0	1.167	1.186	1.154	1.118	1.091	1.070	1.053	1.041
14.0	1.156	1.187	1.172	1.139	1.107	1.080	1.060	1.044

(b) Total

Energy (Mev)								
10 ⁻⁷	1.493	2.344	4.863	18.65	12.17	14.74	19.00	27.10
10 ⁻⁵	1.357	1.772	3.204	5.390	5.967	6.196	6.743	6.623
10 ⁻³	1.303	1.489	2.421	4.836	6.028	8.317	12.41	20.51
0.1	1.951	3.384	7.076	17.80	18.58	51.71	66.17	90.32
1.0	1.363	1.782	2.720	3.395	9.648	11.86	4.588	6.256
10.0	1.341	1.702	1.869	2.247	2.217	1.943	2.226	1.993
14.0	1.334	1.533	2.004	2.423	3.319	2.710	2.341	2.138

NAVSWC TR 91-16

TABLE G-17. NEUTRON BUILDUP FACTORS FOR POLYETHYLENE, GEOMETRY G
($h_s = 10a$, $\rho_D = 0$, $z_D = 11a$)

Thickness, a (mfp)	0.5	1.0	2.0	3.0	4.0	5.0	6.0	7.0
Energy (Mev)								
10 ⁻⁷	1.202	1.252	1.243	1.200	1.159	1.126	1.101	1.083
10 ⁻⁵	1.218	1.345	1.454	1.457	1.412	1.350	1.287	1.230
10 ⁻³	1.149	1.231	1.296	1.293	1.262	1.222	1.181	1.145
0.1	1.390	1.499	1.450	1.324	1.215	1.138	1.087	1.055
1.0	1.118	1.138	1.118	1.087	1.062	1.044	1.031	1.022
10.0	1.151	1.160	1.119	1.082	1.056	1.039	1.027	1.019
14.0	1.144	1.165	1.142	1.108	1.078	1.056	1.039	1.028

(b) Total

Energy (Mev)								
10 ⁻⁷	1.465	2.248	4.992	20.23	12.91	18.51	20.87	29.27
10 ⁻⁵	1.377	1.934	3.409	6.026	5.957	6.324	9.076	10.46
10 ⁻³	1.295	1.575	2.581	4.486	9.370	7.091	8.947	15.44
0.1	1.863	3.273	5.944	10.78	18.42	27.88	36.81	33.63
1.0	1.377	1.492	2.821	4.796	3.767	4.035	8.537	26.74
10.0	1.424	1.594	1.622	2.597	2.391	1.810	1.386	1.253
14.0	1.279	1.549	1.483	1.484	1.534	1.496	1.391	1.249

TABLE G-18. NEUTRON BUILDUP FACTORS FOR CONCRETE, GEOMETRY G
($h_s = 10a$, $\rho_D = 0$, $z_D = 11a$)

Thickness, a (mfp)	0.5	1.0	2.0	3.0	4.0	5.0	6.0	7.0
Energy (Mev)								
10 ⁻⁷	1.184	1.235	1.244	1.216	1.184	1.155	1.131	1.112
10 ⁻⁵	1.262	1.363	1.419	1.393	1.339	1.279	1.223	1.175
10 ⁻³	1.224	1.303	1.339	1.312	1.265	1.216	1.171	1.134
0.1	1.339	1.439	1.441	1.365	1.280	1.207	1.151	1.109
1.0	1.392	1.601	1.837	1.959	2.024	2.056	2.068	2.068
10.0	1.222	1.277	1.283	1.249	1.209	1.171	1.138	1.111
14.0	1.199	1.248	1.252	1.219	1.180	1.147	1.119	1.099

(b) Total

Energy (Mev)								
10 ⁻⁷	1.395	2.210	3.836	16.63	14.71	27.04	45.11	48.74
10 ⁻⁵	1.523	2.012	2.991	5.566	5.939	6.616	6.513	7.050
10 ⁻³	1.391	1.916	2.640	4.476	7.006	12.560	8.492	8.769
0.1	1.889	2.731	7.325	14.04	25.84	31.37	40.08	32.07
1.0	1.622	2.650	4.468	9.914	21.21	37.79	61.79	112.6
10.0	1.417	1.778	3.440	5.237	4.451	5.900	6.306	14.5
14.0	1.337	1.552	2.212	4.563	3.729	13.57	5.668	6.108

TABLE G-19. NEUTRON BUILDUP FACTORS FOR ALUMINUM, GEOMETRY H
($h_s = 0$, $\rho_D = 2a$, $z_D = 2a$)

LOS Thickness (mfp)	0.5	1.0	2.0	3.0	4.0	5.0	6.0	7.0
Energy (Mev)								
10 ⁻⁷	1.354	1.589	1.933	2.213	2.477	2.747	3.035	3.356
0.1	1.294	1.424	1.578	1.689	1.791	1.897	2.017	2.156
1.0	1.344	1.540	1.771	1.920	2.045	2.172	2.313	2.479
7.0	1.250	1.401	1.595	1.739	1.870	2.003	2.148	2.313

(b) Total

Energy (Mev)								
10 ⁻⁷	1.523	2.196	4.235	7.899	14.45	26.53	48.42	88.28
0.1	1.657	2.535	5.729	13.34	32.43	82.86	206.7	530.0
1.0	1.570	2.300	4.421	8.070	14.35	25.35	43.74	76.97
7.0	1.374	1.812	3.020	4.886	7.826	12.04	18.75	28.16

TABLE G-20. NEUTRON BUILDUP FACTORS FOR IRON, GEOMETRY H ($h_s = 0$,
 $\rho_D = 2a$, $z_D = 2a$)

LOS Thickness (mfp)	0.5	1.0	2.0	3.0	4.0	5.0	6.0	7.0
10 ⁻⁷	1.345	1.572	1.903	2.172	2.425	2.684	2.961	3.269
0.1	1.375	1.598	1.881	2.080	2.253	2.428	2.623	2.858
1.0	1.400	1.761	2.631	4.005	6.404	10.79	19.04	34.91
14.0	1.281	1.460	1.716	1.930	2.151	2.409	2.743	3.205

(b) Total

Energy (Mev)								
10 ⁻⁷	1.506	2.140	4.009	7.305	12.98	23.09	40.64	71.38
0.1	1.619	2.476	5.429	12.23	28.39	67.59	155.8	351.6
1.0	1.508	2.181	4.625	10.29	23.80	55.18	131.5	310.5
14.0	1.404	1.885	3.303	5.892	11.21	22.40	46.93	101.8

NAVSWC TR 91-16

TABLE G-21. NEUTRON BUILDUP FACTORS FOR LEAD, GEOMETRY H ($h_s = 0$, $\rho_D = 2a$, $z_D = 2a$)

LOS Thickness (mfp)	0.5	1.0	2.0	3.0	4.0	5.0	6.0	7.0
10 ⁻⁷	1.380	1.629	1.990	2.283	2.558	2.838	3.139	3.473
0.1	1.386	1.638	2.002	2.298	2.575	2.858	3.162	3.499
1.0	1.351	1.550	1.790	1.954	2.098	2.244	2.406	2.594
14.0	1.357	1.585	1.912	2.176	2.425	2.679	2.953	3.258

(b) Total

Energy (Mev)

10 ⁻⁷	1.586	2.387	5.198	11.34	24.83	54.59	119.4	248.8
0.1	1.601	2.429	5.431	12.15	28.26	60.89	130.7	277.5
1.0	1.576	2.333	4.852	9.997	20.46	41.60	82.05	161.7
14.0	1.541	2.243	4.417	8.595	16.19	29.73	53.75	95.84

TABLE G-22. NEUTRON BUILDUP FACTORS FOR WATER, GEOMETRY H ($h_s = 0$, $\rho_D = 2a$, $z_D = 2a$)

LOS Thickness (mfp)	0.5	1.0	2.0	3.0	4.0	5.0	6.0	7.0
10 ⁻⁷	1.448	1.794	2.339	2.795	3.224	3.660	4.127	4.646
0.1	1.613	2.072	2.730	3.213	3.631	4.039	4.473	4.960
1.0	1.347	1.645	2.217	2.840	3.572	4.466	5.577	6.974
14.0	1.288	1.487	1.781	2.018	2.235	2.453	2.681	2.931

(b) Total

Energy (Mev)

10 ⁻⁷	1.654	2.584	5.635	11.57	22.95	44.81	85.81	165.7
0.1	1.960	3.505	9.032	19.05	35.59	63.21	105.2	173.7
1.0	1.431	1.971	3.562	6.188	10.28	16.88	26.84	41.82
14.0	1.406	1.845	2.797	3.918	5.148	6.830	8.787	11.09

NAVSWC TR 91-16

TABLE G-23. NEUTRON BUILDUP FACTORS FOR POLYETHYLENE,
GEOMETRY H ($h_s = 0$, $\rho_D = 2a$, $z_D = 2a$)

LOS Thickness (mfp)	0.5	1.0	2.0	3.0	4.0	5.0	6.0	7.0
10^{-7}	1.450	1.797	2.342	2.798	3.226	3.661	4.127	4.646
0.1	1.609	2.064	2.718	3.200	3.617	4.024	4.457	4.943
1.0	1.292	1.510	1.840	2.100	2.331	2.556	2.786	3.035
14.0	1.288	1.481	1.754	1.964	2.152	2.337	2.530	2.743

(b) Total

Energy (Mev)

10^{-7}	1.657	2.591	5.619	11.54	22.78	44.69	85.69	166.4
0.1	1.957	3.487	9.012	19.11	36.41	64.27	110.0	178.8
1.0	1.392	1.863	2.973	4.228	5.718	7.513	9.841	13.12
14.0	1.411	1.854	2.751	3.678	4.736	5.888	7.230	8.768

TABLE G-24. NEUTRON BUILDUP FACTORS FOR CONCRETE, GEOMETRY H
($h_s = 0$, $\rho_D = 2a$, $z_D = 2a$)

LOS Thickness (mfp)	0.5	1.0	2.0	3.0	4.0	5.0	6.0	7.0
10^{-7}	1.446	1.784	2.308	2.740	3.148	3.566	4.020	4.531
0.1	1.484	1.824	2.315	2.692	3.028	3.360	3.712	4.106
1.0	1.404	1.750	2.466	3.357	4.578	6.327	8.898	12.74
14.0	1.270	1.449	1.706	1.914	2.112	2.315	2.537	2.786

(b) Total

Energy (Mev)

10^{-7}	1.651	2.583	5.604	11.48	22.75	44.820	85.06	166.3
0.1	1.786	3.006	7.759	17.94	38.36	77.52	148.3	275.2
1.0	1.518	2.193	4.512	9.458	20.30	43.83	94.63	204.2
14.0	1.378	1.812	2.954	4.654	7.214	10.74	16.02	24.17

APPENDIX H

GAMMA-RAY ALBEDO FACTOR TABLES, GEOMETRIES F-H

10 PAGES

REFERENCED IN CHAPTER 1, INTRODUCTION, AND
CHAPTER 6, SAMPLE PROBLEM ANALYSIS

TABLE H-1. GAMMA-RAY ALBEDO FACTORS FOR ALUMINUM, GEOMETRY F ($h_s=0$, $\rho_D=0$, $z_D=-10a$)

(a) Single-scatter		0.5	1.0	2.0	3.0	4.0	5.0	6.0	7.0
Thickness (mfp)									
Energy (Mev)									
0.10	0.1791E+03	0.2100E+00	0.2222E+00	0.2245E+00	0.2255E+00	0.2260E+00	0.2260E+00	0.2264E+00	0.2268E+00
1.0	0.4087E-01	0.4716E-01	0.4996E-01	0.5079E-01	0.5120E-01	0.5145E-01	0.5145E-01	0.5163E-01	0.5177E-01
7.0	0.1361E-01	0.1491E-01	0.1543E-01	0.1562E-01	0.1570E-01	0.1575E-01	0.1575E-01	0.1579E-01	0.1581E-01
(b) Total scatter									
Energy (Mev)									
0.10	0.2760E+00	0.3760E+00	0.4300E+00	0.4413E+00	0.4460E+00	0.4473E+00	0.4473E+00	0.4488E+00	0.4498E+00
1.0	0.7963E-01	0.1137E+00	0.1329E+00	0.1373E+00	0.1398E+00	0.1408E+00	0.1408E+00	0.1409E+00	0.1417E+00
7.0	0.3392E-01	0.4203E-01	0.4464E-01	0.4547E-01	0.4612E-01	0.4643E-01	0.4643E-01	0.4657E-01	0.4661E-01

TABLE H-2. GAMMA-RAY ALBEDO FACTORS FOR IRON, GEOMETRY F ($h_s=0$, $\rho_D=0$, $z_D=-10a$)

(a) Single-scatter		0.5	1.0	2.0	3.0	4.0	5.0	6.0	7.0
Thickness (mfp)									
Energy (Mev)									
0.10	0.7484E-01	0.8484E-01	0.8824E-01	0.8898E-01	0.8937E-01	0.8956E-01	0.8956E-01	0.8972E-01	0.8983E-01
1.0	0.3969E-01	0.4549E-01	0.4806E-01	0.4888E-01	0.4928E-01	0.4953E-01	0.4953E-01	0.4968E-01	0.4980E-01
7.0	0.1826E-01	0.2012E-01	0.2083E-01	0.2105E-01	0.2115E-01	0.2122E-01	0.2122E-01	0.2126E-01	0.2129E-01
(b) Total scatter									
Energy (Mev)									
0.10	0.8648E-01	0.1008E+00	0.1059E+00	0.1070E+00	0.1075E+00	0.1078E+00	0.1078E+00	0.1080E+00	0.1081E+00
1.0	0.7124E-01	0.9513E-01	0.1068E+00	0.1091E+00	0.1112E+00	0.1122E+00	0.1122E+00	0.1127E+00	0.1130E+00
7.0	0.3740E-01	0.4628E-01	0.4958E-01	0.5042E-01	0.5064E-01	0.5110E-01	0.5110E-01	0.5125E-01	0.5135E-01

TABLE H-3. GAMMA-RAY ALBEDO FACTORS FOR LEAD, GEOMETRY F ($h_s=0$, $\rho_D=0$, $z_D=-10a$)

(a) Single-scatter		0.5	1.0	2.0	3.0	4.0	5.0	6.0	7.0
Thickess (mfp)									
Energy (Mev)									
0.10	0.5480E-02	0.7137E-02	0.8261E-02	0.8583E-02	0.8707E-02	0.8756E-02	0.8787E-02	0.8805E-02	
1.0	0.1791E-01	0.1955E-01	0.2052E-01	0.2086E-01	0.2104E-01	0.2114E-01	0.2121E-01	0.2126E-01	
7.0	0.2283E-01	0.2471E-01	0.2534E-01	0.2553E-01	0.2561E-01	0.2568E-01	0.2571E-01	0.2574E-01	
(b) Total scatter									
Energy (Mev)									
0.10	0.5598E-02	0.7427E-02	0.8881E-02	0.9505E-02	0.9899E-02	0.1021E-01	0.1049E-01	0.1073E-01	
1.0	0.2210E-01	0.2460E-01	0.2613E-01	0.2676E-01	0.2700E-01	0.2724E-01	0.2734E-01	0.2746E-01	
7.0	0.2927E-01	0.3253E-01	0.3367E-01	0.3405E-01	0.3425E-01	0.3422E-01	0.3438E-01	0.3443E-01	

TABLE H-4. GAMMA-RAY ALBEDO FACTORS FOR WATER, GEOMETRY F ($h_s=0$, $\rho_D=0$, $z_D=-10a$)

(a) Single-scatter		0.5	1.0	2.0	3.0	4.0	5.0	6.0	7.0
Thickess (mfp)									
Energy (Mev)									
0.10	0.2034E+00	0.2408E+00	0.2561E+00	0.2590E+00	0.2603E+00	0.2610E+00	0.2612E+00	0.2616E+00	
1.0	0.4098E-01	0.4729E-01	0.5015E-01	0.5095E-01	0.5134E-01	0.5163E-01	0.5179E-01	0.5190E-01	
7.0	0.1067E-01	0.1166E-01	0.1213E-01	0.1229E-01	0.1237E-01	0.1241E-01	0.1245E-01	0.1246E-01	
(b) Total scatter									
Energy (Mev)									
0.10	0.3524E+00	0.5452E+00	0.7202E+00	0.7692E+00	0.7838E+00	0.7911E+00	0.7977E+00	0.7991E+00	
1.0	0.8112E-01	0.1205E+00	0.1461E+00	0.1523E+00	0.1544E+00	0.1547E+00	0.1556E+00	0.1561E+00	
7.0	0.2934E-01	0.3622E-01	0.3825E-01	0.3914E-01	0.3965E-01	0.3967E-01	0.3990E-01	0.3999E-01	

TABLE H-5. GAMMA-RAY ALBEDO FACTORS FOR POLYETHYLENE, GEOMETRY F ($h_s=0$, $\rho_D=0$, $z_D=-10a$)

(a) Single-scatter		0.5	1.0	2.0	3.0	4.0	5.0	6.0	7.0
Thickness (mfp)	Energy (Mev)								
0.10	0.2062E+00	0.2442E+00	0.2600E+00	0.2630E+00	0.2642E+00	0.2649E+00	0.2654E+00	0.2657E+00	
1.0	0.4098E-01	0.4732E-01	0.5011E-01	0.5096E-01	0.5137E-01	0.5162E-01	0.5183E-01	0.5193E-01	
7.0	0.9726E-02	0.1063E-01	0.1108E-01	0.1124E-01	0.1131E-01	0.1136E-01	0.1139E-01	0.1141E-01	
(b) Total scatter									
Thickness (mfp)	Energy (Mev)								
0.10	0.3668E+00	0.5875E+00	0.8586E+00	0.9662E+00	0.1001E+01	0.1016E+01	0.1025E+01	0.1026E+01	
1.0	0.8153E-01	0.1228E+00	0.1577E+00	0.1623E+00	0.1649E+00	0.1663E+00	0.1671E+00	0.1676E+00	
7.0	0.2813E-01	0.3550E-01	0.3809E-01	0.3851E-01	0.3889E-01	0.3909E-01	0.3927E-01	0.3936E-01	

TABLE H-6. GAMMA-RAY ALBEDO FACTORS FOR CONCRETE, GEOMETRY F ($h_s=0$, $\rho_D=0$, $z_D=-10a$)

(a) Single-scatter		0.5	1.0	2.0	3.0	4.0	5.0	6.0	7.0
Thickness (mfp)	Energy (Mev)								
0.10	0.1763E+00	0.2066E+00	0.2183E+00	0.2205E+00	0.2216E+00	0.2222E+00	0.2225E+00	0.2228E+00	
1.0	0.4084E-01	0.4709E-01	0.4990E-01	0.5072E-01	0.5115E-01	0.5141E-01	0.5157E-01	0.5167E-01	
7.0	0.1299E-01	0.1420E-01	0.1473E-01	0.1489E-01	0.1498E-01	0.1504E-01	0.1507E-01	0.1509E-01	
(b) Total scatter									
Thickness (mfp)	Energy (Mev)								
0.10	0.2685E+00	0.3641E+00	0.4147E+00	0.4240E+00	0.4281E+00	0.4298E+00	0.4312E+00	0.4317E+00	
1.0	0.7931E-01	0.1130E+00	0.1326E+00	0.1370E+00	0.1386E+00	0.1397E+00	0.1402E+00	0.1404E+00	
7.0	0.3275E-01	0.4044E-01	0.4285E-01	0.4396E-01	0.4414E-01	0.4454E-01	0.4452E-01	0.4464E-01	

TABLE H-7. GAMMA-RAY ALBEDO FACTORS FOR ALUMINUM, GEOMETRY G ($h_s=10a$, $\rho_D=0$, $z_D=10a$)

(a) Single-scatter		0.5	1.0	2.0	3.0	4.0	5.0	6.0	7.0
Thickness (mfp)									
Energy (Mev)									
(b) Total scatter	0.10	0.1511E+00	0.1632E+00	0.1462E+00	0.1247E+00	0.1056E+00	0.8926E-01	0.7528E-01	0.6345E-01
	1.0	0.2898E-01	0.2974E-01	0.2556E-01	0.2109E-01	0.1716E-01	0.1384E-01	0.1109E-01	0.8840E-02
	7.0	0.6599E-02	0.5770E-02	0.3907E-02	0.2541E-02	0.1607E-02	0.9964E-03	0.6082E-03	0.3666E-03
Energy (Mev)									
(b) Total scatter	0.10	0.2320E+00	0.2948E+00	0.3406E+00	0.3524E+00	0.2730E+00	0.2277E+00	0.2789E+00	0.1560E+00
	1.0	0.5391E-01	0.8461E-01	0.6573E-01	0.9122E-01	0.4351E-01	0.3405E-01	0.2832E-01	0.2561E-01
	7.0	0.2165E-01	0.1687E-01	0.1001E-01	0.1572E-01	0.5228E-01	0.3660E-01	0.2568E-01	0.1926E-01

TABLE H-8. GAMMA-RAY ALBEDO FACTORS FOR IRON, GEOMETRY G ($h_s=10a$, $\rho_D=0$, $z_D=10a$)

(a) Single-scatter		0.5	1.0	2.0	3.0	4.0	5.0	6.0	7.0
Thickness (mfp)									
Energy (Mev)									
(b) Total scatter	0.10	0.5412E-01	0.5458E-01	0.4542E-01	0.3670E-01	0.2950E-01	0.2365E-01	0.1892E-01	0.1512E-01
	1.0	0.2701E-01	0.2728E-01	0.2307E-01	0.1879E-01	0.1508E-01	0.1201E-01	0.9497E-02	0.7464E-02
	7.0	0.1000E-01	0.9127E-02	0.6652E-02	0.4681E-02	0.3229E-02	0.2193E-02	0.1470E-02	0.9762E-03
Energy (Mev)									
(b) Total scatter	0.10	0.6152E-01	0.6659E-01	0.5218E-01	0.4762E-01	0.4288E-01	0.8425E-01	0.1020E+00	0.1258E+00
	1.0	0.4750E-01	0.5241E-01	0.4716E-01	0.4074E-01	0.3046E-01	0.2960E-01	0.2276E-01	0.1847E-01
	7.0	0.2187E-01	0.3567E-01	0.1914E-01	0.1667E-01	0.7988E-02	0.2062E-01	0.3995E-02	0.3465E-02

TABLE H-9. GAMMA-RAY ALBEDO FACTORS FOR LEAD, GEOMETRY G ($h_s=10a$, $\rho_D=0$, $z_D=10a$)

(a) Single-scatter		0.5	1.0	2.0	3.0	4.0	5.0	6.0	7.0
Thickness (mfp)									
Energy (Mev)									
0.10	0.1005E-01	0.1578E-01	0.2126E-01	0.2335E-01	0.2415E-01	0.2439E-01	0.2439E-01	0.2438E-01	0.2423E-01
1.0	0.5588E-02	0.4238E-02	0.2262E-02	0.1162E-02	0.5827E-03	0.2868E-03	0.2868E-03	0.1395E-03	0.6724E-04
7.0	0.1126E-01	0.9768E-02	0.6554E-02	0.4239E-02	0.2682E-02	0.1667E-02	0.1667E-02	0.1020E-02	0.6180E-03

(b) Total scatter		0.5	1.0	2.0	3.0	4.0	5.0	6.0	7.0
Thickness (mfp)									
Energy (Mev)									
0.10	0.1030E-01	0.1649E-01	0.2278E-01	0.2587E-01	0.2717E-01	0.2821E-01	0.2821E-01	0.2898E-01	0.2941E-01
1.0	0.6200E-02	0.6291E-02	0.6216E-02	0.1429E-02	0.7902E-03	0.4035E-03	0.4035E-03	0.1567E-03	0.8223E-04
7.0	0.1432E-01	0.1114E-01	0.2640E-01	0.7164E-02	0.3922E-02	0.2584E-02	0.2584E-02	0.1707E-02	0.1178E-02

TABLE H-10. GAMMA-RAY ALBEDO FACTORS FOR WATER, GEOMETRY G ($h_s=10a$, $\rho_D=0$, $z_D=10a$)

(a) Single-scatter		0.5	1.0	2.0	3.0	4.0	5.0	6.0	7.0
Thickness (mfp)									
Energy (Mev)									
0.10	0.1787E+00	0.1967E+00	0.1794E+00	0.1549E+00	0.1329E+00	0.1136E+00	0.1136E+00	0.9692E-01	0.8264E-01
1.0	0.2915E-01	0.2993E-01	0.2579E-01	0.2129E-01	0.1733E-01	0.1401E-01	0.1401E-01	0.1124E-01	0.8966E-02
7.0	0.4720E-02	0.3998E-02	0.2566E-02	0.1566E-02	0.9257E-03	0.5343E-03	0.5343E-03	0.3027E-03	0.1691E-03

(b) Total scatter		0.5	1.0	2.0	3.0	4.0	5.0	6.0	7.0
Thickness (mfp)									
Energy (Mev)									
0.10	0.3190E+00	0.4790E+00	0.4933E+00	0.7141E+00	0.6837E+00	0.7687E+00	0.7687E+00	0.7369E+00	0.4972E+00
1.0	0.5875E-01	0.7264E-01	0.6492E-01	0.2240E+00	0.1084E+00	0.7092E-01	0.7092E-01	0.5504E-01	0.4124E-01
7.0	0.1286E-01	0.6253E-01	0.7196E-02	0.1318E-01	0.3797E-02	0.3492E-02	0.3492E-02	0.3637E-02	0.3770E-02

TABLE H-11. GAMMA-RAY ALBEDO FACTORS FOR POLYETHYLENE, GEOMETRY G ($h_s=10a$, $\rho_D=0$, $z_D=10a$)

(a) Single-scatter		0.5	1.0	2.0	3.0	4.0	5.0	6.0	7.0
Thickness (mfp)	Energy (Mev)								
0.10	0.1821E+00	0.2008E+00	0.1836E+00	0.1589E+00	0.1363E+00	0.1167E+00	0.0997E+00	0.08520E-01	0.8520E-01
1.0	0.2917E-01	0.2997E-01	0.2578E-01	0.2129E-01	0.1735E-01	0.1402E-01	0.1125E-01	0.08974E-02	0.8974E-02
7.0	0.4160E-02	0.3486E-02	0.2194E-02	0.1309E-02	0.7544E-03	0.4240E-03	0.2339E-03	0.1272E-03	0.1272E-03

(b) Total scatter		0.5	1.0	2.0	3.0	4.0	5.0	6.0	7.0
Thickness (mfp)	Energy (Mev)								
0.10	0.3373E+00	0.4852E+00	0.8075E+00	0.1054E+01	0.1044E+01	0.4996E+00	0.7703E+00	0.9856E+00	0.9856E+00
1.0	0.5969E-01	0.7812E-01	0.1141E+00	0.6530E-01	0.5476E-01	0.7122E-01	0.7962E-01	0.7325E-01	0.7325E-01
7.0	0.1149E-01	0.1488E-01	0.3729E-02	0.9393E-02	0.8915E-02	0.4851E-02	0.5280E-02	0.3616E-02	0.3616E-02

TABLE H-12. GAMMA-RAY ALBEDO FACTORS FOR CONCRETE, GEOMETRY G ($h_s=10a$, $\rho_D=0$, $z_D=10a$)

(a) Single-scatter		0.5	1.0	2.0	3.0	4.0	5.0	6.0	7.0
Thickness (mfp)	Energy (Mev)								
0.10	0.1481E+00	0.1599E+00	0.1429E+00	0.1217E+00	0.1030E+00	0.8694E-01	0.7327E-01	0.6166E-01	0.6166E-01
1.0	0.2895E-01	0.2967E-01	0.2551E-01	0.2103E-01	0.1712E-01	0.1382E-01	0.1106E-01	0.8816E-02	0.8816E-02
7.0	0.6182E-02	0.5363E-02	0.3596E-02	0.2308E-02	0.1441E-02	0.8805E-03	0.5294E-03	0.3143E-03	0.3143E-03

(b) Total scatter		0.5	1.0	2.0	3.0	4.0	5.0	6.0	7.0
Thickness (mfp)	Energy (Mev)								
0.10	0.2247E+00	0.2975E+00	0.3404E+00	0.2523E+00	0.2586E+00	0.4001E+00	0.2845E+00	0.1465E+00	0.1465E+00
1.0	0.5913E-01	0.7961E-01	0.8599E-01	0.1375E+00	0.6337E-01	0.5024E-01	0.4499E-01	0.3879E-01	0.3879E-01
7.0	0.1913E-01	0.1146E-01	0.7610E-02	0.1181E-01	0.6725E-02	0.3429E-02	0.2374E-02	0.2529E-02	0.2529E-02

TABLE H-13. GAMMA-RAY ALBEDO FACTORS FOR ALUMINUM, GEOMETRY H ($h_s=0$, $\rho_D=2a$, $z_D=-a$)

(a) Single-scatter		0.5	1.0	2.0	3.0	4.0	5.0	6.0	7.0
LOS Thickness	(mfp)								
Energy (Mev)									
0.10	0.1943E+00	0.2506E+00	0.2782E+00	0.2825E+00	0.2828E+00	0.2826E+00	0.2823E+00	0.2823E+00	0.2820E+00
1.0	0.6813E-01	0.9406E-01	0.1130E+00	0.1193E+00	0.1220E+00	0.1235E+00	0.1243E+00	0.1243E+00	0.1249E+00
7.0	0.2174E-01	0.2822E-01	0.3280E-01	0.3451E-01	0.3539E-01	0.3590E-01	0.3622E-01	0.3622E-01	0.3646E-01
(b) Total scatter									
Energy (Mev)									
0.10	0.2642E+00	0.3878E+00	0.4742E+00	0.4876E+00	0.4881E+00	0.4827E+00	0.4804E+00	0.4804E+00	0.4778E+00
1.0	0.9586E-01	0.1564E+00	0.2065E+00	0.2208E+00	0.2247E+00	0.2251E+00	0.2256E+00	0.2256E+00	0.2245E+00
7.0	0.3779E-01	0.5487E-01	0.6584E-01	0.6710E-01	0.6870E-01	0.6927E-01	0.7006E-01	0.7006E-01	0.7046E-01

TABLE H-14. GAMMA-RAY ALBEDO FACTORS FOR IRON, GEOMETRY H ($h_s=0$, $\rho_D=2a$, $z_D=-a$)

(a) Single-scatter		0.5	1.0	2.0	3.0	4.0	5.0	6.0	7.0
LOS Thickness	(mfp)								
Energy (Mev)									
0.10	0.8166E-01	0.1025E+00	0.1119E+00	0.1135E+00	0.1136E+00	0.1136E+00	0.1135E+00	0.1134E+00	0.1133E+00
1.0	0.6679E-01	0.9201E-01	0.1104E+00	0.1167E+00	0.1195E+00	0.1209E+00	0.1217E+00	0.1217E+00	0.1222E+00
7.0	0.2472E-01	0.3148E-01	0.3566E-01	0.3708E-01	0.377E-01	0.3820E-01	0.3847E-01	0.3847E-01	0.3863E-01
(b) Total									
Energy (Mev)									
0.10	0.9056E-01	0.1172E+00	0.1296E+00	0.1313E+00	0.1312E+00	0.1308E+00	0.1305E+00	0.1305E+00	0.1302E+00
1.0	0.9140E-01	0.1425E+00	0.1821E+00	0.1955E+00	0.1991E+00	0.2014E+00	0.2012E+00	0.2012E+00	0.2013E+00
7.0	0.4060E-01	0.5759E-01	0.6805E-01	0.7058E-01	0.7103E-01	0.7093E-01	0.7150E-01	0.7150E-01	0.7145E-01

TABLE H-15. GAMMA-RAY ALBEDO FACTORS FOR LEAD, GEOMETRY H ($h_s=0$, $\rho_D=2a$, $z_D=-a$)

(a) Single-scatter									
LOS Thickness	0.5	1.0	2.0	3.0	4.0	5.0	6.0	7.0	
(mfp)									
Energy (Mev)									
0.10	0.5981E-02	0.8686E-02	0.1100E-01	0.1190E-01	0.1233E-01	0.1257E-01	0.1273E-01	0.1282E-01	
1.0	0.3769E-01	0.5086E-01	0.6153E-01	0.6552E-01	0.6741E-01	0.6847E-01	0.6903E-01	0.6941E-01	
7.0	0.2584E-01	0.3089E-01	0.3322E-01	0.3389E-01	0.3425E-01	0.3447E-01	0.3460E-01	0.3470E-01	
(b) Total scatter									
Energy (Mev)									
0.10	0.6048E-02	0.8876E-02	0.1144E-01	0.1261E-01	0.1327E-01	0.1372E-01	0.1410E-01	0.1441E-01	
1.0	0.4217E-01	0.5925E-01	0.7342E-01	0.7878E-01	0.8130E-01	0.8219E-01	0.8328E-01	0.8317E-01	
7.0	0.3172E-01	0.3927E-01	0.4328E-01	0.4426E-01	0.4477E-01	0.4505E-01	0.4501E-01	0.4518E-01	

TABLE H-16. GAMMA-RAY ALBEDO FACTORS FOR WATER, GEOMETRY H ($h_s=0$, $\rho_D=2a$, $z_D=-a$)

(a) Single-scatter									
LOS Thickness	0.5	1.0	2.0	3.0	4.0	5.0	6.0	7.0	
(mfp)									
Energy (Mev)									
0.10	0.2522E+00	0.3584E+00	0.4432E+00	0.4762E+00	0.5030E+00	0.5095E+00	0.5143E+00	0.0000E+00	
1.0	0.5358E-01	0.7911E-01	0.1037E+00	0.1157E+00	0.1272E+00	0.1303E+00	0.1327E+00	0.0000E+00	
7.0	0.1526E-01	0.2125E-01	0.2672E-01	0.2931E-01	0.3181E-01	0.3249E-01	0.3301E-01	0.0000E+00	
(b) Total									
Energy (Mev)									
0.10	0.3443E+00	0.6027E+00	0.9432E+00	0.1139E+01	0.1297E+01	0.1337E+01	0.1357E+01	0.0000E+00	
1.0	0.7679E-01	0.1369E+00	0.2164E+00	0.2570E+00	0.2951E+00	0.3051E+00	0.3099E+00	0.0000E+00	
7.0	0.2802E-01	0.4609E-01	0.6357E-01	0.7145E-01	0.7932E-01	0.8086E-01	0.8223E-01	0.0000E+00	

TABLE H-17. GAMMA-RAY ALBEDO FACTORS FOR POLYETHYLENE, GEOMETRY H ($h_s=0$, $\rho_D=2a$, $z_D=-a$)

(a) Single-scatter		0.5	1.0	2.0	3.0	4.0	5.0	6.0	7.0
LOS Thickness (mfp)									
Energy (Mev)									
0.10		0.2234E+00	0.2908E+00	0.3246E+00	0.3300E+00	0.3306E+00	0.3304E+00	0.3298E+00	0.3295E+00
1.0		0.6823E-01	0.9423E-01	0.1131E+00	0.1195E+00	0.1223E+00	0.1237E+00	0.1246E+00	0.1250E+00
7.0		0.1937E-01	0.2580E-01	0.3080E-01	0.3276E-01	0.3378E-01	0.3434E-01	0.3473E-01	0.3501E-01
(b) Total									
Energy (Mev)									
0.10		0.3269E+00	0.5448E+00	0.7993E+00	0.9094E+00	0.9505E+00	0.9449E+00	0.9388E+00	0.9295E+00
1.0		0.9782E-01	0.1600E+00	0.2213E+00	0.2374E+00	0.2391E+00	0.2423E+00	0.2412E+00	0.2405E+00
7.0		0.3322E-01	0.5074E-01	0.6118E-01	0.6380E-01	0.6434E-01	0.6586E-01	0.6630E-01	0.6612E-01

TABLE H-18. GAMMA-RAY ALBEDO FACTORS FOR CONCRETE, GEOMETRY H ($h_s=0$, $\rho_D=2a$, $z_D=-a$)

(a) Single-scatter		0.5	1.0	2.0	3.0	4.0	5.0	6.0	7.0
LOS Thickness (mfp)									
Energy (Mev)									
0.10		0.1912E+00	0.2465E+00	0.2734E+00	0.2777E+00	0.2780E+00	0.2779E+00	0.2775E+00	0.2771E+00
1.0		0.6802E-01	0.9400E-01	0.1128E+00	0.1192E+00	0.1219E+00	0.1233E+00	0.1242E+00	0.1247E+00
7.0		0.2136E-01	0.2781E-01	0.3245E-01	0.3420E-01	0.3509E-01	0.3562E-01	0.3597E-01	0.3620E-01
(b) Total scatter									
Energy (Mev)									
0.10		0.2571E+00	0.3780E+00	0.4607E+00	0.4715E+00	0.4694E+00	0.4652E+00	0.4634E+00	0.4608E+00
1.0		0.9613E-01	0.1561E+00	0.2062E+00	0.2187E+00	0.2228E+00	0.2234E+00	0.2224E+00	0.2226E+00
7.0		0.3709E-01	0.5418E-01	0.6428E-01	0.6745E-01	0.6815E-01	0.6813E-01	0.6826E-01	0.6830E-01

APPENDIX I

NEUTRON ALBEDO FACTOR TABLES, GEOMETRIES F-H

10 PAGES

REFERENCED IN CHAPTER 1, INTRODUCTION, AND
CHAPTER 6, SAMPLE PROBLEM ANALYSIS

NAVSWC TR 91-16

TABLE I-1. NEUTRON ALBEDO FACTORS FOR ALUMINUM, GEOMETRY F ($h_s=0$, $\rho_D=0$, $z_D=-10a$)

(a) Single-scatter

Thickness (mfp)	0.5	1.0	3.0	5.0	7.0
Energy (Mev)					
10 ⁻⁷	0.2840E+00	0.3367E+00	0.3609E+00	0.3624E+00	0.3623E+00
0.10	0.2343E+00	0.2524E+00	0.2583E+00	0.2582E+00	0.2575E+00
1.0	0.2701E+00	0.3118E+00	0.3293E+00	0.3306E+00	0.3306E+00
14.0	0.1953E+00	0.2297E+00	0.2453E+00	0.2461E+00	0.2459E+00

(b) Total

Energy (Mev)					
10 ⁻⁷	0.4582E+00	0.6827E+00	0.9853E+00	0.1031E+01	0.1040E+01
0.10	0.5966E+00	0.9046E+00	0.1459E+01	0.1712E+01	0.1854E+01
1.0	0.5079E+00	0.7762E+00	0.1118E+01	0.1164E+01	0.1172E+01
14.0	0.3241E+00	0.4826E+00	0.6639E+00	0.6769E+00	0.6841E+00

TABLE I-2. NEUTRON ALBEDO FACTORS FOR IRON, GEOMETRY F ($h_s=0$, $\rho_D=0$, $z_D=-10a$)

(a) Single-scatter

Thickness (mfp)	0.5	1.0	3.0	5.0	7.0
Energy (Mev)					
10 ⁻⁷	0.2831E+00	0.3361E+00	0.3609E+00	0.3622E+00	0.3622E+00
0.10	0.3142E+00	0.3685E+00	0.3915E+00	0.3929E+00	0.3926E+00
1.0	0.3055E+00	0.3789E+00	0.4261E+00	0.4308E+00	0.4316E+00
14.0	0.2254E+00	0.2664E+00	0.2857E+00	0.2870E+00	0.2870E+00

(b) Total

Energy (Mev)					
10 ⁻⁷	0.4491E+00	0.6609E+00	0.9301E+00	0.9664E+00	0.9747E+00
0.10	0.5775E+00	0.9025E+00	0.1482E+01	0.1641E+01	0.1683E+01
1.0	0.4179E+00	0.6169E+00	0.9535E+00	0.1076E+01	0.1134E+01
14.0	0.3504E+00	0.5093E+00	0.7265E+00	0.7781E+00	0.7925E+00

NAVSWC TR 91-16

TABLE I-3. NEUTRON ALBEDO FACTORS FOR LEAD, GEOMETRY F ($h_s=0$, $\rho_D=0$, $z_D=-10a$)

(a) Single-scatter

Thickness (mfp)	0.5	1.0	3.0	5.0	7.0
Energy (Mev)					
10 ⁻⁷	0.3165E+00	0.3756E+00	0.4031E+00	0.4046E+00	0.4046E+00
0.10	0.3207E+00	0.3806E+00	0.4084E+00	0.4100E+00	0.4100E+00
1.0	0.2993E+00	0.3513E+00	0.3732E+00	0.3741E+00	0.3739E+00
14.0	0.2954E+00	0.3499E+00	0.3750E+00	0.3764E+00	0.3763E+00

(b) Total

Energy (Mev)					
10 ⁻⁷	0.5336E+00	0.8321E+00	0.1380E+01	0.1532E+01	0.1569E+01
0.10	0.5446E+00	0.8557E+00	0.1461E+01	0.1639E+01	0.1680E+01
1.0	0.5312E+00	0.8256E+00	0.1303E+01	0.1400E+01	0.1415E+01
14.0	0.4894E+00	0.7412E+00	0.1096E+01	0.1145E+01	0.1160E+01

TABLE I-4. NEUTRON ALBEDO FACTORS FOR WATER, GEOMETRY F ($h_s=0$, $\rho_D=0$, $z_D=-10a$)

(a) Single-scatter

Thickness (mfp)	0.5	1.0	3.0	5.0	7.0
Energy (Mev)					
10 ⁻⁷	0.8990E-01	0.1064E+00	0.1172E+00	0.1180E+00	0.1173E+00
0.10	0.3982E-01	0.4708E-01	0.5038E-01	0.5055E-01	0.5059E-01
1.0	0.1360E+00	0.1647E+00	0.1804E+00	0.1815E+00	0.1817E+00
14.0	0.1060E+00	0.1244E+00	0.1330E+00	0.1339E+00	0.1339E+00

(b) Total

Energy (Mev)					
10 ⁻⁷	0.2290E+00	0.3976E+00	0.7008E+00	0.7633E+00	0.7786E+00
0.10	0.1826E+00	0.3857E+00	0.7173E+00	0.7688E+00	0.7865E+00
1.0	0.1897E+00	0.2768E+00	0.3717E+00	0.3813E+00	0.3851E+00
14.0	0.1857E+00	0.2588E+00	0.3114E+00	0.3169E+00	0.3189E+00

NAVSWC TR 91-16

TABLE I-5. NEUTRON ALBEDO FACTORS FOR POLYETHYLENE, GEOMETRY F
($h_s=0$, $\rho_D=0$, $z_D=-10a$)

(a) Single-scatter

Thickness (mfp)	0.5	1.0	3.0	5.0	7.0
Energy (Mev)					
10 ⁻⁷	0.9019E-01	0.1069E+00	0.1177E+00	0.1185E+00	0.1178E+00
0.10	0.4779E-01	0.5645E-01	0.6039E-01	0.6064E-01	0.6061E-01
1.0	0.5690E-01	0.6702E-01	0.7166E-01	0.7201E-01	0.7206E-01
14.0	0.9409E-01	0.1102E+00	0.1174E+00	0.1179E+00	0.1178E+00

(b) Total

Energy (Mev)					
10 ⁻⁷	0.2298E+00	0.3976E+00	0.7051E+00	0.7653E+00	0.7800E+00
0.10	0.1987E+00	0.4125E+00	0.7621E+00	0.8116E+00	0.8302E+00
1.0	0.1134E+00	0.1767E+00	0.2243E+00	0.2298E+00	0.2321E+00
14.0	0.1761E+00	0.2452E+00	0.2877E+00	0.2921E+00	0.2940E+00

TABLE I-6. NEUTRON ALBEDO FACTORS FOR CONCRETE, GEOMETRY F ($h_s=0$,
 $\rho_D=0$, $z_D=-10a$)

(a) Single-scatter

Thickness (mfp)	0.5	1.0	3.0	5.0	7.0
Energy (Mev)					
10 ⁻⁷	0.9414E-01	0.0000E+00	0.0000E+00	0.1104E+00	0.1116E+00
0.10	0.2144E+00	0.2529E+00	0.2678E+00	0.2709E+00	0.2709E+00
1.0	0.2692E+00	0.3308E+00	0.3682E+00	0.3714E+00	0.3719E+00
14.0	0.1863E+00	0.2201E+00	0.2356E+00	0.2365E+00	0.2364E+00

(b) Total

Energy (Mev)					
10 ⁻⁷	0.2350E+00	0.0000E+00	0.0000E+00	0.7661E+00	0.7760E+00
0.10	0.4843E+00	0.8586E+00	0.1362E+01	0.1725E+01	0.1746E+01
1.0	0.3787E+00	0.5592E+00	0.8408E+00	0.9264E+00	0.9518E+00
14.0	0.2926E+00	0.4241E+00	0.5590E+00	0.5701E+00	0.5712E+00

NAVSWC TR 91-16

TABLE I-7. NEUTRON ALBEDO FACTORS FOR ALUMINUM, GEOMETRY G
($h_s=10a$, $\rho_D=0$, $z_D=10a$)

(a) Single-scatter

Thickness (mfp)	0.5	1.0	3.0	5.0	7.0
Energy (Mev)					
10 ⁻⁷	0.1762E+00	0.1523E+00	0.3858E-01	0.8105E-02	0.1621E-02
0.10	0.4863E-01	0.1884E-01	0.3021E-03	0.4987E-05	0.8176E-07
1.0	0.1451E+00	0.1161E+00	0.2548E-01	0.4931E-02	0.9413E-03
14.0	0.1122E+00	0.9214E-01	0.2039E-01	0.3924E-02	0.7409E-03

(b) Total

Energy (Mev)					
10 ⁻⁷	0.3493E+00	0.5693E+00	0.4754E+00	0.8727E+01	0.3642E+00
0.10	0.3495E+00	0.4742E+00	0.1566E+01	0.1665E+01	0.2134E+01
1.0	0.3295E+00	0.5082E+00	0.1033E+01	0.2950E+00	0.7097E+00
14.0	0.2174E+00	0.2851E+00	0.2994E+00	0.1672E+00	0.2377E+00

TABLE I-8. NEUTRON ALBEDO FACTORS FOR IRON, GEOMETRY G ($h_s=10a$,
 $\rho_D=0$, $z_D=10a$)

(a) Single-scatter

Thickness (mfp)	0.5	1.0	3.0	5.0	7.0
Energy (Mev)					
10 ⁻⁷	0.1755E+00	0.1517E+00	0.3844E-01	0.8071E-02	0.1616E-02
0.10	0.1778E+00	0.1438E+00	0.2879E-01	0.4780E-02	0.7679E-03
1.0	0.3065E+00	0.3659E+00	0.2763E+00	0.1667E+00	0.9783E-01
14.0	0.1370E+00	0.1169E+00	0.2960E-01	0.6883E-02	0.1828E-02

(b) Total

Energy (Mev)					
10 ⁻⁷	0.3442E+00	0.4199E+00	0.4765E+00	0.5297E+00	0.2595E+00
0.10	0.4033E+00	0.6510E+00	0.1603E+01	0.1375E+01	0.1281E+01
1.0	0.4288E+00	0.6343E+00	0.8583E+00	0.9997E+00	0.8239E+00
14.0	0.2382E+00	0.3399E+00	0.2911E+00	0.4291E+00	0.2548E+00

NAVSWC TR 91-16

TABLE I-9. NEUTRON ALBEDO FACTORS FOR LEAD, GEOMETRY G ($h_s=10a$, $\rho_D=0$, $z_D=10a$)

(a) Single-scatter

Thickness (mfp)	0.5	1.0	3.0	5.0	7.0
Energy (Mev)					
10 ⁻⁷	0.1969E+00	0.1700E+00	0.4301E-01	0.9028E-02	0.1807E-02
0.10	0.1992E+00	0.1719E+00	0.4334E-01	0.9076E-02	0.1813E-02
1.0	0.1573E+00	0.1203E+00	0.1775E-01	0.2028E-02	0.2206E-03
14.0	0.1809E+00	0.1551E+00	0.3881E-01	0.8155E-02	0.1640E-02

(b) Total

Energy (Mev)					
10 ⁻⁷	0.4128E+00	0.7082E+00	0.8891E+00	0.5428E+00	0.8626E+00
0.10	0.4423E+00	0.6389E+00	0.1056E+01	0.1874E+01	0.9160E+00
1.0	0.3830E+00	0.4760E+00	0.1158E+01	0.7214E+00	0.6042E+00
14.0	0.3499E+00	0.5232E+00	0.9298E+00	0.5395E+00	0.4142E+00

TABLE I-10. NEUTRON ALBEDO FACTORS FOR WATER, GEOMETRY G ($h_s=10a$, $\rho_D=0$, $z_D=10a$)

(a) Single-scatter

Thickness (mfp)	0.5	1.0	3.0	5.0	7.0
Energy (Mev)					
10 ⁻⁷	0.4184E-01	0.3161E-01	0.5143E-02	0.7741E-03	0.1246E-03
0.10	0.2401E-01	0.2030E-01	0.4780E-02	0.9314E-03	0.1730E-03
1.0	0.1029E+00	0.1005E+00	0.3932E-01	0.1293E-01	0.4098E-02
14.0	0.5968E-01	0.4886E-01	0.2400E-01	0.2070E-02	0.3827E-03

(b) Total

Energy (Mev)					
10 ⁻⁷	0.1325E+00	0.2269E+00	0.6656E+00	0.3926E+00	0.3502E+00
0.10	0.1329E+00	0.2581E+00	0.1231E+01	0.8823E+00	0.1974E+00
1.0	0.1519E+00	0.2287E+00	0.1763E+00	0.8883E-01	0.9775E-01
14.0	0.1192E+00	0.1551E+00	0.1433E+00	0.2028E-01	0.8689E-02

NAVSWC TR 91-16

TABLE I-11. NEUTRON ALBEDO FACTORS FOR POLYETHYLENE, GEOMETRY G
($h_s=10a$, $\rho_D=0$, $z_D=10a$)

(a) Single-scatter

Thickness (mfp)	0.5	1.0	3.0	5.0	7.0
Energy (Mev)					
10 ⁻⁷	0.4211E-01	0.3188E-01	0.5215E-02	0.7904E-03	0.1280E-03
0.10	0.2857E-01	0.2405E-01	0.5557E-02	0.1061E-02	0.1929E-03
1.0	0.3330E-01	0.2764E-01	0.6065E-02	0.1092E-02	0.1864E-03
14.0	0.5078E-01	0.4059E-01	0.8168E-02	0.1393E-02	0.2289E-03

(b) Total

Energy (Mev)					
10 ⁻⁷	0.1394E+00	0.2309E+00	0.6565E+00	0.3892E+00	0.3312E+00
0.10	0.1559E+00	0.2971E+00	0.3551E+00	0.1634E+00	0.2158E+00
1.0	0.8151E-01	0.8108E-01	0.1095E+00	0.9172E-01	0.7314E-01
14.0	0.1058E+00	0.1303E+00	0.9901E-01	0.8405E-01	0.6540E-01

TABLE I-12. NEUTRON ALBEDO FACTORS FOR CONCRETE, GEOMETRY G
($h_s=10a$, $\rho_D=0$, $z_D=10a$)

(a) Single-scatter

Thickness (mfp)	0.5	1.0	3.0	5.0	7.0
Energy (Mev)					
10 ⁻⁷	0.3874E-01	0.3052E-01	0.6567E-02	0.1274E-02	0.2411E-03
0.10	0.1245E+00	0.1023E+00	0.2124E-01	0.3588E-02	0.5778E-03
1.0	0.2309E+00	0.2457E+00	0.1285E+00	0.8651E-01	0.2560E-01
14.0	0.1106E+00	0.9306E-01	0.2224E-01	0.1014E-01	0.9198E-03

(b) Total

Energy (Mev)					
10 ⁻⁷	0.1654E+00	0.2758E+00	0.6096E+00	0.3481E+00	0.2366E+00
0.10	0.3871E+00	0.6850E+00	0.2045E+01	0.1954E+01	0.2968E+01
1.0	0.3645E+00	0.5806E+00	0.5944E+00	0.5891E+00	0.7373E+00
14.0	0.1867E+00	0.2809E+00	0.2929E+00	0.2397E+00	0.1773E+00

TABLE I-13. NEUTRON ALBEDO FACTORS FOR ALUMINUM, GEOMETRY H
($h_s=0$, $\rho_D=2a$, $z_D=-a$)

(a) Single-scatter

LOS Thickness (mfp)	0.5	1.0	3.0	5.0	7.0
Energy (Mev)					
10 ⁻⁷	0.2786E+00	0.3596E+00	0.3908E+00	0.3832E+00	0.3787E+00
1.0	0.2680E+00	0.3372E+00	0.3560E+00	0.3468E+00	0.3419E+00
14.0	0.1949E+00	0.2491E+00	0.2681E+00	0.2624E+00	0.2590E+00

(b) Total

Energy (Mev)

10⁻⁷

1.0

14.0

TABLE I-14. NEUTRON ALBEDO FACTORS FOR IRON, GEOMETRY H ($h_s=0$,
 $\rho_D=2a$, $z_D=-a$)

(a) Single-scatter

LOS Thickness (mfp)	0.5	1.0	3.0	5.0	7.0
Energy (Mev)					
10 ⁻⁷	0.2765E+00	0.3564E+00	0.3875E+00	0.3801E+00	0.3754E+00
1.0	0.3002E+00	0.4078E+00	0.4804E+00	0.4785E+00	0.4752E+00
14.0	0.2221E+00	0.2854E+00	0.3094E+00	0.3033E+00	0.2997E+00

(b) Total

Energy (Mev)

10⁻⁷

1.0

14.0

NAVSWC TR 91-16

TABLE I-15. NEUTRON ALBEDO FACTORS FOR LEAD, GEOMETRY H ($h_s=0$, $\rho_D=2a$, $z_D=-a$)

(a) Single-scatter

LOS Thickness (mfp)	0.5	1.0	3.0	5.0	7.0
Energy (Mev)					
10 ⁻⁷	0.3076E+00	0.3962E+00	0.4292E+00	0.4208E+00	0.4155E+00
1.0	0.2907E+00	0.3668E+00	0.3882E+00	0.3799E+00	0.3755E+00
14.0	0.2883E+00	0.3701E+00	0.4001E+00	0.3923E+00	0.3877E+00

(b) Total

Energy (Mev)					
10 ⁻⁷	0.4424E+00	0.7208E+00	0.1177E+01	0.1273E+01	0.1282E+01
1.0	0.4392E+00	0.7041E+00	0.1107E+01	0.1165E+01	0.1146E+01
14.0	0.4092E+00	0.6528E+00	0.9819E+00	0.9989E+00	0.9740E+00

TABLE I-16. NEUTRON ALBEDO FACTORS FOR WATER, GEOMETRY H ($h_s=0$, $\rho_D=2a$, $z_D=-a$)

(a) Single-scatter

LOS Thickness (mfp)	0.5	1.0	3.0	5.0	7.0
Energy (Mev)					
10 ⁻⁷	0.1567E+00	0.2171E+00	0.2543E+00	0.2466E+00	0.2404E+00
1.0	0.1621E+00	0.2227E+00	0.2679E+00	0.2692E+00	0.2683E+00
14.0	0.1382E+00	0.1844E+00	0.2134E+00	0.2124E+00	0.2108E+00

(b) Total

Energy (Mev)					
10 ⁻⁷	0.2501E+00	0.4505E+00	0.8095E+00	0.8588E+00	0.8440E+00
1.0	0.2008E+00	0.3174E+00	0.4761E+00	0.4858E+00	0.4799E+00
14.0	0.1965E+00	0.3039E+00	0.3994E+00	0.3912E+00	0.3845E+00

NAVSWC TR 91-16

TABLE I-17. NEUTRON ALBEDO FACTORS FOR POLYETHYLENE, GEOMETRY H
($h_s=0$, $\rho_D=2a$, $z_D=-a$)

(a) Single-scatter

LOS Thickness (mfp)	0.5	1.0	3.0	5.0	7.0
Energy (Mev)					
10 ⁻⁷	0.1567E+00	0.2173E+00	0.2546E+00	0.2471E+00	0.2408E+00
1.0	0.9338E-01	0.1301E+00	0.1624E+00	0.1653E+00	0.1657E+00
14.0	0.1305E+00	0.1748E+00	0.2030E+00	0.2017E+00	0.1999E+00

(b) Total

Energy (Mev)					
10 ⁻⁷	0.2499E+00	0.4515E+00	0.8082E+00	0.8577E+00	0.8445E+00
1.0	0.1339E+00	0.2244E+00	0.3253E+00	0.3274E+00	0.3210E+00
14.0	0.1918E+00	0.2976E+00	0.3792E+00	0.3710E+00	0.3636E+00

TABLE I-18. NEUTRON ALBEDO FACTORS FOR CONCRETE, GEOMETRY H ($h_s=0$,
 $\rho_D=2a$, $z_D=-a$)

(a) Single-scatter

LOS Thickness (mfp)	0.5	1.0	3.0	5.0	7.0
Energy (Mev)					
10 ⁻⁷	0.1591E+00	0.2224E+00	0.2738E+00	0.2761E+00	0.2747E+00
1.0	0.2775E+00	0.3784E+00	0.4456E+00	0.4435E+00	0.4401E+00
14.0	0.1925E+00	0.2495E+00	0.2733E+00	0.2681E+00	0.2649E+00

(b) Total

Energy (Mev)					
10 ⁻⁷	0.2533E+00	0.4500E+00	0.8166E+00	0.8921E+00	0.8679E+00
1.0	0.3479E+00	0.5503E+00	0.8699E+00	0.9455E+00	0.9621E+00
14.0	0.2614E+00	0.4040E+00	0.5218E+00	0.5382E+00	0.5249E+00

DISTRIBUTION

	<u>Copies</u>		<u>Copies</u>
Naval Sea Systems Command		Department of Energy	
Attn: SEA-06GN		Attn: EH-41 (J. Rabovsky)	1
(Dr. J. C. Taschner)	2	Office of Health	
SEA-08 (Chuck Burrows)	1	ER-20 (Ms. N. Rao)	1
PMS-423 (Carter Kolb)	1	Office of Energy Research	
Washington, DC 20362-5101		Dr. P. B. Hemmig	1
		Safety and Physics Branch	
Chief of Naval Operations		Washington, DC 20545	
Attn: OP-455		Director	
(CDR Karl Mendenhall)	1	Defense Nuclear Agency	
2211 Jefferson Davis Hwy.		Attn: RARP	
Arlington, VA 22022		(Dr. R. Young)	1
Commanding Officer		(MAJ R. Kehlet)	1
Naval Medical Research and		(Dr. D. L. Auton)	1
Development Command		6801 Telegraph Road	
Attn: CAPT Woody	1	Alexandria, VA 22310-3398	
CDR Wolfe	1	Office of the Assistant Manager	
Bethesda, MD 20814-5044		for Energy Research and	
		Development	
Department of the Navy		Department of Energy	
Strategic Systems Programs		Oak Ridge Operations	
Attn: SP-27211 (George Garrott)	1	P.O. Box 2001	
Washington, DC 20376		Oak Ridge TN 37831	1
Commanding Officer		Office of Scientific and Technical	
Naval Weapons Evaluation Facility		Information	
Attn: Sam Mauk	1	P.O. Box 62	
Kirtland Air Force Base		Oak Ridge, TN 37830	1
Albuquerque, NM 87117		Radiation Shielding Information	
Director		Center	
Armed Forces Radiobiology		Oak Ridge National Laboratory	
Research Institute		Attn: D. Trubey	1
Attn: MRA	1	Library	1
MRAD		Oak Ridge, TN 37832-6362	
(CAPT R. L. Bumgarner)	1		
Bethesda, MD 20814-5145			

DISTRIBUTION (Cont.)

	<u>Copies</u>		<u>Copies</u>
Department of Commerce National Institute of Standards and Technology Attn: C. Eisenhower Gaithersburg, MD 20899	1	Commander U.S. Army Foreign Science and Technology Center Attn: AIFRTA (Mr. Charles Ward) 220 7th Street, NE Charlottesville, VA 22901-5396	1
FBI Property Bomb Data Center Attn: Agent David Holmes Room 879 10th and Pennsylvania Ave. Washington, DC 20535	1	Los Alamos National Laboratory Attn: Code X-6, MS B226 (Dr. G. P. Estes, INRAD Project Leader) C-DOT, MS-B281 (Dr. Paul Whalen) Los Alamos, NM 87454	1 1
Commanding Officer Naval Research Laboratory Attn: Code 1240 (Mr. T. Johnson) 4555 Overlook Avenue, SE Washington, DC 20375	1	Lawrence Livermore National Laboratory Attn: Dr. Don Goldman P. O. Box 808 Livermore, CA 94550	1
Commander U.S. Army Combat Systems Test Activity Attn: STECS-NE (Dr. A. H. Kazi) (Dr. C. Heimbach) Aberdeen Proving Ground MD 21005-5059	1 1	Quantum Research Services, Inc. Attn: W. L. Dunn A. M. Yacout F. O'Foghludha P.O. Box 52391 Durham, NC 27717-2391	1 1 1
Director Harry Diamond Laboratories Attn: SLCHD-NW-P (Mr. J. Corrigan) (Mr. K. Kerris) 2800 Powder Mill Road Adelphi, MD 20783-1197	1 1	Science Applications Corp. Attn: Mr. D. C. Kaul 10260 Campus Point Drive San Diego, CA 92121	1
Commander U.S. Army Center for EQ/RSTA Attn: AMSEL-RSK (Dr. Stanley Kroneberg) Fort Monmouth, NJ 07703	1	Library of Congress Attn: Gift & Exchange Division Washington, DC 20540	4
Commander U.S. Army Nuclear and Chemical Agency Attn: MONA-NU (CPT Henry Snyder) 7500 Backlick Road, Bldg. 2073 Springfield, VA 22150-3198	1	Defense Technical Information Center Cameron Station Alexandria, VA 22304-6145	12

NAVSWC TR 91-16

DISTRIBUTION (Cont.)

Copies

Internal Distribution:

E221 (B. Stewart)	1
E231	2
E232	3
R41	1
R41 (G. Riel)	3
R41 (B. Lee)	1
R42 (D. Rule)	1

REPORT DOCUMENTATION PAGE			Form Approved OMB No. 0704-0188	
Public reporting burden for this collection of information is estimated to average 1 hour per response, including the time for reviewing instructions, searching existing data sources, gathering and maintaining the data needed, and completing and reviewing the collection of information. Send comments regarding this burden estimate or any other aspect of this collection of information, including suggestions for reducing this burden, to Washington Headquarters Services, Directorate for Information Operations and Reports, 1215 Jefferson Davis Highway, Suite 1204, Arlington, VA 22202-4302, and to the Office of Management and Budget, Paperwork Reduction Project (0704-0188), Washington, DC 20503				
1. AGENCY USE ONLY (Leave blank)		2. REPORT DATE 30 September 1990		3. REPORT TYPE AND DATES COVERED 21 Nov 1988 to 30 Sep 1990
4. TITLE AND SUBTITLE Boltzmann Transport Equation Algorithms for Infinite-Slab Buildup and Albedo Factors			5. FUNDING NUMBERS Pgm. Element: 6354LN Proj./Task No. S1580 Work Unit: R41 CJ, GE N60921-88-C-0175	
6. AUTHOR(S) W. L. Dunn, A. M. Yacout, and F. O'Foghludha				
7. PERFORMING ORGANIZATION NAME(S) AND ADDRESS(ES) Quantum Research Services, Inc. 100 Capital Drive Durham, NC 27713			8. PERFORMING ORGANIZATION REPORT NUMBER 22002	
9. SPONSORING/MONITORING AGENCY NAME(S) AND ADDRESS(ES) Naval Surface Warfare Center White Oak Laboratory (Code R41) 10901 New Hampshire Avenue Silver Spring, MD 20903-5000			10. SPONSORING/MONITORING AGENCY REPORT NUMBER NAVSWC TR 91-16	
11. SUPPLEMENTARY NOTES Sponsor: COMNAVSEASYS COM (SEA-06GN, SSP-27211)				
12a. DISTRIBUTION/AVAILABILITY STATEMENT Approved for public release; distribution is unlimited.			12b. DISTRIBUTION CODE	
13. ABSTRACT (Maximum 200 words) This report describes the development of improved algorithms for use in the Mathematical Radiation Model for Ships (MREMS) code, which estimates dose equivalent at a matrix of many detector points due to a set of gamma-ray and neutron emitting source points. The algorithms consist of models with adjustable parameters, which are averagable over arbitrary source spectra, for buildup and albedo factors. These models can be used directly in the point kernel model that MREMS employs. Buildup and albedo factors were calculated for six materials in a point-source, slab, point-detector geometry using a decomposition of the solution to the Boltzmann transport equation (and appropriate boundary conditions) into single- and multiple-scatter components. A rigorous solution for the single-scatter component was used that improves the efficiency of the calculations. A detailed model-fitting procedure was employed to fit these factors to simplified models, and the model constants were evaluated for each of several source energies. Finally, a procedure was implemented to determine average model constants for arbitrary source spectra. Slab buildup and albedo factors are presented for various source-slab-detector configurations, both in tabular form and in graphs that also show the fitted models.				
14. SUBJECT TERMS gamma-ray neutron photon code buildup attenuation kernel algorithm Boltzmann radiation transport			15. NUMBER OF PAGES 252	
			16. PRICE CODE	
17. SECURITY CLASSIFICATION OF REPORT UNCLASSIFIED	18. SECURITY CLASSIFICATION OF THIS PAGE UNCLASSIFIED	19. SECURITY CLASSIFICATION OF ABSTRACT UNCLASSIFIED	20. LIMITATION OF ABSTRACT UL	

GENERAL INSTRUCTIONS FOR COMPLETING SF 298

The Report Documentation Page (RDP) is used in announcing and cataloging reports. It is important that this information be consistent with the rest of the report, particularly the cover and its title page. Instructions for filling in each block of the form follow. It is important to *stay within the lines* to meet optical scanning requirements.

Block 1. Agency Use Only (Leave blank).

Block 2. Report Date. Full publication date including day, month, and year, if available (e.g. 1 Jan 88). Must cite at least the year.

Block 3. Type of Report and Dates Covered. State whether report is interim, final, etc. If applicable, enter inclusive report dates (e.g. 10 Jun 87 - 30 Jun 88).

Block 4. Title and Subtitle. A title is taken from the part of the report that provides the most meaningful and complete information. When a report is prepared in more than one volume, repeat the primary title, add volume number, and include subtitle for the specific volume. On classified documents enter the title classification in parentheses.

Block 5. Funding Numbers. To include contract and grant numbers; may include program element number(s), project number(s), task number(s), and work unit number(s). Use the following labels:

C - Contract	PR - Project
G - Grant	TA - Task
PE - Program Element	WU - Work Unit Accession No.

BLOCK 6. Author(s). Name(s) of person(s) responsible for writing the report, performing the research, or credited with the content of the report. If editor or compiler, this should follow the name(s).

Block 7. Performing Organization Name(s) and Address(es). Self-explanatory.

Block 8. Performing Organization Report Number. Enter the unique alphanumeric report number(s) assigned by the organization performing the report.

Block 9. Sponsoring/Monitoring Agency Name(s) and Address(es). Self-explanatory.

Block 10. Sponsoring/Monitoring Agency Report Number. (If Known)

Block 11. Supplementary Notes. Enter information not included elsewhere such as: Prepared in cooperation with...; Trans. of...; To be published in... . When a report is revised, include a statement whether the new report supersedes or supplements the older report.

Block 12a. Distribution/Availability Statement.

Denotes public availability or limitations. Cite any availability to the public. Enter additional limitations or special markings in all capitals (e.g. NOFORN, REL, ITAR).

DOD - See DoDD 5230.24, "Distribution Statements on Technical Documents."
DOE - See authorities.
NASA - See Handbook NHB 2200.2
NTIS - Leave blank.

Block 12b. Distribution Code.

DOD - Leave blank.
DOE - Enter DOE distribution categories from the Standard Distribution for Unclassified Scientific and Technical Reports.
NASA - Leave blank.
NTIS - Leave blank.

Block 13. Abstract. Include a brief (*Maximum 200 words*) factual summary of the most significant information contained in the report.

Block 14. Subject Terms. Keywords or phrases identifying major subjects in the report.

Block 15. Number of Pages. Enter the total number of pages.

Block 16. Price Code. Enter appropriate price code (*NTIS only*)

Blocks 17.-19. Security Classifications. Self-explanatory. Enter U.S. Security Classification in accordance with U.S. Security Regulations (i.e., UNCLASSIFIED). If form contains classified information, stamp classification on the top and bottom of the page.

Block 20. Limitation of Abstract. This block must be completed to assign a limitation to the abstract. Enter either UL (unlimited) or SAR (same as report). An entry in this block is necessary if the abstract is to be limited. If blank, the abstract is assumed to be unlimited.